Perceptual continuity across saccades

Perceptuele continuïteit over saccades heen

(met een samenvatting in het Nederlands)

Proefschrift

ter verkrijging van de graad van doctor aan de Universiteit Utrecht op gezag van de rector magnificus, prof. dr. H.R.B.M. Kummeling, ingevolge het besluit van het college voor promoties in het openbaar te verdedigen op vrijdag 6 september 2019 des middags te 12.45 uur

door

Jasper Hajo Fabius

geboren op 28 maart 1989 te Amsterdam
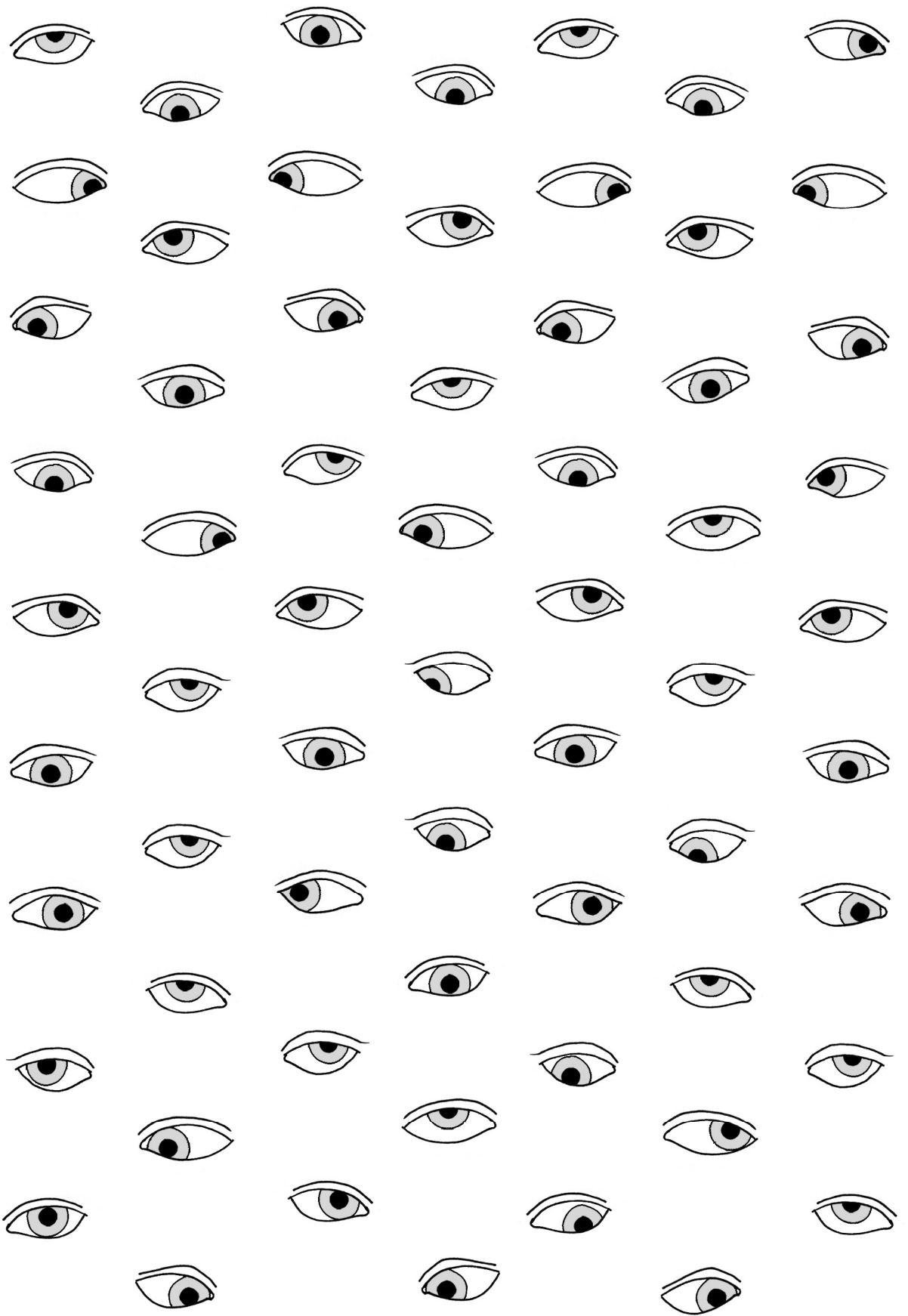
Promotor: Prof. dr. S. Van der Stigchel

Copromotoren: Dr. T.C.W. Nijboer

                            Dr. A. Fracasso

Contents

Chapter 1

General introduction

Example

While you wander around a forest you stumble upon an ant hill (Figure 1A). You see thousands of ants moving across the hill, carrying seeds, long pine needles and small brown leaves. You can perceive the ants and their goods because light reflects off their bodies onto your retina, where photoreceptors transform the electromagnetic radiation into a neural firing pattern that cascades down the visual system (Purves et al., 2008). You can see the ants move because as they move, their reflections move on your retina. As you observe them for a while, a small silhouette suddenly shows up several meters behind the ant hill. Because you were studying the ants, you only see the silhouette from the corner of your eye. To determine the identity of the silhouette you will have to make an eye movement towards it, such that the silhouette falls on the central part of your visual field where visual acuity is highest (Strasburger, Rentschler, & Jüttner, 2011). You saw the silhouette was moving rightwards, towards a tall tree. If you don't make the eye movement now it might have gone out of sight before you can identify what it was. With a delay of only a few hundred milliseconds you make the eye movement (Liversedge, Gilchrist, & Everling, 2011). The silhouette, the ant hill, the thousands of ants, and in fact the entire visual field sweeps across your retina with high velocity. Now you fixate the silhouette and you can easily identify the creature right before it disappears behind the tall tree. A squirrel.

Remarkably, you saw the ants move because the light reflected from their bodies onto your retina. And similarly, you saw the squirrel move in the periphery. But you did not see the entire forest move when you made the eye movement from the ant hill towards the squirrel. Introspectively, the world remained stable and perception appeared continuous despite the drastic change in retinal stimulation caused by the eye movement (Figure 1B). Clearly, the ability to make quick eye movements allows us to aim our fovea's – the part of the retina where cone density is highest (Curcio, Sloan, Kalina, & Hendrickson, 1990) – at the most relevant parts of a scene. At the same time, the ability to make quick eye movements introduces potential ambiguity in the source of retinal stimulation. It can be external (a moving squirrel) or self-generated (an eye movement). However, the perceptual quality of these two sources is introspectively very different. External motion is easily detected, while displacements caused by your own eye movements go largely unnoticed. This raises the question: how does the visual system give rise to perceptual continuity across eye movements?
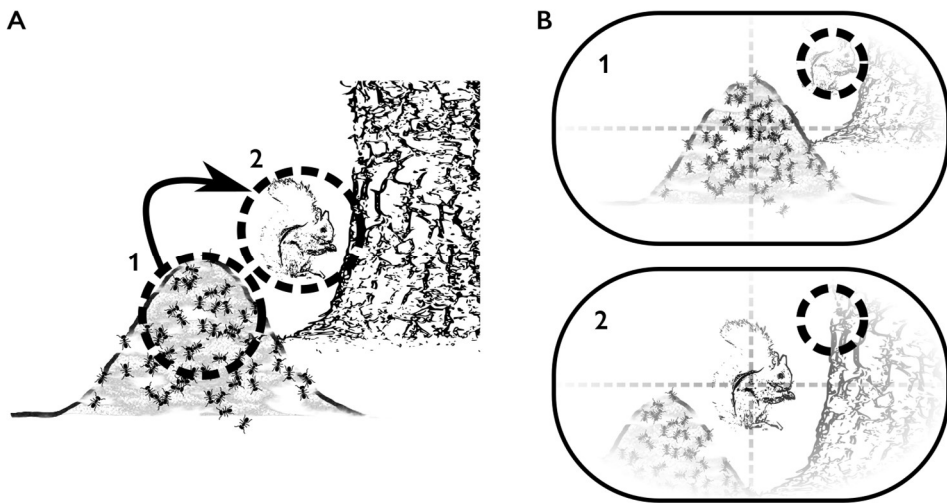
1

Figure 1. Example problem of perceptual continuity across eye movements. **A.** Scene in spatiotopic coordinates. 1 = pre-saccadic fixation location, 2 = post-saccadic fixation location. **B.** Impression of perceptual image under pre-saccadic fixation (1) and post-saccadic fixation (2). Dashed circle depicts the pre-saccadic retinal location of the squirrel. As is clear from the comparison of panel 1 and 2, the squirrel is projected on two different retinal locations across the saccade. After the saccade, the tree is occupying the original retinal location of the squirrel. Dashed straight lines depict central axes of the perceptual field.

Thesis outline

In Chapters 2, 3 and 4 of this thesis I investigated the fundamental nature of perceptual continuity across saccades using human psychophysics (Chapter 2 and 3) and magnetoencephalography (Chapter 4). In Chapter 5 I investigated how perceptual continuity is affected by a lesion to the posterior parietal cortex, a cortical area where neurons show dynamics that suggest involvement in enabling perceptual continuity. In Chapter 6 I developed a clinical screening instrument that is sensitive to impairments in spatial working memory, which I hypothesize might result in impaired perceptual continuity. Chapters 7 and 8 are more exploratory in nature. In these chapters I investigated whether and how locations are remembered over a short period of time. In Chapter 7 I explored the extent to which humans use the history of where they have already looked to determine where they are going to look next. In Chapter 8 I explored what happens to covert attention when observers are asked to keep a peripheral location in memory. But first I will provide the reader with background information on perceptual continuity across saccades.

The principle of re-afference

The dominant explanation of perceptual continuity involves the interaction between neural signals that originate in photoreceptors (afferent signals) and signals that originate in the oculomotor system and are projected to the extraocular muscles (efferent signals). The first rough drafts of this idea can be traced back to at least the 17th century as described in book 3 of the Opticorum Libri Sex by Francisus Aguilonius (Aguilonius, 1613). In succeeding centuries, the idea was further developed by, most notably, Steinbuch, Purkyně, von Helmholtz and von Uexküll (Grüsser, 1995). The idea became firmly established by the work of Von Holst and Mittelstaedt (1950) and Sperry (1950). They explained that the visual system has access to extra-retinal information (Box 1 at the end of this Chapter). With the extra-retinal information, the afferent information caused by the eye movement could be compensated (Sperry, 1950; Von Holst & Mittelstaedt, 1950). This is called the principle of re-afference. With the re-afference principle, perceptual continuity could arise from a forward model (Miall & Wolpert, 1996; Webb, 2004). A forward model is a term in control theory describing part of a system that predicts the outcome of a change in the system before the change is implemented (Figure 2). Because perception is suppressed during the eye-movement, minimizing the visibility of any retinal smear during the eye movement (Volkmann, 1962) – although not completely invisible (Castet, Jeanjean, & Masson, 2002; Castet & Masson, 2000)– I will only discuss the retinal image before and after an eye movement in this thesis, in line with the majority of studies in this research field. Thus, the forward model uses the pre-saccadic retinal image and extra-retinal information about the upcoming eye movement to make a prediction about the post-saccadic retinal image.

Use of extra-retinal information in localization

The forward model predicts that retinal displacements as the result of saccades (Box 1) can be separated from retinal displacements as the result of motion in the external world. With an influential experiment Bridgeman and colleagues tested this hypothesis. They asked observers to detect small target displacements when they occur during a saccade. They instructed observers to make a saccade to a single target (e.g. the squirrel from the example). During the saccade the target was displaced by the experimenters (e.g. moving the squirrel to the left of the ant hill). Thus, there was a mismatch between the actual post-saccadic retinal location of the stimulus and the predicted location according to the forward model. If the visual system compares the predicted and actual retinal locations,
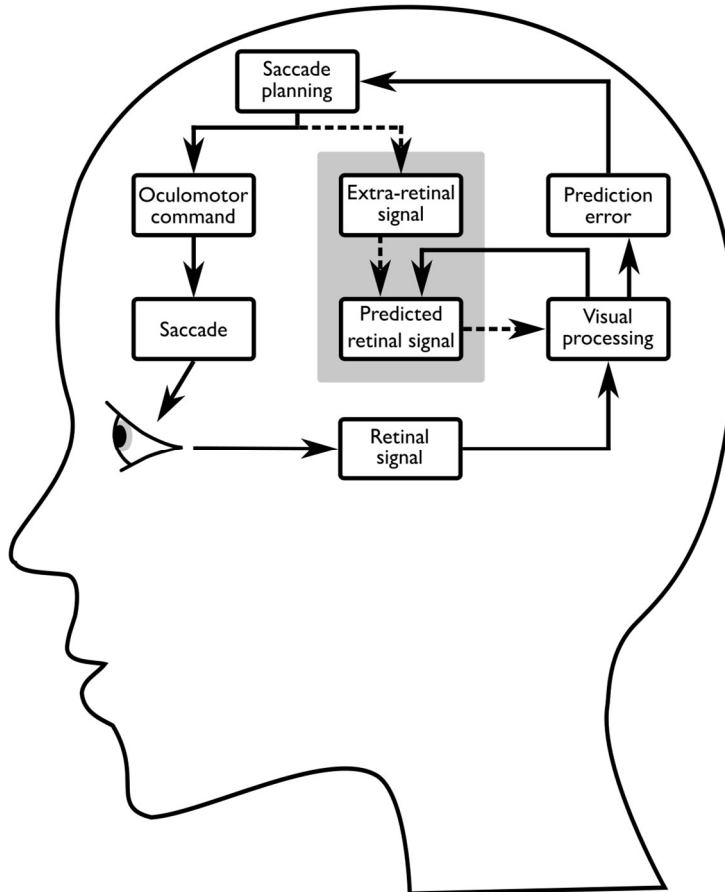
Figure 2. Diagram of visual perception across saccades, involving a forward model (grey box). The forward model predicts the sensory consequences (retinal signal) of an upcoming saccade using extra-retinal signals (e.g. a copy of the oculomotor command or corollary discharge) and visual information. Note that locations of the boxes are not matched to the most likely locations in the brain where each component of the model is thought to be localized. This diagram is based on Miall & Wolpert (1996) and Crapse & Sommer (2008)

the mismatch should be detected. However, remarkably large displacements went unnoticed to the observer, even though the task is trivially easy when the observers maintain stable fixation (Bridgeman, Hendry, & Stark, 1975). This phenomenon became known as saccadic suppression of image displacement (SSID). SSID shows that intra-saccadic displacements must cross a threshold before we can reliably detect them, so it seems the extra-retinal information that provides details of the displacement caused by the saccade is very imprecise. Interestingly, SSID scales with saccade amplitude: displacements of roughly 25% of the saccade amplitude remain undetectable. Moreover, later studies showed that

sensitivity to displacements is particularly low when the displacements are made in parallel to the saccade vector (Bray, Bansal, & Joiner, 2016; Niemeier, Crawford, & Tweed, 2003; Wexler & Collins, 2014).

But the story does not stop here. In an intriguing variation of the intra-saccadic displacement paradigm, the target is briefly removed at saccade onset, such that when the saccade ends there is no target; the stimulus display is blank. The target reappears only 250 ms after the saccade ended. With this blank, smaller displacements become detectable (Deubel, Schneider, & Bridgeman, 1996). This has been aptly called "the blank effect". The authors concluded that by removing the stimulus from the screen, the observers rely only on extra-retinal signals for their judgments when no visual information is available immediately after the saccade ended. Hence, two pieces of evidence suggest from SSID suggest that the extra-retinal signals that influence localization across saccades contain information about the saccade vector. First, SSID scales with saccade amplitude, the larger the amplitude, the larger displacements can be to go unnoticed to the observer (Bridgeman et al., 1975; Deubel et al., 1996). Second, because SSID is specific to the saccade direction (that is, strongest insensitivity for displacements in the same direction as the saccade) extra-retinal signals must contain information about the direction of the saccade. Together, SSID and the blank effect suggest that although extra-retinal signals are available for localization across saccades, there is strong prior assumption that the targets generally do not move during a saccade. Therefore the predicted and actual displacements do not have to match exactly for perceptual continuity (Bridgeman, Van der Heijden, & Velichkovsky, 1994; Mackay, 1972; McConkie & Currie, 1996).

It was later demonstrated that the extent to which extra-retinal signals influence localization depends on the reliability of the oculomotor command. In SSID there is a mismatch between expected and actual retinal displacement across a saccade. Although this mismatch is introduced by the experimenter, another source of mismatch could arise from oculomotor error. Repeated saccades to a single target will not end at the same identical location. Instead, they will fall in elliptical areas around the target. The major axis of the elliptical area that describes oculomotor variance runs parallel to the saccade direction, and scales with saccade amplitude (van Opstal & van Gisbergen, 1989). In addition, the length of the major axis and the ratio between the major and minor axis varies across subjects. Observers with a high ratio (i.e. a strongly elongated ellipse) have been shown to have higher displacement thresholds, so they detect displacements only when they are large (Niemeier et al., 2003). This relationship between saccade endpoint precision and SSID
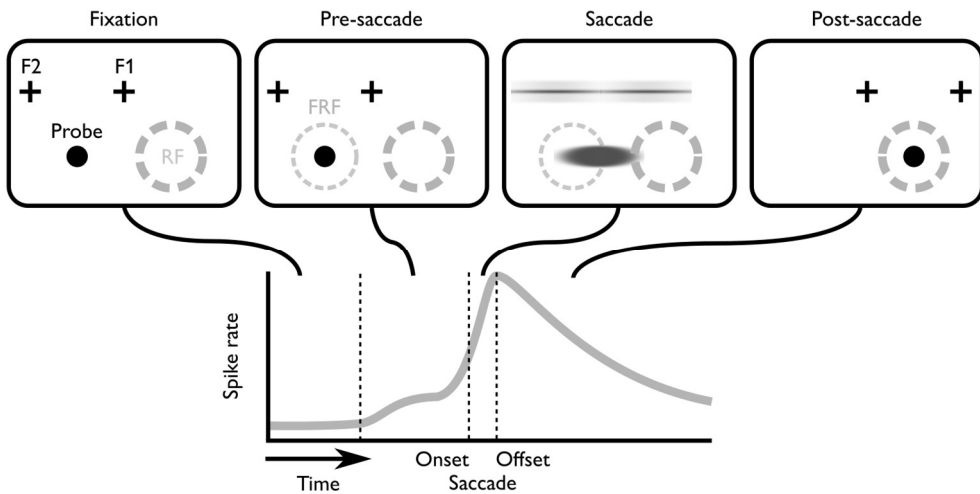
Figure 3. Predictive remapping of receptive fields. Top panels show an of example visual stimulation (black) and neural receptive field (gray) across a saccade. F1 = fixation point 1. F2 = fixation point 2. RF = receptive field. FRF = future receptive field. The bottom panel shows neural spike rate across time, with time locked to saccade onset (after Sommer & Wurtz, 2006). Even before the probe is inside the receptive field of the neuron it starts to respond before saccade onset.

shows that the visual system uses both retinal and extra-retinal information, as proposed by the re-afference principle, but extended with the notion both sources of information are weighted according to their general reliabilities.

Neural implementation

The principle of re-afference – and in fact the problem of perceptual continuity per se – alludes to the neural mechanisms of the visual system. Therefore, I will review the neurophysiological properties of neurons in the visual system that are thought to play a major role in processing re-afferent information. A neural property that could contribute to perceptual continuity is (predictive) remapping of receptive fields (Box 1). Neurons throughout the visual cortex have "receptive fields", which means they respond to stimuli at specific locations on the retina (Hartline, 1938; Hubel & Wiesel, 1959). These receptive fields remain retinotopically organized at multiple levels of the visual system (Gardner, Merriam, Movshon, & Heeger, 2008). Predictive remapping of receptive fields (Figure 3) means that the spatial tuning of neurons is transiently altered shortly before the onset of a saccade, or more colloquially, these neurons exhibit "shifting receptive fields" (Duhamel, Colby, & Goldberg, 1992). Receptive fields can be measured by briefly flashing probes (small points of light) at different retinal locations, while simultaneously recording the responses

of neurons to the probes. To demonstrate remapping, this protocol is used in combination with the execution of saccades. The neural responses in reaction to the probes can then be locked in time to the onset or offset saccade. Remapping had been observed in various brain areas of the macaque, such as the superior colliculus (Walker, Fitzgibbon, & Goldberg, 1995), the frontal eye field (Umeno & Goldberg, 1997) and the parietal cortex (Duhamel, Colby, et al., 1992). Still, it is currently debated in which direction and when these shifts occur – parallel to the saccade vector vs. attraction to the saccade target before the saccade/anticipatory or after/memory-based (Hartmann, Zirnsak, Marquis, Hamker, & Moore, 2017; Mirpour & Bisley, 2016; Neupane, Guitton, & Pack, 2016; Zirnsak, Steinmetz, Noudoost, Xu, & Moore, 2014). The changes in receptive field properties might be the neural signal that represents the predicted post-saccadic retinal stimulation, i.e. re-afferent information (Duhamel, Colby, et al., 1992).

The studies of Wurtz, Sommer and colleagues showed a pathway that processes extra-retinal signals related to saccade execution, consisting of the superior colliculus, the medial dorsal nucleus of the thalamus and frontal eye fields (Sommer & Wurtz, 2002, 2006). It has been suggested that with the extra-retinal information conveyed in this pathway, the frontal eye fields code the evaluation of the afferent and re-afferent information. Crapse and Sommer (2012) investigated the responses properties of neurons in FEF to stimulus changes during a saccade. They presented stimuli before a saccade and during the saccade they displaced the stimulus. or changed its features (colour or size). When the stimulus would fall into the receptive field of the FEF neurons after the saccade, they would respond more strongly if any of the stimulus properties had changed than when they had remained stable and continuous (Crapse & Sommer, 2012). Thus, it seems that these neurons assess the continuity of a stimulus across a saccade. Moreover, inactivation of the medial dorsal nucleus of the thalamus in monkeys results in behaviour that is expected when extra-retinal information is not available, e.g. localization based more on retinotopic coordinates that spatiotopic coordinates (Cavanaugh, Berman, Joiner, & Wurtz, 2016). These findings suggest that together, the superior colliculus, the medial dorsal nucleus of the thalamus and frontal eye fields are a likely candidate to be the neural implementation of the forward model.

Stimulus location vs. Stimulus features

It has been extensively debated what the content of the re-afferent signal is. Some have argued that only 'attentional pointers' to relevant locations are updated. This could be

1

sufficient to prepare the visual system for prioritized processing of visual information at a specific location (Cavanagh, Hunt, Afraz, & Rolfs, 2010), whereas others have argued that more detailed information about the visual features of a stimulus, such as colour or shape, can be predictively remapped (Melcher & Colby, 2008; Subramanian & Colby, 2014). As illustrated by the phenomenon of change blindness, substantial changes can be made to a visual scene without the observer noticing them (Simons & Rensink, 2005). In line with change blindness, psychophysical experiments have demonstrated that perceptual continuity is not the result of a complete fusion of the pre-saccadic and post-saccadic retinal images: when an array of elements (e.g. 20 small lines) was displayed in two halves across a saccade (e.g. 10 of the elements before and 10 after the saccade) observers could not accurately perceive the integrated combination of the two halves, even though they could do this easily when maintaining stable fixation (Bridgeman & Mayer, 1983; Irwin, Yantis, & Jonides, 1983; O'Regan & Lévy-Schoen, 1983). The lack of trans-saccadic fusion shows that a substantial portion of the pre-saccadic retinal information is lost across a saccade.

Another paradigm to study the extent to which retinal information is carried across saccades has been the adaptation after-effect. In general (outside the context of perceptual continuity) an adaptation after effect refers to an altered perception of specific stimulus after a prolonged exposure to a similar stimulus. For example, when a moving stimulus is presented to an observer for several seconds, the observer gets adapted to the motion of the stimulus. When the moving stimulus is taken away and replaced by a static one, the static stimulus appears to move in the opposite direction for the observer. Several groups have studied the spatial specificity of adaptation after effects. The question for perceptual continuity was, if the adaptation is spatially specific, then what happens when a saccade is made between the adapter and the test stimulus? Unfortunately, results with this paradigm have been controversial, with some finding evidence for after effects in spatiotopic coordinates (Melcher, 2005; Nakashima & Sugita, 2017; Wolfe & Whitney, 2015; Zimmermann, Morrone, Fink, & Burr, 2013), and others finding strictly retinotopic effects that move along with each saccade (Knapen, Rolfs, & Cavanagh, 2009; Knapen, Rolfs, Wexler, & Cavanagh, 2010; Mathôt & Theeuwes, 2013; Wenderoth & Wiese, 2008). In total, neither the spatiotopic fusion experiments, nor the spatiotopic adaptation experiments provide evidence for low-level interactions of the pre- and post-saccadic retinal image.

Spatiotopic updating

As the reader might have noticed by this point, the history of experiments on visual perception across eye movements can be rather confusing. With the formulation of the principle of re-afference in the 50's, perceptual continuity seemed to have a plausible neurological foundation. However, psychophysical in the following decades demonstrated that the introspective impression of perceptual continuity is not reflected in behavioural responses to stimuli that change during a saccade. At least, continuity in the form of a full picture-like translation from the pre-saccadic retinal image to the post-saccadic retinal image is not measurable. In contrast, more recent psychophysical studies (discussed in the next paragraph) showed evidence for perceptual judgments that do suggest some feature information is transferred across saccades, albeit not for all the stimuli in the visual field. To describe the effects of a pre-saccadic stimulus on the perception of a post-saccade stimulus I will use the term "spatiotopic updating" (Box 1). Speculatively, the perceptual representations that can be spatiotopically updated are similar to those stored in visual working memory, as several authors have argued (Irwin, Zacks, & Brown, 1990; Schut, Van der Stoep, Postma, & Van der Stigchel, 2017; Van der Stigchel & Hollingworth, 2018).

The discrepancy between introspection and the results of the spatiotopic fusion experiments, prompted the critique that the experimental paradigms with spatiotopic fusion do not resemble the typical visual stimulation during trans-saccadic perception. Stimuli are seldom completely different across a saccade. In contrast, stimuli typically remain continuously the same across a saccade. Therefore, experiment with highly transient stimuli (such as brief flashes of light or the arrays from spatiotopic fusion experiments) do not resemble stimuli where an observer would experience perceptual continuity. As an alternative to spatiotopic fusion, it has been proposed that high-level percepts of stimuli can be updated in spatiotopic coordinates (Box 1). The hypothesis is that the high-level representation of a stimulus (i.e. representations in high-level visual areas) is updated rather than low-level visual features (i.e. representations in striate cortex). Multiple studies have demonstrated that the presence of a pre-saccadic stimulus affected the percepts of a post-saccadic stimulus if the pre-saccadic and post-saccadic stimuli are similar to each other (Irwin et al., 1990; Jüttner & Röhler, 1993; Pollatsek, Rayner, & Collins, 1984). Recently, similar experimental paradigms provided more evidence, for spatiotopic updating of orientation (Fornaciai, Binda, & Cicchini, 2018; Ganmor, Landy, & Simoncelli, 2015; Prime, Niemeier, & Crawford, 2006; Wolf & Schütz, 2015), colour (Oostwoud Wijdenes, Marshall,

1

& Bays, 2015; Wittenberg, Bremmer, & Wachtler, 2008), and motion (Fracasso, Caramazza, & Melcher, 2010; Melcher & Fracasso, 2012; Ong, Hooshvar, Zhang, & Bisley, 2009; Szinte, Wexler, & Cavanagh, 2012). In addition, both displacements and changes in visual features can be detected more readily when one of the two changed across a saccade (Atsma, Maij, Koppen, Irwin, & Medendorp, 2016; Demeyer, De Graef, Wagemans, & Verfaillie, 2010).

Time course of spatiotopic updating

Because the oculomotor system executes a saccade roughly every 300 ms (Henderson & Hollingworth, 1998), spatiotopic updating should operate within a small time window to facilitate perceptual continuity across saccades. Within a single fixation, pre-saccadic information should be updated and be available directly after the saccade. In **Chapter 2**, we demonstrate a direct link between the motion information in the pre-saccadic and immediate post-saccadic information, as hypothesized from the results earlier studies (Deubel, Bridgeman, & Schneider, 1998; Jüttner, 1997). However, it has been suggested that spatiotopic updating can only be observed when the saccade can be planned for 500 ms or more (Zimmermann, Morrone, & Burr, 2013, 2014; Zimmermann, Morrone, Fink, et al., 2013). This is surprisingly long because the visual system typically processes stimuli much quicker (Kirchner & Thorpe, 2006) and saccade are typically executed every 300 ms. In **Chapter 3**, we argue that the slow estimated time course of spatiotopic updating follows from a selective interpretation of the results of the aforementioned studies. In addition, we provide evidence that the spatiotopic updating can observed for fast visually-guided saccades (with latencies of ~150 ms) using a similar paradigm as in Chapter 2.

Feature specificity of spatiotopic updating

The results presented in Chapter 2 and 3 both suggest that spatiotopic updating does contain information specific to the visual features of the stimulus. In **Chapter 4** we investigated this further using magnetoencephalography (MEG). Neuroimaging studies with human subjects have also provided evidence for updating of spatial coordinates of visual targets in the posterior parietal cortex, using functional magnetic resonance imaging (fMRI) (Dunkley, Baltaretu, & Crawford, 2016; Fairhall, Schwarzbach, Lingnau, Van Koningsbruggen, & Melcher, 2017; Medendorp, Goltz, & Vilis, 2006; Medendorp, Goltz, Vilis, & Crawford, 2003; Merriam, Genovese, & Colby, 2003, 2007) and magneto-/electroencephalography (M/EEG) (Bellebaum & Daum, 2006; Edwards, VanRullen, & Cavanagh, 2018; Parks &

Corballis, 2010; Van Der Werf, Buchholz, Jensen, & Medendorp, 2013). In these studies, receptive fields are typically operationalized as hemifield, where each hemisphere represents the contralateral hemifield. For example, Parks and Corballis (2008, 2010) showed observers a large stimulus in the left or right visual field. Subjects were instructed to make a saccade across the stimulus, bringing it from the left to the right visual field. Shortly before saccade onset, the potential over the hemisphere ipsilateral to the stimulus increased. Because the ipsilateral hemisphere would become the contralateral hemisphere after the saccade, the increased potential was interpreted to reflect remapping or spatiotopic updating.

Although the results from the EEG studies might relate to the processing of re-afferent information it does not show whether re-afferent information contains feature information about the stimulus. Feature specificity has been investigated with fMRI. Feature specific updating has been demonstrated in modulations of blood-oxygen level-dependent (BOLD) response amplitudes when presenting either the same stimulus across a saccade or changing it (Dunkley et al., 2016). However, another fMRI study suggested that although visual features might potentially be present in the re-afferent information, feature information is not automatically updated (Lescroart, Kanwisher, & Golomb, 2016). Unfortunately, fMRI does not have the temporal resolution to dissociate between pre- and post-saccadic effects due to the long impulse response function of the BOLD response function. Therefore, we investigated spatiotopic updating with magnetoencephalography in chapter 4. Similar to the EEG study of Parks & Corballis (2008, 2010), we observed stronger responses to the combination of a stimulus and a saccade than the responses to only a stimulus or only a saccade. Using multivariate pattern analysis (MVPA), we further investigated whether the information about the stimulus features in the MEG data were spatiotopically updated. We observed an effect that could be related to spatiotopic updating after saccade offset. Rather than predictive spatiotopic updating of visual features, our results showed that the pre-saccadic representation of the spatial frequency of the stimulus lingered in retinotopic coordinates after saccade offset. However, quickly after saccade offset, only ~50 ms after saccade offset there was an additional representation in post-saccadic retinotopic coordinates. Thus, at the same time we could decode spatial frequency using either the pre- or post-saccadic representation. These results do not reflect predictive updating of stimulus features before saccade onset – although the absence of evidence does not equal evidence for absence – but are more in line with a memory-based account of spatiotopic updating,

1

where the pre-saccadic stimulus and post-saccadic stimulus can be compared once both have been processed using retinotopic afferent information.

Perceptual discontinuity after stroke

In addition to neuroimaging, several studies have investigated spatiotopic updating in patients with lesions to the areas that have been demonstrated to show either remapping of receptive fields (e.g. posterior parietal cortex) or to process extra-retinal information (e.g. medial dorsal nucleus of the thalamus). Around the same time as the discovery of predictive remapping (Duhamel, Colby, et al., 1992), two studies presented patients with frontoparietal lesions that exhibited oculomotor behaviour that suggested an impairment in spatiotopic updating (Duhamel, Goldberg, Fitzgibbon, Sirigu, & Grafman, 1992; Heide, Blankenburg, Zimmermann, & Kompf, 1995). More recently however, these conclusions have been criticized to result from very strict definitions of a saccade in the analysis (Rath-Wilson & Guitton, 2015). Because responses in those studies (double-step saccades) were not perceptual judgements it could be that lesions to the posterior parietal cortex specifically affect perceptual judgements, but not oculomotor responses. To directly assess the influence of extra-retinal signals on perception, we tested patients with lesions to the posterior parietal cortex with the intrasaccadic displacement task in **Chapter 5**. Performance on this task is affected in patients with lesions to the medial dorsal nucleus of the thalamus (Ostendorf, Liebermann, & Ploner, 2010, 2013). Specifically, the blank effect – illustrative for the availability of extra-retinal signals – was reversed, i.e. when the blank was introduced between saccade offset and displacement onset, even larger displacement went unnoticed than without the blank. This is the opposite of what healthy observers show. The data presented in chapter 5 does not suggest that patients with a lesion to the posterior parietal cortex have a deficit similar to patients with thalamus lesions. In most of the patients we tested, even those with substantial lesions to the posterior parietal cortex, displacement sensitivity improved with the introduction of a blank, suggesting an influence of extra-retinal signals on visual perception across saccades.

Maintenance of visuospatial information

The study presented in Chapter 5 is fundamental in nature. We examined the psychophysical data for evidence of perceptual discontinuity in patients with a lesion to the

parietal cortex. But the data did not provide this evidence One explanation for the presence of perceptual continuity in patients with PPC lesions is the possibility that there are multiple neural circuits that could give rise to perceptual continuity, i.e. degeneracy (Edelman & Gally, 2001; Price & Friston, 2002). For example, it has been proposed that perceptual continuity can be established by using an efference copy of the motor command as extra-retinal signals (Von Holst & Mittelstaedt, 1950), but also by using proprioceptive signals from the eye (Steinbach, 1987; Sun & Goldberg, 2016). The data presented in Chapter 5 cannot make a distinction between these different sources. Moreover, the study did not explore the clinical consequences of the hypothetical perceptual discontinuity for the affected patient.

Symptoms of visuospatial neglect resemble problems with memory-based spatiotopic updating (Husain & Rorden, 2003). Although the core-deficit in visuospatial neglect is defined as a lateralized attention disorder, several patients also exhibit impaired spatial working memory performance when spatial information has to be maintained across saccades, resulting in repetitive re-examination of the same stimuli on the intact side of their visual field (Husain et al., 2001; Mannan et al., 2005; Ptak, Schnider, Golay, & Muri, 2007; Wojciulik, Husain, Clarke, & Driver, 2001). In **Chapter 6** we present a newly developed task to assess spatial working memory performance and can be administered in clinical settings. With this task we collected data of stroke patients in the sub-acute phase with and without visuospatial neglect. These data demonstrate a relationship between the precision of spatial information and performance in visual search, which are in turn both correlated with the presence of visuospatial neglect. Moreover, the task proved to be easily assessable in a clinical population and clinical setting (unlike the intra-saccadic displacement task, which requires an advanced eye tracker and 1-2 hours to conduct). This makes it a promising tool to screen for spatial working memory impairments.

The capability to store and update visual information is inherent to perceptual continuity. In **Chapter 7** we investigate this by examining the extent to which previous fixation locations guide saccade direction. It has been suggested that saccades are biased away from previously fixated locations (Boot, McCarley, Kramer, & Peterson, 2004; Klein, 1988; McCarley, Wang, Kramer, Irwin, & Peterson, 2003). However, it is not straightforward to establish a proper baseline rate of fixations at a specific location in a scene (Bays & Husain, 2012). Since the classic work of Yarbus it is known that observers look at specific parts of a scene, others are rarely fixated (Yarbus, 1967). We circumvented this problem using an artificial display where only two saccade targets are presented at every fixation, and previous targets are removed from the screen (McCarley et al., 2003). We

1

observed that re-fixation rates increased when a fixation had been fixated before but a 'long' time ago. This effect was modulated by task (whether or not re-fixating affected task performance) and the presences of spatial references. The effect of spatial references suggests that spatial information is more easily transferred across saccades when visual stimuli are continuously present (Golomb, Pulido, Albrecht, Chun, & Mazer, 2010; Lisi, Cavanagh, & Zorzi, 2015).

In **Chapter 8** we explored how covert attention is deployed while subjects maintain stable fixation but have to remember a single location for several seconds. In this experiment we used the pupillary light response to measure the location of attention (Binda, Pereverzeva, & Murray, 2013; Mathôt, Dalmaijer, & Grainger, 2014; Mathôt, van der Linden, Grainger, & Vitu, 2013). In this experiment observers were presented with a display in which one half was bright, the other half was dark. A brief flash indicated the location that had to be remembered. This location was either on the bright or the dark background. The observer's task was to accurately remember the location because after a delay of 8 seconds, a second flash would be presented slightly displaced from the initial location (cf. displacement task for SSID). The observer had to indicate in which direction the displacement was. When the to-be-remembered location was on the dark background pupil size increased, relative to when the location was on a bright background. We did not observe a continuous difference in pupil size throughout the entire delay, but for several seconds at the beginning of the memory interval, and several seconds before the end.

Summary

To summarize, the first impression of the squirrel, while you were still watching the ants, influenced your perception of the squirrel, immediately after your eye movement towards the squirrel ended (Chapter 2 and 3). You did not see the entire forest move because extra-retinal signals influenced your perception, enabling spatiotopic updating of the representation of the squirrel after the saccade ended (Chapter 4). The extra-retinal signals still influence perception after a stroke to the posterior parietal cortex – a cortical area that is likely involved in processing extra-retinal signals (Chapter 5). Now that you have identified the squirrel you continue to marvel at the complexity of the ant hill. Or, if you are actively looking for other small forest dwellers – such as a hedgehog – you will probably not direct your gaze back to the same location on the ant hill (Chapter 7). However, when the ability to remember locations is impaired, for example after a stroke, your ability to

search for the hedgehog is likely also impaired (Chapter 6). Finally, if you saw something rustle in the periphery, but did not make an eye movement towards it because the ants you were inspecting were too fascinating, you might have been able to keep your attention at the rustled location (Chapter 8). When the rustling increases, you make a saccade towards it, experiencing perceptual continuity across saccades.

Box 1. Definitions

Perceptual continuity

Introspective continuous and stable visual percept. I prefer perceptual continuity over the more frequently used term perceptual stability. Stability implies static objects, whereas continuity more strongly conveys that the percept appears uninterrupted. Multiple authors have recently made this consideration (Herwig, 2015; Rao, Abzug, & Sommer, 2016; Rolfs, 2015; Schut, 2019; Wurtz, 2018).

Extra-retinal information

In the scope of this thesis, extra-retinal information refers to signals that influence visual perception but do not arise in the retina. Extra-retinal signals provide re-afferent information, i.e. afferent signals caused by movement of receptors as result of efferent signals (Von Holst & Mittelstaedt, 1950). The principle of re-afference goes beyond the human visual system and includes all animals and sensory organs (Crapse & Sommer, 2008a). Example signals that could provide extra-retinal signals are an efference copy and a corollary discharge and proprioception. The difference between the efference copy and corollary discharge is minimal. The former was coined by von Holst and Mittelstaedt (1950), the latter by Sperry (1950). Conceptually, the corollary discharge can arise at multiple stages during saccade planning and therefore originate from multiple brain areas, whereas the efference copy is a direct copy of the command send to the extraocular muscles (Straka, Simmers, & Chagnaud, 2018).

Saccade

Fast, jerky eye movement (Liversedge et al., 2011). Saccades contrast with other, slower types of eye movements where the eyes are locked to a stimulus, e.g. when the eyes follow a moving object or when the eyes follow a static stimulus during locomotion. Although during the latter forms of eye movement there is also the problem of dissociating self-generated retinal motion vs. retinal motion generated by the stimulus, these were not subject to the studies presented in this thesis.
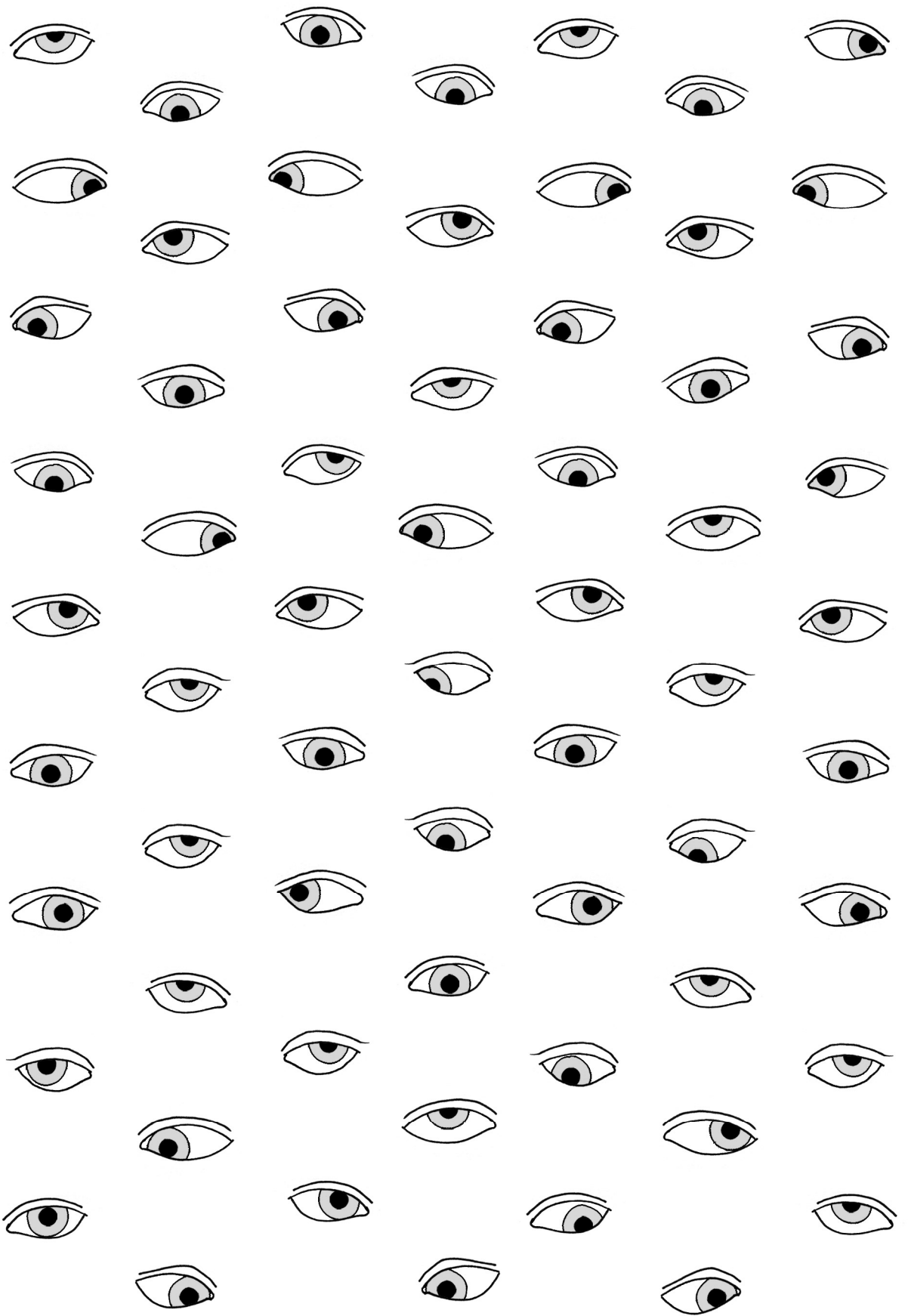
Spatiotopic updating

Refers to perception and behavioural responses. Across a saccade, a stimulus stimulates two different locations on the retina. Updating refers to the change in percept of the stimulus when it is presented multiple times. Spatiotopic means in world-centered coordinates*. Together spatiotopic updating refers the updating of the percept of a stimulus when it stimulates two different retinotopic locations across a saccade but remained stable in world-centered coordinates. In the example described in the first paragraph, the moving silhouette you saw before the eye movement probably gave you the impression it was some kind of small animal. After the eye movement you updated your percept of the moving stimulus by identifying it as a squirrel.

The distinction between spatiotopic (world-centered), craniotopic (head-centered) and body-centered goes beyond the scope of this thesis. In the presented studies body and head position are fixed. Therefore, I use retinotopic to refer to coordinates on the retina and spatiotopic to refer to coordinates in the world.

Remapping

Refers to neural responses. Remapping is a property of neurons with a spatial tuning, i.e. a receptive field (Hartline, 1938; Hubel & Wiesel, 1959). Remapping of receptive fields is a transient change in tuning which can be observed around the time of a saccade (Duhamel, Colby, & Goldberg, 1992).

Chapter 2

Spatiotopic updating facilitates perception immediately after saccades

Author contributions

JHF and AF contributed equally to this work. JHF, AF and SvdS conceptualized and designed experiments. JHF programmed experiments and collected data. JHF and AF performed analyses. JHF, AF and SvdS wrote and revised manuscript.

Abstract

As the neural representation of visual information is initially coded in retinotopic coordinates, eye movements (saccades) pose a major problem for visual stability. If no visual information were maintained across saccades, retinotopic representations would have to be rebuilt after each saccade. It is currently strongly debated what kind of information (if any at all) is accumulated across saccades, and when this information becomes available after a saccade. Here, we use a motion illusion to examine the accumulation of visual information across saccades. In this illusion, an annulus with a random texture slowly rotates, and is then replaced with a second texture (motion transient). With increasing rotation durations, observers consistently perceive the transient as large rotational jumps in the direction opposite to rotation direction (backward jumps). We first show that accumulated motion information is updated spatiotopically across saccades. Then, we show that this accumulated information is readily available after a saccade, immediately biasing postsaccadic perception. The current findings suggest that presaccadic information is used to facilitate postsaccadic perception and are in support of a forward model of transsaccadic perception, aiming at anticipating the consequences of eye movements and operating within the narrow perisaccadic time window.

Introduction

When inspecting the world, visual information travels from the retina to the visual cortex in a retinotopic reference frame. Yet, the eyes are continuously moving, creating large shifts in retinal images and thereby posing a serious problem for visual stability. Are perceptual representations updated across saccades, in a spatiotopic reference frame, or do they start anew upon each fixation? This question has gained increasing interest since the presentation of neurophysiological evidence of perisaccadic shifts of receptive fields, suggesting that information is exchanged between neurons around the time of saccades (Duhamel, Colby, et al., 1992; Kusunoki & Goldberg, 2003; Umeno & Goldberg, 1997).

As illustrated by the phenomenon of change blindness, not the entire visual scene is updated across saccades (Simons & Rensink, 2005). It has been argued that only the behaviourally relevant features at saccade endpoint are updated spatiotopically (Deubel et al., 1996; McConkie & Currie, 1996). This presaccadic acquisition of visual features at the saccade target can then be used to predict the perceptual consequences of the eye movement at the fovea (Mathôt & Theeuwes, 2011; Melcher & Colby, 2008; Sommer & Wurtz, 2008b), compatible with forward models where sensory processing is influenced by the predicted consequences of upcoming, self-generated movements (Crapse & Sommer, 2008a; Miall & Wolpert, 1996; Webb, 2004). Recently, several behavioural studies have indeed provided evidence for spatiotopic updating of feature information such as orientation, colour, shape and motion (Biber & Ilg, 2011; Demeyer, De Graef, Wagemans, & Verfaillie, 2009; Ganmor et al., 2015; Melcher & Morrone, 2003; Oostwoud Wijdenes et al., 2015; Wolf & Schütz, 2015).

However, others studies did not find transfer of visual features from a retinotopic into a spatiotopic representation (Knapen et al., 2009; Mathôt & Theeuwes, 2013; Morris et al., 2010; Wenderoth & Wiese, 2008), prompting the hypothesis that not feature information, but only spatial information can be updated spatiotopically using 'attentional pointers' (Cavanagh et al., 2010). This hypothesis has primarily been investigated using cueing effects, showing that a cue presented before a saccade is effective soon after a saccade in spatiotopic coordinates (Hilchey, Klein, Satel, & Wang, 2012; Jonikaitis & Theeuwes, 2013; Pertzov, Zohary, & Avidan, 2010). Whether this also holds for trans-saccadic integration remains

unknown, as there are currently no studies addressing the time course of spatiotopic updating of perceptual representations after a saccade.

Here, we address the issue of spatiotopic visual stability by taking advantage of a recently described motion illusion – High Phi (Wexler, Glennerster, Cavanagh, Ito, & Seno, 2013) – to measure the rapid induction of a motion percept. Using this illusion, the current experiments address whether and when presaccadic visual features influence postsaccadic perception. In the High Phi illusion, an annulus with a random texture (inducer) rotates slowly clockwise or counter-clockwise and is then replaced with several different textures (transient). With increasing inducer durations, participants report the transient more and more as large rotational jumps in the direction opposite to inducer direction (backward jumps). Importantly, the successive different textures, that trigger the illusory jump, are presented transiently, allowing for direct manipulation of perception onset. By manipulating the reference frame of the inducer with respect to the transient we were able to compare the benefit of spatiotopic representations on the speed of building a perceptual representation after a saccade. The data of two experiments are compellingly in favour of rapid spatiotopic interpretations of visual information after eye movement offset. This supports the hypothesis of a perceptual system where object representations can be updated spatiotopically across saccades, taking into account both object features and position. Thereby, this system enables fast spatiotopic interpretations of visual information immediately after saccade offset.

Results

Experiment 1 – Reference frame of the High Phi illusion

The fast temporal characteristics of the High Phi illusion make it an ideal tool to investigate the rapid building of a perceptual representation. However, when investigating transsaccadic perception, this is only useful when the accumulated motion information can be updated spatiotopically. Previous investigations into spatiotopic accumulation of motion information have yielded mixed results with some studies showing spatiotopic (Biber & Ilg, 2011; Melcher & Morrone, 2003) and others showing strictly retinotopic representations of motion (Knapen et al., 2009; Wenderoth & Wiese, 2008). Moreover, some of the spatiotopic effects have been accounted for by more general decision biases, irrespective of either the spatiotopic or retinotopic location of the stimulus (Morris et al., 2010).
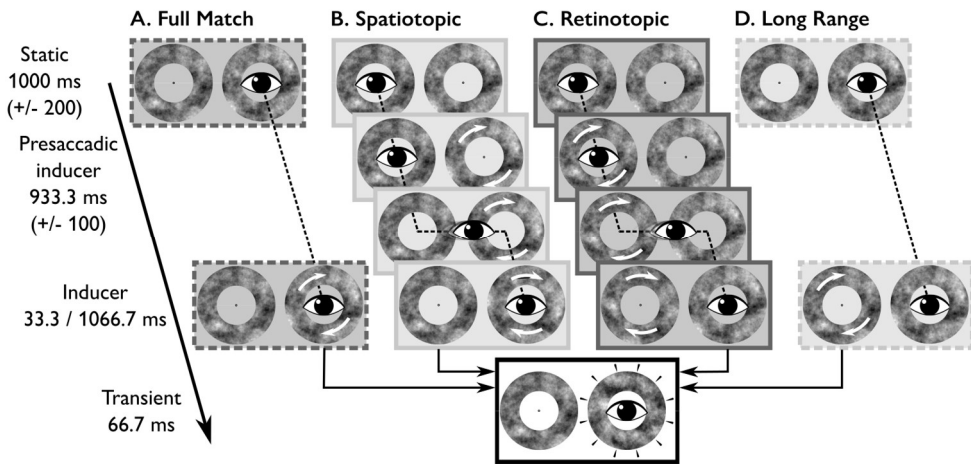
Figure 1. Trial sequences in Experiment 1. The eyes and dotted lines between the eyes depict gaze position. White arrows on the annuli depict rotations of that particular annulus. All trials started with a period of fixation with two static annuli on screen. **A, D.** In the fixation trials (Full Match and Long Range) the static annuli were followed by a rotation of one the two annuli (Inducer, 33.3 or 1066.7 ms). The annulus around fixation rotated in case of the Full Match trials, or in the periphery, in case of the Long Range trials, and was then succeeded by the presentation of series of 4 different textures (Transient). **B.** In the Spatiotopic trials, the peripheral ring started rotating while the eyes remained fixated (Presaccadic inducer). Here, the position of the Presaccadic inducer was spatiotopically matched to the position of the Transient. After an auditory cue, a saccade was initiated to the peripheral, rotating annulus. After the saccade, the annulus rotated around fixation (Inducer), and was then replaced by the Transient. **C.** In Retinotopic trials, the position of the Presaccadic inducer was initially around fixation, and therefore retinotopically matched to the position of the Transient. After an auditory cue, a saccade was executed, and the Inducer was no longer retinotopically matched. Then, the Transient was presented centrally. In all trial types, the Transient would always be presented around the current fixation point. Subjects responded whether they perceived a clockwise or counter clockwise rotational jump, by pressing the right or the left arrow key on a standard keyboard. Note that the Inducer durations as described in this figure correspond to the inducer durations reported in Table 1 (Methods) and Fig. 2 that were analysed.

Therefore, we examined the reference frame in which the High Phi illusion can be induced in Experiment 1. We adapted the illusion into a transsaccadic paradigm with four different trial types (Figure 1). In our display, subjects were always presented with two annuli with different textures, thus enabling manipulation of the reference frame in which the inducer and the transient were presented.

In 12 naïve human subjects we tested the effects of an inducer on perceived jump direction when the inducer and the transient were (A) fully, (B) only spatiotopically, (C) only retinotopically or (D) not matched (we refer to the latter type as Long Range trials). Beside this spatial manipulation, we also varied the inducer duration in order to investigate the temporal development of the illusion.

In Full Match and Long Range trials (Fig. 1A, D), subjects remained fixation, enabling full control over the duration of the inducer which was set to either 0, 33.3 or 1066.7 ms (presented at a 60 Hz refresh rate). We were primarily interested in the 33.3 or 1066.7 ms conditions but included the 0 to keep the number of trials in fixation and saccade blocks balanced (see Methods: Data preprocessing). In Spatiotopic and Retinotopic trials (Fig. 1B,C), inducers rotated both before and after subjects made a saccade. The duration of the postsaccadic inducer was of main interest to our analysis, as we wanted to investigate whether the presaccadic inducer affected the strength of the postsaccadic inducer. During the experiment, postsaccadic inducer duration was probed gaze-contingently with 16.7, 33.3 or 50.0 ms, randomly drawn from a uniform distribution. A posteriori, we determined the actual postsaccadic inducer duration with respect to saccade offset, as set by the native Eyelink saccade detection algorithm. In all trial types, the transient was presented immediately after the inducer, and subjects reported whether they perceived a clockwise or counter clockwise jump. These responses were coded with respect to the preceding inducer rotation direction. Forward jumps were coded as 1, backward jumps as − 1. All trials that met our inclusion criteria (see Methods: Data preprocessing) were analysed using a linear logit mixed effects model (Baayen, Davidson, & Bates, 2008; Jaeger, 2008). The reported coefficients are in logits and relative to the baseline level in the model, comprising the Full Match trials with 33.3 ms of inducer.

Baseline High Phi effect

In Full Match trials, subjects fixated a single fixation point, and the positions of the inducer and the transient were fully matched, i.e. both spatio- and retinotopically. Hence, this condition, was very similar to the original paradigm of Wexler and colleagues (Wexler et al., 2013), with the addition of a second static annulus in the periphery. As depicted by the dark striped bars in Figure 2, subjects perceived more backward than forward jumps after an inducer as brief as 33.3 ms (β = -0.44, z = 4.63, p < 0.001), and this bias grew even stronger after 1066.7 ms (β = -1.95, z = 12.54, p < 0.001). Subjects tended to perceive the changing textures (transient) as backward jumps when it was preceded by an inducer of sufficient duration.

Retinotopic reference frame

As was to be expected from motion aftereffect studies (Knapen et al., 2009; Wenderoth & Wiese, 2008), there was a significant bias in perceived jump direction when the inducer was only retinotopically matched to the transient that was presented 33.3 ms after saccade
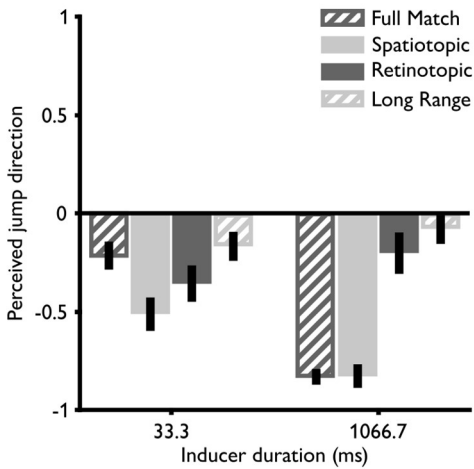
Figure 2. Perceived jump direction in Experiment 1 (error bars represent bootstrapped 95%-confidence intervals of the model estimates). Negative values represent backward jumps, positive values forward jumps (N = 12). In case of the Spatiotopic and Retinotopic trials, inducer duration refers to postsaccadic inducer duration (see Fig. 1 and Table 1). We observed a strong High Phi illusion with Full match trials (dark striped bar at 1066.7 ms of inducer duration). Moreover, the High Phi illusion could be stored retinotopically across saccades, similar to motion after effects (dark solid bar at 33.3 ms of inducer duration). The retinotopic effect faded out at 1066.7 ms of inducer duration, because after saccade execution the Inducer was no longer retinotopically matched with the Transient (see Fig. 1 for description of the trial sequence). Interestingly, the accumulated motion information can also be updated spatiotopically (light solid bar at 33.3 ms of inducer duration). The spatiotopic effect was larger than what was observed in Full match trials (dark striped bar at 33.3 ms of inducer duration) and could not be explained as a long range or decisional bias, since the effect was larger than in the Long Range condition (light striped bar at 33.3 ms of inducer duration).

offset (β = -0.39, z = 2.35, p = 0.019, as compared to the Full Match 33.3 ms condition; Figure 2, dark solid bars). However, this retinotopic effect wears off over time (post-hoc comparison between 33.3 and 1066.7 ms in the Retinotopic trials; β = 0.34, z = 2.16, p = 0.03), most likely because the inducer and the transient are no longer retinotopically matched after the saccade. Indeed, in a control experiment (see Supplementary Figure S1) we showed that the bias in the Retinotopic condition is as strong as in the Spatiotopic condition when the inducer motion is transferred along with the saccade (see Supplementary Figure S2).

Spatiotopic reference frame

Interestingly, beside a retinotopic effect, a spatiotopic effect was observed (Figure 2, light solid bars). Shortly after saccade offset, subjects reported more backward jumps than in the Full Match condition, i.e. when the postsaccadic inducer duration lasted only 33.3 ms (β = -0.69, z = 4.76, p < 0.001). This bias, like the Full Match condition grew stronger over time (post hoc comparison between 33.3 and 1066.7 ms in the Spatiotopic trials; β = 1.24, z = 5.25, p < 0.001), but the difference between a short and long inducer was not as large as in the Full Match trials (β = 0.71, z = 2.51, p = 0.012). In other words, even though the

inducer rotated for 933.3 ms (on average) in the periphery before saccade onset, in Spatiotopic trials the average perceived jump direction after 33.3 ms was not as consistently backward as in the Full Match after 1066.7 ms.

Long range induction of High Phi

To control for potential long range effects in the High Phi illusion, or a decisional bias of a peripheral inducer on the perceived jump direction of a centrally presented transient, we examined the effect of a peripheral inducer per se, that is, without a saccade towards it. In the Long Range condition after 33.3 ms, a bias for backward jumps was observed, not significantly different from the bias observed after 33.3 ms of inducer in the Full Match condition ($\beta = 0.10$, $z = 0.901$, $p = 0.368$; Figure 2, light striped bars). In contrast to the Full Match condition, this bias did not change with longer inducer duration (post hoc comparison between 33.3 and 1066.7 ms in the Long Range trials; $\beta = -0.18$, $z = 1.68$, $p = 0.096$). We re-ran the mixed effects model with the Spatiotopic trials as a reference level to test whether the observed long range effect is statistically different from the observed Spatiotopic effect after 33.3 ms of inducer. This model confirms that the long range effect after 33.3 ms is smaller than in the Spatiotopic condition after 33.3 ms (post-hoc $\beta = 0.79$, $z = 5.45$, $p < 0.001$). The absence of a strong long range effect is indicative for a spatially selective effect of the inducer on the perceived jump direction. The transient and the inducer have to be matched in at least a retinotopic or – and critically – a spatiotopic reference frame in order to effectively induce perceived backward jumps. Together, the results from the Long Range and Spatiotopic condition suggest that a peripherally presented inducer can effectively induce the High Phi illusion but only when the inducer becomes spatially aligned with the transient.

Experiment 2 – Time course of spatiotopic facilitation

In Experiment 1, we showed that the High Phi illusion can be stored retinotopically across saccades, similar to motion aftereffects. In addition, the accumulated motion information can also be updated spatiotopically. The spatiotopic effect is present shortly after saccade offset. In Experiment 2, we addressed whether this observed spatiotopic effect is related to a faster development of the illusion, with respect to the Full Match trials (i.e. an increased effect of inducer duration in Spatiotopic trials) or to a general tendency to observe the transient as backward jumps immediately from the beginning of fixation (i.e. a change in offset in Spatiotopic trials).
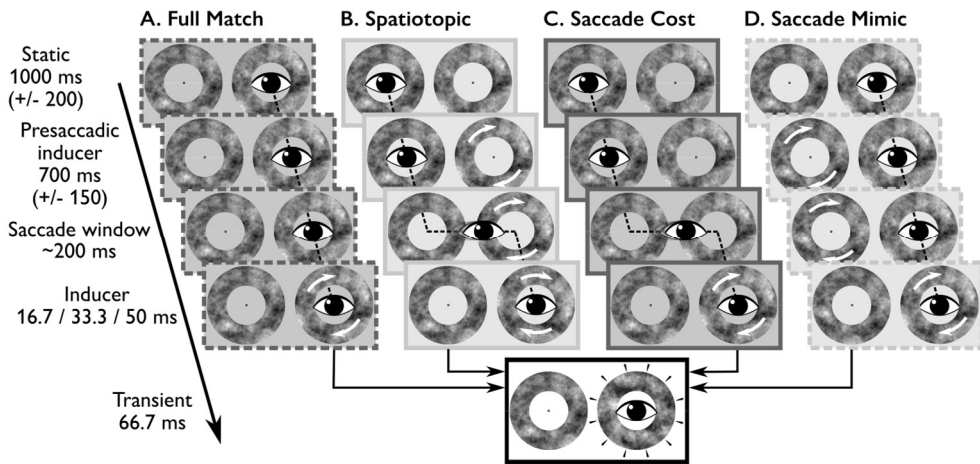
Figure 3. Trial sequences in Experiment 2. The eyes and dotted lines between the eyes depict gaze position. White arrows on the annuli depict rotations of that particular annulus. Like in Experiment 1, all trials started with a period of fixation with two static annuli on screen. **A.** In Full Match trials, subjects remained at fixation with the static annuli for as long as the presaccadic inducer time in Spatiotopic and Saccade Cost trials. After this period of fixation, the Inducer rotated for 16.7, 33.3 or 50.0 ms. In addition, in Full Match trials, the inducer could also rotate for 800 ms. Then, the Transient was presented. **B.** Spatiotopic trials were similar to the Spatiotopic trials in Experiment 1. **C.** In Saccade Cost trials subjects remained fixation and the annuli remained static up until saccade offset. A saccade was executed after an auditory cue. Upon saccade landing, the annulus around fixation started rotating (Inducer), succeed by the Transient. **D.** In Saccade Mimic trials, the retinal input of Spatiotopic trials was mimicked, without the execution of a saccade. The Presaccadic inducer phase consisted of a peripheral rotating annulus and a central static annulus. Then, the peripheral annulus stopped rotating and the central annulus rotated for 16.7, 33.3 or 50.0 ms. In all trial types, the Transient would always be presented around the current fixation point.

The spatiotopic effect in Experiment 1 seemed to be different from a long range or decisional bias, since the observed spatiotopic effect was larger than the long range effect. However, in the Spatiotopic condition, after saccade offset, the postsaccadic inducer and the transient position were fully matched, whereas in the Long Range condition the inducer and the transient were never matched. Hence, we tested the long range effect more conservatively in Experiment 2 (see Methods, Saccade Mimic trials), to further control for a long range explanation of the spatiotopic effect (Morris et al., 2010).

12 different naïve subjects were tested on four different trial types (Figure 3), with a higher temporal resolution with respect to inducer duration. Similar to Experiment 1, there were Full Match and Spatiotopic trials (Figure 3 A/B). Inducer duration was set to 16.7, 33.3 or 50 ms (presented at a 60 Hz refresh rate). In Full Match trials, the inducer could also rotate for 800 ms, in order to obtain a measure of the potency of the High Phi illusion at its strongest. In addition to the Full Match and Spatiotopic trials, we included Saccade Cost
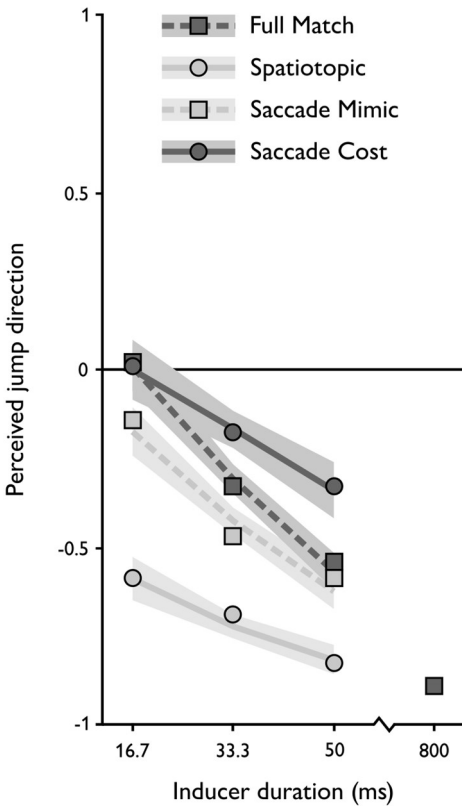
Figure 4. Perceived jump directions in Experiment 2. Positive values represent forward jumps, negative values backward jumps. Lines depict linear interpolation between the estimates of the linear logit mixed effects model. Shaded region represents the bootstrapped 95%-confidence intervals of the model estimates. Bootstrapped averages are depicted by the small dots (N = 12). We observed the rapid induction of the illusion, as illustrated by the slope in the Full Match condition (dark dashed line), similar to the Saccade mimic condition (light dashed line). In the Saccade Cost condition, the illusion developed more slowly over time (dark solid line). In the Spatiotopic condition, the illusion was induced more strongly than in the Full Match condition, even when the transient was presented after only a single frame of the post-saccadic inducer (light solid line). Similarly, in the Spatiotopic condition, the illusion was induced more strongly than in the Saccade Mimic condition (light dashed line), even when the transient was presented after only 16.7 ms of the post-saccadic inducer.

trials to investigate the potential cost of a saccade preceding the transient on the proportion of reported backward jumps (Figure 3C). In these trials, subjects fixated within a static annulus, and made a saccade towards the peripheral annulus, that had also remained static. The inducer started rotating only after the saccade had ended. Hence, the retinal input was essentially similar to the Full Match trials, with the exception that a saccade was made before inducer presentation. The fourth trial type, Saccade Mimic controlled conservatively for long range effects (Figure 3D). In these trials, a peripheral inducer rotated for 700 ms (± 150, uniformly distributed), resembling the peripheral inducer duration in Spatiotopic trials, followed by an additional 200 ms (± 100, uniformly distributed), approximately simulating the saccadic latency and saccadic duration in Spatiotopic trials. Then, the peripheral inducer stopped rotating and the central inducer rotated for 16.7, 33.3 or 50 ms, followed by the transient. As in Experiment 1, we analysed the perceived jump direction as a function of trial type and inducer duration with a linear logit mixed effects model.

Temporal development of High Phi after saccades

The baseline for the development of the High Phi illusion is the effect of 16.7 ms of inducer in the Full Match condition. The rapid induction of the illusion is illustrated by the observed slope in the Full Match condition, along inducer duration (β = -0.65, z = 11.18, p < 0.001; Figure 4, dark dashed line). However, in the same condition, 16.7 ms of inducer was not sufficient to induce a bias for backward jumps (β = 0.02, z = 0.15, p = 0.882). After 800 ms of inducer in the Full Match condition, the average response was -0.89 (± 0.03 s.e.m.) very similar to what was observed in Experiment 1 after 1066.7 of inducer in the Full Match condition (-0.83 ± 0.04 s.e.m.). After a saccade this initial bias was similarly absent (difference between Full Match and Saccade Cost at 16.7 ms of inducer: β = 0.02, z = 0.15, p = 0.878; Figure 4 dark solid line). However, the illusion developed more slowly over time (effect of inducer duration in Saccade Cost, as compared to the effect of inducer duration in Full Match trials: β = 0.27, z = 3.01, p = 0.003), though significantly (post-hoc β = -0.27, z = 3.01, p = 0.003).

Note that both in the Full Match trials (Exp. 1 and Exp. 2) as well as in the Saccade Cost trials, the direction of the perceived jumps is slightly different from the results obtained by Wexler and colleagues (2013). With short inducer durations (16.7 or 33.3 ms) their subjects reported primarily forward jumps, whereas here subjects already had a slight bias to report backward jumps when a transient followed a short inducer. A potential explanation for this difference might be found in the duration of the transient (Wexler, personal communication). In their study, the transient comprised a single change in texture, here, four different textures were used. We used more textures because the perceived jump tends to increase with more different textures (Wexler et al., 2013). However, the transient duration might have also affected the direction of the perceived jump. Yet, given the internal consistency and replication of the High Phi effect in the current study (see Control Analyses and Figure 5b), we believe the results of the Full Match condition can serve as a valid baseline for the Spatiotopic condition.

Temporal development after a saccade with spatiotopic preview

In contrast to the Saccade Cost condition, when a presaccadic Spatiotopic preview of the inducer was provided, the illusion was induced more strongly than in the Full Match condition (Figure 4, light solid line), even when the transient was presented after only 16.7 ms of the post-saccadic inducer (β = -1.33, z = 10.78, p < 0.001). The development of the

illusion (slope) was not significantly different in the Spatiotopic condition, with respect to the slope in the Full Match condition (interaction $\beta = 0.14$, $z = 1.24$, $p = 0.215$).

Long range induction of High Phi

The Saccade Mimic condition was included to provide the most conservative control for the observed spatiotopic effect. In this condition a peripheral inducer rotated for at least 550 ms and was then succeeded by a central inducer of 16.7, 33.3 or 50 ms. In these trials, there was a larger bias than in the Full Match condition after 16.7 ms inducer ($\beta = -0.37$, $z = 3.74$, $p < 0.001$; Figure 4 light dashed line), but the slope was similar to the slope in the Full Match trials ($\beta = 0.10$, $z = 1.17$, $p = 0.242$). We re-ran the model with the Saccade Mimic trials as a reference level to further investigate the long range effects. First, this shows that the initial bias is not only stronger than in the Full Match trials but is actually also statistically different from zero after even 16.7 ms of central inducer (post-hoc $\beta = -0.35$, $z = 2.79$, $p = 0.005$). Second, crucially, the initial bias observed after 16.7 ms of inducer in the Saccade Mimic condition was smaller than in the Spatiotopic condition (post-hoc $\beta = 0.96$, $z = 7.74$, $p < 0.001$).

Control analyses

Decision bias induced by familiarity with the illusion

Beside the aforementioned long range effects, we warranted some additional caution in interpreting the Spatiotopic effect. We suspected that, given the strength of the visual illusion, subjects might have hypothesized that long inducers were always followed by backward jumps. If this were true and subjects were able to identify the inducer direction in the Spatiotopic conditions, they might have based their response on that hypothesis. To control for this effect, we ran another linear mixed effects model (for each experiment separately), where we added a random slope of Trial number within each subject. Trial number corresponded to the actual trial number that was used in the experiment. With likelihood ratio tests, we compared these new models to the original models, where Trial number was not included. Neither in Experiment 1, nor in Experiment 2 did Trial number increase the fit of the models (Exp. 1 $\chi^2(2) = 4.03$, $p = 0.133$; Exp. 2 $\chi^2(2) = 4.73$, $p = 0.094$). Therefore, we conclude that the observed Spatiotopic effect is not likely to be attributable to decision biases related to familiarity with the High Phi illusion.
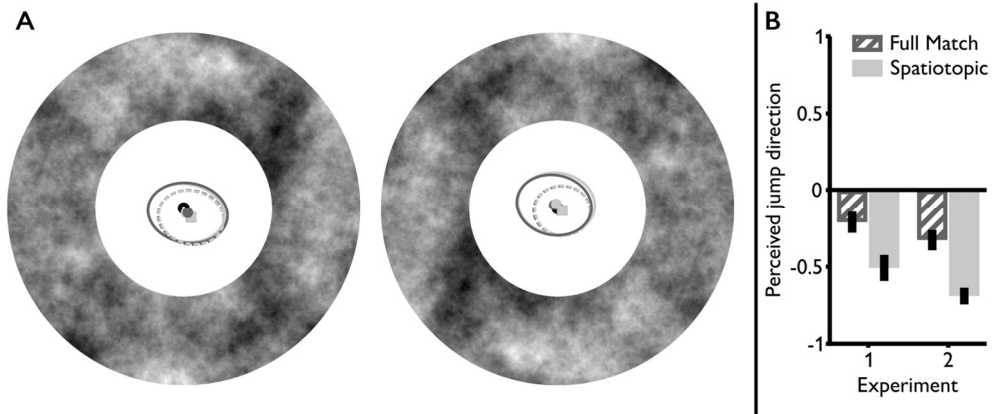
Figure 5. Control analyses. **A.** Ellipses inside annuli represent the area where fixation was during transient presentation on 95% of the trials. Left and Right annuli represent Experiment 1and 2, respectively. The spread of fixation coordinates during transient presentation was larger for trials where subjects made a saccade prior to transient presentation (solid ellipses), than when they maintained fixation (dashed ellipses). **B.** Comparison in average perceived jump direction in Experiment 1 (N = 12) and Experiment 2 (N = 12) after 33.3 ms of (postsaccadic) inducer. The effect of a spatiotopic inducer on average perceived jump direction was stronger in Experiment 2 than in Experiment 1, yet the difference between the bias in the Full Match condition and the Spatiotopic condition was not statistically different between Experiments, even though two different samples were tested.

Gaze position

In both experiments, subjects were required to make a saccade in two conditions, whereas in the other two conditions they could remain stable fixation over the entire course of the trial. First, we analysed the average horizontal gaze positions during the transient across the different conditions. Overall, there was more variability in the conditions with saccades than in the conditions without (Figure 5a and see Supplementary Material online). Next, we analysed the precision of fixation during transient presentation (variance in gaze coordinates during transient) and fixation error (between inducer presentation and transient presentation). When precision and error were included as random effects in our mixed effects models, inferences on the fixed effects did not change (see Supplementary Table S1). The variability in fixation precision and error does therefore not account for the observed differences in perceived jump direction across the different conditions.

Robustness of spatiotopic effect

Figure 5b shows the average perceived jump direction after 33.3 ms of inducer in Experiment 1 and Experiment 2. As can be clearly seen, the Spatiotopic benefit was present

in both experiments, even though two different samples of subjects were used. An additional linear mixed effects analysis with Experiment and Condition as fixed effects and Subject as a random effect was ran to test this. In both samples, there was a bias in the Full Match condition after 33.3 ms of inducer motion (β = -0.45, z = 2.98, p = 0.003), and the bias was stronger in the Spatiotopic condition in both experiments, compared to the Full Match condition (β = -0.69, z = 4.63, p < 0.001). The Spatiotopic was stronger in Experiment 2 than in Experiment 1 (β = -0.64, z = -2.55, p = 0.011). However, the interaction between experimental condition (Spatiotopic and Full Match) and Experiment number was not significantly different (β = 0.37, z = 1.81, p = 0.07). Together, these results show that the trans-saccadic High Phi paradigm as developed in this study yields robust and consistent results across observers.

Discussion

We investigated whether and when presaccadic visual information is integrated with postsaccadic information. Using the fast temporal dynamics of the High Phi illusion, we demonstrated that presaccadically acquired information influences perception immediately after a saccade. We excluded potential long range explanations of this spatiotopic facilitation with several control conditions. Our data support the hypothesis of a perceptual system that uses predictions based on presaccadic information to efficiently process postsaccadic information (Crapse & Sommer, 2008b; Sommer & Wurtz, 2008b). These predicted consequences are commonly thought to enable the cancellation of self-generated changes from external changes in visual input, as observed in saccadic suppression of intrasaccadic displacement paradigms (Bays & Husain, 2007; Bridgeman et al., 1975; Crapse & Sommer, 2012; Currie, McConkie, Carlson-Radvansky, & Irwin, 2000; Deubel et al., 1996). In addition to this cancellation property, our data suggest that the same prediction might also facilitate postsaccadic perception under circumstances where nothing changed externally during the saccade. By actively integrating the prediction (based upon prior presaccadic information) with the postsaccadic information, perception can be accurately biased towards presaccadic input. When the world remained stable across a saccade, this could potentially increase sensory sampling efficiency.

The investigation of the time course of transsaccadic integration has thus far mainly focussed on the pre-saccadic acquisition of feature information (Demeyer et al., 2009; Ganmor et al., 2015; McConkie & Currie, 1996; Oostwoud Wijdenes et al., 2015; Wolf &

Schütz, 2015). One study showed that presaccadic information is integrated with information that is available upon fixation onset, by measuring participant critical spacing on crowding stimuli (Harrison & Bex, 2014). Here, we extend this finding by providing direct empirical evidence that the presaccadically acquired features facilitate postsaccadic perception immediately after saccade offset. This time course is compatible with several reports of early spatiotopic attentional effects briefly after saccade offset (Golomb, Nguyen-Phuc, Mazer, McCarthy, & Chun, 2010; Hilchey et al., 2012; Jonikaitis & Theeuwes, 2013). Our data are in favour of a visual system that seems to anticipate the consequences of an upcoming saccade in order to readily process postsaccadic visual information using that same prediction (Mathôt & Theeuwes, 2011; Melcher & Colby, 2008; Wurtz, Joiner, & Berman, 2011).

It should be noted that in the current study we did not manipulate or highly restrict the time in which the system could build a spatiotopic prediction before saccade onset. Instead, we allowed subjects to view the peripheral rotating inducer for at least 596 ms (945 ms on average). Interestingly, previous studies suggested that constructing a spatiotopic prediction of visual information might actually take approximately 400 ms (Zimmermann, Morrone, & Burr, 2013; Zimmermann, Morrone, Fink, et al., 2013). Here, we did not attempt to investigate the presaccadic build-up of spatiotopic representations. Potentially, saccadic suppression of motion stimuli might reduce the strength of a peripheral inducer when it is only visible shortly before saccade onset, since motion signals are strongly suppressed during saccades (Shioiri & Cavanagh, 1989). On the other hand, rotational motion is used to induce the High Phi illusion, effectively providing motion energy in all directions. This might minimize suppression, because it has been shown that sensitivity for displacements during saccades is primarily reduced on the axis parallel to the saccade, but not so much in orthogonal directions (Bansal, Jayet Bray, Peterson, & Joiner, 2015; Wexler & Collins, 2014). Hence, the paradigm presented here could be a good candidate to investigate the suggested slowly developing spatiotopic representations (Zimmermann, Morrone, Fink, et al., 2013).

Apart from the time course of integration, it is currently also debated exactly which features are updated spatiotopically across saccades. In Experiment 1 we showed that the accumulated motion information can be stored both in a retinotopic and in a spatiotopic reference frame. The storing of motion information in a retinotopic reference frame is a common finding (Knapen et al., 2009; Wenderoth & Wiese, 2008). However, spatiotopic updating of accumulated motion information is controversial. On a behavioural level, one

study showing spatiotopic motion integration (Melcher & Morrone, 2003) has been criticized to lack a strict long range control condition that accounted for the presumed spatiotopic effects (Morris et al., 2010). Here, we carefully controlled for these potential long range effects, and show that despite the presence of a small long range bias, this cannot fully account for the observed spatiotopic updating of accumulated motion information.

Additionally, spatiotopic updating of motion information has previously been investigated using motion after effects (Knapen et al., 2009; Wenderoth & Wiese, 2008). The results of those studies suggested that motion cannot be updated spatiotopically but is strictly represented retinotopically. The retinotopic conditions in Experiment 1 and the control experiment (see Supplementary Information) show that inducer motion energy in the High Phi phenomenon can be similarly accumulated in a retinotopic reference frame across saccades. When the inducer is not rotating retinotopically after the saccade, the effectiveness of the inducer wears off. This might suggest a common mechanism underlying the High Phi phenomenon and motion after effects. However, our findings are in conflict with the conclusion that updating of feature information is restricted to a retinotopic reference frame. Unfortunately, the exact mechanism underlying the High Phi phenomenon remains unknown, so there is no direct explanation why the High Phi illusion can be induced spatiotopically, whereas traditional motion after effects cannot. Hypothetically, High Phi and traditional motion after effects might represent separate phenomena of motion processing. Wexler and colleagues (Wexler et al., 2013) mention two important differences between the High Phi illusion and traditional motion after effects. First, the amplitude of the perceived jump tends to be equivalent to, or slightly exceeding D_{max}, whereas the classical motion after effect tends to have the same amplitude and speed as the inducer (Wexler et al., 2013). Second, the inducer duration can be very brief for the High Phi illusion, whereas in traditional motion after effects, inducers tend to be effective after longer inducer durations, e.g. ±400 ms for rapid motion after effects (Kanai & Verstraten, 2005).

How the effects observed here can be explained at the level of neural systems remains a question for future studies. Spatiotopicity of (population) receptive fields in motion sensitive area MT has been suggested (Crespi et al., 2011; d'Avossa et al., 2007) but debated (Gardner et al., 2008). More in general, the neural mechanisms of transsaccadic integration are still largely controversial. Classical findings of shifting receptive field around the time of saccades have recently been re-investigated. It was originally interpreted that the visual neurons anticipated the consequences of an upcoming saccade by shifting their receptive fields in the direction of the saccade (Duhamel, Colby, et al., 1992). However, recently it

was shown that the receptive fields actually converge towards the saccade target, instead of linearly shifting in the direction of the saccade (Zirnsak et al., 2014). Yet, even more recently, several studies showed at least two different types of shifts in receptive fields: anticipatory vs. memory-based (Inaba & Kawano, 2016; Neupane et al., 2016; Yao, Treue, & Krishna, 2016). Unfortunately, the link between these neurophysiological findings and the observed behavioural effects in transsaccadic integration still remain unknown (Higgins & Rayner, 2015; Marino & Mazer, 2016). We believe the fast temporal dynamics and the robustness of the effects across subjects show that the current paradigm might provide a valuable tool to further investigate the link between perisaccadic neurophysiology and perception.

To conclude, the current experiments show two main findings. First, accumulated motion information can be updated spatiotopically. Second, presaccadically acquired information influences perception immediately upon saccade landing. The fast, or even instant effect of spatiotopically updated information on postsaccadic perception supports the hypothesis that at least the processing of the saccade target is preceded by a forward model aiming at anticipating the consequences of the eye movement (Currie et al., 2000; Miall & Wolpert, 1996; Webb, 2004; Zirnsak & Moore, 2014), where the postsaccadic retinal input is predicted based upon the presaccadic retinal input and the characteristics of the upcoming eye movement (Cavanaugh et al., 2016; Sommer & Wurtz, 2008b).

Methods

Subjects

24 subjects (age 18–29, 4 male) with normal or corrected-to-normal vision participated after giving written informed consent. All were naïve to the High Phi illusion and the purpose of the study. 12 subjects participated in Experiment 1, 12 in Experiment 2. This study was approved by the local ethical committee of the Faculty of Social Sciences of Utrecht University. The approved methods were carried out in accordance with the Declaration of Helsinki.

Setup

Subjects were seated in a darkened room with their heads resting on a chinrest. They were seated 70 cm in front of an LG 24 MB65PM LCD-IPS monitor with a spatial resolution

of 1280×800 pixels and a refresh rate of 60 Hz. All stimuli were created and presented using MATLAB (The MathWorks Inc., Natick MA, 2012) and the Psychophysics Toolbox 3.0 (Brainard, 1997; Pelli, 1997). Eye movements were recorded with an Eyelink 1000 (SR Research Ltd. Ottawa ON; sampling rate of 1000 Hz). The Eyelink was calibrated using the native 9-point calibration routine.

Stimuli

Subject were presented two annuli with different random textures. One annulus was 7.5° visual angle (VA) to the left of screen centre, the other 7.5° VA to the right. The inner radius of the annuli was 3° VA, the outer 6° VA. In the centre of each annulus was a small fixation point (black, diameter 0.4° VA). The textures of the annuli were random black and white pixels, low pass filtered with circular averaging (bandwidth 1.24 cycles per degree VA). To induce the illusion, the annuli rotated at 20°/sec (Inducer). After the inducer, the texture of the annulus was rapidly replaced by a succession of 4 different, random textures (Transient).

Procedure Experiment 1

All trials started with a single fixation point combined with the Eyelink 1000 drift check. A trial started when gaze was closer than 2° to the fixation point and the subject pressed the spacebar. Then, the two annuli appeared, remaining static for 1000 ms (± 200 ms, uniformly distributed). In Full match and Long Range trials subjects were required to maintain fixation over the entire trial, whereas in Spatiotopic and Retinotopic trials subjects made a saccade. Fixation and saccade trials were presented in separate, interleafed blocks. All trials were flagged invalid and repeated at the end of a block when subjects blinked or when gaze deviated more than 3° VA from fixation during the presentation of the (presaccadic) inducer.

Full match

During the presentation of the static annuli, the imminence of the inducer was cued by an auditory beep (261.62 Hz, 50 ms). This beep was not strictly necessary for the task but was included to keep saccade and fixation trials as similar as possible. Inducer onset was delayed with respect to this cue by 300 ms (± 200 ms, uniformly distributed). The inducer rotated for 0, 33.3 1066.7 (60 trials per inducer duration) before transient onset (Fig. 1A).

We were primarily interested in the 33.3 and 1066.7 ms conditions but included the 0 to keep the number of trials in fixation and saccade blocks balanced (see Data Preprocessing).

Spatiotopic match

After 1000 ms (± 200) of static annuli, the peripheral annulus started rotating for 700 ms (Fig. 1B). An auditory cue (440 Hz, 50 ms) instructed subjects to make a saccade to the fixation point at the centre of the peripheral inducer (required saccade amplitude: 15° VA). When gaze was detected within a rectangular area around the peripheral fixation point (width x height: 1° x 4° VA), the inducer kept rotating for an additional 16.7, 33.3 or 50 ms (120 trials) or 1066.7 ms (60 trials) before the transient was presented. We included these 3 possible inducer rotations to obtain a reasonable amount of data points for each participant, when a posteriori computing the postsaccadic inducer duration with respect to saccade offset (see Data Preprocessing).

Retinotopic match

In retinotopic trials, the presaccadic inducer rotated for 700 ms around fixation, followed by an auditory cue (440 Hz, 50 ms) that instructed the subject to make a saccade to the centre of the peripheral static annulus (Fig. 1C). Postsaccadically, the inducer (now peripheral) kept rotating for an additional 16.7, 33.3 or 50 ms (120 trials) or 1066.7 ms (60 trials) before the transient was presented. Then, the transient was presented around fixation. Thus, after the saccade the inducer and the transient were not matched.

Long range

An auditory beep (261.62 Hz, 50 ms) cued the inducer that would be presented 300 (± 200) ms later. The inducer rotated peripherally for 0, 33.3 or 1066.7 ms and was followed by a transient around fixation (Fig. 1D).

Procedure Experiment 2

Full match

These trials were similar to the Full match trials in Experiment 1 (Fig. 3A). However, inducer durations were set to 16.7, 33.3 and 50 ms (60 trials per inducer duration). Additionally, the inducer could rotate for 800 ms to verify the effectiveness of the illusion in each subject (60 trials).

Spatiotopic match

Procedurally similar to the spatiotopic trials in Experiment 1 with two changes (Fig. 3B). However, we only tested postsaccadic inducer duration of 16.7, 33.3 and 50 ms, randomly drawn from a uniform distribution (180 trials), not 1066.7 ms as in Experiment 1.

Saccade cost

These trials were identical to Spatiotopic trials, with the exception that there was no presaccadic inducer (Fig. 3C).

Saccade mimic

After the static annuli, a peripheral inducer rotated for 700 ms (± 150, uniformly distributed), followed by an auditory beep (Fig. 3D). The peripheral inducer kept rotating for an additional 200 ms (± 100 ms), matching the saccadic latencies from Experiment 1. Then, the peripheral annulus stopped rotating and the central annulus rotated for 16.7, 33.3 or 50 ms (60 trials per inducer duration), followed by the transient.

Screening

In order to verify that subjects could reliably report jump directions, each subject completed a screening task prior to the actual experiment. Here, trials were similar to the Full match trials, with the exception that the transient was substituted by an actual clockwise or counter clockwise rotational jump of 15°. Subjects received feedback on their response: fixation point turned green for correct responses, or red for incorrect responses. All participants performed well above chance on this task (average proportion correct: 0.95, range: 0.75 – 1.0).

Data pre-processing

Saccade detection

Saccades were detected offline using the Eyelink velocity-based algorithm, with a velocity threshold of 35°/s and an acceleration threshold of 9500°/s². Trials were only included when saccade onset was > 100 ms, and the amplitude was > 8° VA.

Table 1. Median number of trials per inducer duration in the Saccade conditions, with the minimum and maximum number trials across subjects in parentheses.

Experiment	Condition	Inducer duration in frames (ms)			
		1 (16.7)	2 (33.3)	3 (50)	64 (1066.7)
1	Spatiotopic	–	30.5 (16-38)	–	27 (12-43)
	Retinotopic	–	33 (24-42)	–	27.5 (15-42)
2	Spatiotopic	45.5 (15-67)	49 (34-64)	35.5 (13-56)	–
	Saccade cost	26.5 (11-55)	44.5 (30-57)	39 (19-60)	–

Postsaccadic inducer duration

To compute the number of rotational steps of the postsaccadic inducer in frames with respect to saccade offset, we subtracted the time of saccade offset from the time of transient onset. Differences in the interval [16,32] were considered as a single step, [33,49] as two steps and [50,65] as three steps. This calculation was used in order to analyse identical inducer durations in Saccade and Fixation trials. Additionally, in the Saccade Cost condition, we only included trials where the onset of the postsaccadic inducer started within 100 ms upon saccade offset. The median number of trials per subject, per trial type and per inducer duration in frames (and milliseconds) in Experiment 1 and Experiment 2 are summarized in Table 1. Only trials that included a saccade are represented in the table. The fixation conditions contained at least 46 trials per subject per trial type (60 on average).

Data analysis

Given the imbalance in trial numbers across conditions and subjects we analysed the data using linear logit mixed effects models (Baayen et al., 2008; Jaeger, 2008). In these models we included Condition and Inducer duration as fixed effects. Subjects were modelled as random offsets. Responses were -1 for backward jumps, and 1 for forward jumps. In Experiment 1, condition and inducer duration were modelled as factors, not numerically. Thus, the expected average response of subject j in condition i is given by

$$p_{ij} = \frac{2}{1+e^{-(\beta_0 + \beta_i X + S_j)}} - 1, \text{ where}$$

β_i are the coefficients (with one coefficient for each row in the design matrix, and β_0 is the coefficient in the Full Match condition after 33.3 ms of inducer), X is the full factorial design matrix of Trial type (4 levels), Delay (2 levels) and their interaction, S is the subject-

specific coefficient. In Experiment 1, we did not include 0 ms of inducer because responses are coded with respect to inducer direction. Hence, with no inducer there is no inducer direction to code the responses to. For the analysis of Experiment 2, a similar model was used. However, here Inducer duration was modelled numerically, from 0 to 2, where 0 represents the baseline of 16.7 ms of inducer.

Chapter 2 – Supplementary information

Control experiments

Methods

All included subjects scored at least 75% correct on the screening (as described in the main manuscript). Two additional subjects were tested but failed to reach this inclusion threshold. They therefore did not perform the experimental conditions. Similar to Experiment 1 and 2, all trials started with a single fixation point combined with the Eyelink 1000 drift check and required the subjects to start the trial by pressing the spacebar. Then, the two annuli appeared, remaining static for 800-1000. After that each trial proceeded differently. Trials in the Full Match and Spatiotopic condition were similar to the same conditions in Experiment 1 and 2. 1) Full Match – In these trials, the annuli remained static for another 650-800 ms. Then the auditory beep was played, and 200-300 ms later the inducer was presented. The inducer rotated for 33.3 or 800 ms before transient onset. 2) Spatiotopic – The peripheral annulus started rotating for 650-800 ms. Then the beep was played, and subjects made a saccade towards the rotating annulus. After gaze was detected within a rectangular ROI (1x4° VA) the inducer kept rotating for another 33.3 or 50 ms. A posteriori we determined the actual inducer duration with respect to saccade offset. 3) Purely retinotopic – The annulus around fixation rotated for 650-800 ms. Then the beep was played, and subjects made a saccade towards the rotating annulus. After gaze was detected within a rectangular ROI (1x4° VA) the other annulus, (now around fixation) rotated for 33.3 or 50 ms. The annulus that rotated initially stopped rotating when the other started (Figure S1).

Data preprocessing

After setting transient onset with respect to inducer onset we had on average 20 trials per subject in the spatiotopic condition (range: 17-26) and 20 trials per subject in the retinotopic condition (range: 13-29).
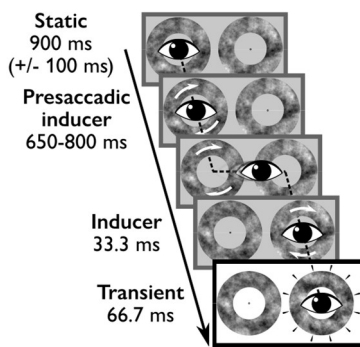
Figure S1. Purely Retinotopic trial. The position of the presaccadic inducer was initially around fixation. After an auditory cue, a saccade was executed and the inducer motion was shifted along with the saccade. After the saccade, the inducer would rotate for another 33.3 ms. Then, the transient was always presented around the last fixation point.

Perceived jump direction

We analysed the effects of condition in the trials with short inducers (33.3 ms) on the perceived jump direction in a linear mixed effects analysis (Figure S1). The reported effects are reported in reference to the Full Match condition. Like in the other experiments, 33.3 ms of inducer was sufficient to produce a bias in perceived jump direction (β = -0.92, z = 5.28, p < 0.001), and this bias was stronger when a spatiotopic preview of the inducer was provided (β = -1.15, z = 4.33, p < 0.001). Moreover, like in Experiment 1, the observed bias was also stronger when a retinotopic preview was provided (β = -1.08, z = 4.11, p < 0.001). There was no significant difference between the Spatiotopic and Retinotopic conditions (β = 0.08, z = 0.22, p = 0.83). To test our hypothesis more directly, we also compared both 'saccade'-conditions to the Full Match trials where the inducer rotated for 48 frames. There was a very strong bias in these Full Match trials (β = -3.32, z = 8.89, p < 0.001), that was stronger than the bias in both the Spatiotopic (β = 1.03, z = 3.10, p = 0.002) and the Retinotopic trials (β = 1.13, z = 3.42, p < 0.001). The difference between the Retinotopic trials and the long Full Match trials might be explained by a potential cost of the intervening saccade.

Control analyses

Fixation position

As can be seen in Figure 5a in the main text, there was more variance in the average fixation positions during transient presentation between the different conditions. We used Levene's test to test the differences in horizontal variance of the average fixation positions. First, we compared the conditions with saccades versus conditions without in Experiment (Full Match and Long Range versus Spatiotopic and Retinotopic). There was more variance in the conditions with saccades ($F(1)$ = 58.03, p < 0.001). However, there was no difference
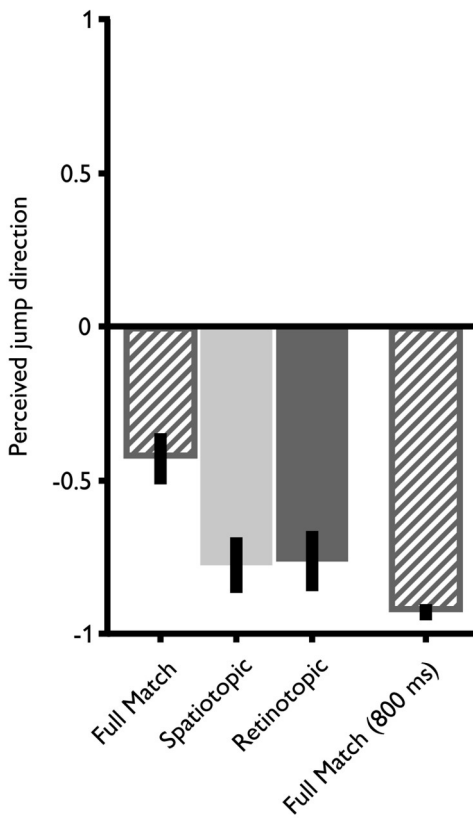
Figure S2. Perceived jump direction in Experiment 3. Error bars represent bootstrapped 95%-confidence intervals of the model estimates. The three left bars, are the average response after 33.3 ms of (post-saccadic) inducer.

2

in the variance of the Full Match and the Long Range condition ($F(1) = 0.01$, $p = 0.91$), nor between the Spatiotopic and the Retinotopic condition ($F(1) = 0.41$, $p = 0.52$). We followed the same procedure for Experiment 2 (Full Match and Saccade Mimic versus Spatiotopic and Saccade Cost). Again, there was a difference between the conditions with and without saccades ($F(1) = 322.96$, $p < 0.001$), but not between the different types of fixation ($F(1) = 0.56$, $p = 0.46$) or saccade conditions ($F(1) = 2.73$, $p = 0.10$). Given the difference in fixation position during the presentation of the transient between the conditions with and without saccade we analysed to more measures of fixation position.

Fixation variance

This is a measure of the stability of fixation. We defined fixation variance as the average distance of raw x-y gaze coordinates from average gaze position during transient presentation (per trial).
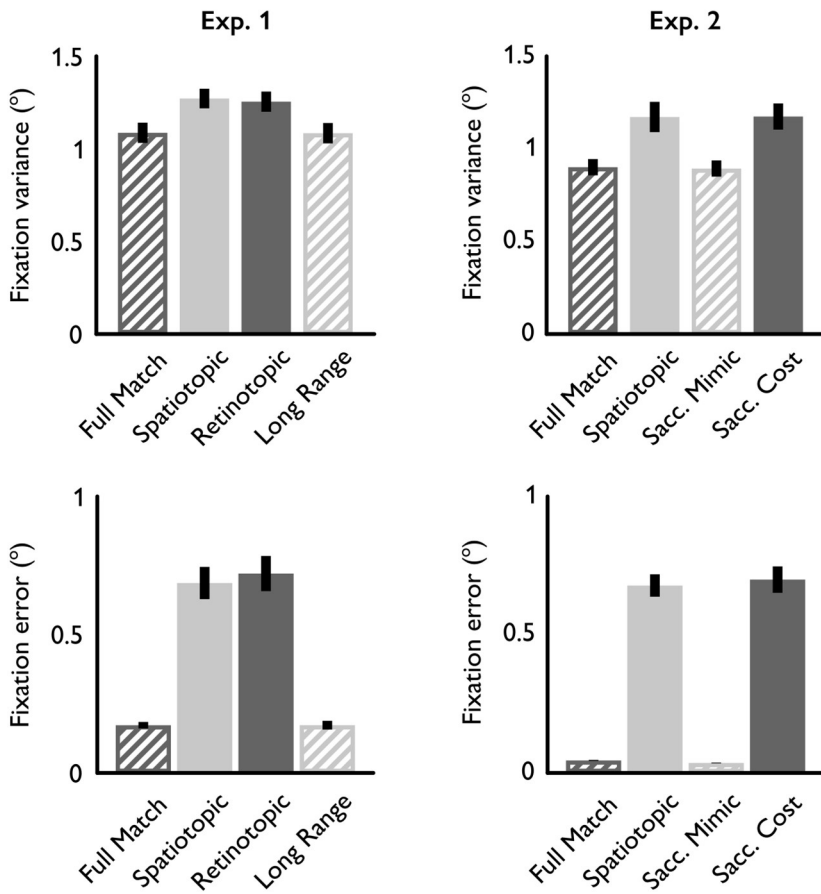
Figure S3. Fixation parameters in Experiment 1 and 2. **Top panels**. Average fixation variance across subjects (± s.e.m.) for the different conditions in Experiment 1 (left) and Experiment 2 (right). This is a measure of the stability of fixation. **Bottom panels.** Average fixation error across subjects (± s.e.m.) for the different conditions in Experiment 1 (left) and Experiment 2 (right). This is measure of the retinal mismatch of the annuli around fixation during the presentation of the (pre-saccadic) inducer and during the transient.

Fixation error

This is a measure of the retinal mismatch of the annuli around fixation during the presentation of the (pre-saccadic) inducer and during the transient. We defined fixation error as the distance between the fixation position during the presentation of the (presaccadic) inducer and the transient. These are positions are taken with respect to the fixation dot.

Experiment 1

Fixation variance (Figure S3, top left)

We constructed linear mixed effects models for the variance in fixation during transient presentation, with condition as a fixed effect and subject as a random effect. The Full Match condition was taken as the reference level. This analysis showed a difference in average spread of coordinates between trials with saccades (Spatiotopic and Retinotopic conditions) and trials without (Full Match and Long Range conditions). The average spread during presentation of the transient was 1.17° VA in the Full Match trials (t = 23.26) and not significantly different from Long Range trials (β = 0.02° VA, t = 0.69). In Spatiotopic trials this spread was 0.18° VA larger (t = 4.87), in Retinotopic trials 0.16° VA (t = 4.49).

Fixation error (Figure S3, bottom left)

Another linear mixed effects model was constructed to analyse fixation error (as defined above), with condition as a fixed effect and subject as a random effect. In Full Match trials there was only a small difference between average fixation position during the inducer and during the transient (β = 0.12° VA, t = 4.63), not significantly different from the fixation error in Long Range trials (β < -0.01° VA, t = 0.59). The fixation error was 0.61° VA larger in Spatiotopic trials (t = 46.41) and 0.67° VA larger in Retinotopic trials (t = 52.08).

Fixation variance and error as random effects

We added random slopes of the trial by trial fixation variance (as defined above) and fixation error (as defined above) within each subject as two random effects to our original logit linear mixed effects model. We compared the models with and without (the original model) with a log likelihood test. The additional random effects did not improve the fit of the model ($\chi^2(5) = 3.22$, p = 0.67).

Experiment 2

Fixation variance (Figure S3, top right)

We followed the same analysis procedure for Experiment 2 as for Experiment 1. This analysis showed a difference in average spread of coordinates between trials with saccades (Spatiotopic and Retinotopic conditions) and trials without (Full Match and Long Range conditions). The average spread during presentation of the transient was 1.00° VA in the Full Match trials (t = 16.12) and not significantly different from Saccade Mimic trials (β = -

Table S1. Comparison of fixed effects in the original model (as used in the manuscript) and with the addition of two random effects: fixation variance and fixation error. Although the model with the two additional random effects fits the data better, the inferences on the fixed effects are similar for both models.

|	Model 1			Model 2		
	response ~ condition * inducer duration + (1|subject)			response ~ condition * inducer duration + (1 + fixation variance + fixation error|subject)		
Fixed effect	β value	z value	p value	β value	z value	p value
Intercept (Full Match)	0.02	0.15	0.882	0.02	0.16	0.876
Spatiotopic	-1.33	-10.78	< 0.001	-1.30	-9.57	< 0.001
Saccade Mimic	-0.37	-3.74	< 0.001	-0.37	-3.75	<0.001
Saccade Cost	0.02	0.15	0.878	0.05	0.43	0.665
Inducer duration	-0.65	-11.18	< 0.001	-0.66	-11.21	< 0.001
Inducer duration:Spatiotopic	0.14	1.24	0.215	0.13	1.20	0.230
Inducer duration:Saccade Mimic	0.10	1.17	0.242	0.10	1.18	0.238
Inducer duration:Saccade Cost	0.27	3.01	0.003	0.27	2.91	0.004

0.02° VA, t = 0.91). In Spatiotopic trials this spread was 0.31° VA larger (t = 11.18), similar to the Saccade Cost trials (β = 0.30° VA, t = 11.01).

Fixation error (Figure S3, bottom right)

In Full Match trials there was only a small difference between average fixation position during the inducer and during the transient (β = 0.04° VA, t = 2.34), not significantly different from the fixation error in Long Range trials (β < -0.01° VA, t = 0.10). The fixation error was 0.70° VA larger in Spatiotopic trials (t = 80.44) and 0.69° VA larger in Retinotopic trials (t = 77.27).

Fixation variance and error as random effects

Again, we added the trial by trial fixation variance and fixation error to our original logit linear mixed effects model of Experiment 2. We compared the models with and without (the original model) with a log likelihood test. In contrast to Experiment 1, the additional random effects did improve the fit of the model ($\chi^2(5)$ = 16.28, p = 0.007). However, inferences based on the estimated parameters stay the same as without the random effects (Table S1).

2
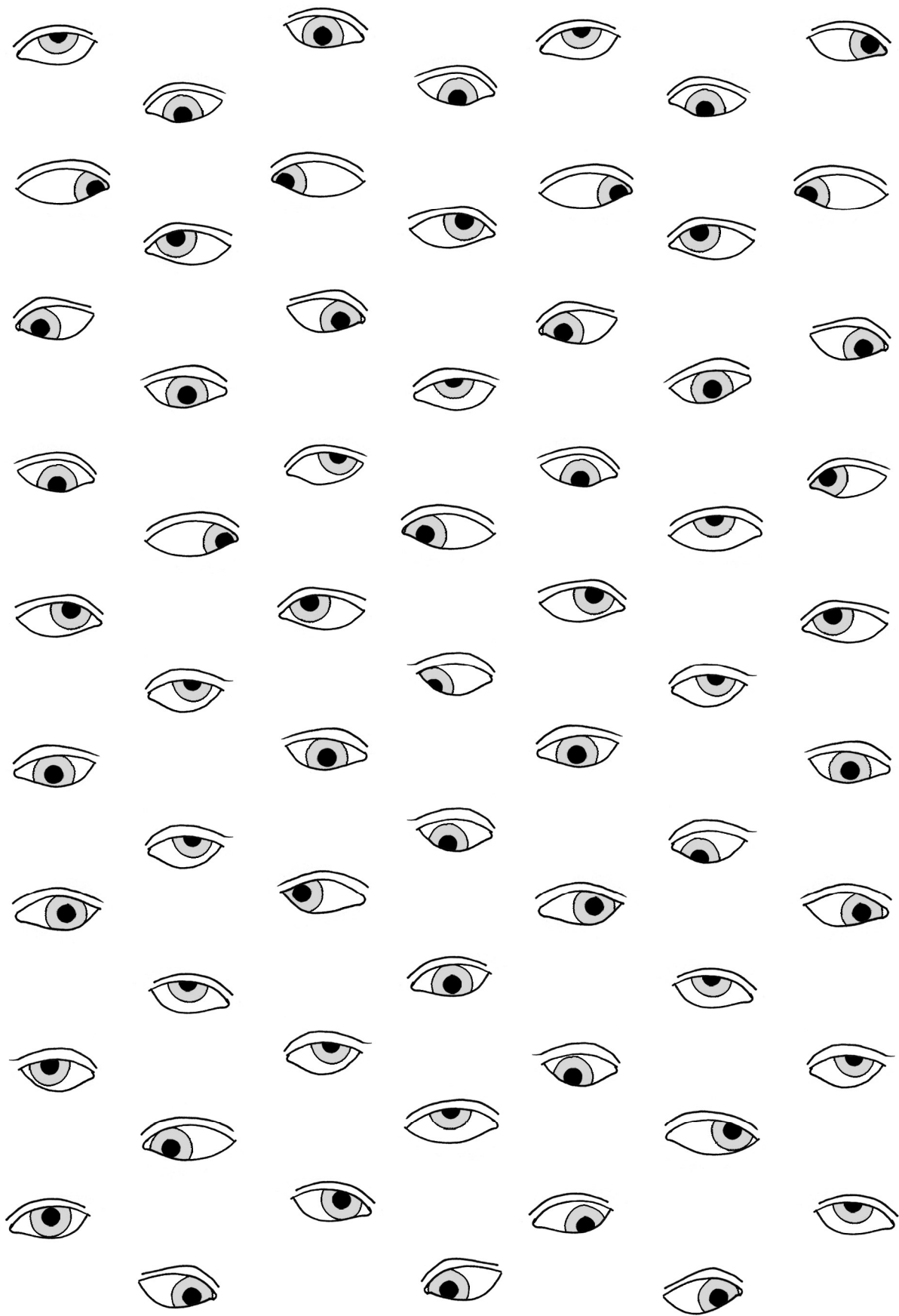
Chapter 3

Time course of spatiotopic updating across saccades

Author contributions

JHF, AF and SvdS conceptualized and designed experiments. JHF programmed the experiments, collected the data and performed analyses. JHF, AF, TCWN and SvdS wrote and revised manuscript.

Abstract

Humans move their eyes several times per second, yet we perceive the outside world as continuous despite the sudden disruptions created by each eye movement. To date, the mechanism that the brain employs to achieve visual continuity across eye movements remains unclear. While it has been proposed that the oculomotor system quickly updates and informs the visual system about the upcoming eye movement, behavioural studies investigating the time course of this updating suggest the involvement of a slow mechanism, estimated to take more than 500 ms to operate effectively. This is a surprisingly slow estimate, because both the visual system and the oculomotor system process information faster. If spatiotopic updating is indeed this slow, it cannot contribute to perceptual continuity, because it is outside the temporal regime of typical oculomotor behaviour. Here, we argue that the behavioural paradigms that have been used previously are suboptimal to measure the speed of spatiotopic updating. In this study, we used a fast gaze-contingent paradigm, using high phi as a continuous stimulus across eye movements. We observed fast spatiotopic updating within 150 ms after stimulus onset. The results suggest the involvement of a fast updating mechanism that predictively influences visual perception after an eye movement. The temporal characteristics of this mechanism are compatible with the rate at which saccadic eye movements are typically observed in natural viewing.

Introduction

Humans sample the visual world by making fast, ballistic eye movements: saccades (Findlay & Gilchrist, 2003). Because acuity is not homogenous across the visual field (Curcio et al., 1990), the fovea is directed to those locations that need to be inspected in closer detail. Saccades are made frequently – roughly every 200 to 300 ms (Fig. 1C) (Henderson & Hollingworth, 1998) – causing stimuli to fall on different locations on the retina several times per second. Still, feedforward processing of visual information in the brain is even faster – it is possible to decode stimulus specific representations within 100 ms after stimulus onset (Carlson, Tovar, Alink, & Kriegeskorte, 2013), and humans can discriminate a peripheral object and make a saccade towards it in 120 ms (Crouzet, 2010; Kirchner & Thorpe, 2006). However, given that the visual system is largely retinotopically organized (Wandell, Dumoulin, & Brewer, 2007), saccades repeatedly create temporal discontinuities and spatial instabilities in the retinotopic representations, posing a problem for continuity in visual processing. Yet introspectively most humans perceive a continuous and stable visual world without these distortions generated by saccades.

How is perceptual continuity established? One prominent hypothesis is that the visual system anticipates the change in sensory input caused by a saccade based on a corollary discharge from the oculomotor system that carries information about the upcoming saccade (Guthrie, Porter, & Sparks, 1983; Sommer & Wurtz, 2008b). Close to saccade onset, a subset of neurons respond to different retinotopic locations than they do under stable fixation (Duhamel, Colby, et al., 1992; Mirpour & Bisley, 2012; Neupane et al., 2016; Walker et al., 1995; X. Wang et al., 2016; Zirnsak et al., 2014). This anticipatory remapping of receptive fields could give rise to a transient non-retinotopic representation called spatiotopic updating (Cicchini, Binda, Burr, & Morrone, 2013; Crapse & Sommer, 2012). Spatiotopic updating has been used to explain both the subjective impression of a continuous stream of visual perception across saccades (Higgins & Rayner, 2015; Melcher & Colby, 2008), as well as the objective psychophysical evidence for trans-saccadic integration of orientation, colour, motion or higher-level features (Demeyer et al., 2009; Fabius, Fracasso, & Van der Stigchel, 2016; Fracasso et al., 2010; Ganmor et al., 2015; Harrison & Bex, 2014; Jüttner & Röhler, 1993; Melcher & Fracasso, 2012; Ong et al., 2009; Oostwoud Wijdenes et al., 2015; Szinte & Cavanagh, 2011; Wittenberg et al., 2008; Wolf & Schütz, 2015; Wolfe & Whitney, 2015; Zimmermann, Weidner, & Fink, 2017). In these studies, a

3

pre-saccadic probe affected perception of a post-saccadic stimulus at the same spatiotopic location.

Because the oculomotor system executes about 3-4 saccades per second, spatiotopic updating should operate within a small time-window to facilitate perceptual continuity across saccades. Within a single fixation, pre-saccadic information should be updated and be available directly after the saccade. Concerning the post-saccadic availability, different experiments demonstrated that spatiotopic updating primarily affects perception immediately after saccades (Deubel et al., 1998, 1996; Fabius et al., 2016; Jüttner, 1997). But concerning the pre-saccadic updating of visual information, spatiotopic representations have been estimated to develop surprisingly slow, requiring fixation durations of more than 500 ms (Nakashima & Sugita, 2017; Zimmermann, Morrone, & Burr, 2015, 2013; Zimmermann, Morrone, et al., 2014; Zimmermann, Morrone, Fink, et al., 2013). This raises a question: if visual processing is fast – content specific representations in 100 ms – and the saccade system is fast – 250 ms between two saccades – why is spatiotopic updating slow?

We hypothesized that the apparent slow speed of spatiotopic updating resulted from the nature and interpretation of the psychophysical tasks that have been used. The tilt aftereffect (TAE) is one such example (Nakashima & Sugita, 2017; Zimmermann, Morrone, Fink, et al., 2013), although updating of the TAE is not without controversy (Knapen et al., 2010; Mathôt & Theeuwes, 2013). The TAE is a perceptual aftereffect where the perceived orientation of a test stimulus is changed after prolonged exposure of another oriented grating, the adapter. When the test stimulus is presented with an orientation away from the adapter, perceptual reports tend to be even further away from the adapter (Gibson & Radner, 1937). Because the TAE is a slow process – still increasing in magnitude after 10 minutes (Greenlee & Magnussen, 1987) – it might not be a particularly sensitive paradigm to investigate fast visual processing across saccades. To investigate spatiotopic updating, the TAE has been tested in a spatiotopic reference frame where a saccade was made between the presentation of the adapter and the test stimulus. The time-course of spatiotopic updating was inferred to take a long time because the TAE increases in strength when saccades were delayed. This increase continues for delays up to 1000 ms. Similar results were obtained for delayed saccades with saccadic suppression of intrasaccadic displacement (Zimmermann, Morrone, & Burr, 2013) and perisaccadic mislocalization (Zimmermann et al., 2015). However, although the effects were strongest for the longest delays, they were already apparent even for short delays. Finally, it should be noted that in most trans-saccadic experiments, like these with the TAE, two essentially different stimuli are presented before

and after the saccade, violating the assumption of a stable, continuous visual world across the saccade. Indeed, psychophysical evidence shows that when visual stimuli are continuous across saccades, observers perceive the continuity, whereas if reliable intra-saccadic changes are made to the stimuli, observers expect stimuli to change during a saccade (H. M. Rao, Abzug, & Sommer, 2016). To study visual continuity, the experimental stimulus should also be continuous (Mirpour & Bisley, 2016).

To test spatiotopic updating within the time-window of 250 ms before saccade onset, we used our recently developed psychophysical, gaze-contingent paradigm (Fabius et al., 2016) with a fast motion illusion: high phi (Wexler et al., 2013). This paradigm allows for the examination of the complete time-course of spatiotopic updating. In high phi, subjects see an annulus with a random low-pass filtered texture. This annulus rotates slowly (inducer), after which its texture is sequentially replaced by four different random textures (transient). This creates an illusory transient percept of a large rotational step in the opposite direction from the preceding inducer. Previous experiments with high phi have shown that high phi can be experienced with inducers as brief as 50 ms (Fig. 1B). In our previous study, we observed that it is possible to induce the illusion in a spatiotopic reference frame, when testing with long inducer previews (>500 ms).

Here, we presented an inducer in the peripheral visual field (inducer preview) and asked subjects to make a saccade to the center of the inducer as soon as it appeared, i.e. visually guided saccades. After the saccade the inducer continued to rotate briefly (post-saccadic inducer), followed by the transient. If the rotational motion of the inducer preview is spatiotopically updated across the saccade, the rotational information of the preview should be added to the rotational information of the post-saccadic inducer, resulting in stronger high phi. Alternatively, if the rotational motion of the inducer preview is not (yet) spatiotopically updated, the strength of high phi is only related to the post-saccadic inducer. To test whether spatiotopic updating can indeed be observed within the temporal regime of visually guided saccades (Henderson & Hollingworth, 1998), we kept the duration of the inducer preview as long as (Experiment 1) or shorter than (Experiment 2) the saccade latencies of our subjects. Thus, we were able to dissociate whether spatiotopic updating itself is slow, or whether updating occurs at a shorter time-scale but previous paradigms were not sensitive to this fast process.
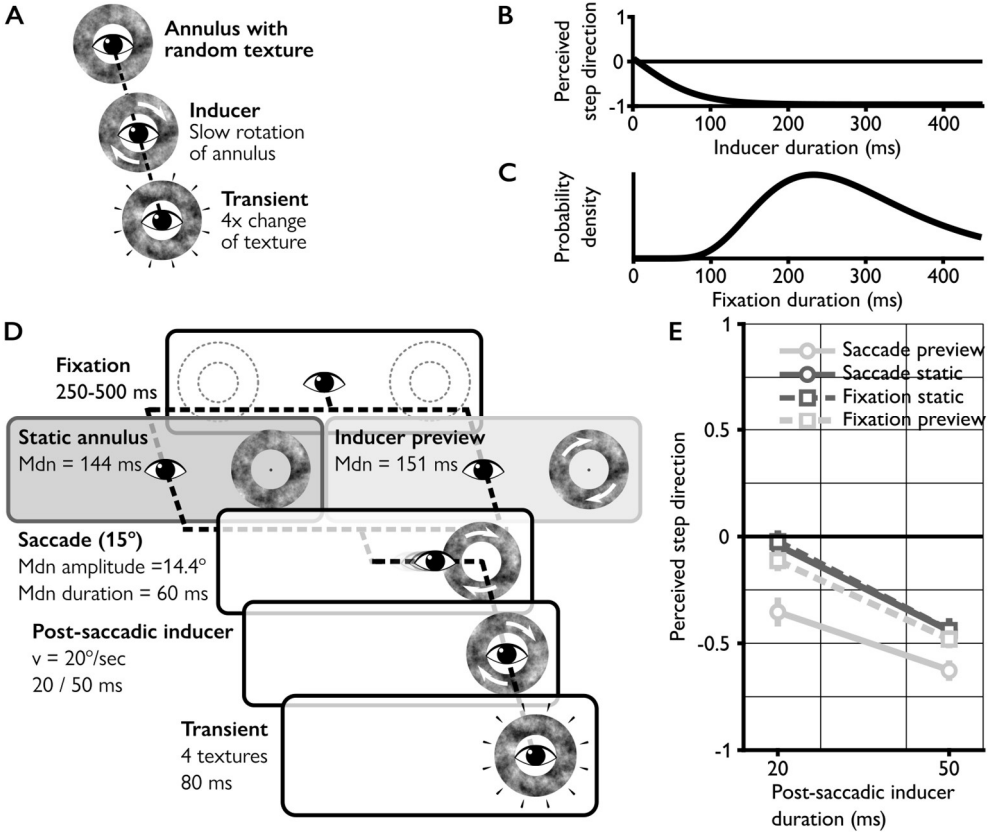
Figure 1. Experiment 1, design and results. **A.** High phi example (48). An annulus of random low-pass filter noise is presented around the point of fixation. The annulus starts rotating slowly (inducer), clockwise (CW) or counter clockwise (CCW). Then, the random noise texture is replaced rapidly by four different textures, 20 ms per texture (transient). The transient induces the percept of a large rotational step in the opposite direction from the inducer. The percept of a backward step is illusory because, on average, the change of textures does not contain global motion in CW or CCW direction. **B.** Perceived step direction with high phi as a function of inducer duration. Observers indicate whether they perceived a CW or CCW step when the transient was presented. Their responses were recoded to forward (1) or backward (−1) with respect to the rotation direction of the preceding inducer. More negative numbers reflect a stronger bias to perceive backward steps, and thus a stronger high phi. High phi increases with longer inducers but is already apparent after brief inducers. **C.** Example distribution of fixation durations in natural viewing tasks (based on ref. 3). Comparing B and C, it can be noted that high phi can be induced within the temporal limits of a typical fixation. **D.** Gaze-contingent conditions in experiment 1. The two conditions proceeded almost identically, with the only exception that the annulus remained static until saccade onset (saccade static, dark grey) or started rotating immediately upon onset (saccade preview, light grey). Subjects maintained fixation until the annuli appeared. The dotted lines in the first panel were not actually visible but merely illustrate that the stimuli could appear at two locations (equal probability). The eye indicates gaze position in each panel. Arrows on the annuli illustrate that the annulus rotated in that phase of the trial. Median saccade parameters in rows 2 and 3 were obtained from the trials that were included in the analysis. **E.** Model estimates of the average perceived step direction, where the error bars represent the 95% CI of the estimates obtained with nonparametric bootstrapping.

Results

Rapid spatiotopic updating

In Experiment 1, we measured the strength of high phi in four conditions (Supplementary Information), two trans-saccadic conditions (Fig. 1D) and two additional conditions where subjects maintained fixation to control for a spatial invariant effect (see next section: Control for spatially invariant effect). The direct test for spatiotopic updating is the comparison between the two trans-saccadic conditions. In the Saccade preview condition, subjects were presented the inducer before saccade onset, whereas in the Saccade static condition, subjects were presented a static annulus before saccade onset. After the saccade the annulus rotated briefly for 20 or 50 ms in both conditions, followed by the transient. Subjects indicated whether they perceived a large clockwise or counter clockwise step. We analysed responses with a logistic linear mixed effects model, with condition and post-saccadic inducer duration as fixed effects. The estimated intercept of the model gives the log odds of the transient being reported as a forward rotational step in the saccade preview condition. The other estimated coefficients (β) are relative to this intercept (Fig. 3A). A negative coefficient indicates a higher probability of perceiving the transient as a backward rotational step.

Longer durations of the post-saccadic inducer lead to more frequent percepts of backward rotational steps ($\beta = -0.36/10$ ms, 95%-CI = [-0.41, -0.31], $F(1,7957) = 80.98$, $p < 0.001$). This shows that high phi rapidly increases in strength with longer inducers, similar to previous the results of previous experiments (Fabius et al., 2016; Wexler et al., 2013). Importantly, if the inducer is previewed in the periphery before saccade execution (Saccade preview, Fig. 1E, light solid line), high phi is stronger than in the Saccade static condition after the saccade (Fig. 1E, dark solid line; $\beta = 0.63$, 95%-CI = [0.33, 0.91], $F(1,7957) = 17.54$, $p = 0.001$). The preview effect can be interpreted as a spatiotopically transferred effect of the inducer preview: the visual system updated the location of the rotating inducer to a spatiotopic reference frame before the saccade. As a result, the inducer preview and the post-saccadic inducer jointly biased perception after the saccade, inducing a stronger high phi. We estimate that the preview resulted in an approximate 17.5 ms (95%-CI = [10.7, 27.3] ms) 'head start' in visual processing after saccades with latencies of 150 ms, by taking the ratio of the coefficient of the Saccade static condition ($\beta = 0.63$) and the coefficient of the post-saccadic inducer ($\beta = -0.36/10$ ms). This preview effect generalizes to annuli that

3

cover different and more peripheral portions of the visual field (inner, outer radius = [2.6, 5.0]° and [6.0, 9.25]°), as observed in a control experiment with different subjects (Supplementary Information).

Control for spatially invariant effect

The observed spatiotopic preview effect could potentially be explained by a general, spatially invariant induction of high phi. Such an effect should also be observed without the execution of a saccade. Therefore, we measured high phi in two conditions without saccades, where subjects maintained fixation at the center of the screen and either an inducer (Fixation preview) or static annulus (Fixation static) was presented in the periphery before the annulus was presented around fixation (Fig. S1; Supplementary Information). The results of the Fixation preview (Fig. 1E, light dashed line) condition demonstrate that a spatially invariant effect cannot fully account for the observed spatiotopic effect, because the illusion was less strong in the Fixation preview condition than in the Saccade preview condition (β = 0.37, 95%-CI = [0.11, 0.63]; $F_{(1,7957)}$ = 10.13, p = 0.006). However, high phi in the Fixation preview condition was slightly stronger than in the Fixation static (Fig. S1A) condition ($F_{(1,7957)}$ = 7.85, p = 0.015). In short, we observed a limited spatially invariant effect, but this cannot fully account for the trans-saccadic preview effect.

Duration of pre-saccadic preview and strength of post-saccadic bias

In Experiment 1, the inducer preview biased post-saccadic perception of the same stimulus when it was presented in the same spatiotopic location. In general, the strength of high phi depends on inducer duration. We examined whether the strength of the preview effect similarly depends on preview duration. In Experiment 1, the duration of the inducer preview coincides with saccade latency. We constructed a second mixed effects model, using only data from the Saccade preview condition. Preview duration and post-saccadic inducer duration were fixed effects, and we included random effects per subject for the fixed effects and inducer rotation direction. We compared this model to a null-model without a fixed effect for preview duration. Preview duration did not improve the model fit ($\chi^2(1)$ = 0.82, p = 0.36), so it seems that the preview effect was not modulated by preview duration. However, if the preview effect is perceptual in nature it should be related to the strength of the preview. To test the limits of the preview effect, in Experiment 2 we uncoupled preview duration and saccade latency for even shorter preview durations than in Experiment 1.
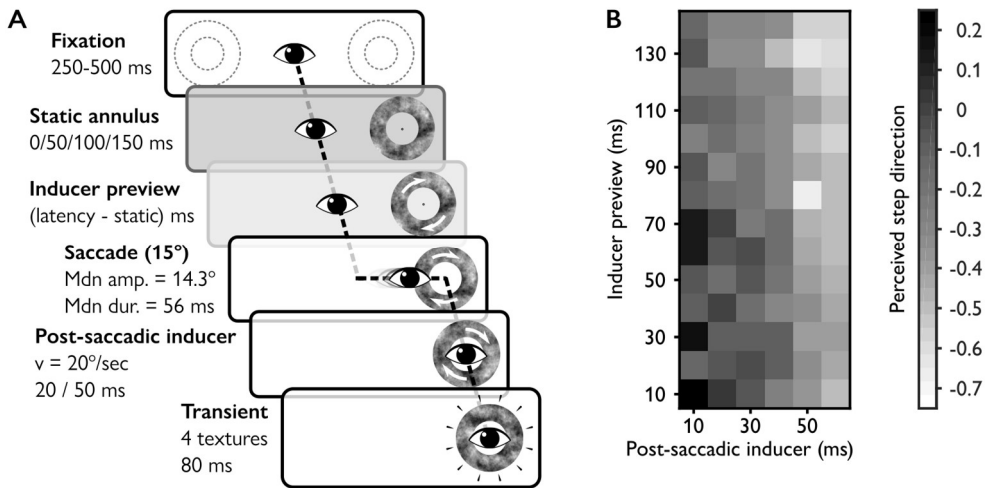
Figure 2. Experiment 2, design and results. **A.** Subjects fixated a fixation target for 250 ms to 500 ms. An annulus appeared in the periphery. The annulus remained static for 0, 50, 100, or 150 ms, and then started rotating. The annulus continued to rotate throughout the saccade and 20 or 50 ms after (post-saccadic inducer). If subjects moved their eyes before the annulus started rotating, it started rotating when gaze was detected >3° away from the fixation target. After the postsaccadic inducer, the texture of the annulus was replaced by four different, random textures (20 ms per texture). Subjects indicated whether they perceived the change in textures as a step in CW or CCW direction. Responses were recoded to "backward" and "forward" with respect to the rotation direction of the preceding inducer. **B.** Estimated perceived step direction from the mixed effects model as a function of inducer preview (y axis) and postsaccadic inducer (x axis). Brighter grey values indicate more frequent percepts of backward steps. The range of the colormap goes from 0.25 to −0.75.

In Experiment 2, each preview consisted of a mixture of a static annulus followed by an inducer preview (Fig. 2A; Supplementary Information). The data were analysed with a mixed effects model, with fixed effects for preview duration and post-saccadic inducer duration and random effects per subject. The model with preview duration as a fixed effect was a better fit for the data than the model without it ($\chi^2(1)$ = 8.99, p = 0.003). In this model, a longer preview duration results in more frequent percepts of a backward step (Fig. 2B; β = -0.05/10 ms, 95%-CI = [-0.07, -0.02], F(1, 3799) = 13.99, p < 0.001). In addition to the effect of the inducer preview, the post-saccadic inducer also induced a strong bias, similar to Experiment 1 (β = -0.30/10 ms, 95%-CI = [-0.35, -0.25], F(1, 3799) = 91.90, p < 0.001). The estimated coefficients are displayed in Fig. 3B. In sum, both in Experiment 1 and 2 we observed spatiotopic updating within 150 ms after stimulus onset. Moreover, the duration of the preview increases the strength of the spatiotopic effect.
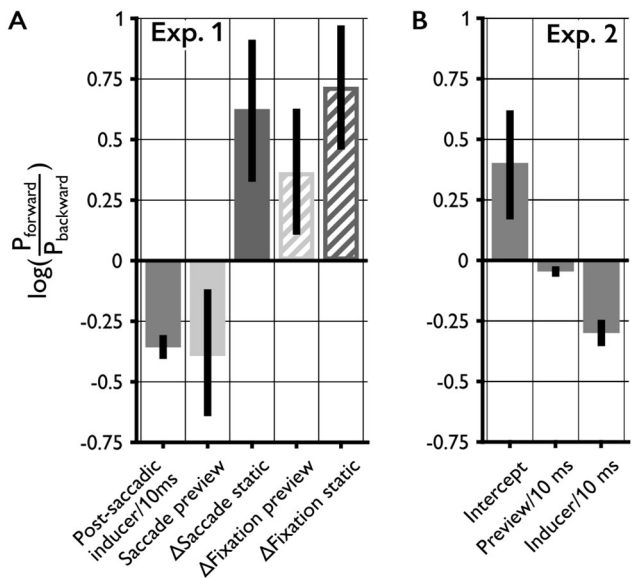
Figure 3. Bootstrapped coefficient estimates of the mixed effects model from experiment 1. (**A**) and experiment 2 (**B**). Estimates are obtained with non-parametric bootstrapping (2,000 samples). Error bars represent empirical 95% CI of the coefficient estimates. In experiment 1, the coefficient estimates of saccade static, fixation preview, and fixation static are relative to the saccade preview condition. In experiment 2, the intercept refers to trials with 10 ms of preview and 10 ms of inducer.

Discussion

We examined spatiotopic updating of visual information across saccades. The current experiments demonstrate a fast updating mechanism in the visual system that predictively influences perception after an eye movement. We observed a direct link between post-saccadic perception and the strength of the pre-saccadic stimulus for stimuli that covered the parafovea after a saccade – in a control experiment (Supplementary Information) we also observed this link for larger stimuli (inner, outer radius = [6.0, 9.25]°), in the same eccentricity range typically used in spatiotopic updating experiments (~5 to 10 degrees in the periphery). The time-scale on which this link is established is compatible with typical fixation durations observed in natural viewing (Henderson & Hollingworth, 1998) and represents a behavioural index of spatiotopic updating expressed as a perceptual bias in the direction of the pre-saccadic visual information, comparable to a 17.5 ms head start in visual processing.

The current study differs in two important aspects from the studies with tilt-adaptation to assess the time-course of spatiotopic updating (Nakashima & Sugita, 2017; Zimmermann, Morrone, et al., 2014; Zimmermann, Morrone, Fink, et al., 2013). First, the stimulus we used to assess spatiotopic updating is fast in nature. High phi can be induced in the order of tens

of milliseconds, whereas tilt adaptation is typically induced in the order of hundreds of milliseconds (Greenlee & Magnussen, 1987). Second, the stimulus feature that had to be updated (inducer rotation direction) was stable and continuous across saccades, enabling the assessment of perceived visual continuity in an environment where the assumption of continuity across saccades is true (Mirpour & Bisley, 2012; H. M. Rao et al., 2016).

Rapid spatiotopic updating is plausible when considering the speed of processing in the human visual system, which contains stimulus specific representations rapidly after stimulus onset – in the order of 100 ms – as demonstrated in psychophysical studies (Crouzet, 2010; Kirchner & Thorpe, 2006) and neuroimaging studies (Carlson et al., 2013). This rapidly acquired information is used by the visual system to predict the sensory changes induced by saccades. It facilitates post-saccadic visual processing by anticipating the post-saccadic retinal input based on pre-saccadic input (Herwig, 2015). Three fMRI studies support this idea by showing spatiotopic and feature-specific repetition suppression (Dunkley et al., 2016; Fairhall et al., 2017; Zimmermann, Weidner, Abdollahi, & Fink, 2016). Repetition suppression in neurophysiological measures is observed when the same stimulus is presented twice (Grill-Spector, Henson, & Martin, 2006). Hence, repetition suppression in spatiotopic coordinates can be interpreted as a neurophysiological measure of the visual system regarding the post-saccadic stimulus to be 'the same' as the pre-saccadic stimulus, even though it was presented at different retinotopic coordinates. Although these effects are in line with the current findings, the time-scale of fMRI studies is limited by the slow blood-oxygen level-dependent response. Interestingly, a recent EEG study provides more direct neurophysiological correlate of our behavioural findings (Edwards et al., 2018). Edwards and colleagues used time-resolved decoding of a post-saccadic stimulus while varying the correspondence between the pre- and post-saccadic stimuli. The post-saccadic stimulus could be decoded faster when it matched the pre-saccadic stimulus than when it was different from the pre-saccadic stimulus. This indicates that information about the pre-saccadic stimulus affects the neural responses to the post-saccadic stimulus in a way that suggests more efficient processing when the two stimuli match. The current results show that this fast facilitation in post-saccadic visual processing is not only reflected in neurophysiological measures but can be quantified in human behaviour.

Still, although we observed spatiotopic updating on a short time-scale, we would not generalize the results to all stimuli in the visual field. The reason for this caution is that while there is ample evidence in favour of spatiotopic updating of visual information, there are also studies that fail to observe this with either behavioural measures (Knapen et al., 2009,

3

2010; Mathôt & Theeuwes, 2013) or with fMRI (Lescroart et al., 2016). One important restriction on spatiotopic updating seems to be that it is limited to attended stimuli, passive visual stimulation does not automatically result in spatiotopic updating (Melcher, 2009; Mirpour & Bisley, 2016). The introspective feeling of visual continuity thus could arise from a match between the predicted post-saccadic retinal image and observed retinal image of an attended stimulus (Cavanagh et al., 2010; Herwig, 2015).

Predicting upcoming stimuli is a fundamental characteristic of the brain, as stated by theories of predictive coding (R. P. N. Rao & Ballard, 1999). Anticipating the consequences of an upcoming saccade is a frequently recurring example of a scenario where the principles of predictive coding are applied (Friston, Adams, Perrinet, & Breakspear, 2012; Spratling, 2017; Vetter, Edwards, & Muckli, 2012). This anticipation could be implemented as a forward model (Crapse & Sommer, 2008b), where a corollary discharge from the oculomotor system enables the dissociation between internal and external changes in retinal input (Cavanaugh et al., 2016). Here, we observed effects of a spatiotopic prediction on post-saccadic perception within the temporal regime of the typical latencies of visually guided saccades. With these findings, rapid spatiotopic updating of visual information is a plausible mechanism that contributes to perceptual continuity across saccades in natural viewing.

Methods

Subjects

52 subjects (age: M = 22.6, range = [18,37], 26 female) with normal or corrected-to-normal acuity participated after giving written informed consent (N = 20 in Experiment 1, N = 12 in Experiment 2, N = 20 in Supplementary Information, Control Experiment). The sample size of Experiment 1 was based on the effect sizes of our previous study with high phi (Fabius et al., 2016). The sample size in Experiment 2 was lower because we planned to make fewer statistical comparisons with fewer experimental conditions. This study was approved by the local ethical committee of the Faculty of Social Sciences of Utrecht University. All subjects were naïve to high phi prior to the experiments and completed a screening procedure (Supplementary Information, screening) to ensure they could reliably report the motion direction of a rotating annulus. Moreover, we verified whether subjects perceived backward steps with high phi after a long inducer (500 ms; Supplementary

Information, screening; Fig. S2). One subject was excluded from the dataset of Experiment 1 because of a failure to meet this criterion (Supplementary Information, preprocessing).

Setup

Stimuli were displayed on a 48.9° by 27.5° Asus RoG Swift PG278Q, an LCD twisted nematic monitor with a spatial resolution of 52 pixels/° and a temporal resolution of 100 Hz (AsusTek Computer Inc., Taipei, TW). The ultra low motion blur backlight strobing option of the monitor was enabled (maximum pulse width) for higher temporal precision (Zhang et al., 2018). Eye position of the left eye was recorded with an Eyelink 1000 at 1000 Hz (Sr Research Ltd., Mississauga, ON, Canada). The eye-tracker was calibrated using a 9-point calibration procedure. All stimuli were created and presented in MATLAB 2016a (The Math Works, Inc., Natick, MA.) with the Psychophysics Toolbox 3.0 (Kleiner, Brainard, & Pelli, 2007) and the Eyelink Toolbox (Cornelissen, Peters, & Palmer, 2002). Visual onsets and eye-movement data were synchronized using photodiode measurements (Supplementary Information, synchronization).

Stimuli

Stimuli were annuli (inner radius ≈ 3°, outer radius ≈ 6°) with random greyscale textures, created by low pass filtering random black (0.09 cd/m^2) and white (88.0 cd/m^2) pixels with a pillbox average (radius = 1.24°). For rotating annuli, the rotational velocity was 20°/sec. Fixation targets were black dots (radius ≈ 0.2°) with a grey point in the center (radius ≈ 0.075°). All stimuli were presented on a uniform grey background (44.1 cd/m^2). We tested the spatial generalizability of the preview effect observed in Experiment 1 by repeating the saccade conditions using stimuli with different radii (Supplementary Information).

Analysis

Before the statistical analysis, eye movement data were pre-processed (Supplementary Information, preprocessing) and visual onsets were aligned to the eye movement data based on photodiode measurements (Supplementary Information, synchronization; Fig S5). We analysed the perceived step direction (i.e. the probability of a 'forward step' response: $p_{forward}$) with a logistic linear mixed effects model (Bates, Mächler, Bolker, & Walker, 2015). $p_{forward} = \frac{2}{1 + e^{-(X\beta + Zy)}} - 1$, where X is the design matrix, β is a vector with the fixed effects coefficients, Z the random effects design matrix and y the random effect coefficients. All

estimates of fixed effects coefficients are reported relative to the intercept condition, here the Saccade preview condition with an inducer of 10 ms (Fig. 1D). In Experiment 1, the mixed effects model contained fixed effects of inducer duration and condition, and random effects of inducer duration, condition and inducer rotation direction per subject (Supplementary Information, statistics Exp. 1). Condition was modelled as a categorical variable and inducer duration as a continuous variable. We only allowed inducer durations between 10 and 60 ms. We did not include the interaction between condition and inducer duration because a model comparison showed that, all other things kept equal, the interaction did not improve the model ($\chi^2(3) = 4.16$, $p = 0.245$). We compared conditions among each other with planned contrasts. Reported p-values for planned contrasts are corrected with the Holm-Bonferroni method (Holm, 1979). In Experiment 2, the model contained fixed effects for pre-saccadic inducer duration and post-saccadic inducer duration, and random effects of pre-saccadic inducer duration, post-saccadic inducer duration and rotation direction per subject (Supplementary Information, statistics Exp. 2). Both inducer durations were modelled as continuous variables. We used non-parametric bootstrapping to obtain 95%-confidence intervals of the estimated fixed effects coefficients. 2000 bootstrap samples were constructed by stratified sampling from the original dataset, with stratification according to the fixed effects but not the random effects. Trials were sampled with replacement. Bootstrapped coefficient estimates and 95%-confidence intervals are displayed in Fig. 3. Individual variation across these estimates are displayed in Fig. S3.

Saccade latencies

We set out to investigate spatiotopic updating across saccades unconstrained latencies. Saccade latencies in natural viewing conditions are typically around 250 ms (Henderson & Hollingworth, 1998). In Experiment 1, the average median saccade latency was 146 ms (range = 111-177 ms across subjects). In Experiment 2, the average median saccade latency was 136.8 ms (range = 112-178 ms across subjects).

Chapter 3 – Supplementary information

Experimental Procedures

Experiment 1

With Experiment 1 we tested the hypothesis that visual information can be spatiotopically updated in a time window as short as the saccade latency. Subjects performed a gaze-contingent version of the high phi illusion (Fig. 1D). Each trial started with a drift check of 500 ms at the central fixation target (target radius ≈ 0.2°, radius of ROI for fixation control = 3°), followed by an additional fixation period of 250-500 ms. Then, an annulus with a random texture appeared, with its center 15° either to the left or to the right of the fixation target (equal probability). Subjects made a saccade to the center of the annulus. To increase the variability of the saccade latencies, we varied the synchrony of stimulus onset and fixation target offset with gaps of -150, 0 or 150 ms, taking advantage of the gap-effect (Saslow, 1967). Saccades were slower with longer temporal overlap (Fig. S4). Importantly, before the saccade was executed, the annulus was either static (Saccade static) or rotated with 20°/s (Saccade preview). In case of the Saccade static condition, the annulus started rotating during the saccade, i.e. as soon as gaze position was ≥3° away from the initial fixation target. The annulus rotated for another 20 or 50 ms after saccade offset (the post-saccadic inducer), i.e. when gaze was detected within ≤2° of the saccade target. Then, the texture of the annulus was rapidly replaced by four different random textures (20 ms/texture). Subjects indicated whether they perceived a rotational step clockwise or counter clockwise (2AFC). Responses were recoded to forward (1) and backward (-1) with respect to the rotation direction of the preceding inducer. Trials were presented in 12 blocks of 48 trials, where the following factors were presented factorially in random order within a block: preview (static/inducer), post-saccadic inducer duration (20/50 ms), inducer rotation direction (CW/CCW), saccade direction (L/R) and gap duration (-150/0/150 ms).

Subjects also performed two control conditions in separate blocks to test whether high phi can also be induced for a transient around fixation but with an inducer in the periphery. In these conditions we matched the visual input as close as possible to the saccade conditions while subjects maintained fixation during the whole trial (Fig. S1A). Subjects were presented a fixation target in the center of the screen. After 250-500 ms of stable fixation, an annulus with a random texture appeared in the periphery, at the same location as in the

Saccade conditions. Again, this peripheral annulus was either static (Fixation static) or rotated with 20°/s (Fixation preview). For each trial, the duration of the peripheral annulus was sampled from the distribution of saccade latencies that were collected in the saccade conditions. The distributions were estimated via non-parametric kernel density estimation, bounded on the closed interval [80, 500] ms. This sampling procedure was performed per individual subject, to match the durations of visual input between conditions with and without saccades as accurately as possible (Fig. S1B). Next, the peripheral stimulus disappeared, and the screen was blank (apart from the central fixation point) for a duration that was sampled from the smoothed distribution of saccade durations in the conditions with saccades. This sampling procedure was similar to the aforementioned sampling procedure, with the difference that it was bounded on the closed interval [20, 80] ms (Fig. S1C). The blank was followed by an annulus presented around the central fixation target. This annulus had the same random texture as the peripheral annulus and rotated for 20 or 50 ms (akin to the post-saccadic inducer in the conditions with a saccade). Then, the texture was replaced by four other random texture (20 ms/texture), after which subjects gave their response. In the Fixation static condition, we implemented an additional 'post-saccadic inducer' duration of 500 ms, to test whether a long, and therefore strong, inducer reliably induces the high phi illusion in every subject. We used the Fixation preview condition to test for a spatially invariant effect of the inducer. Blocks with and without saccades were interleaved. Before the start of the experiment, subjects practiced one block with and one without saccades. For the actual experiment subjects completed 6 blocks of the Fixation conditions and 12 blocks of the Saccade conditions.

Experiment 2

The data from Experiment 1 show that even within a time window as brief as the latency of a visually guided saccade, pre-saccadic perception of a stimulus biases post-saccadic perception of the same spatiotopically localized stimulus. With Experiment 2 we examined whether the duration of the pre-saccadic preview affects the strength of the post-saccadic bias. As suggested previously, spatiotopic updating might become detectable with behavioural measures only when sufficiently long saccade latencies are allowed. Here, we worked the other way around, where we tried to minimize the observed spatiotopically induced bias, since we already observed a bias with short saccade latencies. Therefore, we decoupled saccade latency and preview duration in Experiment 2 by making each preview a mixture of a static preview followed by an inducer preview. Yet note that under natural viewing conditions, the preview duration is as long as the saccade latency (like in Experiment

1). The task in Experiment 2 was similar to Experiment 1. However, rather than being presented with either a static preview or an inducer preview (Experiment 1), subjects were presented with a mixture of both (Fig. 2A). Specifically, when the annulus appeared in the periphery, it started rotating after a delay 0, 50, 100 or 150 ms. Again, subjects were instructed to make a saccade to the center of the annulus immediately after the onset of the annulus. Thus, the total inducer preview duration was determined both by the saccade latency of the subjects and the rotation delay of the stimulus and continued rotating for either 20 or 50 ms after saccade offset. Additionally, subjects performed trials where they maintained fixation, and the inducer and transient were presented around the fixation point. These trials included no peripheral inducers. Subjects practiced one block of the Saccade condition, and one block of the Fixation condition. In the actual experiment, subjects completed 6 blocks of 24 trials of the Fixation condition and 24 blocks of 32 trials of the Saccade condition.

Screening

Long inducers – The high phi illusion is a subjective, non-random interpretation of a random stimulus: the direction of the transiently changing textures is interpreted as a large rotational step in backwards direction with respect to the preceding rotational motion. To make sure the illusion could successfully be induced in all subjects, we verified the perceptual interpretation of the transient after a long inducer (500 ms) in the Fixation static conditions in both experiments. An inducer of 500 ms should evoke a strong percept of a large backward step (cf. Wexler et al. 2013; Fabius et al. 2016). Subjects would be excluded when their binomial confidence interval would include 0, i.e. no clear sign of a successfully induced high phi illusion with a strong inducer. All but 1 subject reliably reported backward jumps with this long inducer (Fig. S2). One subject was excluded from the analysis based on this criterion (Subject 19 in Experiment 1).

Large physical step – Because the high phi illusion is a subjective measure, we verified whether subjects were able to accurately dissociate the direction of a physical rotational step – i.e. not illusory – from the rotation direction of a slowly rotating inducer. All subjects performed a screening experiment prior to the main experiment. In the screening, subjects fixated a fixation target on the left (-10°), center (0°) or right (10°) side of the screen. A static annulus appeared after 500 ms of stable fixation at the fixation target (i.e. all recorded gaze samples were within 3° of the fixation target). The annulus remained static for 600 ms, and then rotated clockwise or counter clockwise for 1000 ms., akin to a long inducer in the
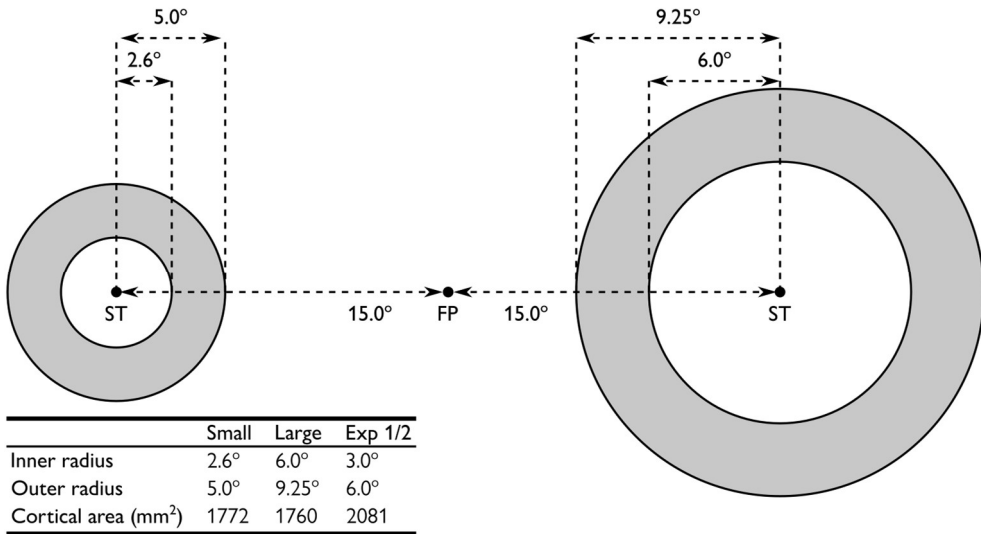
	Small	Large	Exp 1/2
Inner radius	2.6°	6.0°	3.0°
Outer radius	5.0°	9.25°	6.0°
Cortical area (mm²)	1772	1760	2081

Figure C1. Design of the control experiment. The size of the stimulus was changed with respect to Experiment 1 and 2. One annulus had a slightly smaller inner and outer radius than the annulus used in Experiments 1 and 2, and the other annulus had an inner radius that was similar to the outer radius as the annulus in Experiment 1 and 2. The surface of these two annuli were roughly comparable when accounting for the cortical magnification factor, although smaller than the stimuli used in Experiment 1 and 2. FP = initial fixation point. ST = saccade target, only one saccade target and stimulus would be shown on each trial. Stimulus sizes were counterbalanced across screen sides.

high phi illusion. Rotational velocity was 20°/sec, i.e. rotational steps of 0.2° presented at 100 Hz (the refresh rate of our monitor). After the rotation, the annulus made a rotational step of 12° and stopped rotating. Subjects indicated the direction of the large step by pressing the left arrow ('counter clockwise') or right arrow ('clockwise'). The direction of the large step, the direction of the preceding rotational motion and the location were counterbalanced over 36 trials (3 repetitions per combination). To assess accuracy, we computed the proportion correct responses over all trials. Every subject performed well above chance level (p = 0.5) in Experiment 1 (M = 0.95, range = 0.81-1.00) and Experiment 2 (M = 0.97, range = 0.75-1.00).

Control experiment

Introduction

To investigate spatiotopic updating for more peripheral targets we decided to test the preview effect from Experiment 1 with stimuli of different sizes. The rationale here is that although the annuli in Experiment 1 are not stimulating the fovea after the saccade – and
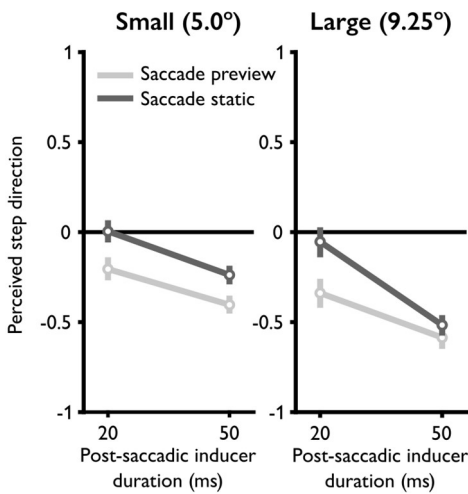
Figure C2. Model estimates of the average perceived step direction, where the error bars represent the 95%-CI of the estimates obtained with non-parametric bootstrapping. The perceived step direction became more biased to backward steps with increased post-saccadic inducer duration both for the small and the large annulus. Additionally, there was a stronger bias in the Saccade preview condition (light grey) than in the Saccade static condition (dark grey), for both annulus sizes.

3

so do not coincide with the saccade target – they are closer to the fovea (inner radius of the annulus = 3°) than typically seen in similar experiments on spatiotopic updating, which is usually between 5 and 10 degrees. In this control experiment, we used annuli with different radii than in Experiment 1, one smaller (inner radius = 2.6°, outer radius = 5°) and one larger (inner radius = 6°, outer radius = 9.25°). It is important to remark that the eccentricity range for the large annulus lies in the same eccentricity regimes typically seen in spatiotopic updating experiments (5-10 degrees in the periphery). Most importantly, the larger annulus' distance from the initial fixation point and the saccade target is almost the same on the vertical midline of the screen, i.e. the retinal stimulation before and after the saccade was parafoveally (Wandell, 1995). See Figure C1 for an illustration of these sizes. When accounting for the cortical magnification factor, the surface of these two sizes was roughly equal, although smaller than the surface of the stimuli in Exp. 1 and Exp. 2.

Methods

We repeated the Saccade conditions from Experiment 1, i.e. 50% of trials contained a preview of the inducer before saccade onset, on the other 50% the inducer was static until the saccade had started. Additionally, the annulus could be large or small. Within a block of 64 trials, all unique combinations of preview (with/without), annulus size (small/large), saccade direction (left/right), rotation direction (cw/ccw) and inducer duration (20/50 ms) were repeated twice. Subjects completed 15 of these blocks. Additionally, before the Saccade conditions, subjects completed 3 blocks of a Fixation condition, where subjects
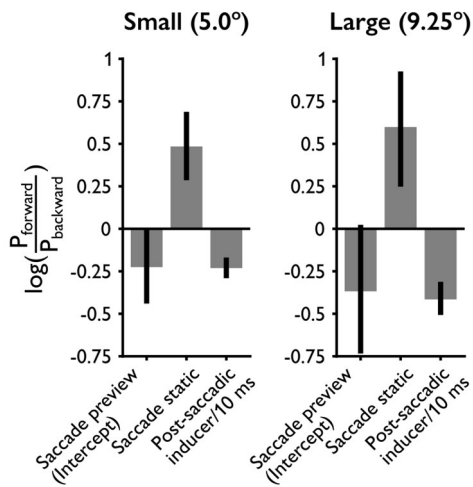
Small (5.0°)   Large (9.25°)

Figure C3. Bootstrapped coefficient estimates of the generalized linear mixed effects model from trials with a small annulus (left panel) and trials with a large annulus (right panel). Estimates are obtained with non-parametric bootstrapping (2000 samples). Error bars represent empirical 95%-confidence intervals of the estimated coefficients. The estimated coefficients of the 'Saccade static' conditions are relative to the 'Saccade preview' conditions in each panel. The bias to backward steps is observed in the Saccade preview condition is larger than in the Saccade static for both the small and the large annulus.

were required to maintain fixation at a fixation point (either on the left or right side of the screen, similar to the locations used in the Saccade conditions). The High phi illusion was then presented around that fixation point. Each block in the Fixation condition consisted of 48 trials. Similar to Exp. 1 and Exp. 2, we only included participants who scored above chance level on a screening test, where we presented an inducer of 1 s, followed by a physical step of 12°. Next, we only included data in the analysis from participants who reliably reported backward jumps after a long inducer (500 ms) in an additional Fixation condition. 2/20 subjects were excluded based on the second criterion. Additionally, we applied the same inclusion criteria that are summarized in the Supplementary Information (Preprocessing). In Exp. 3, the 95th percentile of saccade latencies (inclusion criterion 6) was 480 ms, and the 2.5th and 97.5[th] percentiles of the manual response times were 310 and 1413 ms. Analysis of the data was identical to the analysis of Experiment 1. We analysed the data for the small and large stimuli separately with generalized linear mixed effects models. These models had the same fixed and random effects structure as the model that was used to analyse Exp. 1. With these models, we performed non-parametric bootstrapping to obtain 95% confidence interval of the fixed effect coefficients and model predictions.

Results

The average median saccade latencies in trials with the small annulus was 161 ms (range = 117-261 ms), and 164 ms in trials with the large annulus (range = 119-276 ms). Both for the small and the large annulus, the perceived step direction became more biased to

backward steps with increased post-saccadic inducer durations (small annulus: β = -0.23, 95%-CI = [-0.29, -0.16], $F_{(1, 4953)}$ = 90.58, p <0.001; large annulus: β = -0.42, 95%-CI = [-0.51, -0.31], $F_{(1, 3640)}$ = 88.15, p <0.001). So, for both annulus sizes, the High phi illusion could reliably be induced. Regarding the preview effect for the small annulus, the observed bias in the Saccade Static condition was smaller than in the Saccade Preview condition ($\Delta\beta$ = 0.48, 95%-CI = [0.29, 0.69], $F_{(1, 4953)}$ = 5.48, p = 0.019). Similarly, for the large annulus the observed bias in the Saccade Static condition was also smaller than in the Saccade Preview condition ($\Delta\beta$ = 0.60, 95%-CI = [0.25, 0.93], $F_{(1, 3640)}$ = 7.20, p = 0.007). To estimate the size of the preview benefit in time we took the ratio between the effect of the post-saccadic inducer per 10 ms and the difference between the Saccade static and Saccade preview conditions. For the small annulus this preview benefit is 20.9 ms (bootstrapped 95%-CI = [11.6, 32.2] ms), for the large annulus this is 14.3 ms (bootstrapped 95%-CI = [7.4, 24.6] ms). See Figure C2 for an illustration of the estimated perceived step direction per condition and per inducer duration for the two different annulus sizes. See Figure C3 for the bootstrapped model estimates.

Discussion

In this control experiment, we replicated the spatiotopic preview effect from Experiment 1. Moreover, we measured and observed spatiotopic updating of the inducer effect for an annulus that was presented in the peripheral, parafoveal visual field. This larger annulus stimulated peripheral parts of the visual field in which previous effects of spatiotopic updating have also been observed. These findings demonstrate that rapid spatiotopic updating can be observed at different locations than the saccade target.

Data analysis

Preprocessing

We only included subjects who could reliably report the direction of rotational steps in the screening (Experiment 1: N = 20/20, Experiment 2: N = 12/12) and whose responses showed a successful induction of the high phi illusion in trials with a long inducer (500 ms) in the Fixation static condition (Experiment 1: N = 19/20, Exp. 2: N = 12/12). One subject (Experiment 1) was excluded because she did not report significantly more backward steps when the high phi illusion was presented with this long inducer (Fig. S2). Even though our paradigm was gaze-contingent, we determined post-saccadic inducer durations offline. Saccades were detected offline using the native SR Research saccade detection algorithm.

The timing of the onset of the stimuli was determined by the timestamps in the Eyelink datafile, corrected for the input lag of 11 ms of the monitor, as measured with a photodiode (Supplementary Information, Synchronization). Next, we only included trials in the analysis where A) the primary saccade had an amplitude > 12°, B) the primary saccade started and ended within 2° of the fixation points (or, in case of Fixation conditions, where the median gaze position over 50 ms after preview onset and inducer onset was within 2° of the fixation points), C) the primary saccade started before the gaze-contingent onset (at least 10 ms), D) the primary saccade ended after the gaze-contingent onset (at least 10 ms), E) the primary saccade had a minimum latency of 80 ms after stimulus onset, F) the primary saccade had maximum latency no higher than the 95th percentile of all saccades that were included after applying criteria 1 to 4 (Experiment 1: 320 ms, Experiment 2: 242 ms), G) where the manual response time was within the 2.5th and 97.5th percentile of all the trials after applying criteria 1 to 4 (Experiment 1: 331-1244 ms, Experiment 2: 320-1240 ms), H) where the post-saccadic inducer duration was in the closed interval [20, 60] ms in Exp. 1, or [10, 60] in Exp. 2. Another inclusion criterion in Experiment 2 was that the inducer preview duration had to be in the closed interval [10, 140] ms. With these criteria we included 7962 trials in Experiment 1 (42.9% of all trials) and 5436 trials in Experiment 2 (49.7% of all trials). For the main analysis of Experiment 2, only the trials from the saccade condition were used (3802 trials, 41.3% of all saccade trials).

Synchronization of visual onsets and eye-movements.

Introduction

For the analysis of the reported experiments, we synchronized eye-movement data from the Eyelink data file (EDF) with stimulus onset (as determined by the timestamps in the EDF). During the experiments, timestamps were sent to the EDF immediately after PsychToolbox reported that the vertical retrace had started. That is, we used the function Eyelink('Message') immediately after using Screen('Flip'). With these timestamps in the EDF, we determined in which trials our online-gaze contingent algorithm performed correctly (e.g. starting the rotation of the inducer during the saccade rather than after the saccade in the Saccade static condition). Hence, to ensure that we only included trials where the stimulus was indeed rotating before the saccade had ended, we only included trials where the time difference between the timestamp of the onset of the inducer and the offset of the saccade was larger than 10 ms (i.e. the duration of 1 frame at 100 Hz). This criterion was also applied to Induce Preview trials. Thus, we entered only those trials in the analysis

where the gaze-contingent onset was at least 10 ms before the offset of the saccade. This method of synchronizing stimulus presentation with eye movement data is only valid if the timestamp in the EDF was indeed synchronized with stimulus onset. However, this is most likely not the case for most LCD monitors because they suffer from input lag (a delay introduced in the hardware of the monitor). To accurately synchronize eye movement data and visual stimulation we measured the input lag of our monitor with a photodiode that was fed directly into the printer port of the Eyelink host PC.

Methods

We used a photodiode (sampling rate = 10 kHz) connected to an Itsy Bitsy microcontroller board (Adafruit Industries, New York City, NY). The output of the Itsy Bitsy was sent to the parallel port (printer port) of the Eyelink host PC, to the 11th pin ('busy' pin). With a custom-written MATLAB script, using the Psychophysics toolbox and Eyelink toolbox, we changed the luminance of the screen every frame. We tested 4 transitions from full dark to 25%, 50%, 75% or 100% luminance. Luminance thresholds for the output were set to 80% of the required luminance level in a given measurement. After the script commanded a luminance change (with the Psychophysics toolbox's Screen('Flip') function) a message was sent to the Eyelink data file (using the Eyelink toolbox's Eyelink('Message') function). Simultaneously, we recorded the output of the photodiode directly into the Eyelink data file. We should note that our LCD monitor uses a feature that is not common in all LCD monitors, called 'ultra low motion blur' (ULMB). With ULMB turned on, the backlight of the LCD panel is strobing at the same rate as the refresh rate of the monitor, in our case 100 Hz (see Fig. S5 for measurements made with oscilloscope). This makes the monitor effectively similarly suited for visual psychophysics as traditional CRT monitors, as recently described by Zhang and colleagues (2018). Because the backlight is strobing, this means that a transition from 100% bright to 50% bright is in fact a transition from 100% to 0% to 50% luminance. We made several photographs from measurements with an oscilloscope to demonstrate this feature of the screen (Figure S6). Given that the screen is always dark between two frames, and the photodiode is a binary signal, we can only consider changes from dark to a certain luminance value. For each luminance level, we reversed the luminance 2000 times (i.e. 1000 from bright to dark and 1000 from dark to bright). We compared the differences between the timestamp of the message and the time of change in photo diode output.

Results and discussion

There was a consistent delay of 11.0 ms (s.d. = 0.5 ms) between the timestamp and the time of contrast reversal as measured with the photodiode (Fig. S6A). This is numerically similar to the input lag measured by Zhang and colleagues (Zhang et al., 2018). The delays were similar across different vertical locations. To correct for the measured input lag, we added 11 ms to all the timestamps in the EDF that indicated the onset of a visual stimulus before we performed our analyses and before we applied the in/exclusion criteria to individual trials. Timings of post-saccadic inducer onsets over eye-positions are visualized in Fig. S6B.

Statistics Experiment 1

We analysed the responses from Experiment 1 with four factors in the following model, with a logit link function. The analysis was run in MATLAB 2016a, with the 'fitglme' function from the Statistics package.

Model structure

Experiment 1 was designed to test for effects of post-saccadic inducer duration and differences in offset between conditions. Thus, we constructed a mixed model with two fixed effects, one for condition and one for post-saccadic inducer duration. For completeness, we compared the model with these fixed effects against two alternative models with different fixed effects (see below). For the random effects, we allowed the size of the fixed effects to vary across subjects, because in most psychophysical experiments the effect sizes can vary across observers. Additionally, we added a random effect of rotation direction that we allowed to vary per subject. This third random effect was included to dissociate a perceptual bias from a response bias. There is a two stage rationale for this. First, the number of trials per rotation direction could not be balanced a priori, because the trial exclusion based on saccade parameters was performed post-hoc. Second, theoretically, subjects could have a default response of, for example, pressing the 'right' button. If a subject with such a bias would also have more trials – after trial exclusion – with counter clockwise rotations, it would seem as though this subject would have a perceptual bias for reporting backward steps, whereas in fact he was just pressing the same button and hence a response bias. We account for this possibility by adding a random effect of rotation direction to vary per subject.

Formula

response ~ condition + inducer + (1 + condition + inducer + rotation | subject)

Factors

	Factor	Class	Levels	Code
0	Response	Categorical	backward	0
			forward	1
1	Condition	Categorical	saccade preview	0
			fixation static	1
			fixation preview	2
			saccade static	3
2	Post-saccadic inducer duration	Continuous	20 ms	0
			⋮	⋮
			60 ms	5
3	Inducer rotation direction	Categorical	clockwise	0
			counter clockwise	1
4	Subject	Categorical	1	1
			⋮	⋮
			19	19

Model comparison

The design of the model for the analysis of Experiment 1 was defined by our experimental questions. However, we did examine whether adding an interaction term to the model would improve the fit. In addition, as a sanity check we compared our model against a model with the same random effects, but without any fixed effects.

Final model

response ~ condition + inducer + (1 + condition + inducer + rotation | subject)

Interaction model

response ~ condition * inducer + (1 + condition + inducer + rotation | subject)

Null model

response ~ 1 + (1 + condition + inducer + rotation | subject)

Final model vs. Interaction model

Theoretical Likelihood Ratio Test

Model	DF	AIC	BIC	LogLik	LRStat	deltaDF	pValue
finalModel	26	8775	8956.5	-4361.5			
interactionModel	29	8776.8	8979.3	-4359.4	4.155	3	0.2452

Final model vs. Null model

Theoretical Likelihood Ratio Test

Model	DF	AIC	BIC	LogLik	LRStat	deltaDF	pValue
nullModel	22	8795.5	8949.1	-4375.8			
finalModel	26	8775	8956.5	-4361.5	28.543	4	9.6774×10^{-6}

Bootstrapped GLME estimated coefficients

Coefficients obtained with non-parametric empirical bootstrapping. For the bootstrapping procedure we randomly sampled an equal number of responses per inducer duration per condition as in the original model (i.e. stratification over the fixed effects), without stratifying over the random effects (i.e. subject and rotation direction). Thus, for each sample we had 7962 observations, and we re-fitted our original model with these random sample of trials. This sampling and re-fitting was repeated 2000 times. To obtain confidence intervals on the estimated coefficients, we calculated empirical confidence intervals. That is, taking the difference between the original model estimates and all the bootstrap estimates: $\delta = b_{bootstrap} - b_{model}$. The bias-corrected estimate of a given coefficient is defined as $b = b_{model} - \delta_{0.5}$, and the 95% confidence interval is [$b_{model} - \delta_{0.025}$, $b_{model} - \delta_{0.975}$].

Planned comparisons between conditions

All estimated coefficients in the mixed effects model of Experiment 1 are relative to the Fixation static condition with a post-saccadic inducer of 20 ms. However, to answer all our experimental questions we also compared conditions among each other with planned comparisons. The reported p-values are Holm-Bonferroni corrected for multiple comparisons. Stars indicate a significant difference with an alpha of 0.05.

Comparison	Fstat	Pvalue
Saccade preview vs. Fixation static	$F(1,7957) = 36.80$	$p < 0.0001^*$
Saccade preview vs. Fixation preview	$F(1,7957) = 10.13$	$p = 0.0059^*$
Saccade preview vs. Fixation static	$F(1,7957) = 17.54$	$p = 0.0001^*$
Fixation static vs. Fixation preview	$F(1,7957) = 7.85$	$p = 0.0153^*$
Fixation static vs. Saccade static	$F(1,7957) = 0.90$	$p > 0.05$
Fixation preview vs. Saccade static	$F(1,7957) = 2.14$	$p > 0.05$

Statistics Experiment 2

Final model

> response ~ preview + inducer + (1 + preview + inducer + rotation | subject)

Interaction model

> response ~ preview * inducer + (1 + preview + inducer + rotation | subject)

Null model

> response ~ inducer + (1 + preview + inducer + rotation | subject)

Final model vs. Interaction model

Theoretical Likelihood Ratio Test

Model	DF	AIC	BIC	LogLik	LRStat	deltaDF	pValue
finalModel	13	4041.0	4122.2	-2007.5			
interactionModel	14	4040.6	4128.0	-2006.3	2.3889	1	0.1222

Final model vs. Null model

Theoretical Likelihood Ratio Test

Model	DF	AIC	BIC	LogLik	LRStat	deltaDF	pValue
nullModel	12	4048.0	4122.9	-2012			
finalModel	13	4041.0	4122.2	-2007.5	8.9919	1	0.0027
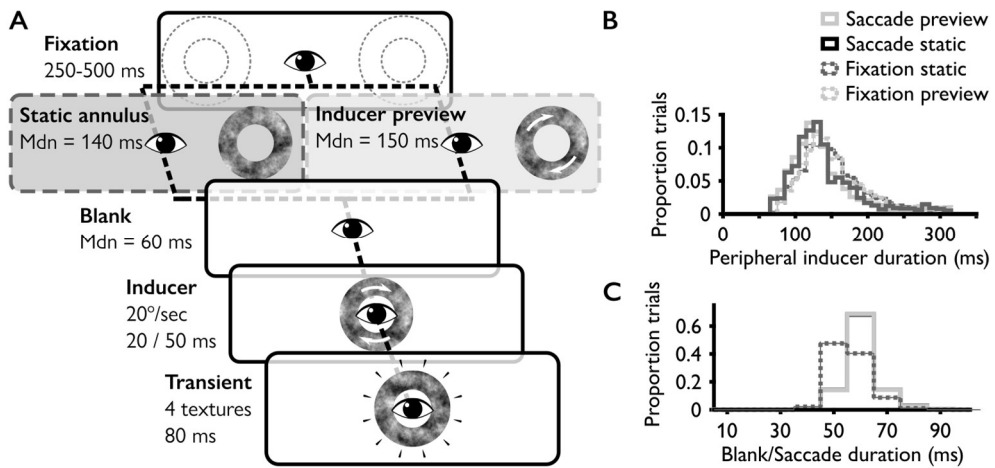
Figure S1. A. Experiment 1, control conditions. The visual input from the experimental saccade conditions was mimicked as close as possible, without the execution of a saccade. The two control conditions proceeded almost identically, with the only exception that the peripheral annulus (panel 2) remained static (Fixation static) or rotated (Fixation preview). Subjects maintained fixation at a fixation target in the center of the screen over the entire course of a trial. The dotted lines in the first panel were not visible but merely illustrate the stimuli could appear at two locations (equal probability). The eye indicates required gaze position in each panel. Arrows on the annulus illustrates that the annulus rotated in that phase of the trial. Median duration of the peripheral stimulus (panel 2) and the blank (panel 3) were sampled from the saccade parameters from the experimental conditions. **B.** Histogram with durations of peripheral preview in control and experimental conditions from Experiment 1. The duration of the peripheral inducer in the control conditions (dashed lines) was sampled online from the distribution of saccade latencies (for each subject individually. Durations of the saccade latencies (solid lines) are corrected for the delay between timestamp and visual onset. **C.** Histogram with the durations of the blanks in the control conditions (dashed lines) and saccade durations (solid lines) in the experimental conditions. The duration of the blank in the control conditions was sampled from the distribution of the saccade durations in the experimental conditions.
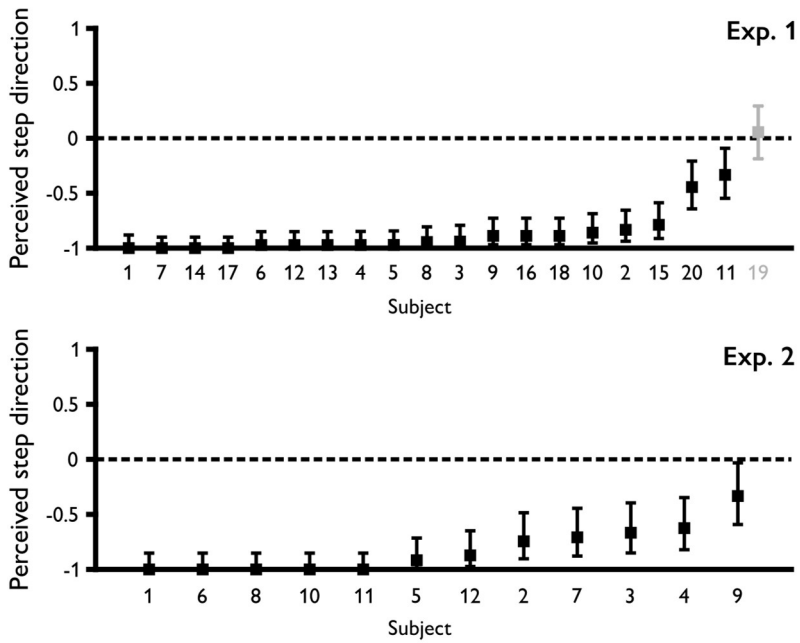
Figure S2. Perceived step direction in the Fixation static condition with an inducer duration of 500 ms. Upper panel Experiment 1. Lower panel Experiment 2. Forward steps are coded +1 and backward steps -1. The average response for each subject is plotted. Subjects are ordered by the strength of their response bias. Error bars represent the binomial 95%-confidence interval.
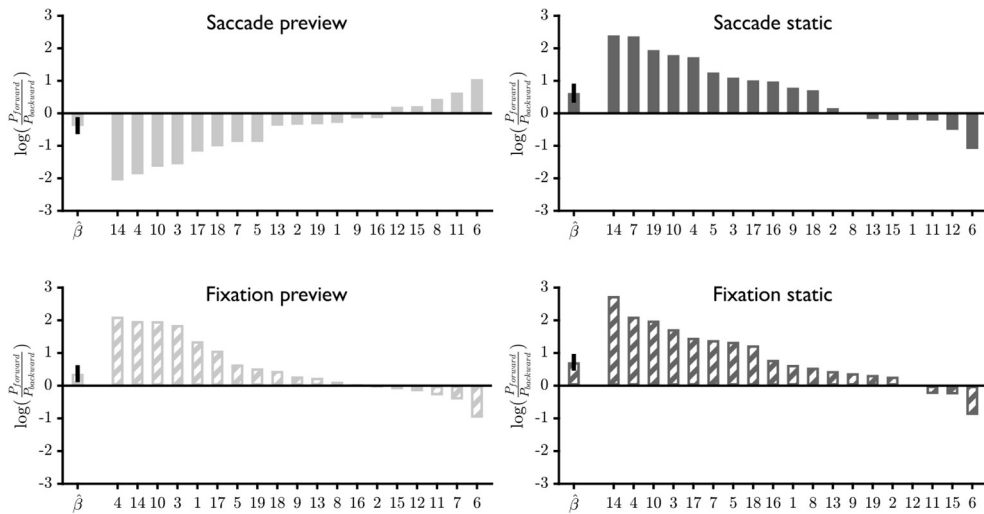
Figure S3. Individual biases per condition in Experiment 1. First bar is the bias as estimated by the generalized linear mixed effects model (error bars are 95% bootstrapped confidence intervals). X tick labels refer to subject ID. In each panel, subjects are ordered by effect size. For each subject, the average response (converted to log odds) per condition with a post-saccadic inducer of 20 or 50 ms. The difference between these averages was divided by 3 to get an estimate of the effect of the post-saccadic inducer of 10. Then, we took the average response after 20 ms of post-saccadic inducer and subtracted the effect of 10 ms inducer. Thus, we had an estimate of the bias after 10 ms of post-saccadic inducer per condition per subject.
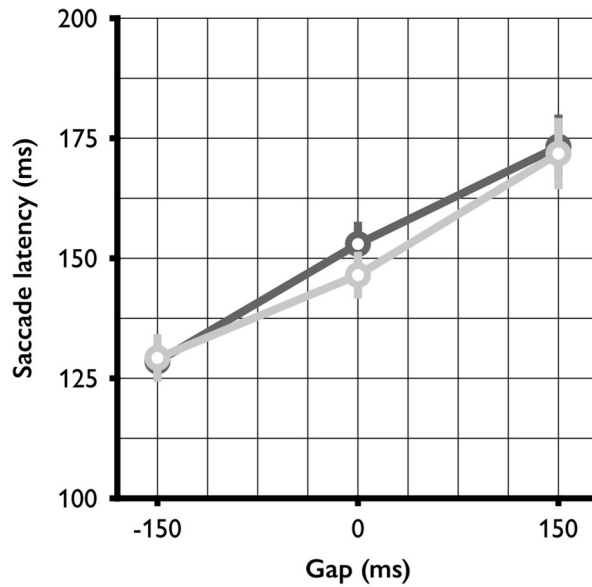
Figure S4. Average saccade latencies in Experiment 1 in the Saccade Preview (yellow) and Saccade static (black) conditions. Error bars represent 1 standard error of the mean over subjects. Gap duration is defined as the time of fixation target offset minus the time of stimulus onset. A two-way repeated measures analysis of variance showed the gap modulation had a significant effect on saccade latencies ($F_{(2,36)} = 31.815$, $p < 0.001$), with no significant difference between the two preview conditions ($F_{(1,18)} = 1.065$, $p = 0.316$), nor a significant interaction between gap duration and preview condition ($F_{(2,36)} = 1.298$, $p = 0.285$).
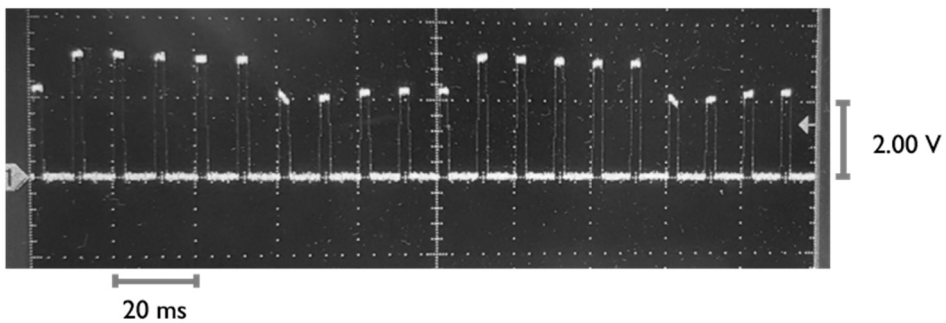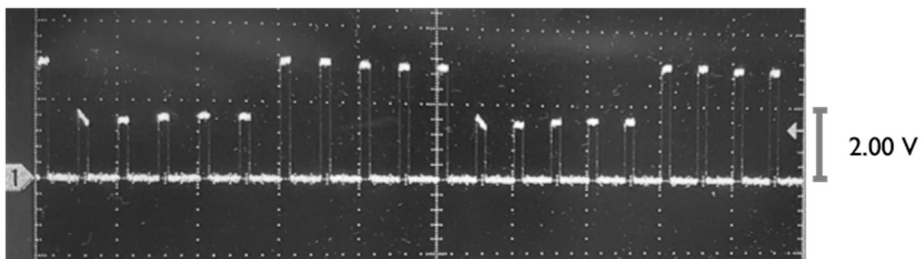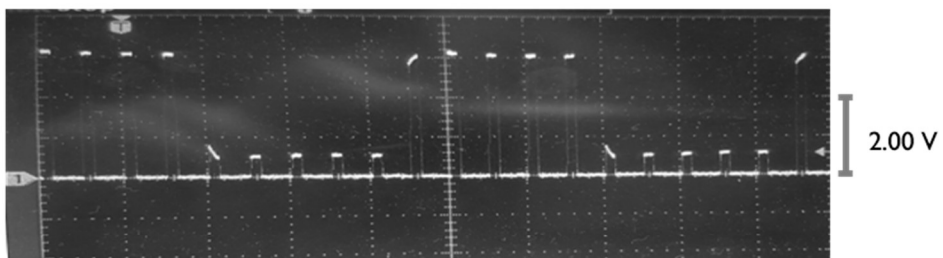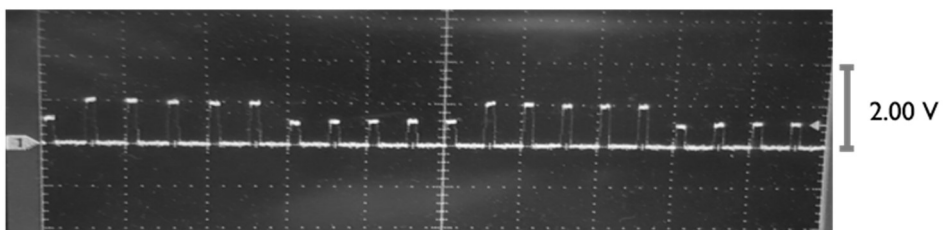
Figure S5. Photographs of oscilloscope measurements of different luminance transitions. Luminance was changed every 5 frames while the monitor was running at 100 Hz, and with the native backlight strobing feature enabled with pulse width of 100%. The desired luminance level was reached within the first frame when the luminance was changed. For large transitions there was a small ramp within the first frame (best visible in the third panel, 12.5% - 75% luminance).
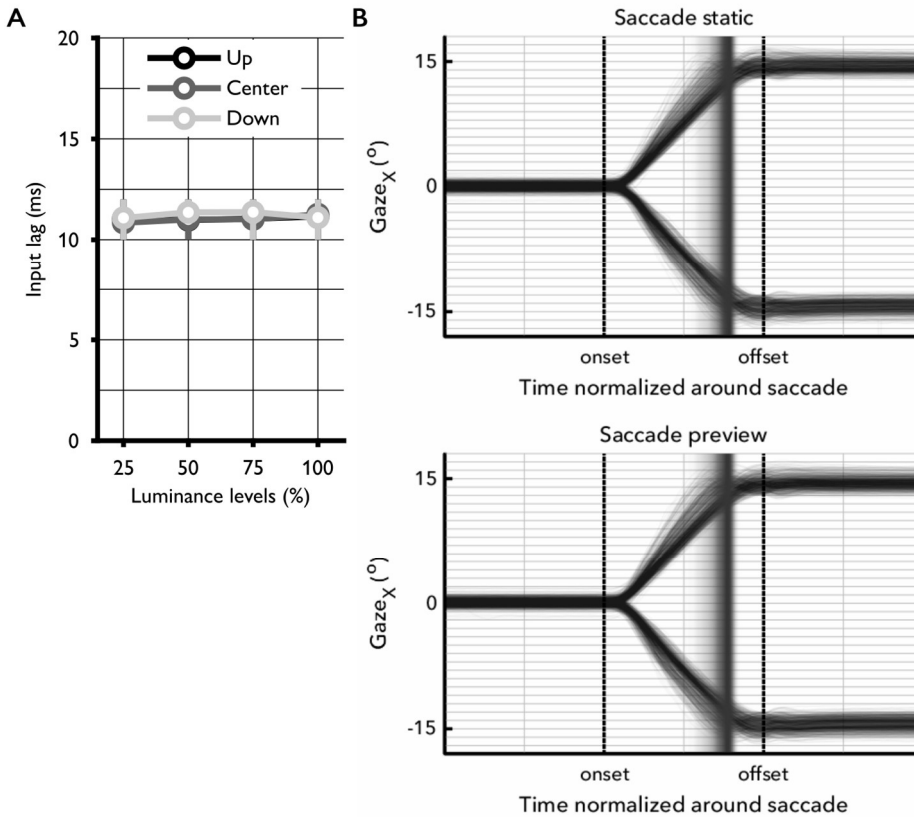
Figure S6. Synchronization of visual onsets and timestamps in Eyelink datafile (EDF). **A.** Average input lag in ms between visual onset (as measured with a photodiode) and the timestamp in the EDF. Lags were measured at three different locations on the left side of the screen (see legend). Delays were measured from black to different luminance levels (see x-axis). Error bars represent interval including 95% measured delays. Rounded to whole milliseconds, all measured input lags were 11 ms. **B.** Horizontal gaze position over time, where time is normalized to saccade onset and offset. Red patch is the onset of the post-saccadic inducer in all trials that were included in the analysis, where the transparency reflects the density of onsets. This onset is the based on the timestamp in the EDF and corrected by 11 ms based on the photodiode measurement as displayed in A. The upper panel includes all trials from the Saccade static condition. The bottom panel includes all trials from the Saccade preview condition.
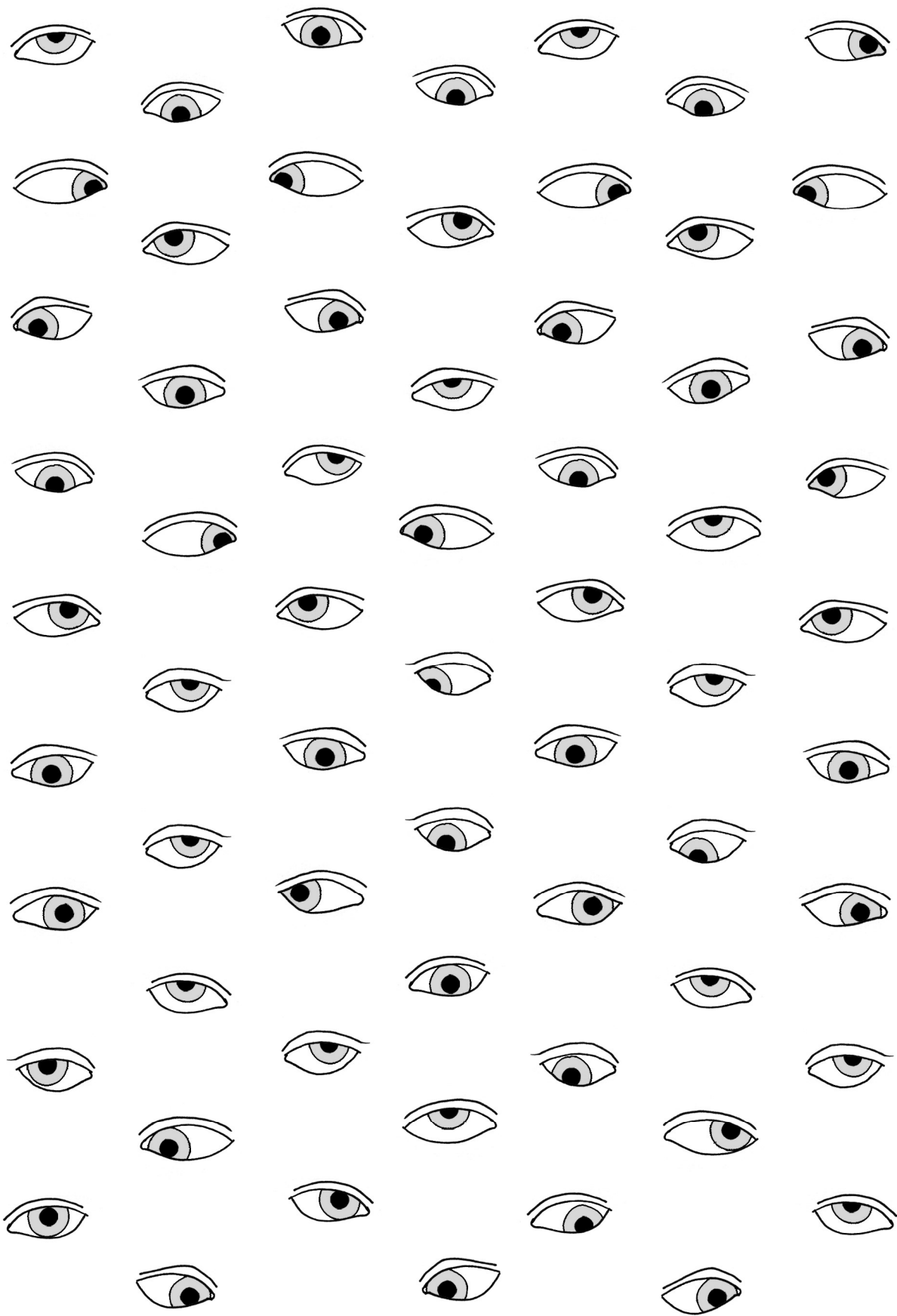
Chapter 4

Time course of spatiotopic updating of visual feature information in MEG data

In preparation as

Fabius, J.H., Fracasso A., Acunzo, D.A., Van der Stigchel, S. & Melcher, D.
Time course of spatiotopic updating of visual feature information in MEG data

Abstract

Despite the retinotopic organization of the visual system, the world appears introspectively stable and continuous across saccades. A long standing question in visual neuroscience has been how perceptual continuity arises from the visual system. The major hypothesis is that visual information is spatiotopically updated. Based on a corollary discharge from the oculomotor system, the visual system can anticipate the shift in visual information. Neurophysiological studies have demonstrated changes in receptive field properties of visual neurons right before saccade offset in monkeys. Similar pre-saccadic changes in visual processing have been demonstrated in humans with electroencephalography. However, it remains unclear what the content of this anticipatory shift is. Here we used magnetoencephalography to investigate visual processing across saccades. We showed observers large sinusoidal gratings in one visual hemifield while they either maintained fixation or made saccade across the stimulus, shifting the stimulus to the other visual hemifield. Our analysis was two-fold. First, we performed a conceptual replication of previous EEG studies, investigating the lateralization of visually evoked field before saccade onset. After stimulus onset event related fields were stronger over the contralateral hemisphere, but this lateralization disappeared briefly before saccade onset. This is congruent with predictive remapping. Second, we used multivariate pattern analysis to investigate the time-course of visual information representation across saccades. We operationalized visual information with the spatial frequency of the stimulus. Before saccade offset spatial frequency was represented similarly as when subjects maintained fixation at the pre-saccadic fixation point. About 40 ms after saccade offset, the representation was similar to when subjects maintained fixation at the post-saccadic fixation point. Importantly, spatial frequency could still be classified based on the pre-saccadic representation after saccade offset. We interpret this temporal overlap of pre- and post-saccadic representations as a "soft handoff" of information transfer. According to this hypothesis, visual feature information can be compared for continuity across saccades after saccade offset, using both the pre- and post-saccadic retinotopic representations of the stimulus.

Introduction

We perceive a stable and continuous visual world, despite frequent spatial changes and temporal disruptions introduced by saccades. This introspective notion is also reflected in psychophysical data, where responses to a post-saccadic stimulus are affected by a pre-saccadic stimulus when presented at the same spatiotopic location, but – because of the saccade – at a different retinotopic location (Demeyer et al., 2009; Fabius, Fracasso, Nijboer, & Van der Stigchel, 2019; Fracasso et al., 2010; Ganmor et al., 2015; Oostwoud Wijdenes et al., 2015; Wittenberg et al., 2008; Wolf & Schütz, 2015). Given that the visual system is largely retinotopically organized (Wandell et al., 2007) this raises the question, how does perceptual continuity arise in our visual system? The major hypothesis is that the visual system integrates retinal and extraretinal signals (Sperry, 1950; Von Holst & Mittelstaedt, 1950). More specifically, the visual system seems to be able to anticipate the distortions created by saccades based on a corollary discharge from the oculomotor system (Grüsser, 1995; Melcher & Colby, 2008; Wurtz, 2008). With the information conveyed by the corollary discharge, visual information can (theoretically) be updated from its current location in the visual field to the upcoming location in the visual field, thereby giving rise to perceptual continuity.

Neurophysiological studies with non-human primates have identified a pathway for the processing of a corollary discharge from the oculomotor system, comprising the superior colliculus, medial dorsal nucleus of the thalamus and the frontal eye fields (Sommer & Wurtz, 2002, 2006). This pathway has also been related to perceptual continuity (Cavanaugh et al., 2016; Joiner, Cavanaugh, FitzGibbon, & Wurtz, 2013). In addition, other neurophysiological studies with non-human primates demonstrated changes in receptive field profiles of visual neurons before the onset of a saccade (Duhamel, Colby, et al., 1992; Kusunoki & Goldberg, 2003; Nakamura & Colby, 2002; Umeno & Goldberg, 1997). It is assumed that the change in receptive field properties is triggered by the corollary discharge such that visual neurons can anticipate the change in visual input caused by the saccade (Mirpour & Bisley, 2016). Evidence from experiments with human subjects point in the same direction, although the effects are only observed after saccade offset (but this could be due to methodological constraints). Multiple fMRI studies (Dunkley et al., 2016; Fairhall et al., 2017; Merriam et al., 2003; Zimmermann, Weidner, et al., 2016) and EEG studies (Edwards et al., 2018; Huber-Huber, Buonocore, Hickey, & Melcher, 2018) showed that a visual stimulus before a saccade affects the processing of a stimulus at the same spatiotopic

location after the saccade, corroborating observations from human psychophysics. Although these studies do show clear post-saccadic effects of a pre-saccadic stimulus, it remains unclear when these effects arise in the human visual system. Previous attempts to address this question with electroencephalography (EEG) have resulted in mixed results. Two studies demonstrated modulations of ERPs related to updating before saccade onset (Parks & Corballis, 2008, 2010), but two other studies only found these effects after saccade offset (Bellebaum & Daum, 2006; Peterburs, Gajda, Hoffmann, Daum, & Bellebaum, 2011). The former two studies specifically found effects ipsilateral to a presented stimulus, suggesting pre-saccadic updating of information to the post-saccadic location of the stimulus. Here, we tried to replicate this finding (modulation of ipsilateral evoked responses before saccade onset) with magnetoencephalography (MEG). While subjects were in the MEG, they were presented a large sinusoidal grating in the lower visual field. In different conditions, subjects either maintained fixation with the grating in the lower left or lower right visual field, or they made a saccade over the grating such that the grating was first in the lower left and then in the lower right visual field. In a subset of trials, the grating was absent, and subjects only made a saccade. This paradigm is similar to other human neuroimaging paradigms investigating updating of visual information across saccades (Dunkley et al., 2016; Fairhall et al., 2017; Parks & Corballis, 2010; Zimmermann, Weidner, et al., 2016). Similar to the aforementioned EEG studies, we observed stronger contralateral responses after stimulus onset in our MEG data. However, this lateralization disappeared close to saccade onset, consistent with pre-saccadic remapping.

Beyond a replication of the pre-saccadic modulation of visually evoked responses, we also went a step further to examine the content of the updated information. Because although a pre-saccadic stimulus influences the post-saccadic processing of the same stimulus, it remains unclear whether signals related to updating across saccades contain detailed information about the stimulus features. It has been argued that only pointers to relevant locations are updated, without any detailed information about the visual characteristics of the stimulus at that location (Cavanagh et al., 2010; Mirpour & Bisley, 2016), whereas others have argued that more detailed information of stimulus features could be updated (Melcher, 2011; Subramanian & Colby, 2014). Here, we used multivariate pattern analysis to decode stimulus information from the pre-saccadic event-related responses to explore when the representation of a stimulus switches from the pre- to the post-saccadic situation. To give our stimuli distinct features we presented grating with a low (0.33 cyc/°) or a high (1.33 cyc/°) spatial frequency. We trained classifiers to distinguish the

spatial frequency of the gratings based on data from trials where subjects remained stable fixation. It has been demonstrated that spatial frequency can be reliably decoded from MEG data, albeit with larger stimuli around the point of fixation (Ramkumar, Jas, Pannasch, Hari, & Parkkonen, 2013). We trained two classifiers: one trained on the data with the gratings in the pre-saccadic visual field, another one trained on the data with the gratings in the post-saccadic visual field. Cross-validation of these classifiers showed rapid above chance classification, about 40 ms after stimulus onset. We then used these classifiers to decode the data from trials in which a saccade brought the grating from one visual hemifield into the other.

The pre-saccadic classifier – trained with data obtained while subjects were keeping fixation during the entire trial, and where the stimulus was in the same hemifield as in the saccade trials before saccade onset – accurately classified the spatial frequency rapidly after stimulus onset (~40 ms). Crucially, spatial frequency was accurately classified, well into the post-saccadic period. The post-saccadic classifier – trained with fixation data when stimulus was in the same hemifield as in the saccade trials after saccade offset – accurately classified spatial frequency only after saccade offset, about 40 ms into the post-saccadic fixation period. Together, the rapid classification and temporal overlap after saccade offset, is reminiscent of a "soft handoff" in information transfer (Drew, Mance, Horowitz, Wolfe, & Vogel, 2014), such as when a person making a cell phone call is moving such that a new cell tower must be used. In the case of a moving stimulus (and stable fixation), for example, when an object transfers across the midline, its representation changes cortical hemispheres. The initially tracking hemisphere continues to represent the object for a period after that object crosses the midline, such that both hemispheres track the object at the same time before the "receiving" hemisphere takes over. In the case of the moving object, the "drop-off" of the initial hemisphere was delayed by several hundred milliseconds when the object moved in a predictable way. In the current experiments, and for saccades in general, the stimulus is moved predictably across the visual field. We discuss the current data and perceptual continuity in light of the idea of a soft handoff.

4

Methods

Subjects

We analysed data of 29 subjects (13 female; mean age = 25.3, range = [20, 35]; 23 righthanded). We collected data of two more subjects, but their data could not be included in the analysis because of technical issues (n = 1) and inability to perform the task (n = 1). In the latter case, the subject was making saccades to the stimulus rather than the saccade target. Of the 29 subjects, one subject was excluded after analysing the behavioural performance. Performance of this subject in the Saccade condition on the orientation change detection task was at chance level both for 0.33 cyc/° (D' = 0.05) and 1.33 cyc/° (D' = 0.11) stimuli.

Setup

Participants were dressed in scrubs. Five head position indicator (HPI) coils were attached. Head coordinate frame, coil position and head shape were determined with the Fasttrack 3D digitization system (Polhemus, Colchester, VT, USA) using the left and right pre-auricular points, the nasion and 500 points distributed across the head. Head position was measured at the beginning of each experimental run. MEG data were acquired with a Vectorview 306 channel MEG machine (Elekta Neuromag Oy, Helsinki, Finland). Eye position data were acquired with an Eyelink 1000+ at 1000 Hz, recording the left eye (SR Research Ltd., Mississauga, ON, Canada). Stimuli were projected with a PROPixx projector (VPixx Technologies, Saint-Bruno, QC, Canada) onto a translucent screen 100 cm away from the subject, with a refresh rate of 120 Hz. The display size was 51 by 38 cm, with a resolution of 1440 by 1080 pixels. Visual onsets were monitored with a photodiode, placed in the lower left corner of the display over a small square that changed polarity with every change in display. Manual responses were recorded with RESPONSEPixx (VPixx Technologies, Saint-Bruno, QC, Canada). Four electrooculography (EOG) and two electrocardiography (ECG) electrodes were attached, but these recordings were not used in the analysis. Electrodes were placed above and below the left eye for measuring the vertical EOG, and on the outer canthi for measuring the horizontal EOG. ECG was recorded using Einthoven's lead II, which used the Left Leg and the Right Arm electrodes.
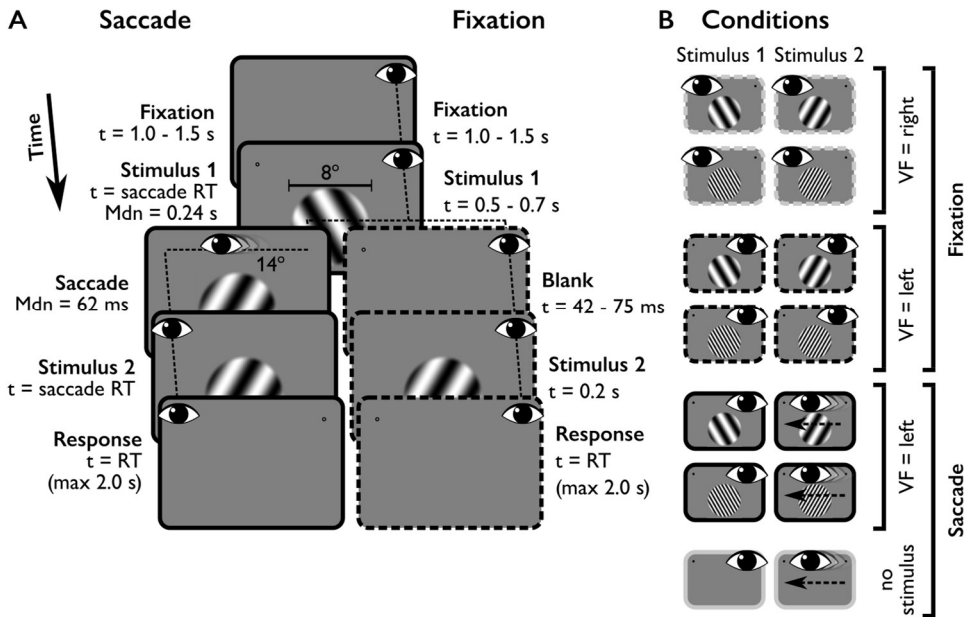
Stimuli

Figure 1. Trial timeline and conditions. **A.** Example trials in the Saccade condition and Fixation condition. Subjects were instructed to detect a change in orientation (60°) between Stimulus 1 and Stimulus 2. The eye and red dotted line depict gaze location in each panel. In the response window, subjects indicated whether the grating had changed orientation or not. **B.** Possible configurations of Stimulus 1 and Stimulus 2 and instructed oculomotor behaviour. In Fixation trials, subjects maintained fixation on a single side of the screen for the entire duration of a trial. The Saccade condition also included trials without a stimulus, but with the onset of the second fixation target. In those trials, subjects were instructed to make a saccade to the second target and do nothing else. **Abbreviations:** Mdn = median, VF = visual field.

Stimulus presentation was controlled with MATLAB Psychtoolbox 3 (Brainard, 1997; Kleiner et al., 2007; Pelli, 1997) and its DATAPixx extension (VPixx Technologies, Saint-Bruno, QC, Canada). The Eyelink extension of the Psychtoolbox (Cornelissen et al., 2002) was used to control the eye-tracker and control the gaze-contingent display. The stimuli were static sinusoidal gratings (ø = 4° visual angle; orientation = -30° or 30° from vertical; spatial frequency = 0.33 or 1.33 cyc/°; phase = 0 or pi, to keep luminance equal). Stimuli were presented at full contrast (black = 1.94 cd/m^2, white = 142 cd/m^2) on a uniform grey background (61.1 cd/m^2). Stimulus contrast was reduced to zero over the outer 0.6° with a raised cosine envelope. The center of the stimuli was located 6° below the horizontal meridian, and horizontally centred on the display. The fixation points consisted of black dots (radius = 0.5°) overlaid with a grey cross and a black point (radius = 0.07°) in the center

of the cross (Thaler, Schütz, Goodale, & Gegenfurtner, 2013). Fixation points were located 7° to the left or right from the center of the display.

Procedure

Subjects performed trials in two different conditions, a Saccade and a Fixation condition (Figure 1A). In the Saccade condition, subjects performed a trans-saccadic change detection task on the orientation of the stimulus. In these trials (416 trials/subject), subjects initially fixated the right fixation point for a random duration of 1.0 to 1.5 seconds (uniformly distributed). Then stimulus 1 (S1) appeared, together with the second fixation point. Subject made a saccade (required amplitude = 14°) to the left fixation point immediately after stimulus onset. In a pilot dataset we observed that this procedure gave rise to median saccade latencies of approximately 0.2 seconds. The maximum saccade latency during the experiment was 1.0 second. If subjects had not executed a saccade by then they were displayed a text encouraging them to make faster saccades. During the saccade, stimulus 2 (S2) was presented. S2 had either the same orientation as S1 or a 60° different orientation. I.e. if S1 had an orientation of -30° from vertical, and the orientation changed during the saccade, S2 would have an orientation of +30°. We only used these two orientations. S2 was presented for the same duration as S1. After the saccade, subjects manually indicated whether S1 and S2 had the same orientation. The maximum response latency during the experiment was 2.0 seconds. If subjects had not responded by then they were displayed a text encouraging them to make faster responses.

Additionally, we included trials without a stimulus (208 trials/subject). In these trials, subjects fixated the right fixation point for 1.0 to 1.5 seconds, before the left fixation point appeared. Subjects made a saccade to the left fixation point. When a saccade was detected, the trial ended after a time equal to the sum of the online saccade latency and an additional 0.5 seconds. Subjects did not give a manual response in these trials. These "saccade, no stimulus" trials were mixed with the trans-saccadic change detection trials. Online saccade detection was position-based, i.e. a 'saccade' was detected as soon as gaze was outside an area of 2° around the right fixation point. For the analysis, saccades were detected offline using a velocity-based algorithm (see Preprocessing).

In the Fixation condition, subject also performed a change detection task, similar to the trans-saccadic change detection task (416 trials/subject). Subjects fixated the left or right fixation point for the entire length of a single trial. S1 was presented for a random duration

between 0.5 to 0.7 seconds (uniformly distributed). Then, S1 was removed for a duration between 42-75 ms (normally distributed; mean = 55; s.d. = 6) and followed by S2 presented with the same duration as S1. The duration between S1 and S2 was matched to the duration of saccades from the pilot data.

Block design

The Saccade and Fixation conditions were presented in separate blocks. Subjects performed 13 blocks of the Saccade condition, and 13 blocks of the Fixation condition. The order of conditions (i.e. fixation first or saccade first) was balanced between subjects. The parameters spatial frequency (high/low), base orientation (-30°/30°), grating phase (0/pi) and change presence (with/without) were factorially presented within each block. In the Saccade condition, trials without a stimulus were implemented as a spatial frequency of 0 in this factorization. In the Saccade condition, all factorial combinations were repeated twice within a block, resulting in 48 trials per block. In the Fixation condition, fixation location (L/R) was included as an additional parameter in the factorization, resulting in 32 trials per block. One block of the Saccade condition and one block of the Fixation condition were combined into one experimental run. The duration of one run was approximately 8 minutes. Before the experiment started, subjects performed one block of the Fixation condition and one block of the Saccade condition as practice. The Fixation condition was always practiced first.

Preprocessing

We visually inspected all data and marked noisy channels. The native Maxwell filter of Elekta Neuromag was applied to filter signals that originated outside the MEG helmet (Taulu & Kajola, 2005; Taulu, Kajola, & Simola, 2003; Taulu, Simola, & Kajola, 2005). Line noise (50 Hz) and its harmonics (100 and 150 Hz) were attenuated using a DFT filter on the continuous data of each run. Data were then cut into epochs from 0.5 s before until 1.5 s after S1 onset. Then, data were downsampled to 500 Hz. The raw Eyelink recordings in the MEG datafile were converted from volt to pixels. We observed a small but consistent lag between the recordings in the MEG datafile and the Eyelink datafile of 7 ms. This lag probably originated during the digital-to-analog conversion and was compensated for by shifting all Eyelink data in the MEG datafile with 7 ms back in time with respect to the MEG data. Saccades were detected with the saccade detection algorithm of Nyström and Holmqvist (Nyström & Holmqvist, 2010), with a minimum fixation duration of 40 ms and a minimum saccade duration of 10 ms. To determine the onset of a visual event we converted the raw photodiode signal to a trinary signal – because we used three grey values: black,
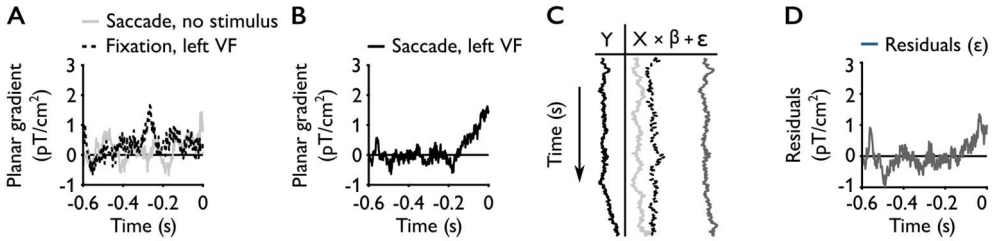
Figure 2. Linear modelling of planar gradients in the of the Saccade, left VF as a weighted linear combination of the Saccade, no stimulus and Fixation, left VF conditions. **A.** Example planar gradients of one combined planar gradiometer in the Saccade, no stimulus and Fixation, left VF conditions. **B.** Example planar gradient in the Saccade, Left VF condition. **C.** Visualization of the general linear model with the planar gradients depicted in A and B. Y = Saccade, left VF. X = [Saccade, no stimulus and Fixation, left VF]. ε = residuals. **D.** Residuals in the general linear model. The residuals represent the surplus of planar gradient in the Saccade, left VF condition, with respect to the planar gradients expected based on the measurements in the Fixation, left VF and Saccade, no stimulus condition.

grey and white – by taking four linearly separated values between the minimum and maximum values of the raw signal. All values below the second boundaries were classified as black (-1). All values between the second and third boundary were classified as grey (0). All values higher than the third boundary were classified as white (1). The absolute difference of the trinary signal was used to obtain the timing of a visual onset.

Epoch exclusion

All epochs from -0.5 to 1.5 after S1 onset were visually inspected for remaining MEG artefacts (e.g. muscle activity). Epochs containing artefacts were removed (mean = 3.9%, min = 0.4%, max = 7.3%). In the conditions with saccades, epochs were included only if 1) there was a single saccade after S1 onset and before S2 onset, 2) the saccade endpoint was at least 4° over the vertical midline of the screen, bringing the stimulus from being entirely in the left visual field to entirely in the right visual field, and 3) the saccade endpoint was higher than 2° below the horizontal midline of the screen, keeping the stimulus entirely in the bottom visual field (mean = 8.2%, min = 0.2%, max = 28.8%). In the Fixation conditions, epochs were included only if subjects 1) maintained gaze within an area of 2° visual angle around the fixation point during the entire epoch and 2) did not make microsaccades with amplitudes larger than 0.5° (mean = 4.2%, min = 0.1%, max = 21.4%). After defining valid epochs, we further included epochs in the saccade condition only when the saccade latency was between 150 and 500 ms. These latencies were selected because we intended to compare the saccade and fixation conditions. The duration of S1 in the fixation conditions was minimally 500 ms. The lower bound of the latency inclusion was more arbitrary: we did

not want saccades to be slow, but we also wanted to have epochs of a considerable length. Thus, we settled for 150 ms.

Event-related planar gradients

We computed event-related planar gradients of the combined gradiometer data with the recordings locked to saccade onset. We used planar gradiometers because their measurements allow for a direct distinction between left and right hemisphere activity, whereas magnetometers do not. We cut epochs from -0.6 to 0 seconds before saccade onset. Then computed the average per sensor and subsequently combined the averaged gradiometers. Lastly, we subtracted the average activity in a baseline period from -0.6 to -0.5 seconds before saccade onset. This baseline period did not include any stimulus-related activity, as we only included trials with a maximum saccade latency of 0.5 seconds. We did not apply any filters before or after computing the planar gradients (other than described in Preprocessing). We estimated responses related to pre-saccadic remapping to be the residual planar gradients from the conditions with both a saccade and a stimulus (i.e. the Saccade, left VF condition), after regressing out the predicted planar gradients based on the linear, weighted combination of the saccade related planar gradients and stimulus related planar gradients (Figure 2). For the saccade related activity, we took the saccade-locked planar gradients from the Saccade, no stimulus condition, because that condition only contains a saccade and no stimulus. For the stimulus related activity, we used the saccade-locked planar gradients from both the combined trials in the Fixation, left VF, 0.33 cyc/° and 1.33 cyc/° conditions. We did not make a distinction between spatial frequencies of the stimulus. For each subject and each combined planar gradiometer, we constructed a linear model, estimated the parameters for the saccade related activity ($\beta_{saccade}$, no stimulus) and the stimulus related activity ($\beta_{fixation}$, left VF). With these parameters, we estimate the predicted planar gradient ($\hat{Y}$) in the conditions with both a saccade and a stimulus (Saccade, left VF, 0.33 cyc/° and 1.33 cyc/°). The residuals were the difference between the actual planar gradient and $\hat{Y}$. We then tested where the residuals deviated from zero (see Methods: Statistics). In addition, we tested the lateralization of the residuals by subtracting the average residual planar gradient of all 48 rights sided sensors from the average residual planar gradient of all 48 left sided sensors (note that we left out 8 sensors from this analysis because they are positioned at the center of the helmet).

Trial length matching

In the analysis of planar gradients, we focused on stimulus related activity with respect to the onset of a saccade. Therefore, we locked epochs to the onset of the saccade (in the Saccade conditions). Because of the natural variability in saccade latencies, not all epochs had the same length. With our inclusion and exclusion criteria we assured that all trials were between 150 and 500 ms (see Methods: Epoch exclusion). By locking all epochs to the onset of the saccade rather than to the onset of S1, the stimulus-related activity would be scrambled across trials and become more convoluted when averaging over all trials in one condition. On the other hand, activity related to saccade onset should become more pronounced. Trials in the Fixation conditions did not have a saccade. Therefore, we matched each trial in these conditions to the duration of the trials in the Saccade conditions. We matched the trials chronologically per subjects. I.e. trial 1 of the Fixation trials was matched in length to trial 1 of the Saccade trials etc. We did not take the stimulus features into account for this procedure. In case a subject had more trials in the Fixation conditions than in the Saccade conditions, the surplus of Fixation trials was matched by randomly sampling from the Saccade trials. In addition, to the chronological match, we made 500 other samples of trial length matches, where Saccade trials and Fixation trials were randomly matched, rather than chronologically. These matchings were used to test whether the residuals used in our planar gradient analysis were robust to different computations of the 'saccade-locked' planar gradient from the Fixation condition.

Multivariate pattern analysis (MVPA)

We performed three different multivariate pattern analyses. All MVPAs were performed using the CoSMoMVPA toolbox for MATLAB (Oosterhof, Connolly, & Haxby, 2016). Firstly, we assessed whether any stimulus features could be decoded from the MEG data. To this extent, we performed 10-fold cross-validation of linear support vector machines (SVM) trained to separate stimulus features (spatial frequency, orientation and phase) from the data of the Fixation conditions. SVMs were trained for each subject separately. Data were aligned to the onset of stimulus 1 (S1), processed at 500 Hz and baseline standardized to -0.2 to 0 s before S1 onset. We used "temporal searchlight" with a radius 10 ms (i.e. 5 samples at 500 Hz). This temporal searchlight means that for each timepoint, classification is based not only on the data of all 306 channels at that timepoint but also 10 neighbouring timepoints, increasing the number of feature dimensions for

classification elevenfold. In each fold of the cross-validation, trials were always balanced for the stimulus feature that would be classified.

Secondly, we examined to which extent classifiers trained on one condition could decode spatial frequency in another condition. We performed cross-condition classification of spatial frequency. Here, SVMs were trained on the MEG data of either the Fixation, left VF or the Fixation right VF condition, to test for spatial invariance of the classification of spatial frequency. Subsequently, we tested on data of the Saccade, left VF and Fixation Right VF, or Saccade, left VF and Fixation, left VF conditions, respectively. Because trials in the training and test set were independent, we did not use cross-validation here. The same preprocessing and temporal searchlight parameters as in the first MVPA analysis were used.

Thirdly, we examined the temporal generalization of cross-condition classification of spatial frequency. The SVMs were trained on data from the Fixation conditions and tested on the data from the Saccade condition. Data were downsampled to 250 Hz and baseline standardized to -0.2 and 0 s before S1 onset. We used a temporal searchlight with a radius of 8 ms (i.e. 2 samples). The test data from the Saccade condition were aligned to S1 onset, saccade onset or saccade offset. Thus, in total six temporal generalizations were made per subject. With this analysis we examined how stimulus related activity changes across a saccade, and whether this progression resembles activity related to stimulus onsets under stable fixation at the pre-saccadic or the post-saccadic fixation location.

Statistics

For the behavioural parameters we calculated the mean or median of a parameter per subject and per condition. These values were analysed with a Bayesian repeated-measures ANOVA either in a 3×2 design (3 conditions × 2 spatial frequencies, excluding the Saccade, no stimulus condition) or in a 3×1 design (3 Saccade conditions). We used the default prior settings in JASP and computed Bayes factors for the fixed effects across matched models (JASP Team, 2018).

For the residuals in the planar gradient analysis, we tested for significant deviations from 0 per sensor and per time-point using one-sample t-tests (α = 0.05, two-tailed). We corrected for multiple comparisons using cluster-based permutations with threshold-free cluster-enhancement (Maris & Oostenveld, 2007; S. Smith & Nichols, 2009). We used 1×10^4 permutations, sensors were clustered based on Delaunay triangulation. Statistics were computed with the CoSMoMVPA toolbox (Oosterhof et al., 2016).
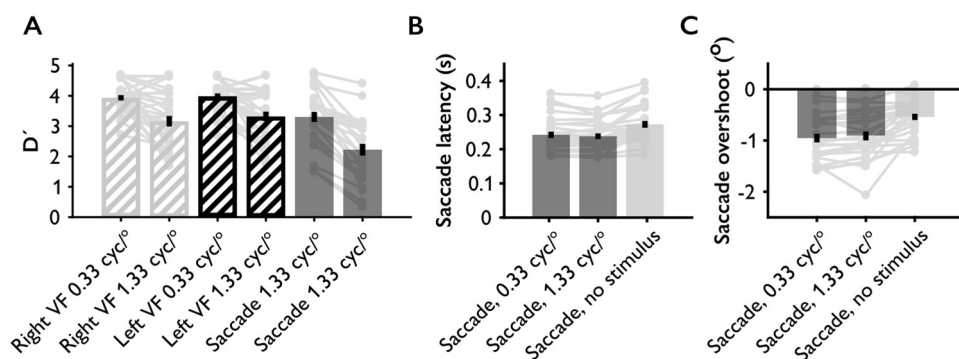
Figure 3. Behavioural performance. In all panels, the bars represent the group average, the error bar is 1 s.e.m. and the grey lines are individual subjects. **A.** Orientation change detection sensitivity expressed as D'. **B.** Saccade latency. **C.** Saccade endpoint error expressed as horizontal undershoot in degrees visual angle. Negative values represent hypometric saccades.

For the MVPAs, classifier performance was assessed against chance level using one sample t-tests, corrected for multiple comparisons using cluster-based permutations, with threshold free cluster-enhancement. Classifier accuracy was computed as "proportion correct" but converted to the log-odds of a correct response before entering the statistical analysis. Chance level were log-odds = 0. We used 1×10^4 permutations. Time points were regarded as clusters within a radius of 10 ms.

Results

Behaviour

Orientation change detection

Overall, sensitivity for changes in orientation was high (average D' = 3.32 ± 0.11 s.e.m.), but there were differences in sensitivity between the different conditions and spatial frequencies (Figure 3A). We assessed these differences with a Bayesian repeated measures ANOVA, with the factors condition (Fixation, right VF, Fixation, left VF and Saccade, left VF) and spatial frequency (0.33 cyc/° and 1.33 cyc/°). There was strong evidence in favour of an effect of both condition ($BF_{10} = 1.43 \times 10^{10}$) and spatial frequency ($BF_{10} = 1.39 \times 10^{12}$), but not for their interaction ($BF_{10} = 0.377$). Post-hoc tests showed that the effect of condition was primarily driven by differences between the Saccade and two Fixation conditions ($BF_{10} = 4.17 \times 10^6$, and $BF_{10} = 7.50 \times 10^7$), but not between the two Fixation

conditions (BF_{10} = 0.316). Subjects had a slight overall bias of reporting a change (average criterion = 0.19 ± 0.03 s.e.m.). The data were inconclusive with regards to effects of condition (BF_{10} = 0.562) or spatial frequency (BF_{10} = 1.04) on this bias, and the data were against an interaction between condition and spatial frequency (BF_{10} = 0.123). Together, these results show that subjects were attending the stimulus in all conditions, but performance was better in the fixation conditions and for stimuli with a low spatial frequency.

Saccades

We analysed the median saccade latencies and mean horizontal accuracies (Figure 3B, 3C). Histograms and 2D density plots are provided in the Supplementary Information (Figure S1). Across the different Saccade conditions, the average of median saccade latencies was 0.251 (±0.009 s.e.m.) seconds (after excluding trials with latencies <0.15 s or >0.50 s). Latencies was different across these different conditions (BF_{10} = 1.45×10^7). This was driven by a difference between the latencies in the Saccade, no stimulus condition versus the Saccade 0.33 cyc/° (BF_{10} = 2.77×10^3) and the Saccade 1.33 cyc/° (BF_{10} = 1.83×10^4) conditions. The data were inconclusive about a difference in saccade latencies between the Saccade 0.33 cyc/° and the Saccade 1.33 cyc/° (BF_{10} = 0.993). On average saccades were hypometric (average overshoot = -0.76° ± 0.07 s.e.m). The saccade amplitudes were also different between the different conditions (BF_{10} = 1.17×10^7), with larger amplitudes in the Saccade, no stimulus condition than in the Saccade, 0.33 cyc/° (BF_{10} = 5.60×10^4) or the Saccade, 1.33 cyc/° (BF_{10} = 2.13×10^3) conditions. But the evidence was inconclusive about a difference between Saccade, 0.33 cyc/° and Saccade, 1.33 cyc/° conditions (BF_{10} = 0.442). Together, these results show that oculomotor behaviour between trials with a stimulus and trials without a stimulus was slightly different (faster but more hypometric when a stimulus was presented), but not very different (if at all) between trials with a stimulus with spatial frequencies of 0.33 cyc/° or 1.33 cyc/°.

Model pre-saccadic planar gradient

In the EEG experiments of Parks and Corballis (2008, 2010), saccade-locked ERPs were stronger in electrodes over the hemisphere ipsilateral to a visual stimulus than over the contralateral hemisphere when the upcoming saccade would shift the stimulus to the other hemifield. The ipsilateral ERP was only significantly different from the contralateral ERP close before saccade onset (-40 to 0 ms). Because of the late timing and ipsilateralization, the authors conclude that the ERP could reflect pre-saccadic remapping. Here, we
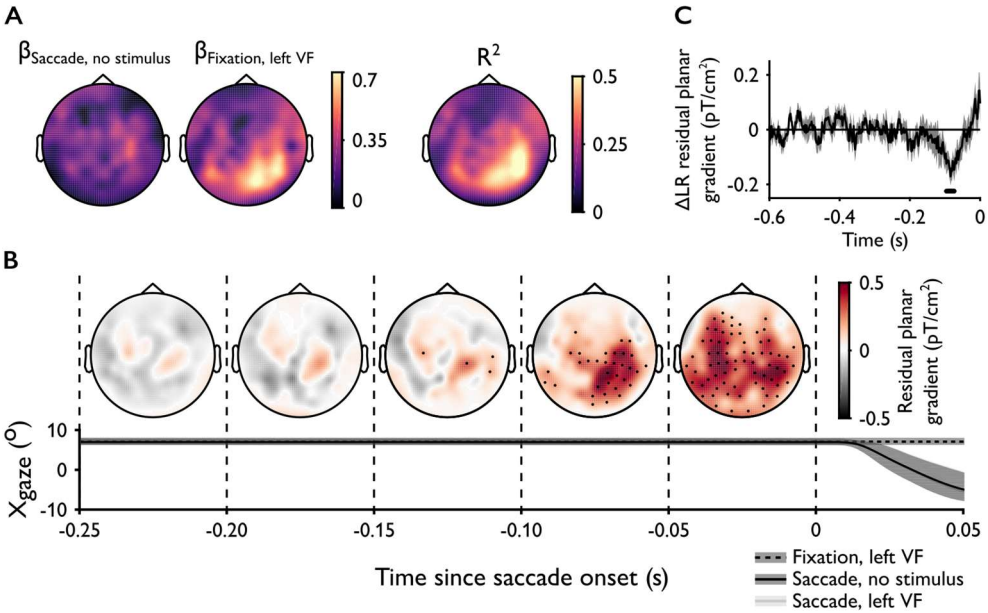
Figure 4. Results of linear modelling of event-related fields in the of the Saccade, left VF as a weighted linear combination of the Saccade, no stimulus and Fixation, left VF conditions. **A.** Topographic heatmap of estimated parameters for the Saccade, no stimulus condition ($\beta_{saccade,\ no\ stimulus}$) and the Fixation, left VF condition ($\beta_{fixation,\ left\ VF}$), and a topographic heatmap of the proportion variance explained (R^2). **B.** Topographical heatmaps of the residuals of the linear models. Values represent group averages. Deviations from 0 were assessed with one-sample t-tests, cluster-corrected in time and space for multiple comparisons ($\alpha = 0.05$, two-tailed). Sensors with a significant deviation from 0 for at least 12.5 ms are highlight with a black point. The average horizontal gaze position over time is plotted below the heatmaps. Lines represent median gaze position over all trials. Shaded area is the 95% interval across all trials. **C.** Lateralization of residuals. Difference in residual planar gradients between left and right lateralized sensors over time. Positive values indicate larger residual planar gradients in the left lateralized sensors than in the right sensors. Solid line represents the group average, shaded area is 1 s.e.m. Red line indicates significant deviation from 0 (corrected for multiple comparisons).

investigated pre-saccadic remapping signatures in the planar gradients of combined planar gradiometers by analysing residual activity in the Saccade, left VF (0.33 cyc/° and 1.33 cyc/° combined) condition, after regressing out the planar gradients of the Saccade, no stimulus and Fixation, left VF (0.33 cyc/° and 1.33 cyc/° combined) conditions. For the group average planar gradients in the different conditions see Figure S2. Overall, regression coefficients and explained variances were larger for sensors on the right (contralateral) side of the helmet (Figure 4A). From 142 ms before saccade onset, average residual planar gradients in several sensors were significantly higher than 0 (Figure 4B). The number of sensors with significant residual planar gradients increased over time to saccade onset to a maximum of 71 sensors. The residual planar gradients were significantly lateralized over the right

(contralateral) hemisphere between -96 and -72 ms before saccade onset (Figure 4C). After this period, lateralization seemed to reverse but was not significantly different from zero. We repeated this analysis 500 times with different trial length matchings between Saccade and Fixation trials (see Methods: Trial length matching). The outcomes of the different trial matchings did not differ substantially from the chronologically matched trials (Figure S3).

In sum, we extracted planar gradients that were potentially related to pre-saccadic updating of visual information. We defined the remapping related planar gradients by taking the residuals from the Saccade, left VF (0.33 cyc/° and 1.33 cyc/° combined) condition after regressing out the stimulus related (the Fixation, left VF condition) and the saccade related planar gradients (the Saccade, no stimulus condition). Following the results of the EEG studies of Parks and Corballis (2008, 2010), we expected the residuals to be ipsilateral to the stimulus shortly before saccade onset. In our data, the residual planar gradients increased in strength closer to saccade onset. For a brief period around 80 ms before saccade onset, the residual planar gradients were lateralized to the hemisphere contralateral to the stimulus. This lateralization seemed to reverse to the ipsilateral hemisphere closer to saccade onset, but there was no significant difference between residual planar gradients in the left and in the right sensors. Still, there was a strong residual planar gradient in a large number of sensors both over the contra- and ipsilateral hemispheres, suggesting stronger neural activity in both hemispheres close to saccade onset.

Stimulus feature decoding with MVPA

In the previous section we investigated whether the planar gradients contained any evidence for pre-saccadic updating. Although we did not observe a clear ipsilateral response, the condition with both a saccade and a stimulus contained stronger planar gradients than would be expected based on the conditions with only a stimulus or only a saccade. In this section we investigated whether the pre-saccadic saccade-locked data contained information about the stimulus features. We took a different approach to this problem by using multivariate pattern analysis (MVPA).

Benchmark decoding of stimulus features in Fixation conditions

We trained linear SVMs to classify the spatial frequency of the stimulus based on all MEG data (magnetometers and gradiometers) from the Fixation conditions. To assess the distinctiveness of the evoked fields, we computed classifier accuracy based on 10-fold cross-validation. We observed significant above-chance classification accuracy (Figure 5A) both in
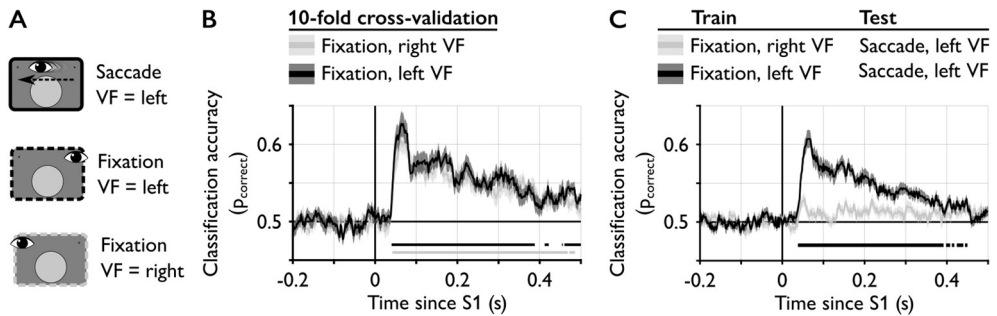
Figure 5. Classification of spatial frequency based on standardized data locked to stimulus 1 (S1) onset. In panels B and C, the lines represent the group average. The shaded areas are 1 s.e.m. Significant above chance ($p_{correct}$ = 0.5) classification is indicated by the horizontal black and grey lines between $p_{correct}$ = 0.45 and 0.5. **A.** Procedure of conditions (repetition of Figure 1B). **B.** Classification accuracy in the two fixation conditions, based on 10-fold cross-validation. **C.** Cross-condition classification accuracy of spatial frequency. Classifiers were trained on the data from the Fixation, right VF (grey) or from the Fixation, left VF condition (black). These classifiers were then tested with data from the Saccade conditions. Both the training and testing MEG data were locked to stimulus 1 onset.

the Fixation, right VF (0.042-0.468 s after S1 onset) and in the Fixation, left VF conditions (0.040-0.388 s after S1 onset. The peak of average classification accuracy in the Fixation, right VF was 0.60 at t = 0.062 s after S1 onset. The peak of average classification accuracy in the Fixation, left VF was 0.63 at t = 0.064 s after S1 onset. The orientation and the phase of the stimulus could not be classified reliably (Figure S4A, S4B).

Next, we tested the spatial specificity of spatial frequency encoding. In visual cortex, each hemisphere represents the contralateral visual field. Therefore, we expected that the evoked fields by a stimulus in the left VF would be substantially different from the fields evoked by a stimulus in the right VF. So, the difference between high and low spatial frequencies would also be different. Thus, we hypothesized that a classifier trained to discriminate spatial frequency of stimuli in the left VF should not perform above chance in classifying stimuli in the right VF. We tested this hypothesis using cross-classification. We had two conditions in which Stimulus 1 was presented in the left visual field (Fixation, left VF a Saccade, left VF), and one in which Stimulus 1 was presented in the right visual field (Fixation, right VF). We expected that an SVM trained to classify spatial frequency from the Fixation, left VF data would be able to classify spatial frequency from the Saccade, left VF data, but not from the Fixation, right VF data. And conversely, an SVM trained to classify spatial frequency from the Fixation, right VF data would not be able to classify spatial frequency from the other two conditions.

We trained data on one of the two Fixation conditions and assessed its performance on the other conditions. SVMs trained on the Fixation, right VF data could not reliably classify spatial frequency from the Saccade, left VF condition (Figure 5B), or the Fixation, left VF condition (Figure S4C). However, SVMs trained on the Fixation, left VF data could also classify data from the Saccade, left VF condition (first above-chance classification cluster = [0.038, 0.392] s after S1 onset, peak accuracy = 0.61, time of peak classification = 0.066 s after S1 onset), but not from the Fixation, right VF condition. This implies that the differences in stimulus-locked data between gratings with 0.33 cyc/° or 1.33 cyc/° spatial frequencies are different for stimuli in the left and stimuli in the right visual field, but these differences do not depend on the instructed oculomotor behaviour (i.e. remain fixation or execute a saccade after stimulus onset)

Temporal generalization of Fixation-Saccade cross-decoding

In the previous sections, we observed that spatial frequency can be decode from the data when locked to stimulus onset. This representation of spatial frequency was specific to the hemifield in which the stimulus was presented. With this final MVPA, we investigated at which time point (with respect to the saccade) the representation of spatial frequency in the Saccade, left VF condition switches from the representation of spatial frequency in the Fixation, left VF to the representation in the Fixation, right VF condition. To investigate this carefully, we examined the cross-condition temporal generalization of classifiers trained on the Fixation conditions and tested on three different alignments of the Saccade condition (Figure 6).

When the test data from the Saccade condition were aligned to S1 onset the classifier trained on data from the Fixation, left VF condition was able to classify significantly above chance (Figure 6D), but the temporal generalization was limited (note the narrow diagonal pattern of classification accuracy in Figure 6D). The classifier train on the Fixation, Right VF data only classified the Saccade, Left VF data correctly in a couple of small time windows, one along the diagonal around 0.4 s after stimulus onset (Figure 6G). At this timepoint, saccades had been executed in the majority of the trials (in the Saccade, left VF data). Thus, this cluster might reflect a second sweep of feedforward processing of visual information after saccade offset. This will become more apparent when inspecting the cross-classification with the test data aligned to saccade offset.
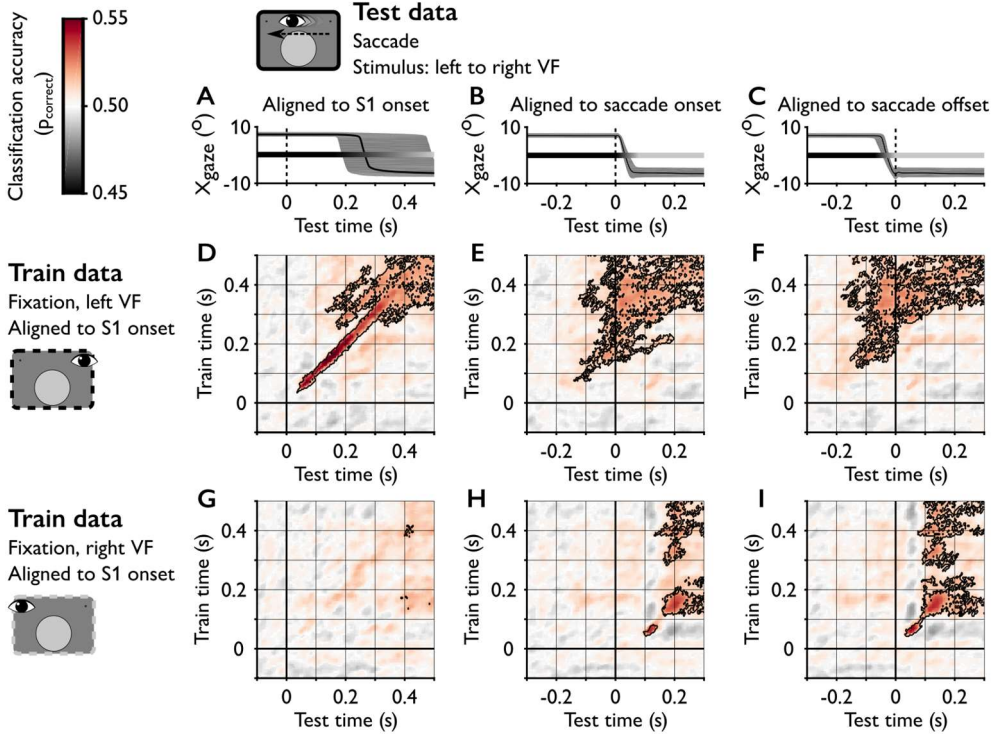
Figure 6. Temporal generalization of spatial frequency cross-classification from the Fixation conditions to the Saccade conditions. Red indicates above chance classification, grey indicates below chance classification. For visualization, classification accuracy was filtered with 5×5 two-dimensional median filter, corresponding to the size of the temporal neighbourhood in the MVPA. Time windows with significant above or below chance classification are outlined. **A., B. and C.** Average horizontal eye position for the three different alignments of the data from the Saccade condition. Shaded area covers eye position in all trials. The horizontal line with a colour gradient from yellow to green depicts the location of the stimulus, with the colour gradient indicating the visual field of the stimulus (black = left VF, grey = right VF). The test data from the Saccade, left VF condition was aligned to three different events. In panels **A** and **D**, the test data is locked to S1 onset. The diagonal line represents time points where train and test time are the same with respect to S1 onset. In panels **B** and **E**, the test data is locked to saccade onset. In panels **C** and **F**, test data is locked to saccade offset. The diagonal line represents time points where train time is the same with respect to S1 onset as the test time is to saccade offset. In panels **D**, **E** and **F**, a classifier was trained to separate the spatial frequency of the stimulus based on data locked to the onset of stimulus 1 (S1) in the Fixation, right VF condition. In panels **G**, **H** and **I**, the classifier was trained on data from the Fixation, left VF condition.

After aligning the Saccade, left VF data to saccade onset it becomes apparent that the classifier trained on the Fixation, left VF is still able to classify spatial frequency from the Saccade data after saccade onset (Figure 6E). Especially the test data between 0 and 0.1 s after saccade onset can be decoded by classifiers trained on Fixation, left VF data from approximately all timepoints between 0.15 to 0.45 s after S1 onset. Crucially, the classifier
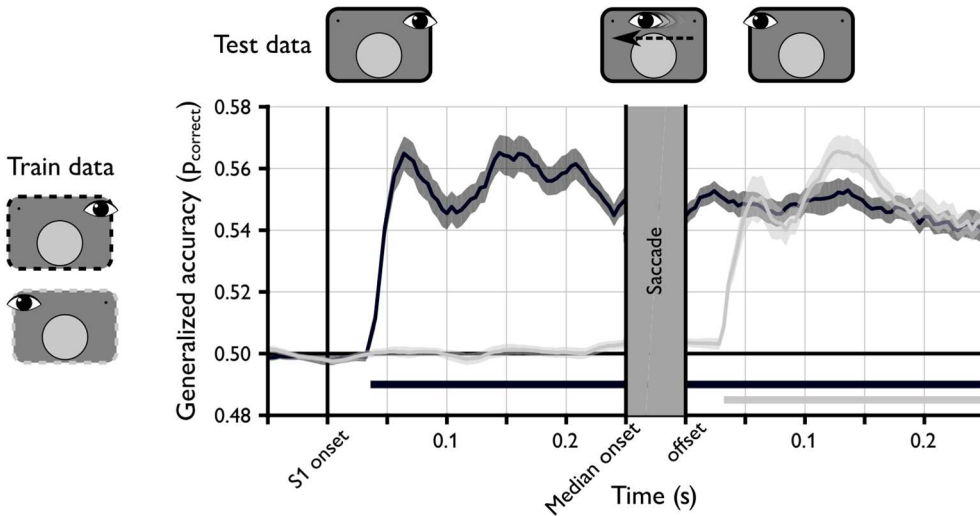
Figure 7. Summary of temporal generalization of cross-classification accuracy presented in Figure 6. Black: train data = Fixation, left VF, test data = Saccade. Grey: train data = Fixation, right VF, test data = Saccade. For each time-point of the test data (Saccade condition), we checked whether at any time-point of the train data (Fixation data) there was significant above chance classification in the temporal generalization of cross-classification, i.e. the columns in the matrices presented in figure 6D, F, G and I. If so, we took the maximum cross-condition classification accuracy in that column. If not, we took the average accuracy over the entire column. Horizontal black and grey line indicate time windows where the maximum was used. For the pre-saccadic time we used the test data locked to stimulus onset, presented in Figure 6D and 6G. For the post-saccadic time we used test data locked to saccade offset, presented in Figure 6F and 6I. Solid line is the group average. Shaded area represents 1 s.e.m. NB: this figure shows a summary of the data in Figure 6 based on both classification accuracy and statistical significance.

trained on the Fixation, right VF data was not able to decode the Saccade data before saccade onset (Figure 6H), but only after ~0.1 s after saccade onset. So, before saccade offset, the patterns in the MEG data do not resemble stimulus evoked patterns when subjects were fixating the post-saccadic fixation location.

After aligning the Saccade, left VF data to saccade offset, the classifier trained on the Fixation right VF data was able to classify significantly above chance, starting 0.032 s after saccade offset (Figure 6I). This above-chance classification is most prominent along the diagonal that time since S1 onset in the training data to the time since saccade offset in the test data. Note that after saccade offset, the stimulus is located in the right visual field, similar to the Fixation, right VF condition. Unlike the narrow temporal generalization in Figure 6D, classifiers trained on timepoints between roughly 0.1 to 0.2 and 0.3 to 0.5 s after S1 onset were able to significantly decode the Saccade data from 0.1 to 0.2 s after saccade offset. The classifier trained on the Fixation, left VF data was able to accurately decode the

Saccade data both before and after saccade offset (Figure 6F). Especially classifiers trained on the time points between 0.3 and 0.4 after S1 onset were able to generalize to the time points in the Saccade data from -0.1 before to 0.3 after saccade offset.

In summary, stimulus locked data contained information about the spatial frequency of the stimulus (Figure 5B), and this information is specific to the visual field in which the stimulus is presented (see cross-classification in Figure 5C). The differences between spatial frequencies of 0.33 cyc/° and 1.33 cyc/° develop rapidly over time (see the limited temporal generalization in Figure 6D). Hence, the representation of spatial frequency might depend primarily on feedforward sweeps of visual information. When a classifier was trained on MEG data evoked by visual input that was similar to the pre-saccadic visual input (Fixation, left VF), it was able to decode the Saccade, left VF data after S1 onset, both before saccade onset and after saccade offset (Figure 7). A classifier trained on responses evoked by visual input that was similar to the post-saccadic visual input (Fixation, right VF), it was able to decode the Saccade, left VF data only after saccade offset (Figure 7). Hence, the response evoked by stimulus onset resembles the response evoked by a stimulus after saccade offset.

Discussion

In this study, we investigated updating of visual information across saccades with magnetoencephalography. Visual information was operationalized as a large sinusoidal grating. In the crucial condition, subjects were presented visual information while also instructed to make a saccade that brought the stimulus from one visual hemifield into the other. In different conditions, we only presented the stimulus but subjects made no saccade, or we did not present a stimulus and subjects only made a saccade.

The spatial profile and temporal development of the evoked response were similar to what would be expected from spatial updating of visual information. In particular, we found a stimulus-contralateral response followed by (also) an ipsilateral response, as previously reported in an EEG study (Parks & Corballis, 2008, 2010). Initially, the event-related planar gradients showed clear responses to the onset of the grating when subjects maintained stable fixation, as expected. Moreover, these responses were stronger in the condition where subjects made a saccade across the grating, shifting it from the left to the right visual field. We modelled the planar gradients from that condition as the weighted linear combination of the planar gradients in response to only a grating but no saccade and in

response only a saccade but no grating. These residual planar gradients were initially lateralized contralateral to the grating. Close to saccade onset, the planar gradients were stronger across the majority of gradiometers, both contralateral and ipsilateral to the grating. One possible interpretation is that this stronger planar gradients reflect updating of visual information from the contralateral hemisphere ("current receptive field") to the ipsilateral hemisphere ("future receptive field"), similar to monkey neurophysiology (Duhamel, Colby, et al., 1992; Kusunoki & Goldberg, 2003; Sommer & Wurtz, 2006) and human EEG (Parks & Corballis, 2008, 2010).

At the same time, behavioural characteristics differed between the conditions. Subjects were essentially performing a dual task in the Saccade, left VF condition – making both a saccade and performing an orientation change detection task – which made the Saccade, left VF task harder than the Fixation, left VF condition. This is reflected in a lower change detection performance in the Saccade, left VF condition. Moreover, because the grating was a strong visual stimulus, saccades towards the stimulus had to be inhibited, and a saccade to the saccade target had to be initiated (Schall, 1995; Van der Stigchel, Meeter, & Theeuwes, 2006). This competition between saccade vectors was absent in the Saccade, no stimulus condition. This is reflected in higher saccade endpoint errors in the Saccade, left VF condition (and one subject who was not able to perform the Saccade, left VF condition at all because she kept making saccades towards the grating). Thus, while the pattern of evoked responses was consistent with spatial updating around the time of saccades, replicating a pattern similar to that reported by Parks and Corballis with EEG (2008, 2010), these responses are open to multiple interpretations. Therefore, in addition to the univariate analysis of average planar gradients, we also used multivariate pattern analysis (MVPA) to examine whether whole-brain MEG responses contained stimulus specific information, operationalized as decoding of spatial frequency.

The multivariate approach focused on performance in decoding spatial frequency across different experimental conditions in order to characterize the spatial and temporal pattern of decoding performance. Data from the Fixation conditions clearly demonstrated that spatial frequency could be decoded from the MEG data. Moreover, these responses were spatially specific: classifiers trained to decode spatial frequency of a grating in the left visual field could not reliably classify spatial frequencies of gratings in the right visual field (or vice versa). In the Fixation conditions, classification accuracy sharply increased ~40 ms after stimulus onset, as observed in a previous study (Ramkumar et al., 2013). Decoding accuracy developed quickly over time and showed very limited temporal generalization. The above

chance classification accuracy and spatial specificity were prerequisites to further use MVPA to investigate when the representation of spatial frequency switches from the left visual field to the right visual field in the Saccade condition. Before saccade onset, the visual stimulation in the Saccade, left VF condition was similar to the visual stimulation in the Fixation, left VF condition. After saccade offset, the visual stimulation in the Saccade, left VF had changed to the stimulation in the Fixation, right VF condition. As summarized in Figure 7, visual stimulation has to match retinotopically before saccade onset for a classifier to be able to decode spatial frequency. Only after the saccade has shifted the stimulus to the other visual hemifield could the other classifier decode spatial frequency. In other words, the response to a spatial frequency after stimulus onset resembles the response to the same spatial frequency after saccade offset. This finding suggests that the spatial frequency classifier primarily uses feedforward information that is retinotopically organized. In addition to these feedforward responses there seems to be lingering representation of the pre-saccadic stimulus after saccade offset. The classifier trained on data from the Fixation, left VF condition could still decode spatial frequency after saccade offset, when the stimulus had been brought from the left into the right visual field in the Saccade, left VF condition. This finding shows that it would be possible, in principle, for higher visual area to read out the spatial frequency of the stimulus during the entire interval, across the saccade.

This pattern of results has several interesting implications for theories of perceptual continuity. First, the results show how stimulus specific information is present from feedforward responses very quickly, after about 40 ms (considering the radius of temporal search light window of 8 ms). This estimate is similar to a previous study that decoded spatial frequency with MEG (Ramkumar et al., 2013). The ultra-low latency of spatial frequency specific information in the MEG data suggests that the classifier used signals from early visual areas. Neurophysiology studies with monkey subjects showed different latencies (30-50 ms) to spatial frequencies in the superior colliculus (Chen, Sonnenberg, Weller, Witschel, & Hafed, 2018) and V1 (Maunsell & Gibson, 1992; Mazer, Vinje, McDermott, Schiller, & Gallant, 2002). One of the key arguments that perceptual continuity across saccades poses a major challenge for the visual system is the delay in the transmission of visual information through the visual system (for example, see Melcher & Colby, 2008). A number of neurophysiological and behavioural studies have shown that pre-saccadic stimulus affects perception of the post-saccadic stimulus immediately after saccade offset (Deubel et al., 1998; Edwards et al., 2018; Fabius et al., 2016; Mirpour & Bisley, 2016). After that period, the new feedforward information develops quickly, as we observed similar rapid

ramping up of feedforward information after saccade offset. Increasing evidence shows that category specific responses develop within 100 ms after stimulus onset as measured with MEG (Carlson et al., 2013) and as reflected in human saccadic responses (Kirchner & Thorpe, 2006; Thorpe, Fize, & Marlot, 1996). The interaction between this rapid feedforward response and the lingering pre-saccadic representation of the stimulus might play an important role in stable and continuous perception across the saccade.

Second, we did not observe statistically significant above-chance decoding from the post-saccadic classifier before saccade onset, but only rapidly after saccade offset (~40 ms). Performance of the pre-saccadic classifier showed above-chance decoding before and across the saccade, well into the new fixation. This could provide another potentially valuable clue as to why perception seems stable and continuous. Given that stimuli do not typically change during the saccade, it would be possible to "read out" the correct spatial frequency of the stimulus continuously across the saccade. About 40 ms after saccade offset, the pre-saccadic and the post-saccadic information about the stimulus would converge. This temporal overlap could reflect a "soft handoff" in information transfer, resembling attentional tracking of a moving object (Drew et al., 2014; Khayat, Spekreijse, & Roelfsema, 2006). Our results are consistent with a "soft handoff", rather than a "hard handoff" in which neurons rapidly cease to represent the pre-saccadic stimulus. It is interesting to note that studies of parietal neurons have shown a wide variety of behaviours, with some cells responding to the future receptive field even prior to the saccade, i.e. predictive remapping (Duhamel, Colby, et al., 1992) but also many maintaining the response to the pre-saccadic receptive field briefly after the saccade ended (Mirpour & Bisley, 2016), which has been suggested to be important for post-saccadic updating (Ong et al., 2009). Thus, one interpretation of the current results is that visual information was not updated before saccade onset, but rather maintained retinotopically, and integrated after saccade offset.

The current results show a pre-saccadic enhancement in event-related planar fields and simultaneously, a long pre-saccadic representation of spatial frequency. Although we cannot test this directly, it seems that the pre-saccadic ERFs do not contain information about spatial frequency. At least not in a similar structure as spatial frequency is processed after stimulus onset. One possible explanation is that the pre-saccadic modulation of ERFs reflects a "predictive remapping of attentional pointers", but not of visual feature information (Cavanagh et al., 2010). After saccade offset, the new retinal location of the stimulus is quickly sampled for new feedforward information. This new information can then be combined with the lingering pre-saccadic information to assess continuity of the visual

features. Hence, perceptual continuity seems to require four ingredients: current visual information and current eye position, as well as lingering pre-saccadic visual information and lingering pre-saccadic eye position. Here, we demonstrate that both the pre- and post-saccadic visual information can be decoded from the MEG data. Moreover, a recent neurophysiological study demonstrated that eye position can be decoded with various lags from the same populations of neurons in LIP, VIP, MT and MST, by reweighting inputs connections between the neurons and the decoder (Morris, Bremmer, & Krekelberg, 2016). Thus, it seems theoretically feasible to obtain the four ingredients to assess perceptual continuity from neural data following a soft handoff of information transfer after rapidly saccade offset.

Chapter 4 – Supplementary information
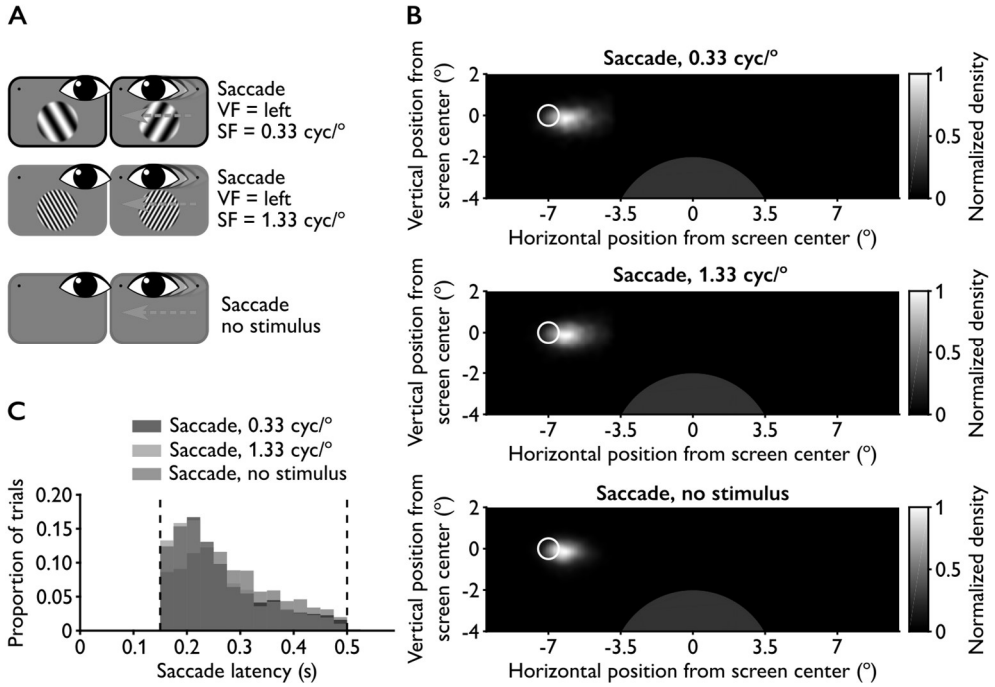
A

B

C

Figure S1. Saccade parameters. **A.** Reminder of the procedure of the Saccade conditions. **B.** Histogram of saccade latencies separated for the three Saccade conditions. The vertical dashed lines represent the inclusion criteria for saccade latencies (i.e. 0.15 and 0.5 s). **C.** Two dimensional density of saccade landing points. Each panel corresponds to one Saccade condition. Densities are normalized to the peak density per condition. Circular patch at (-7, 0) is a lay out of the saccade target. Large circle at (0, -6) represents the outline of the stimulus.
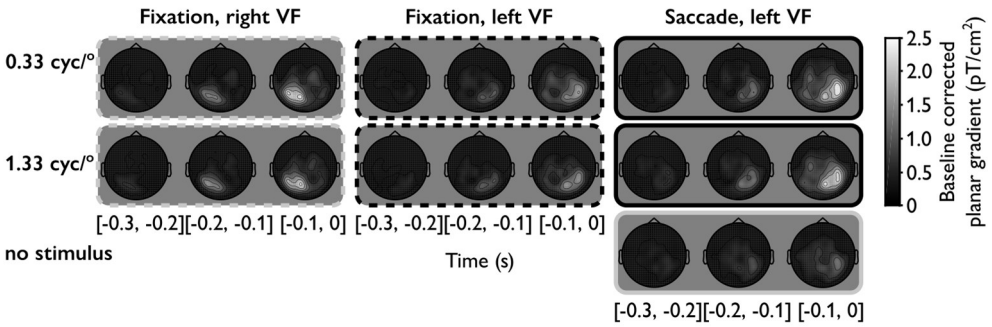
Figure S2. Baseline-corrected event-related planar gradients from combined gradiometers, with data locked to saccade onset. Each panel represents a different condition. Each heatmap within a panel corresponds to a different time window, as displayed beneath the panels. Time is relative to saccade onset. Baseline correction was a subtraction of the average planar gradient in the time-window from -0.6 to -0.5 s before saccade onset. See "Methods: Trial length matching" for the procedure of locking data of the Fixation conditions to 'saccade onset'.
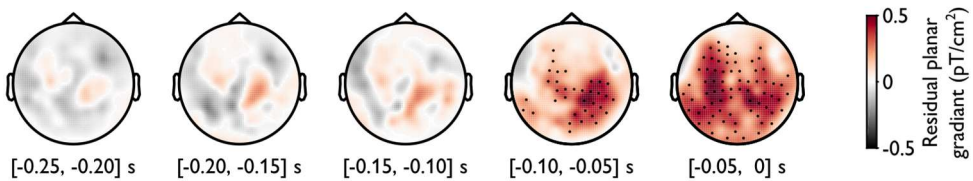

Figure S3. Topographical heatmap of median residual planar gradients of 500 different trial length matchings. Black points indicate sensors where the absolute median z-value of the cluster-summed t-statistic was larger than 1.96 for more than 12.5 ms in a time-window.
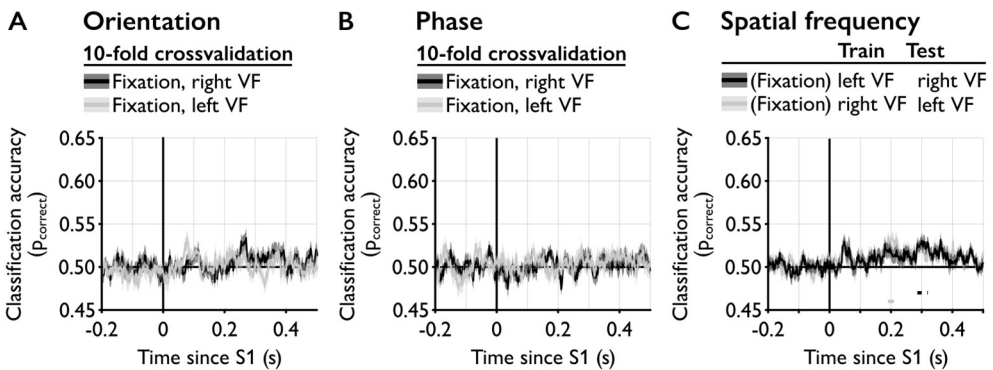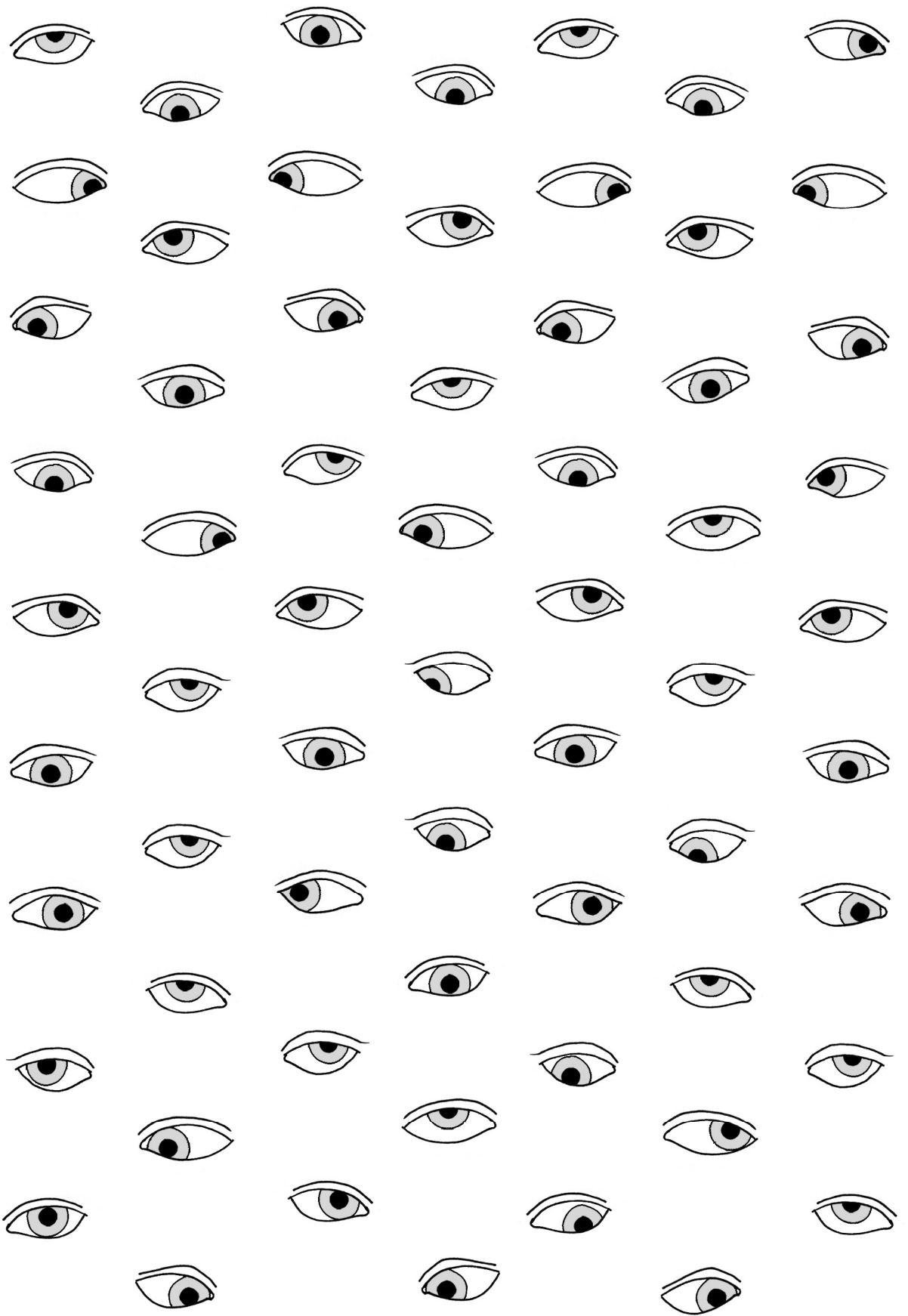

Figure S4. Stimulus 1 locked MVPA results. **A.** Classification of stimulus 1 orientation. **B.** Classification of stimulus 1 phase. **C.** Cross-decoding accuracy of spatial frequency between the two different Fixation conditions.

4

Chapter 5

Perceptual continuity across eye movements after a lesion to the posterior parietal cortex

Abstract

Visual perception is introspectively stable and continuous across eye movements. It has been hypothesized that displacements in retinal input caused by eye movements can be dissociated from displacements in the external world by the use of extra-retinal information, such as a corollary discharge from the oculomotor system. The extra-retinal information can inform the visual system about an upcoming eye movement and accompanying displacements in retinal input. The parietal cortex has been hypothesized to be critically involved in integrating retinal and extra-retinal information. Two tasks have been widely used to assess the quality of this integration: double-step saccades and intra-saccadic displacements. Several studies had indicated that patients with lesions to the parietal cortex showed hypometric second saccades, that critically rely on extra-retinal information. However, recently another study refuted this idea by demonstrating that patients with very similar lesions were able to perform the double step saccades, albeit taking multiple saccades to reach the saccade target. So, it seems that extra-retinal information is still available for saccade execution after a lesion to the parietal lobe. Here, we investigated whether extra-retinal signals are also available for perceptual judgements in nine patients with strokes affecting the posterior parietal cortex. We assessed perceptual continuity with the intra-saccadic displacement task. Patients did not show major differences from control subjects, suggesting that extra-retinal signals still influence perceptual judgements of stimulus displacements across eye movements.

Introduction

Eye movements (saccades) introduce brief disruptions and distortions to the inflow of visual information through the eyes. Yet, introspectively, most humans perceive a stable and continuous visual world. It has been hypothesized that perceptual continuity across eye movements is related to 'remapping of receptive fields' of visual neurons (Cavanaugh et al., 2016; Crapse & Sommer, 2012; Mirpour & Bisley, 2016). This neuronal property is defined as a modulation of the response profile to visual stimuli (retinal information) by neural signals that carry information about eye movements (extra-retinal information). Remapping of receptive fields was first discovered in the lateral intraparietal sulcus of the macaque (Duhamel, Colby, et al., 1992), and later in other areas such as the superior colliculus (Walker et al., 1995), V4 (Tolias et al., 2001) and the frontal eye fields (Umeno & Goldberg, 1997).

These discoveries sparked interest in the behavioural consequences of a lesion to areas where neurons exhibit remapping properties. The hypothesis was that extra-retinal signals are either not available or not used appropriately after a brain lesion and therefore remapping of retinal information would be disrupted (Duhamel, Goldberg, et al., 1992; Heide et al., 1995). To test this hypothesis behaviourally, subjects with lesion affecting the frontal lobe or posterior parietal cortex (PPC) were asked to perform double step saccades (Hallett & Lightstone, 1976). In this task, two flashes of light are presented briefly in sequence. Subjects are asked to make two saccades, from the initial fixation point to the first target and then on to the second target. The rationale for using this paradigm to test for remapping is that the location of the second target must be updated after the first saccade. The retinal location of the second target cannot be used to execute the second saccade because it is not appropriate anymore after the first saccade, i.e. the retinal location of the second target has to be remapped based on the vector of the first saccade. Two studies indeed provided evidence that subjects with lesions to the PPC exhibit hypometric second saccades when the first saccade was directed to the ipsilesional side (Duhamel, Goldberg, et al., 1992; Heide et al., 1995). Later, the same observation was made for patients with a thalamus lesion (Bellebaum, Daum, Koch, Schwarz, & Hoffmann, 2005; Ostendorf et al., 2010). However, recently, the two studies focusing on PPC lesions have been criticized for two main reasons (Rath-Wilson & Guitton, 2015). In the study of Rath-Wilson and Guitton (2015), 6 patients with nearly identical lesions as the patients in the older studies

5

performed the same double-step saccade task and two other variation thereof. The first criticism was that the trial exclusion criteria were too conservative in the older studies. Although the second saccade was hypometric according to the original analysis, these saccades tended to be followed by one or more saccades bringing the fixation location close to the second target. When analysing this 'composite second saccade', performance was on par with controls. The second criticism was that the classic double step task can be confusing, and subject tend to mix up the order of the two targets. With two variations on the classic double step task, where this problem was circumvented, patients performed again on par with controls. Hence, extra-retinal signals seem to guide saccades after a lesion to the PPC.

Double step saccades assess the accuracy and precision of extra-retinal signals for motor control, but not for perception. To directly assess the influence of extra-retinal signals on perception, the intrasaccadic displacement task has been used in both humans (Bridgeman et al., 1975; Deubel et al., 1996) and monkeys (Cavanaugh et al., 2016). This task has also been used in patients with thalamus lesions (Ostendorf et al., 2010, 2013), but not yet in patients with PPC lesions. The intrasaccadic displacement task consists of two conditions. In the first condition (STEP), subjects are asked to make a saccade to a target when it appears. The saccade target is displaced during the saccade, and subjects are asked to indicate the direction of the displacement. In the second version (BLANK), the saccade target is removed during the saccade, and then reappears displaced 300 ms after saccade offset. In the STEP condition, surprisingly large displacements go unnoticed to an observer, with thresholds around 30% of the saccade amplitude. However, the temporal gap between saccade offset and target onset in the BLANK condition improves detection sensitivity, with thresholds around 10% of the saccade amplitude (Deubel et al., 1998, 1996). The failure to detect a displacement in the STEP condition suggests that subjects primarily use visual information rather than extra-retinal information in trans-saccadic perception (Deubel et al., 1998; see also Fabius, Fracasso, & Van der Stigchel, 2016). However, the availability and use of extra-retinal signals is highlighted by the improvement after a brief post-saccadic blank period. In other words, the increase in sensitivity from the STEP condition to the BLANK condition indicates the availability of extra-retinal information for perceptual judgements.

The increase in sensitivity from the STEP to the BLANK condition has been used to study impairments in extra-retinal signals. Patients with thalamus lesions demonstrated a sensitivity decrease instead of increase from the STEP to the BLANK condition, i.e. they

performed worse when they had to rely on extra-retinal signals (Ostendorf et al., 2010, 2013). Although no studies have used this task in patients with PPC lesions, there are two studies that have assessed location memory across saccades with a more cognitive task (Russell et al., 2010; Vuilleumier et al., 2007). Subjects with right hemisphere lesions were instructed to keep the location of a peripheral stimulus in memory and make a saccade such that the memorized location moved from the left to right visual field (or vice versa). After a delay, a second stimulus appeared either at the same location or displaced from the remembered location. Sensitivity was abnormally low when the stimulus was moved from the right to the left visual field, with an ipsilesional saccade (Russell et al., 2010; Vuilleumier et al., 2007). Although the time scale of this task differs from the intra-saccadic displacement task – and therefore putting more emphasis on working memory – their results suggest that spatial memory is degraded after an ipsilesional saccade in patients with PPC lesions.

Here, we test the hypothesis that lesions to the PPC specifically affect the integration of retinal and extra-retinal signals for perception using the intrasaccadic displacement task. If the hypothesis is correct, then a lesion to the PPC should result in a decreased sensitivity in the BLANK condition as compared to the STEP condition. Neurophysiological evidence suggests that neurons in the PPC are important for the integration of retinal and extra-retinal signals for visual perception (Duhamel, Colby, et al., 1992; Mirpour & Bisley, 2016; Subramanian & Colby, 2014). Evidence from patients with PPC lesions demonstrates that the PPC is not crucial for the use of extra-retinal signals in motor control (Rath-Wilson & Guitton, 2015). The use of extra-retinal signals for motor control seems to be related more to the functioning of a network between the thalamus and the frontal eye fields (Ostendorf et al., 2010; Sommer & Wurtz, 2002, 2006). Possibly, lesions to the PPC specifically affect the integration of retinal and extra-retinal signals for perception, but not for motor control.

Methods

Subjects

12 patients in the chronic phase post-stroke onset (>4 months) with chronic stroke damage and 13 healthy control subjects participated. Patients were invited for participation after inspection of their clinical imaging data (MRI or CT scan) from existing databases at the UMC Utrecht that are available for scientific purposes. This database contains patients who had been admitted because of (suspected) cerebrovascular problems. Patients included

5

Table 1. Demographics. The rows are ordered according to (1) PPC damage and (2) lesion volume.

ID	Age[1]	Sex[2]	Modified[3] Rankin Scale (after 3 months)	Years since CVA	Scan	Lesion volume (ml)	Percentage damaged[4]				
							PPC	SPL	IPG	SMG	AG
L	55	0	2	1.85	CT	167.2	51.97	0.08	41.06	94.80	64.99
A	65	0	3	4.43	MRI	187.6	47.08	2.93	43.53	93.18	42.14
C	76	1	1	5.43	CT	48.2	25.47	54.79	20.51	0.04	28.29
K	47	1	2	6.10	MRI	37.2	23.69	56.16	36.59	2.18	4.44
D	57	1	2	2.53	MRI	26.4	14.12	0	8.28	42.42	0
I	41	0	1	5.92	MRI	47.5	12.97	0	0.80	20.80	27.05
H	63	0	2	3.48	CT	64.2	5.05	0	0	14.39	3.26
M	59	1	2	0.34	MRI	6.6	4.77	0	5.71	0	14.88
J	48	0	2	5.91	MRI	1.4	0.91	0.01	3.41	0.84	0
E	51	0	0	4.17	MRI	57.4	0	0	0	0	0
B	81	1	2	1.90	MRI	0.9	0	0	0	0	0
F	75	0	3	5.15	MRI	-	-	-	-	-	-
Average[5]	56.8	0.44	1.89	4.00	-	65.2	20.67	12.66	17.77	29.85	20.56
Controls	53.6 [39, 66]	0.54	-	-		-	-	-	-	-	-

[1] For the controls the average is noted, and the min and maximum individual values are noted between brackets.

[2] 0 = female, 1 = male

[3] The modified Rankin scale ranges from 0 (no symptoms) to 6 (dead)

[4] PPC = posterior parietal cortex, SPL = superior parietal lobule, IPG = inferior parietal gyrus, SMG = superior marginal gyrus AG = angular gyrus

[5] The average is the average of subjects with lesions to the PPC (i.e. not subject E, B or F).

in this database provided informed consent to have their imaging data be inspected for scientific purposes. Patients were included in the current study when there appeared to be

a lesion to the right posterior parietal cortex (PPC). In practice, the right PPC was defined as lesions found A) posterior to the postcentral gyrus, B) dorsal to the posterior horn of the right lateral ventricle and C) not posterior to the parieto-occipital sulcus. Later, lesion locations were determined exactly by an expert neurologist. Patients were not included when they had exhibited clinical signs of visual field defects, a history of substance abuse, or an inability to understand the task instructions. See Table 1 for the demographic data of all patients and a summary of the healthy controls.

Lesion location

Lesions were drawn by a trained neurologist and projected to the MNI-152 anatomical template using MRIcron (Chris Rorden & Brett, 2000). We parcellated the posterior parietal cortex into four anatomically defined areas with the Automated Anatomical Labeling atlas (Tzourio-Mazoyer et al., 2002) available in MRIcron. We defined the PPC to comprise the superior parietal lobule (SPL), inferior parietal gyrus (IPG), supramarginal gyrus (SGM) and angular gyrus (AG). For the entire PPC and each subarea, we computed the percentage of lesioned voxels of the MNI-template in MATLAB. These data are summarized in Table 1.

Experimental setup

Stimuli were displayed on a 48.9° by 27.5° Asus RoG Swift PG278Q, an LCD-TN monitor with a spatial resolution of 52 pixels/° and a temporal resolution of 120 Hz (AsusTek Computer Inc., Taipei, TW) in a darkened room. The ultra low motion blur backlight strobing option of the monitor was disabled. Eye position of the left eye was recorded with an Eyelink 1000 at 1000 Hz (SR Research Ltd., Mississauga, ON, Canada). The eye-tracker was calibrated using a 9-point calibration procedure. All stimuli were created and presented in MATLAB 2016a (The Math Works, Inc., Natick, MA.) with the Psychophysics Toolbox 3.0 (Kleiner et al., 2007) and the Eyelink Toolbox (Cornelissen et al., 2002). Visual onsets and eye-movement data were synchronized offline based on independent photodiode measurements (Fabius et al., 2019). To this end, we added 11 ms to the timestamps in the Eyelink data files that indicated visual onset during the experiment. This lag of 11 ms is most likely caused by input lag of the monitor and similar in magnitude to measurements by another group (Zhang et al., 2018).

Intrasaccadic displacement task (Figure 1A)

Fixation targets were grey circles (13.01 cd/m^2, ø = 0.5°) with a superimposed black cross (line width = 0.15°) and grey point (Thaler et al., 2013), presented on a black background (0.06 cd/m^2). A stimulus appeared after a period of stable fixation (randomly sampled from the uniform distribution on the open interval [500, 1000] ms). Stimuli were red circles (5.40 cd/m^2, ø = 0.5°) presented 10° to the left or to the right of the fixation target, on the same horizontal axis as the fixation target. Subjects made a saccade towards the stimulus. When gaze was detected within a radius of 8° around the target, the stimulus was either displaced on the horizontal axis (STEP condition) or it disappeared for 300 ms and was displaced when it reappeared (BLANK condition). Subjects indicated the direction
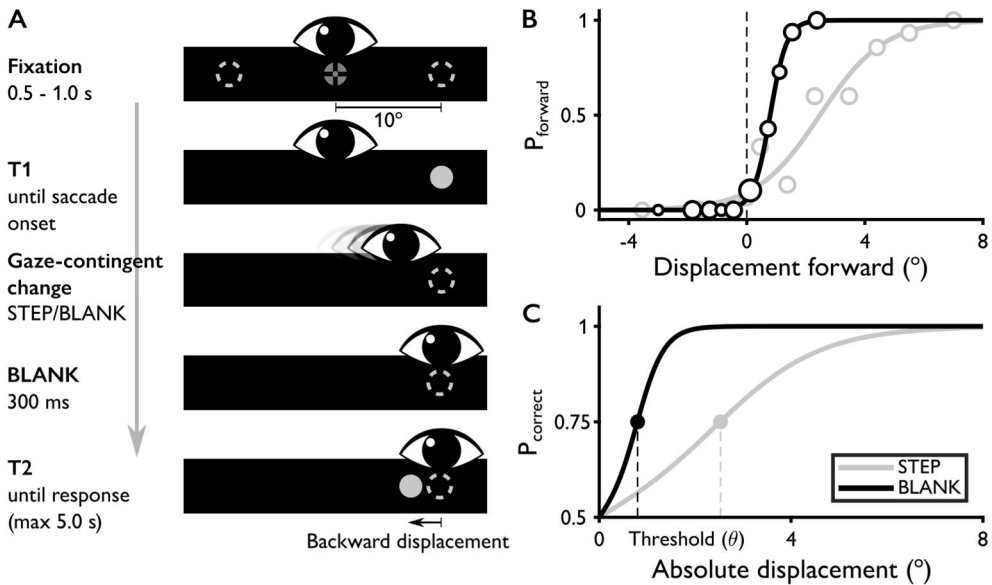
Figure 1. Experiment methods and example results. **A.** Trial sequence in the BLANK condition. Target size is not to scale. The BLANK was absent in the STEP condition, insteadT2 (or, the displaced target) appeared during the gaze-contingent change. **B.** Example psychometric function of the STEP (grey) and BLANK (black) condition for leftward saccades of one control subject. Circles represent the average proportion 'forward' responses in a bin. The size of the circles scales with the number of trials in that bin. Lines represent the fitted psychometric functions. The psychometric functions were fitted with two free parameters: the mean and the width. **C.** To make comparisons across conditions and subjects easier, we converted the psychometric functions to proportion correct. We defined the threshold (θ) as the absolute displacement where performance was 0.75 correct. With the thresholds from the STEP and the BLANK conditions we calculated an index to capture the availability of extra-retinal information: Δthreshold index = (θ_{STEP}-θ_{BLANK}) / (θ_{STEP}+θ_{BLANK}).

of the displacement by pressing the left or right arrow key on a standard keyboard. When no responses or no saccade was detected after 10 seconds, the trial was aborted and later repeated. Trials were divided into block of 32 trials. We collected as many trials as possible for patients within a time limit of 2 hours including breaks.

Adaptive range of displacements

The displacement size varied from trial to trial and was sampled (without replacement) from a set of 32 displacement sizes that was compiled at the start of each block. This set was based on performance in all preceding blocks. In the first block, the displacement set was equal for all subjects, consisting of 2 repetitions of 15 linearly spaced displacements ranging from -5.8° to 5.8° in the STEP condition and from -3.5° to 3.5° in the BLANK condition. Additionally, we added two displacements of 0 (i.e. no displacement) to each set.

Because we planned to fit psychometric function to the displacement data, we wanted to capture an appropriate range of displacements. However, we also wanted subjects to understand the task, and avoid confusion. To this end we implemented some adaptive variation to the limits of the displacement set. We adjusted the upper and lower limit of the displacement set after each block based on a simple logistic fit (i.e. only fitting the slope and offset, but keeping the asymptotes fixed to 0 and 1). The limits were set to the estimated displacement size to get to a performance of 0.99 and 0.01. The upper limit was constrained to be <= 7.5°, the lower limit was constrained to be >= -2°. In addition to the 30 linearly spaced displacements in this range (15 unique values repeated twice), we added two displacements of zero to each block, like in the first block. With these constrains we ensured that each block contained trials with leftward and rightward displacements, and trials without any physical displacement.

Preprocessing

Saccades were detected with the algorithm by Nyström and Holmqvist, with a minimum saccade duration of 10 ms, a minimum fixation duration of 40 ms (Nyström & Holmqvist, 2010). To ensure the online gaze-contingency worked adequately, all trials were visually inspected by plotting the x coordinate, y coordinate, velocity profile and x-y gaze path, with markings for the timing of visual on- or offsets. Trials where saccade latency was < 80 ms, saccade amplitude was < 2°, eye velocity was < 150°/s or the difference between saccade offset and T1 offset was < 10 ms were highlighted to the inspector. Moreover, trials where response time < 200 ms or > 5000 ms were removed automatically.

Psychometric functions

We fitted a logistic function with two free parameters (mean and width) to the proportion 'forward' responses as a function of displacement size using Psignifit 4.0 (Schütt, Harmeling, Macke, & Wichmann, 2016). We fitted four psychometric functions, one per condition (STEP, BLANK) and saccade direction (left, right). Figure 1B shows example fits for the STEP and the BLANK condition for one subject for leftward saccades. As an estimate of the quality of the fitted psychometric function, we correlated the measured proportion forward responses with the predicted proportions from the fitted psychometric function (Wichmann & Hill, 2001). Following Ostendorf et al. (2010, 2013), we converted the fits to proportion correct as a function of the absolute displacement size (Figure 1C). Next, we defined the threshold (θ) as the absolute displacement where performance equals a

proportion of 0.75 correct. This measure captures the mean and the width of the function simultaneously. With the thresholds from the STEP and the BLANK conditions we calculated an index to capture the availability of extra-retinal information: Δthreshold index $= \frac{\theta_{STEP} - \theta_{BLANK}}{\theta_{STEP} + \theta_{BLANK}}$. Positive values indicate that the threshold in the STEP condition was higher than in the BLANK condition, and thus that detection sensitivity improved in the BLANK condition. Negative values indicate a worse performance in the BLANK condition that in the STEP condition.

Analysis

We performed two analyses, one confirmatory and one exploratory. For the confirmatory analysis, we tested the hypothesis that damage to the PPC impairs behavioural performance that relies on extraretinal signals. The behavioural performance is here operationalized as the Δthreshold index (see Psychometric functions). Following this hypothesis, the Δthreshold index should be ≤ 0, or more leniently, the index should at least be lower than the indices of the control group. We also assessed the group difference between patients and controls in thresholds and Δthreshold indices with Bayesian mixed design ANOVA's. In an exploratory analysis, we analysed the relationships between damage in specific subregions of the PPC and the Δthreshold index. These relationships were assessed using Bayesian interpretations of Kendall rank correlations (van Doorn, Ly, Marsman, & Wagenmakers, 2016).

Results

Demographics

Of the 12 subjects included based on an initial inspection of the available medical imaging data, 9 subjects had a lesion in the PPC (Figure 2). Patient E had extensive bilateral lesions that cover the superior frontal lobes but did not extend entirely to the PPC. Patient B only had two small lesions, with one in the white matter tracts beneath the PPC. Although Patient F had multiple lesions the available scans were not suitable for manual labelling of the lesion. We will further discuss the performance of the other patients relative to the controls, but for completeness, the values of patients B, E and F will be displayed in tables and figures but will not be included in the averages of the patient group. The group of
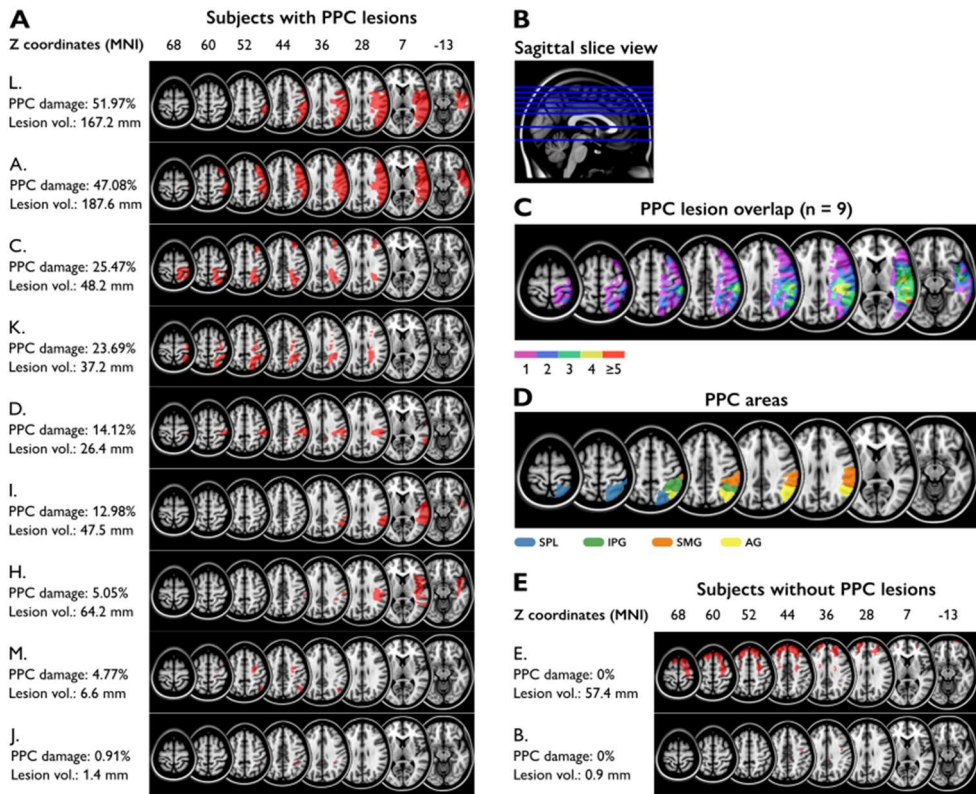
Figure 2. Lesions projected onto MNI template brain. **A.** Individual lesions of all subjects with lesions in the posterior parietal cortex (PPC). Subjects are ordered according PPC damage and lesion volume. Percentage of damage is calculated based on location of the superior parietal lobule, inferior parietal gyrus, supramarginal gyrus and angular gyrus according to the Automated Anatomical Labelling atlas. **B.** Sagittal view of slices. Slices are chosen to facilitate the inspection of the PPC. **C.** Lesion overlap of the 9 subjects with lesions to the PPC. **D.** Areas that define the posterior parietal cortex (PPC) according to the AAL atlas. **Abbreviations:** SPL = superior parietal lobule, IPG = inferior parietal gyrus, SMG = supramarginal gyrus, AG = angular gyrus. **E.** Individual lesions of the subjects without lesions to the PPC.

patients with PPC lesions did not differ substantially in age (BF_{10} = 0.492) or female-male ratio (BF_{10} = 0.491) from the group of controls.

Psychometric functions

Because we constrained data collection to a time limit rather than a trial limit, we could not anticipate the number of trials per condition or saccade direction. Still, we needed to fit 4 psychometric functions on the available data: for leftward and rightward saccades in the STEP and in the BLANK conditions. For all control subjects we had on average 165 trials per function (min = 129, max = 192). For patients, we had 123 trials on average.

However, for patient A we had only 39 and 42 trials for leftward saccades in the STEP and BLANK condition, respectively. For F we only had 47 and 46 trials in the STEP condition for left- and rightward saccades respectively. Therefore, the data from these patients in these conditions should be interpreted with caution. In all other cases we had more than 100 trials per condition and saccade direction to estimate the parameters of the psychometric function. All estimated psychometric functions are displayed in Figure S1. Correlations between measured proportion forward and estimation from the fitted psychometric function were high and all significantly larger than zero ($\alpha = 0.05$, one-sided) for the data of control subjects (mean $r = 0.98$, s.d. = 0.01). For patients with PPC lesions, most correlations were high and significantly larger than zero as well (mean $r = 0.93$, s.d. = 0.15), except for the fitted psychometric functions on the data of leftward saccades of patient A, in both the STEP ($r = 0.52$, $p = 0.05$) and BLANK conditions ($r = 0.26$, $p = 0.22$). These correlations show that the quality of the fitted psychometric functions was high, except for the data for leftward saccades of patient A.

Displacement sensitivity

The thresholds are displayed for each patient and summarized for the control group in Figure 3 (and Table S1). We tested for difference in thresholds using a Bayesian mixed-design ANOVA, with the factors group (patient/control) condition (STEP/BLANK) and saccade direction (left/right). For this analysis we took the log transformed thresholds. The data provide strong evidence for a main effect of condition, with higher thresholds in the STEP than in the BLANK condition ($BF_{10} = 5.26 \times 10^4$). In addition, the data are suggestive of higher thresholds in the patient group than in the control group ($BF_{10} = 7.14$). The data provide inconclusive evidence about the main effect of saccade direction or any of the interaction effects ($0.29 \leq$ all $BF_{10} \leq 2$). Together, this analysis shows that, in general, displacement sensitivity is higher in the BLANK than in the STEP condition, and that subjects with a lesion to the PPC are generally less sensitive to accurately discriminate the displacement directions than controls irrespective of saccade direction or condition.

ΔThreshold index

To directly examine the availability of extra-retinal information, we calculated an index to capture the difference in sensitivity between the STEP and in the BLANK condition (Figure 3C, 3D). Values above zero indicate a lower threshold in the BLANK than in the STEP condition and therefore suggest the use of extra-retinal information. As is apparent
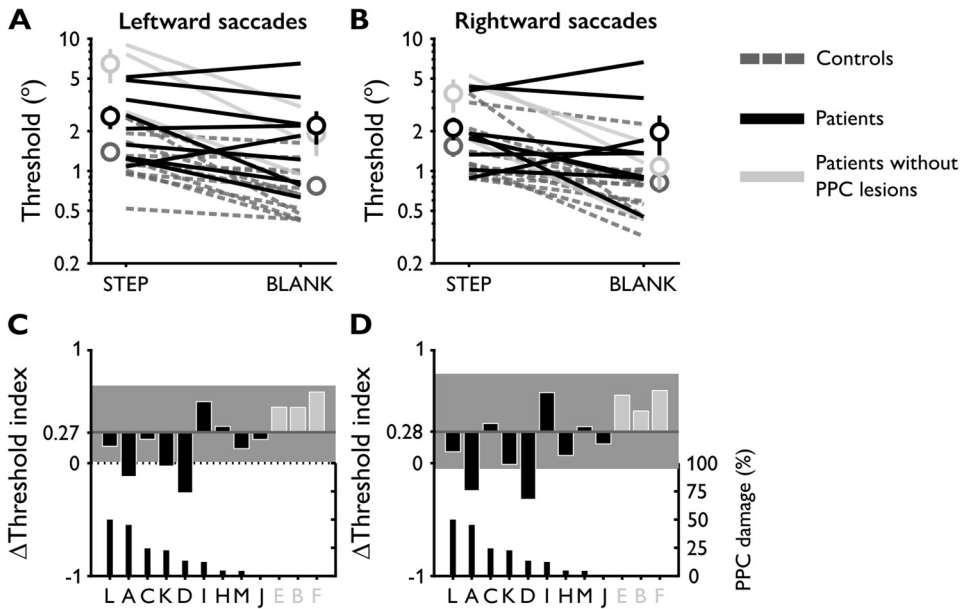
Figure 3. Displacement sensitivity. In panel A and B, each line represents one subject. Circles represent the group averages, error bars 1 s.e.m. Solid black represents subjects from the patient group, dashed dark grey the control group, solid light grey the patients without PPC damage (B, E, F). **A.** Thresholds for leftward saccades. Note that the y-axis is logarithmically scaled to increase visibility of the majority of subjects with low thresholds. **B.** Like A but for rightward saccades. **C.** Δthreshold index for leftward saccades. Each bar represents one subject of the patient group. The grey patch covers the minimum and maximum of the control group. The horizontal solid gray line is the average of the control group. Bars on the x-axis represent the percentage of damage in the PPC as marked by the righthanded y-axis. **D.** Layout identical to C but for rightward saccades.

from the number in Table 3, not all patients with lesions to the PPC have a negative Δthreshold index, nor do they all score below the control subjects. In addition to this conservative analysis, we performed a Bayesian ANOVA on Δthreshold index with the factors direction and group. The data are inconclusive about the effect of group (BF_{10} = 1.00), direction (BF_{10} = 0.30) or the interaction effect (BF_{10} = 0.43). This means that although a lesion affected the PPC, these subjects still have access to extra-retinal information as suggested by the presence of a reliable blank-effect (Deubel et al., 1996).

Correlation lesion and Δthreshold index

There was no clear relationship between lesions in the PPC and the availability of extra-retinal signals as captured by the Δthreshold index. However, the Δthreshold index of two patients meet the criteria for a lack of extra-retinal signals as formulated in the Methods, and 1 closely approached these criteria (A, D and K, respectively). As an exploratory
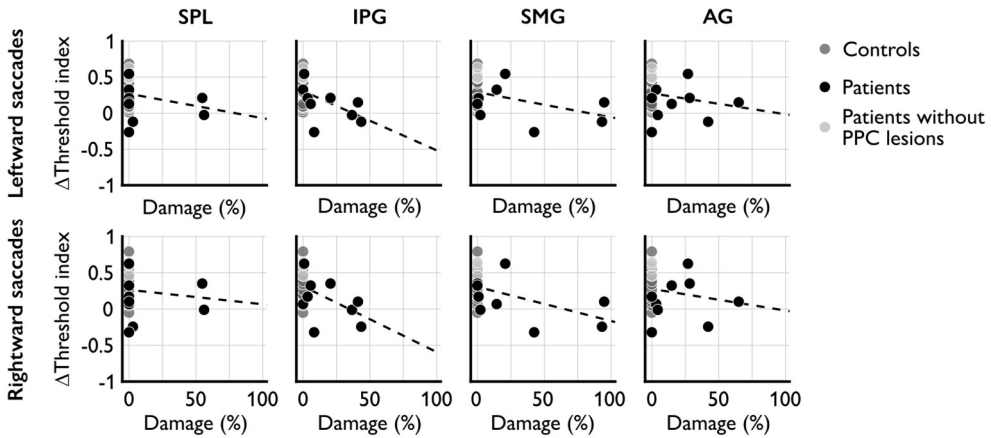
Figure 4. Correlation between the percentage of damage per subarea of the PPC and the Δthreshold index. The upper row of panels contains the Δthreshold index for leftward saccades, the bottom panels for rightward saccades. In each panel, the black circles represent subjects with lesions in the PPC, dark grey circles the control group and light grey circles the subjects with lesions but not in the PPC. The dashed line is the least squares fit. **Abbreviations:** SPL = superior parietal lobule, IPG = inferior parietal gyrus, SMG = supramarginal gyrus, AG = angular gyrus.

analysis, here we correlate the percentage of damage to each of the four subareas of the PPC with the Δthreshold index. In this analysis, all subjects (9 patients with PPC lesions and 13 controls) are included and we use the Bayesian interpretation of Kendall's rank correlation. Bayes Factors are computed for the one-sided hypothesis that more damage is related to lower Δthreshold indices. Please note that these correlations should only be interpreted as exploratory because there are only 9 subjects with PPC lesions in the current dataset. Because we included only patients with right hemisphere lesions, we separated trials with leftward and rightward saccades. For the Δthreshold index of leftward saccades, there is inconclusive evidence for a correlation with the percentage of damage in any of the PPC areas ($-0.29 \leq \tau \leq -0.08$, $0.4 \leq BF_{10} \leq 3$). For the Δthreshold index of rightward saccades, there is suggestive evidence for a correlation with the percentage of damage in the SMG ($\tau = -0.30$, $BF_{10} = 3.26$), but inconclusive for the other areas ($-0.24 \leq \tau \leq -0.08$, $0.4 \leq BF_{10} \leq 1.6$). One careful and typical consideration with lesion-behaviour relationships is the correlation between the size of the lesion and behaviour. A larger lesion is more likely to result in stronger or more general impairments than a smaller lesion. Here, there was inconclusive evidence for a correlation between lesion volume and the Δthreshold index both for leftward ($\tau = -0.17$, $BF_{10} = 0.81$) and rightward saccades ($\tau = -0.23$, $BF_{10} = 1.45$).
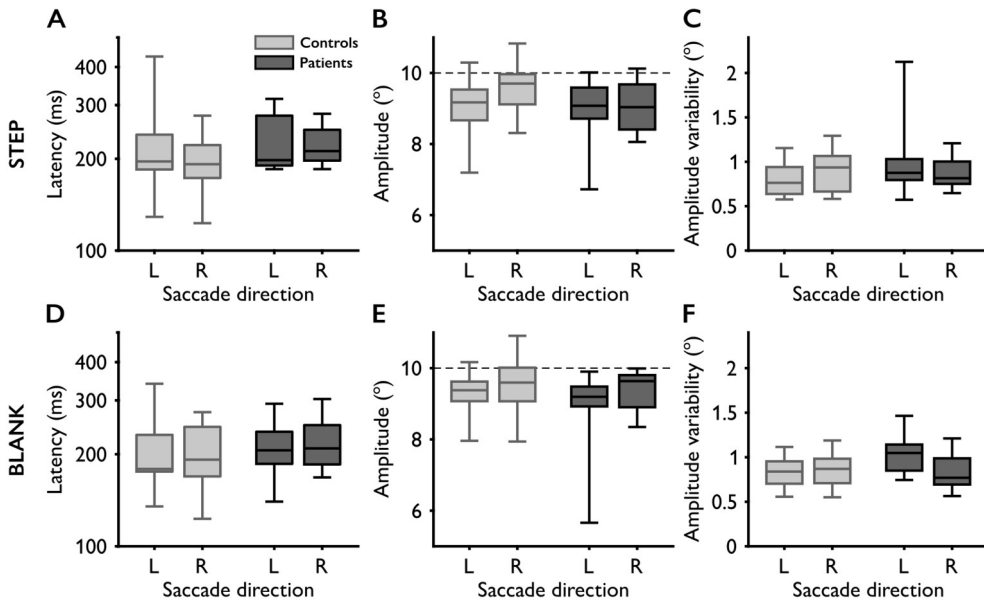
Figure 5. Saccade parameters. Panels A, B, C represent parameters from the STEP condition, Panels D, E, F represent parameters from the BLANK condition. Saccade variability in panels C and F is the standard deviation of all trials included in the analysis per subject. Boxes encompass the 25th to 75th percentile. The whiskers extend to the most extreme values per group. The central lines are the group medians. Grey is the control group, black is group of subjects with PPC lesions.

Saccade parameters

We analysed the saccade parameters with Bayesian mixed-design ANOVA's, with the factors saccade direction (L/R), condition (STEP/BLANK) and group (patient/controls). We added the main effects of condition, direction and the interaction between condition and direction to the null model. Bayes factors for the effects are computed across matched models. We report the average parameters per group and saccade direction, averaged over the two conditions. In the control group the average latencies (Figure 5A, 5D) were 214 (±12 s.e.m.) ms for leftward and 198 (±18 s.e.m.) ms for rightward saccades. In the patient group these latencies were 221 (±16 s.e.m.) and 220 (±12 s.e.m.), respectively. The average amplitudes (Figure 5B, 5E) in the control group were 9.16° (±0.19 s.e.m.) for leftward and 9.53° (±0.21 s.e.m.) for rightward saccades. For the patients the average amplitudes were 8.93° (±0.37 s.e.m.) and 9.21° (±0.21 s.e.m.), respectively. The average amplitude variability (Figure 5C, 5F) in the control group was 0.81° (±0.04 s.e.m.) for leftward and 0.88° (±0.06 s.e.m.) for rightward saccades. For the patients, the average variability was 1.02° (±0.11 s.e.m.) for leftward and 0.86° (±0.04 s.e.m.) for rightward saccades. According to the

Bayesian mixed-design ANOVA's, these data provide inconclusive evidence for an effect of any of the factors (or their interactions) on the saccade latencies or the average saccade amplitudes (all $BF_{10} < 1$). There was suggestive evidence for an interaction effect of group and saccade direction on the variability of saccade amplitudes ($BF_{10} = 28.1$), with the most variability in leftward saccades of the subjects with PPC lesions. In addition to the saccades that were made in the displacement task, we also screened for general visually guided oculomotor behaviour in a brief task before the experiment. In this task, subjects made saccades in 8 different directions starting in the middle of the screen. As can be seen, there was no systematic difference in any of the 8 directions concerning the latencies (Figure S2) or amplitudes (Figure S3) of the saccades.

Discussion

We measured the consequences of a lesion to the posterior parietal cortex (PPC) for perceptual continuity across saccades. Perceptual continuity refers to the apparent stable and fluent visual percept humans experience, despite the disruptions in visual input caused by saccades. We used the intrasaccadic displacement task to measure the availability of extra-retinal signals for perception in 9 patients with lesions to the PPC. We measured reliable psychometric functions for both the STEP and BLANK condition of the intrasaccadic displacement task. Most patients – even with substantial lesions to the PPC (see pt. L) – demonstrated behaviour that indicates the influence of extra-retinal signals on their perceptual judgements. In an explorative analysis, we correlated the amount of influence of extra-retinal signals (Δthreshold index) to the amount of damage in four different subareas of the PPC. There was suggestive evidence for a relationship between the lesion size in the SMG and the size of sensitivity improvement, for the other areas the evidence was inconclusive.

The results of the current study do not support the hypothesis that the PPC is crucial for perceptual continuity across saccades (Heide et al., 1995). This could mean that extra-retinal signals are processed in neural circuits that do not include the PPC, but for example the thalamus and FEF (Sommer & Wurtz, 2008a; Wurtz, 2008). Still, there are many examples that do suggest that the PPC is involved in processing both retinal and extra-retinal signals from human (Dunkley et al., 2016; Fairhall et al., 2017; Medendorp et al., 2003; Merriam et al., 2003) and monkey neurophysiology (Duhamel, Colby, et al., 1992; Mirpour & Bisley, 2016; Subramanian & Colby, 2014). One explanation for the presence of perceptual

continuity in patients with PPC lesions is the possibility that there are multiple neural circuits that could give rise to perceptual continuity, i.e. degeneracy (Edelman & Gally, 2001; Price & Friston, 2002). For example, it has been proposed that perceptual continuity can be established by using an efference copy of the motor command as extra-retinal signals (Von Holst & Mittelstaedt, 1950), but also by using proprioceptive signals from the eye (Steinbach, 1987; Sun & Goldberg, 2016). So far, the efference copy has been considered the most likely candidate, because a network has been mapped that processes an efference copy of the oculomotor command (Cavanaugh et al., 2016; Crapse & Sommer, 2012; Sommer & Wurtz, 2002, 2006). Moreover proprioceptive signals are signal slower than the efference copy (Xu, Wang, Peck, & Goldberg, 2011) and are believed to not contribute for fast processes such as updating memorized saccade targets (Sparks & Mays, 1983; Sparks, Mays, & Porter, 1987). Still, proprioception guides motor control of eye movements over longer periods than single saccades (Poletti, Burr, & Rucci, 2013). The efference copy is believed to be the strongest extra-retinal signal across a single saccade, and is thus expected to be contribute to perceptual continuity across saccades (Cavanaugh et al., 2016). However, proprioception of the eye provides an alternative, slower extra-retinal signal. Thus, hypothetically, if the PCC were crucial to integrating the efference copy with retinal information, patients with lesions to the PPC could still experience perceptual continuity when different and undamaged cortical areas integrate eye proprioception with retinal information.

The main strength of the current study is the data quality. We were able to collect sufficient data and good fits for the psychometric functions of most subjects, including the patients with PPC lesions. The main limitation of the study is the relative low number of patients, although it should be noted that 9 patients with PPC lesions was not (much) lower than comparable studies on this topic (Heide et al., 1995; Rath-Wilson & Guitton, 2015; Russell et al., 2010; Vuilleumier et al., 2007). The only problem is that we could not perform proper lesion symptom mapping, which could be more sensitive to detect subtle lesion-deficit relationships.

To summarize, at the behavioural level, patients with a chronic lesion to the PPC did not show major differences on a task that has extensively been used to study perceptual continuity across saccades in healthy humans, patients and non-human primates (Cavanaugh et al., 2016; Deubel et al., 1998; Ostendorf et al., 2010). This suggests that patients had access to extra-retinal signals, despite lesions to the PPC. Therefore, the current results do not provide evidence for a crucial role of the PPC in monitoring extra-retinal signals for perceptual continuity. It could be that patients with a lesion to the PPC use a different

source of extra-retinal signals than controls (e.g. eye proprioception instead of an efference copy). Given the slower speed of proprioceptive signals, this leads to the hypothesis that perceptual continuity might only be disrupted after a PPC lesion when many saccades are made in a brief period of time. However, the present results show that extra-retinal signals still influence visual perception after a lesion to the PPC, as measured with the intrasaccadic displacement task.

Chapter 5 – Supplementary information

Table S1. Psychometric function parameter estimates. Individual patients are ordered by the percentage of damage to the PPC. Values between square brackets give the minimum and maximum values per group. Patients in grey font did not have any damage to the PPC and are not included in the patient average.

| ID	Threshold				ΔThreshold index	
	STEP		BLANK			
	L	R	L	R	L	R
L	4.87	4.36	3.60	3.56	0.15	0.10
A	5.13	4.05	6.51	6.66	-0.12	-0.24
C	1.26	1.79	0.82	0.86	0.21	0.35
K	2.09	1.33	2.20	1.36	-0.03	-0.01
D	1.08	0.88	1.85	1.71	-0.26	-0.32
I	2.65	1.95	0.78	0.45	0.55	0.63
H	1.24	1.02	0.63	0.89	0.33	0.07
M	1.58	1.76	1.22	0.90	0.13	0.32
J	3.46	1.92	2.26	1.36	0.21	0.17
E	9.02	4.51	3.06	1.66	0.49	0.46
B	2.79	1.73	0.94	0.43	0.50	0.60
F	4.87	5.30	1.74	1.15	0.63	0.64
Average	2.60	2.12	2.21	1.97	0.13	0.12
Controls	1.39	1.55	0.77	0.82	0.27	0.28
	[0.52, 2.54]	[0.88, 3.88]	[0.42, 1.63]	[0.32, 2.26]	[0.01, 0.69]	[-0.05, 0.79]

5
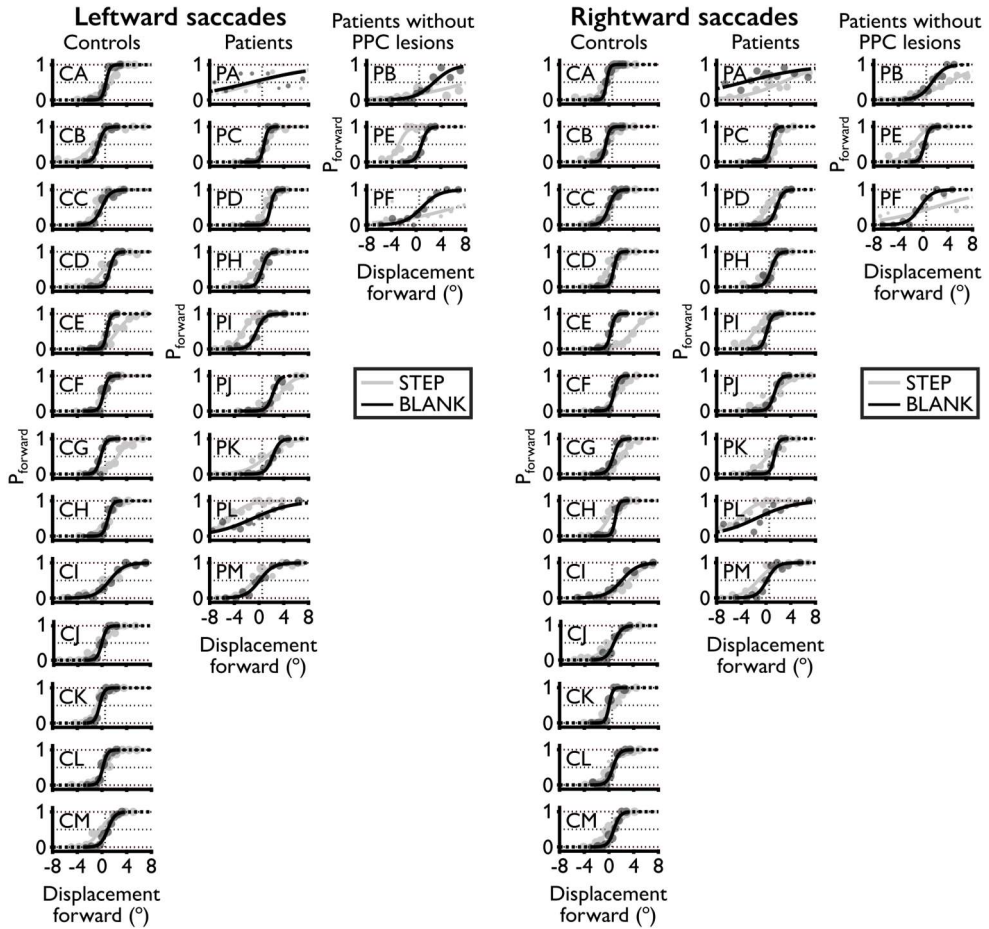
Figure S1. Individual psychometric functions. Grey is used for data from the STEP condition. Black is used for data from the BLANK condition. In each panel, data is binned into equally spaced bins (circles). The size of the circles is logistically scaled with the number of trials in that bin. Fitted psychometric functions are displayed as solid lines (and as dashed lines where the fit is extrapolated from the binned data).
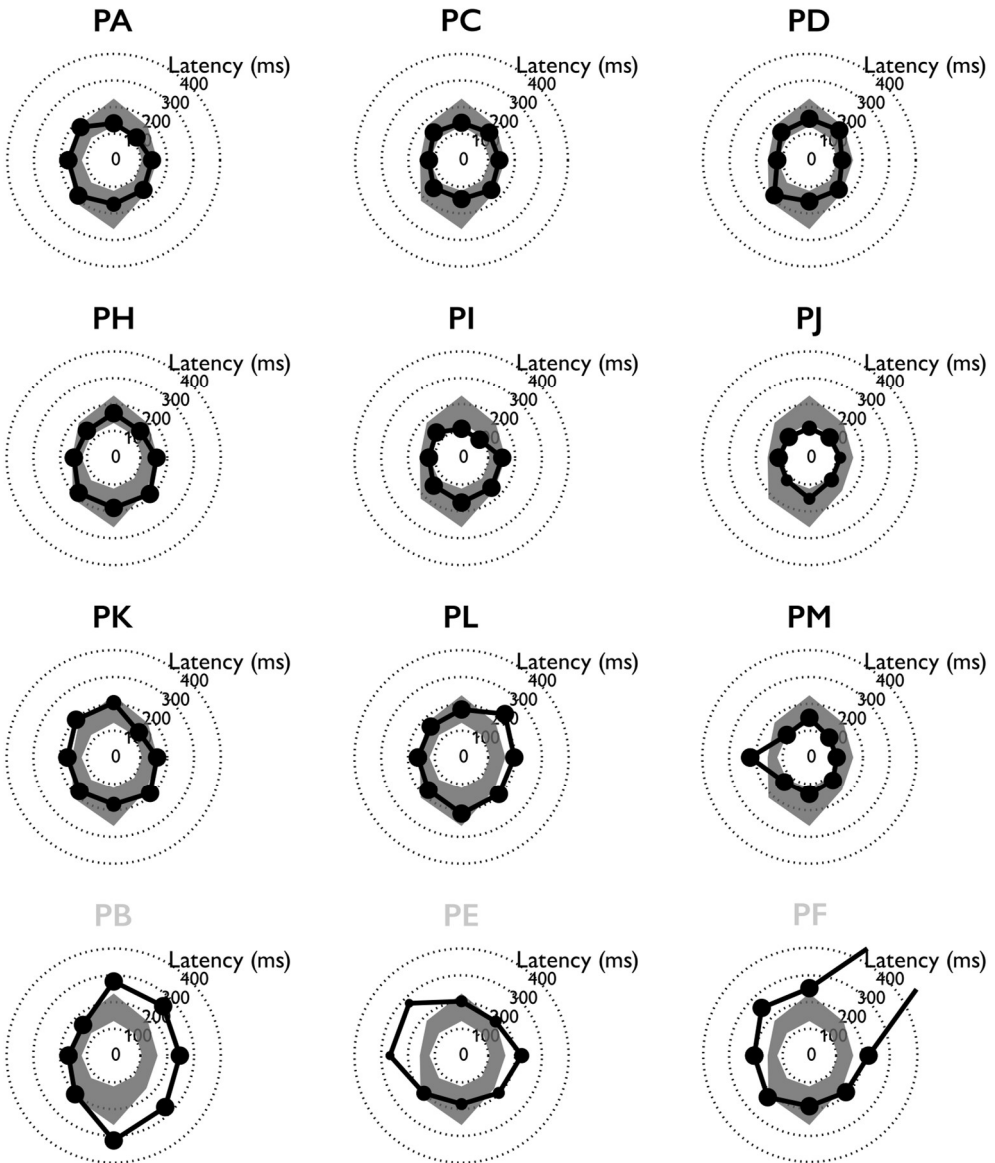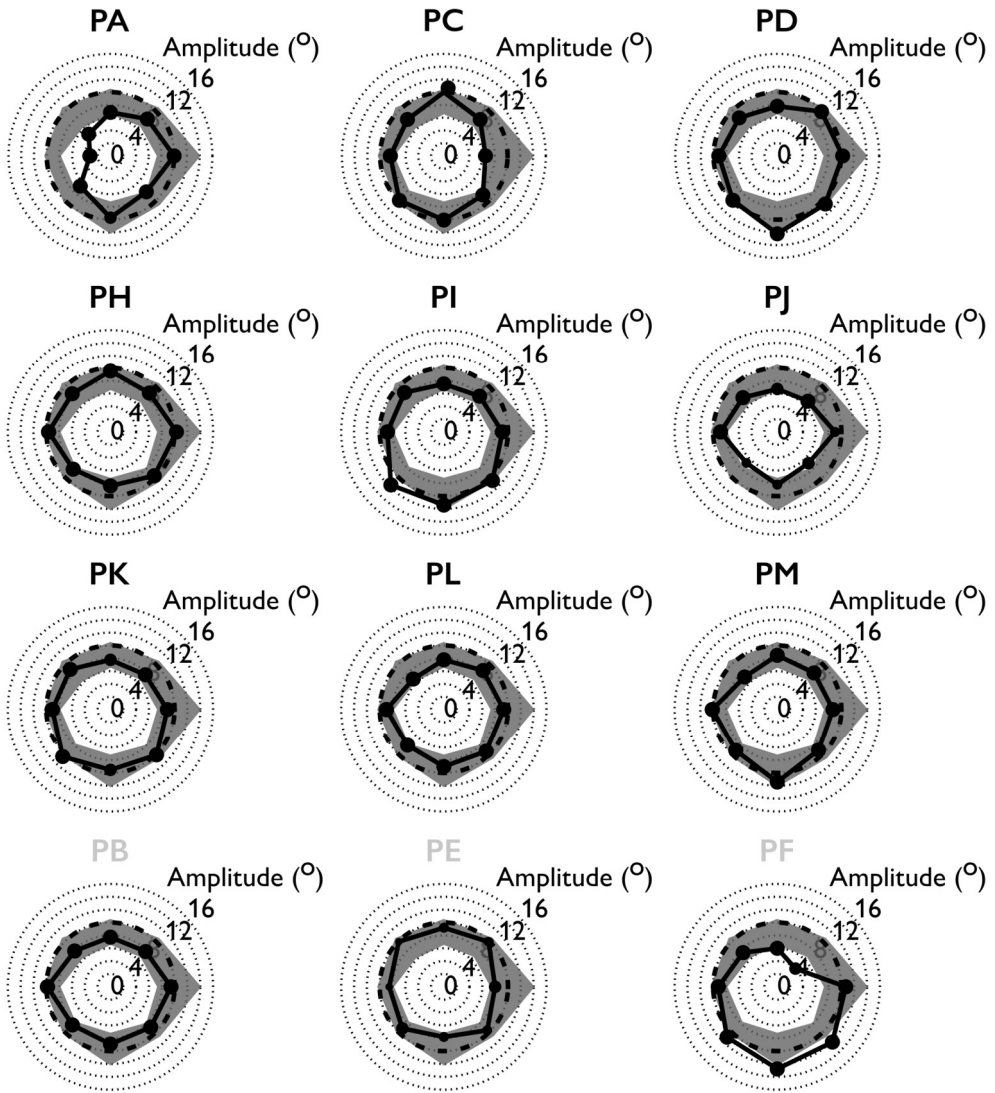
Figure S2. Latencies of saccades in 8 eight different directions. Polar angle corresponds to the direction of the saccade target. The radius of the black points is the average latency of max. 5 saccades in each direction. The size of the points is scaled with the number of saccades. The grey patch covers the minimum and maximum average latency of subjects in the control group. Each panel shows the data of a single subject from the patient group, both with (black font) and without PPC lesions (grey font).

Figure S3. Amplitudes of saccades in 8 eight different directions. Polar angle corresponds to the direction of the saccade target. The radius of the black points is the average amplitude of max. 5 saccades in each direction. The size of the points is scaled with the number of saccades. The black dashed line is the eccentricity at which the saccade target was presented (8°). The grey patch covers the minimum and maximum average amplitude of subjects in the control group. Each panel shows the data of a single subject from the patient group, both with (black font) and without PPC lesions (grey font).

5
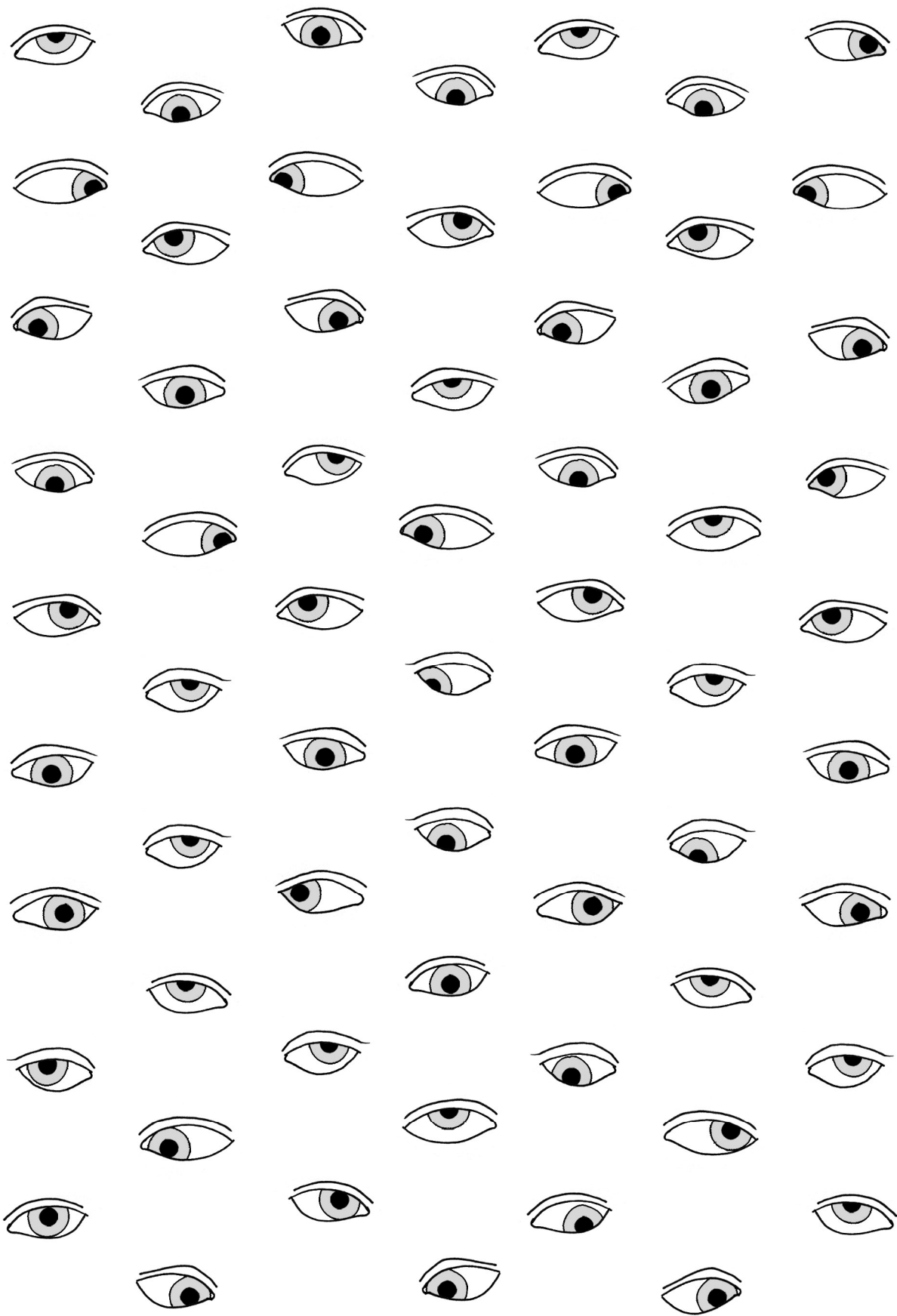
Chapter 6

Spatial working memory impairment and search behaviour in visuospatial neglect

Author contributions

JHF, SvdS and TCNW conceptualized experiments. JHF programmed the experiments and performed analyses. AFTB managed data collection. JHF, AFTB, SvdS & TCWN wrote the manuscript.

Abstract

Objectives: Visuospatial neglect (VSN) is generally characterized by a lateralized attentional deficit. In addition, several studies have suggested that neglect can be better regarded as a syndrome in spatial processing that also comprises non-lateralized impairments, such as an impairment in the temporary storage of spatial information in working memory (spatial working memory; SWM). Impaired SWM is thought to be reflected in disorganized search behaviour in patients with VSN. Although several studies have provided evidence for these non-lateralized impairments, these studies consist of small samples. Here, we performed a conceptual replication with a larger sample and related SWM performance to search behaviour.

Methods: We assessed SWM with novel task in a group of 182 stroke patients (24 with VSN, 158 without) and 65 healthy controls. We related SWM performance to available stroke-related and cognitive data.

Results: Patients with VSN exhibited lower SWM performance than patients without VSN and healthy controls. Additional control analyses indicated that differences in SWM performance are specific to visuospatial processing, instead of e.g. verbal working memory or the general level of physical disability. Last, we related SWM performance to performance on two cancellation tests, one with visible markings and one without visible markings. SWM performance correlated with search organization on the cancellation test without visible markings.

Conclusion: Together, these results from a large sample of stroke patients corroborate the findings of earlier studies, while excluding several alternative explanations: SWM impairment is a part of the VSN syndrome, and SWM impairments are related to search behaviour.

Introduction

Visuospatial neglect (VSN) is a common disorder after brain damage, affecting around 20-50% of patients after a first-ever stroke (Appelros, Karlsson, Seiger, & Nydevik, 2002; Nijboer, Kollen, & Kwakkel, 2013). The core component of VSN is a lateralized attention deficit (Bisiach & Vallar, 1988; Kinsbourne, 1987), reflected in the observations that patients with VSN tend to copy only the right half of a figure (Ronchi, Posteraro, Fortis, Bricolo, & Vallar, 2009), or miss targets in the left half of a search array (Eglin, Robertson, & Knight, 1989). In addition, VSN consists of non-lateralized spatial processing impairments (Husain & Rorden, 2003). VSN is therefore better defined as a syndrome in visuospatial processing, with both lateralized and non-lateralized symptoms. An important non-lateralized symptom regards impairments in spatial working memory (SWM; Striemer, Ferber, & Danckert, 2013). Here, we focus on the assessment of SWM performance in patients with VSN.

Impairments of SWM are thought to be reflected in disorganized visual search (Behrmann, Watt, Black, & Barton, 1997; Husain et al., 2001; Shimozaki et al., 2003; Wojciulik et al., 2001). Indeed, search behaviour of patients with VSN is characterized by unstructured patterns and frequent revisits of already inspected items (Kristjánsson & Vuilleumier, 2010; Mannan et al., 2005; Ten Brink, Van der Stigchel, Visser-Meily, & Nijboer, 2016). Furthermore, patients with VSN show a tendency to cancel the same targets multiple times (Parton et al., 2006), analogous to re-fixations in eye-tracking data of these patients (Mannan et al., 2005; Parton et al., 2006; Ptak et al., 2007). However, other studies suggest that disorganized search is a different impairment from VSN, not necessarily two symptoms of the same syndrome. For example, disorganized search and VSN were not related (Mark, Woods, Ball, Roth, & Mennemeier, 2004) and were found to comprise separate clusters in a cluster analysis (Ten Brink, Visser-Meily, & Nijboer, 2018).

SWM performance has been assessed directly in single cases or small groups of patients with VSN (see Table 1). The experimental tasks consisted of variations of the Corsi task (Malhotra et al., 2005; Malhotra, Mannan, Driver, & Husain, 2004; Wansard et al., 2015, 2014), change detection tasks (Ferber & Danckert, 2006; Pisella, Berberovic, & Mattingley, 2004) and an N-back task (Ravizza, Behrmann, & Fiez, 2005). The tasks were designed to minimize potential interference of the attentional imbalance, for example by presenting stimuli only on a vertical axis. Although SWM was measured with different tasks, all studies

6

Table 1. Literature overview. Studies that assessed spatial working memory (SWM) performance in patients with visuospatial neglect (VSN) directly. The total number of participants are split by patients with visuospatial neglect (VSN+), patients without visuospatial neglect (VSN-) and healthy control subjects. In the rightmost column a brief description of the SWM task is provided.

Study	N				SWM test
	Total	VSN+	VSN-	Control	
Malhotra et al., 2004	7	1	3	3	Corsi task; vertical
Pisella et al., 2004	8	8	–	–	Change detection; 4x4 grid with 4 items; delay of 1s. change in either location, colour or shape of 1 item
Malhotra et al., 2005	20	10	–	10	Corsi task; vertical; identification
Ravizza et al., 2005	14	1	4	14	N-back task; vertical
Ferber & Danckert, 2006	18	4	–	10	Change detection; vertical; 3 items in right visual field; delay of 3s; 1 item; same/new location as one of 3 items in sample.
Wansard et al., 2014	28	14	–	14	Corsi task; increase no. of potential targets to increase difficulty
Wansard et al., 2015	24	12	–	12	Corsi task; increase no. of potential targets to increase difficulty
Current study	247	24	158	65	Spatial discrimination; vertical; delay of 2s; distance between first and second stimulus determined with staircase

concluded that patients with VSN had lower SWM performances than controls. Such a difference in performance was not observed in non-spatial (e.g. feature-based) working memory tasks (Ferber & Danckert, 2006; Malhotra et al., 2005; Pisella et al., 2004; Ravizza et al., 2005). Although these studies present converging evidence that SWM is impaired in patients with VSN, the conclusions are limited by the small sample sizes and (in most studies) the lack of non-VSN stroke control groups.

Here, we assessed SWM performance in a large sample of participants and compared SWM performance between stroke patients with and without VSN. We intentionally define VSN based on a single score: the omission difference score between the left and right side of a cancellation test. This score is the most sensitive test to test for the attentional imbalance which represents the core deficit in VSN (Ferber & Karnath, 2001; Husain & Rorden, 2003; Ten Brink et al., 2018). We chose not to include different diagnostical tests as this may increase the heterogeneity of the VSN+ group by including different subtypes of neglect into a single group, which could likely blur relevant relationships between our

variable of interest (Azouvi et al., 2002; Buxbaum et al., 2004; Ferber & Karnath, 2001). After assessing SWM difference between patients with and without VSN, we examined whether potential SWM impairments relate to impaired functional or cognitive abilities in general. To this end, we related SWM performance with measures of motor functioning, functional independence, general cognitive functioning and specific cognitive domains using existing data from their physical and neuropsychological assessment. These analyses address the potential explanation that a relationship between VSN and SWM can be simply explained because patients with VSN suffer from an overall decline in functional or cognitive performance, resulting in a decreased performance on any kind of (neuropsychological) task irrespective of whether the task depends on visuospatial processing. Last, we explored the relationship between SWM performance and search organization. For this analysis, we correlated SWM performance with several measures of search organization derived from two cancellation tests, one with and one without visible markings.

Methods

Participants

Patients were recruited after admission for in-patient rehabilitation to De Hoogstraat Rehabilitation center (Utrecht, the Netherlands). Patients in this study were patients who had been admitted to De Hoogstraat rehabilitation clinic after being hospitalized elsewhere. In the Netherlands, not all stroke patients are referred to a rehabilitation clinic. To be eligible for rehabilitation, patients need to meet several criteria upon discharge from the hospital (described in Van der Stoep et al., 2013). To summarize these eligibility criteria: a patient is not able to return home yet but is expected to improve sufficiently with rehabilitation. Therefore, the sample in this study is representative for patients with mild stroke. Stroke patients who arrived at De Hoogstraat were scheduled for the neglect screening (see Neglect screening). We aimed to keep our sample of patients as representative possible, so patients were only excluded when they did not comprehend task instructions or when no data was obtained for the cancellation test (due to for example fatigue). All patients who were able to perform the cancellation test were also able to perform the SWM task. We have no data on the number of patients who were excluded, because patients with, for example, severe impairments in language comprehension or severe fatigue were not scheduled for the neglect screening. We included 182 stroke

Table 2. Demographics

	Control	VSN-		VSN+		Statistics		
N	65	158 (87%)		24 (13%)		–	–	–
Gender	0.51	0.65		0.46		$\chi^2(2) = 5.56$	–	p = 0.062[4]
Age	43	59		58		H(2) = 28.4	–	p < 0.001[4]
Days post stroke[1]	–	21		25.5		U = 14090	Z = -1.53	p = 0.127
Hemisphere lesioned (prop.)	–		72.8%[2]		75%[2]	$\chi^2(2) = 5.03$	–	p = 0.081
left	–	0.50		0.22		–	–	–
right	–	0.45		0.72		–	–	–
bilateral	–	0.05		0.06		–	–	–
MoCA[1,5] [0-30]	–	23.0	70.3%[2]	19.0	75.0%[2]	U = 7642	Z = 2.75	p = 0.004
Motricity Index Arm[1] [0-100]	–	87.0	78.5%[2]	83.0	79.2%[2]	U = 9145	Z = 1.17	p = 0.183
Motricity Index Leg[1] [0-100]	–	91.0	77.8%[2]	77.0	79.2%[2]	U = 8948	Z = 0.68	p = 0.340
SAN[1,5] [1-7]	–	6	78.5%[2]	6	75.0%[2]	U = 8886	Z = 0.25	p = 0.903
Barthel[1] [0-20]	–	14.0	79.1%[2]	9.0	70.8%[2]	U = 9274	Z = 1.56	p = 0.034

[1] Reported values are medians per group.

[2] We do not have the clinical data of all patients. The percentage of patients for whom we have these data are in grey.

[3] Statistics are the results of non-parametric tests testing for differences between groups on each parameter.

[4] Statistics in this row entails a comparison between all three groups: controls, VSN- and VSN+

[5] MoCA = Montreal Cognitive Assessment; SAN = Stichting Afasie Nederland (Dutch aphasia test)

patients. Of the 182 patients, 24 were included in the VSN+ group, 158 in the VSN- group. Additionally, 65 healthy control subjects were recruited to perform the novel SWM task. Control subjects were paid €10,- for their participation. See Table 2 for an overview of the demographics of all participants, split by group.

Data collection

Data collection procedures and procedures of neuropsychological tests are described in detail elsewhere (Ten Brink et al., 2018). Briefly, there were three moments of data collection. First, demographical data and diagnostical screening tests for a general level of functioning were administered upon admission by a rehabilitation physician. Later, an extensive neglect screening battery was conducted – the SWM task was included in this neglect screening. Patients were scheduled for neglect screening as part of usual care after admission for in-patient rehabilitation to De Hoogstraat Rehabilitation center (Utrecht, the

Netherlands). Last, a general neuropsychological assessment was performed. All data were provided anonymized to the authors. The procedures were in accordance with the Declaration of Helsinki.

Diagnostical screening

The diagnostical screening tests included the Montreal Cognitive Assessment (MoCA; in some patients the Mini-Mental State Examination was used, these scores were later converted to MoCA scores following Solomon et al., 2014), the "Stichting Afasie Nederland test" (SAN), the Motricity index (arm and leg), and the Barthel index. The MoCA is used to assess a general level of cognition (range = 0-30). The SAN is a Dutch language deficit test for aphasia (range = 1-7). The motricity indices reflect motor strength and coordinates in the legs and arms separately (range = 1-100). The Barthel index assess the level of independence in daily activities (range = 0-20). In all tests, higher scores reflect better performance.

Neglect screening

The second moment of data collection was approximately in the second week of admission to rehabilitation (Mdn = 21 days after stroke, Q_1 = 16, Q_3 = 30 days). Patients were screened for VSN using a computerized version of a shape cancellation task as part of an extended VSN screening (Van der Stoep et al., 2013). The cancellation task was presented at 90 cm from the patient. Most patients performed two versions of the cancellation test, one where their markings remained visible, and one where the markings were invisible to the patient but only registered digitally. The cancellation test with visible markings was used to assess the presence of neglect. Some patients had difficulties in performing the digital versions of the cancellation test. In these patients a traditional pen-and-paper version of the cancellation test was administered (thus, the test with invisible markings was not administered in these patients). The neglect screening consisted of more tests then described here. However, we only report the cancellation tests here for the sake of clarity. All other tests are described by Ten Brink et al. (2018).

Neuropsychological assessment

The third moment of data collection was a broader neuropsychological assessment (Mdn = 7 days after the neglect screening, Q_1 = 4, Q_3 = 14 days). Not all tasks were administered in all patients, rather a selection was made by the neuropsychologist.

6

Therefore, we do not have all neuropsychological data for all patients in our sample. We selected the WAIS Digit Span (verbal working memory), Rey auditory verbal learning test (RAVLT; verbal memory), Delis-Kaplan executive function system Tower test (D-KEFS Tower test; spatial planning, executive functioning) and the Rey-Osterrieth Copy Figure test (ROCFT, visuospatial perception and construction) for different subsamples from our total sample. These tests were selected as they reflect different cognitive functions, so the major cognitive domains are represented; and were assessed most frequently, resulting in a group of at least 5 patients per test. We used the raw test scores of each test: longest span length of the WAIS digit span forward (range = 3-8), longest span length of the WAIS digit span backward (range = 2-8), total number correct words of the RAVLT (range = 0-75), raw score of the ROCFT (range = 0-36) and raw score of the D-KEFS Tower test (range = 0-30). The analysis of these data is provided in the Supplementary Information.

Spatial working memory task

The trial sequence is depicted in Figure 1. A trial started with a fixation point that was displayed for 800-1000 ms. Then Target 1 (T1) was presented for 500 ms. In half of the trials, T1 was presented above the fixation point, in the other half below. After the presentation of T1, the fixation point briefly (100 ms) expanded and contracted to reorient attention back to the fixation point. Target 2 (T2) was presented 2000 ms after the offset of T1, and vertically displaced with respect to the original location of T1. Participants verbally indicated whether T2 was presented above or below the original position of T1 by saying 'higher' or 'lower'. The response was recorded with a keypress on a standard keyboard by the experimenter. T1 and T2 were dots with the same radius (0.3°). T1 was red and T2 was yellow to make them clearly distinct. The background colour was uniformly grey. T2 was always presented in the same vertical hemifield as T1 (e.g. when T1 was presented above the fixation point, so would T2). The difference in location between T1 and T2 was controlled with a staircase: Accelerated Stochastic Approximation (Kesten, 1958; Treutwein, 1995). In the first trial, the displacement size was 4.8°. In the first three trials, the displacement size on the next trial (d_{k+1}) was given by

$$d_{k+1} = d_k - \frac{3.6}{k}(Z_k - 0.8)$$

where d_k is the displacement size used in the current trial, 3.6 is the staircase constant, k is the trial number, Z_k is 1 when a correct response was provided in the current trial or 0 when an incorrect response was provided, and 0.8 is the desired accuracy level. On the
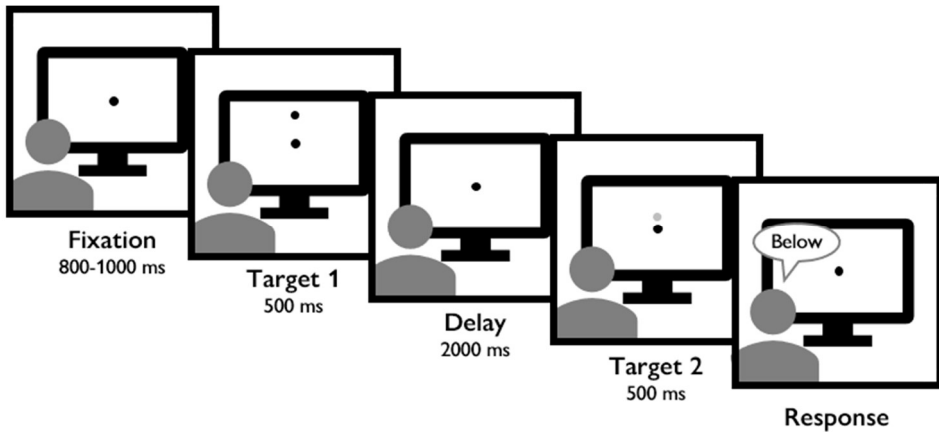
Figure 1. Trial sequence. Participants had to indicate whether Target 2 (grey, actual colour was yellow) was presented above or below the location of Target 1 (black, actual colour was red). The distance between the locations of Target 1 and Target 2 was controlled by a staircase procedure, i.e. the distance was made smaller when the response on the previous trial was correct, and vice versa. In the delay between Target 1 and Target 2, the fixation point briefly expanded and contracted. Responses were given verbally and entered through a standard keyboard by the experimenter. Actual background colour was grey, here depicted as white.

remaining trials, the displacement size was adjusted slightly differently, taking into account the number of switches that had been made, i.e. the switch from a series of correct answers to an incorrect answer or vice versa:

$$d_{k+1} = d_k - \frac{3.6}{2 + m_{switch}}(Z_k - 0.8), k > 3$$

where m_{switch} is the number of switch trials. T1 and T2 were never closer than 1.2° to either the screen edge or the fixation point. The staircase converges to a displacement size at which the proportion correct responses should be 0.8. This displacement size is the threshold. Ideally, the final threshold estimate is taken from the staircase estimates when the displacements reaches a predefined lower limit. However, this means that the duration of the task is undefined. We aimed to keep the task as brief as possible, so we used a low, fixed number of trials (n = 32). Because of this low trial number, we defined the threshold as the weighted average of the last 10 displacements (D),

$$\theta = \sum_{k=1}^{10} D_k w_k$$

where w is the weight vector, given by

$$w = \frac{\{1, 2, 3 \cdots 10\}}{\Sigma_{k=1}^{10} k}$$

Task instructions were verbally explained to the participant. Before the staircase procedure started participants practiced at least 4 trials. Total execution of the task lasted approximately 5 minutes.

Analysis

Group classification

Patients were divided into two groups based on their performance on the cancellation test with visible markings. We took the absolute difference of omissions between the left and right side of the stimulus field. When, for example, more targets on the right side were omitted than on the left, there was an omission difference. When a patient obtained an absolute omission difference of two or more, this patient was included in the VSN+ group, otherwise in the VSN- group (Nijboer, Kollen, et al., 2013; Nijboer, van de Port, Schepers, Post, & Visser-Meily, 2013; Ten Brink et al., 2018; Van der Stoep et al., 2013). We used this criterion because it is used in the rehabilitation clinic as a clinical sign of VSN. Changing the criterion to higher omission difference scores or combining the omission difference scores with the total number of omissions lowers the number of patients in the VSN+ group but does not change the inferences of the group analysis.

Statistical analysis – differences in SWM between groups

For our analysis, we took the base 10 logarithm of these thresholds, because the threshold estimate is positively skewed (by definition). Distributions of the thresholds per group are depicted in Figure 1. We analysed the differences in thresholds between the three groups (i.e. control, VSN-, VSN+) with Bayesian linear models and Bayesian model averaging (Hoeting, Madigan, Raftery, & Volinsky, 1999; Rouder, Morey, Verhagen, Swagman, & Wagenmakers, 2017), using the generalTestBF function from the R-package "BayesFactor", with default prior settings (Morey, Rouder, & Jamil, 2015). To estimate the evidence in favour of a specific factor included in the analysis, we sum the Bayes factors of all models that include that factor and divide it by the proportion of models that include that factor. This division is itself divided by the sum of all Bayes factor without the factor in question divided by the proportion of all models that do not include the factor. To guide the interpretation of the Bayes Factor (BF_{10}) we use the interpretations provided in Table 3, based on Jeffreys (Jeffreys, 1961) and Kass and Raferty (Kass & Raftery, 1995). It is important

Table 3. Proposed interpretation of Bayes Factors.

Bayes Factor (BF$_{10}$)	Subjective interpretation
>100	Strong evidence in favour of the alternative hypothesis, this result is likely to be replicated
10 – 100	Substantial evidence in favour of the alternative hypothesis
3 – 10	Suggestive evidence in favour of the alternative hypothesis, but requires follow-up investigation
⅓ – 3	Inconclusive, experimental data do not add new information to prior
0.1 – ⅓	Suggestive evidence against alternative hypothesis, but requires follow-up investigation
0.1 – 0.01	Substantial evidence against the alternative hypothesis
<0.01	Strong evidence against the alternative hypothesis, this result is likely to be replicated

to note that the size of the BF$_{10}$ is not the same as the effect size, e.g. a high BF$_{10}$ does not reflect a large effect but rather strong evidence in favour of what could very well be a small effect. For the main analysis, we compared the thresholds between the three groups, while controlling for possible effects of age and gender. Hence, we construct seven models to explain the SWM threshold (1. group, 2. age, 3. sex, 4. group+age, 5. group+sex, 6. age+sex, 7. group+age+sex).

Statistical analysis – explanatory effect of general disability on SWM performance

To exclude the possibility that the observed differences in SWM impairments result from a general disability, we examined whether the scores on the diagnostical screening tests influenced the SWM thresholds. As noted in Table 2, we did not have the data of the diagnostical screening tests for all patients who completed the SWM task. For simplicity, we treated the missing values as random and performed the following analyses only on the complete cases (i.e. patients for whom we have data on all 5 tests, the MoCA scores, Barthel indices, SAN, Motricity index arm and Motricity index leg: 96 VSN-, 13 VSN+). Similar to the SWM group analysis, we compared all 63 conceivable models with the combinations of the following 6 predictors: 1. group, 2. MoCA score, 3. Barthel index, 4. SAN score, 5. Motricity index leg, 6. Motricity index arm. All models were compared to the intercept only model. The observed SWM thresholds were the most likely under the model that included both group and MoCA score. In addition, we computed Bayes factors for the inclusion of each effect separately.

Statistical analysis – relation between search behaviour and SWM

We correlated four common measures of search behaviour as assessed with the two cancellation tests from the neglect screening to the SWM thresholds: 1) the absolute

6

difference between the number of omissions left and right, 2) the number of delayed revisits, i.e. re-cancellation of target when at least one other target has been cancelled in between, 3) best R, i.e. a correlation between the order of cancellation and position of cancelled items (Mark et al., 2004), and 4) the intersection rate, i.e. the number of times the path of cancellation crosses itself divided by the total number of markings (Benjamins, Dalmaijer, Ten Brink, Nijboer, & Van der Stigchel, 2018; Dalmaijer, Van der Stigchel, Nijboer, Cornelissen, & Husain, 2015). Note that the absolute omission difference is also the measure we used for group classification. So, rather than an independent measure of search behaviour, this measure reflects the severity of neglect (Ten Brink et al., 2018). We used Bayesian interpretations of the Kendall rank correlation, with a stretched beta prior with a width of 1 (van Doorn et al., 2016). For these correlations, we used the entire sample of patients without making a distinction between VSN- and VSN+ patients.

Results

Differences in SWM between groups

The data are strongly in favour of a difference in SWM threshold between the three groups (BF_{10} = 3.12×10^{14}), with inconclusive evidence for an effect of age (BF_{10} = 0.934) or sex (BF_{10} = 0.374). Therefore, in the following analyses, we will further consider the model with only group as a predictor, but not with age or sex. See Figure 2 for a visualization of the SWM thresholds per group and per group separated for sex or age. We obtained the estimated median SWM thresholds for each group and their 95%-credible intervals (CrI). For the control group, the median threshold was 0.54° (CrI: 0.39-0.75). For the VSN- group this was substantially higher, with a median of 0.84° (CrI: 0.63-1.13), and even higher for the VSN+ group, with a median of 3.32 (CrI: 2.27-4.84). The results of this analysis were similar when we only included patients with right hemisphere lesions in the VSN- and VSN+ groups. Due to the low number of VSN+ patients with left hemisphere lesions (N = 4) we did not interpret the same analysis for left hemisphere patients. To summarize, the SWM threshold of VSN+ patients was higher than that of control subjects and VSN- patients. There was no clear difference between the average threshold of the control group and the VSN- patients.

To assess the possibility that altitudinal neglect (Rapcsak, Cimino, & Heilman, 1988) could explain the difference in SWM performance between the VSN- and VSN+ group, we
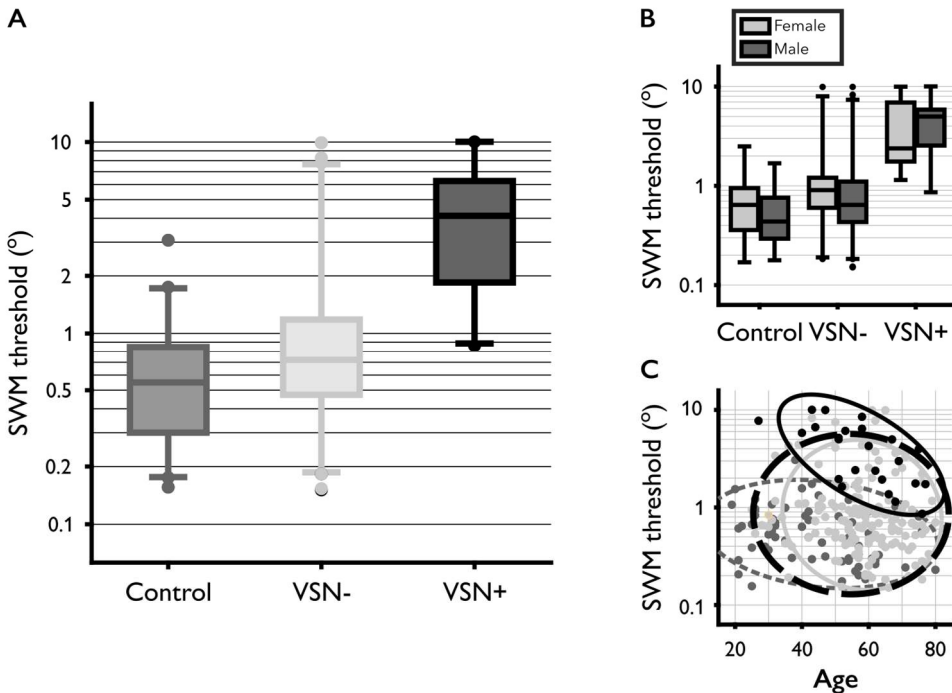
Figure 2. Spatial working memory (SWM) thresholds. For the boxplots, the central horizontal lines indicate the median threshold per group. Boxes encompass the inter-quartile range; whiskers extend to 2.5th and 97.5th quantiles of the group data. Points are participant with scores outside these intervals. **A.** Thresholds per group. There was strong evidence in favour of an effect of group on the SWM thresholds ($BF_{10} = 3.12 \times 10^{14}$). Moreover, the medians per group are different of the medians of the other groups, as indicated by non-overlapping 95% credible intervals. **B.** Thresholds per group and split between males and females. There was no clear evidence for an effect of sex on the SWM thresholds ($BF_{10} = 0.374$). **C.** Thresholds as a function of age. There was no clear evidence for an effect of age on the SWM thresholds ($BF_{10} = 0.934$). Ellipses represent area that holds 95% of the cases per group. **Colours**: dark grey = control, light grey = VSN-, black = VSN+. Black dashed ellipse represents 95% area across all subjects.

also tested whether the vertical center of cancellation (Christopher Rorden & Karnath, 2010) was the same in both groups. The center of cancellation was calculated for most, but not all patients who completed the neglect screening, so the t-test was performed on a subgroup of the VSN- patients (N = 146) and the VSN+ patients (N = 22). A Welch t-test showed no significant difference between the vertical centers of cancellation (t(21.08) = 1.11, p = 0.28), whereas there is a significant difference between the horizontal centers of cancellation (t(21.00) = -2.55, p = 0.019). Therefore, it seems unlikely that altitudinal neglect explains the difference in SWM thresholds between the VSN- and VSN+ groups.
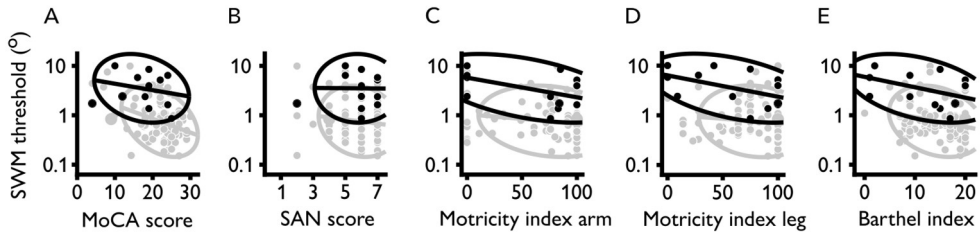
Figure 3. Control analysis. Black represents the VSN+ group. Grey represents the VSN- group. Note that in these analyses we only included a subset of patients for which we had the data (see Table 3). Spatial working memory (SWM) thresholds as a function of **A.** MoCA score (BF$_{10}$ = 141), **B.** SAN score, (Dutch aphasia test; BF$_{10}$ = 0.397), **C.** Motricity Index arm (BF$_{10}$ = 0.490), and **D.** Motricity Index leg (BF$_{10}$ = 0.530), **E.** Barthel index (BF$_{10}$ = 1.16). When accounting for these relations, the VSN+ group still has a higher median threshold than the VSN- group (BF$_{10}$ = 3.49×10^4). In sum, across patients, a lower MoCA score is related to a higher SWM threshold and the presence of VSN predicts an additional increase in SWM threshold., but none of the other measures for general disability was strongly related to SWM performance.

Moreover, in an exploratory analysis, we related the SWM thresholds of the VSN- and VSN+ group to the performance on five tests from the neuropsychological assessment (WAIS digit span forward, WAIS digit span backward, RAVLT, R-OCFT, D-KEFS Tower). See Supplementary Information for all the details of this analysis. The results suggest that, although the VSN+ group scored worse on the SWM task than the VSN- group, this is not due to a general worse performance on any cognitive task. The groups only seem to differ on tasks with an explicit spatial component (i.e. R-OCFT, D-KEFS Tower) but not on other tasks (i.e. WAIS Digit Span forward or backward, RAVLT).

Explanatory effect of general disability on SWM performance

Next, we related SWM thresholds to scores on the diagnostical screening tests (Figure 3). As shown in Table 2, the VSN+ group scores lower on the general cognitive screening task (MoCA) than the VSN- group. Moreover, the VSN+ group has a lower Barthel Index than the VSN- group. For the SAN, and both Motricity indices there was no clear difference between the VSN- and VSN+ groups. When controlling for the effect of these tests, we still observed strong evidence for an effect of group on SWM (BF$_{10}$ = 3.49×10^4). In addition, we also observed strong evidence for an effect of the MoCA score (BF$_{10}$ = 141) on the SWM thresholds, but inconclusive evidence for an effect of the SAN score (BF$_{10}$ = 0.397), the Motricity Index arm (BF$_{10}$ = 0.490), Motricity Index leg (BF$_{10}$ = 0.530), or the Barthel Index (BF$_{10}$ = 1.16). In sum, SWM thresholds were best predicted by a combination of the presence of VSN (VSN+ vs. VSN-) and general cognitive performance (MoCA score). The effect of MoCA score on the SWM threshold can be best described as an increase of 0.025
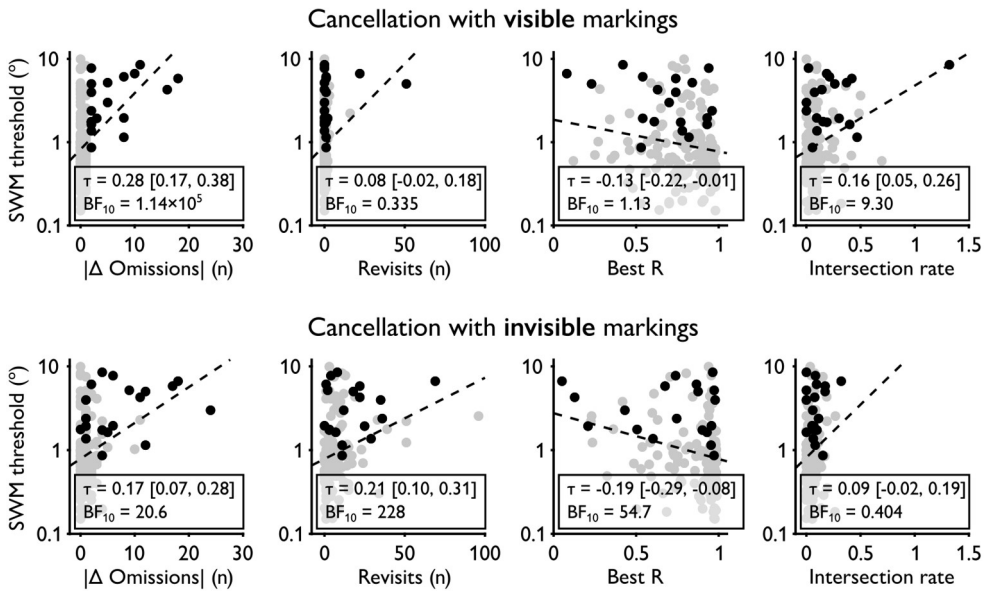
Figure 4. Relationship between different search measures taken from the cancellation task with visible markings (top row) and the SWM threshold, and the cancellation test with invisible markings (bottom row) and the SWM thresholds. Although individual participants are coloured based on group (VSN- = grey, VSN+ = black) the correlation was calculated once across all patients (black dashed line). The legends give the estimated Kendall's tau statistic and 95% credible interval. A suggested interpretation of the Bayes factors (BF$_{10}$) is given in Table 3.

log units (CrI: 0.012-0.037) for every point lost on the MoCA. To conclude, even though the MoCA score was related to the performance on our SWM task, the presence of VSN had an additive effect, with increased SWM thresholds for patients with VSN.

Relation between search behaviour and SWM

Lastly, we related search behaviour on the cancellation tasks in the neglect screening to the SWM thresholds. The cancellation test with invisible markings was available for 19/24 patients in the VSN+ group (79.2%) and for 140/158 in the VSN- group (88.6%). We correlated four common measures of search behaviour to the SWM thresholds: 1) the absolute difference between the number of omissions left and right, 2) the number of delayed revisits, i.e. re-cancellation of target when at least one other target has been cancelled in between, 3) best R, i.e. a correlation between the order of cancellation and position of cancelled items, and 4) the intersection rate (see Figure 4).

For both cancellation tests with and without visible markings there was evidence for a positive correlation between SWM thresholds and the absolute difference between the number of omissions left and right (visible markings: τ = 0.28, BF_{10} = 1.14×10^5; invisible markings: τ = 0.17, BF_{10} = 20.6). SWM thresholds correlated with the number of revisits (visible markings: τ = 0.08, BF_{10} = 0.335; invisible markings: τ = 0.21, BF_{10} = 228), and best R (visible markings: τ = -0.13, BF_{10} = 1.13; invisible markings: τ = -0.19, BF_{10} = 54.7) only when the markings were invisible. Conversely, there was suggestive evidence for a correlation between SWM thresholds and intersection rate only when the markings were visible (visible markings: τ = 0.16, BF_{10} = 9.30; invisible markings: τ = 0.09, BF_{10} = 0.404).

Problems in visual search and VSN can be considered two different cognitive factors (Ten Brink et al., 2018). Although the two factors can be associated, they seem to be two distinct factors. Moreover, problems in visual search have been observed more frequently in patients with right hemisphere damage than in patients with left hemisphere damage (Ten Brink, Biesbroek, et al., 2016). Therefore, we explored this lateralization in the current dataset by repeating the correlation analysis separately for patients with left hemisphere (N = 50) and patients with right hemisphere (N = 46) damage in the VSN- group, for whom we also collected data on their search behaviour. A Bayesian independent samples t-test (Cauchy prior width = 0.707) demonstrated that the data provide inconclusive evidence that the two VSN- subgroups differ in their average SWM thresholds (BF_{10} = 0.437). For the left hemisphere group, none of the correlations provided suggestive evidence for a correlation between the SWM thresholds and any of the search measures in both cancellation tasks (-0.22 < all τ < 0.19, all BF_{10} < 1.9). For the right hemisphere group, the data provide suggestive evidence for a correlation between the SWM thresholds and the number of delayed revisits in the cancellation task with invisible markings (τ = 0.28, BF_{10} = 7.0), but not for any of the other measures (-0.22 < all τ < 0.19, all BF_{10} < 1.7).

Discussion

We assessed SWM performance in 182 stroke patients and 65 healthy controls. 24 of the stroke patients demonstrated VSN on a cancellation test, 158 did not. On average, patients with VSN had lower SWM performance than patients without VSN and healthy controls, and across all patients a higher left-right omission difference correlated with lower SWM performance. Moreover, the data suggest that the SWM impairment in VSN patients does not reflect a general functional or cognitive impairment but a specific impairment in

visuospatial processing. SWM thresholds were related to performance on the ROCFT (visuospatial perception and construction), and to a lesser extent to the D-KEFS Tower test (spatial planning and executive functioning), but the SWM thresholds were not strongly related to performance on the WAIS digit span (verbal working memory) or RALVT (verbal learning and memory), similar to previous findings (Malhotra et al., 2005, 2004; Ravizza et al., 2005).

The relations between SWM performance and the ROCFT and the D-KEFS Tower test are perhaps unsurprising given that both the ROCFT and the D-KEFS Tower test are used to assess visuospatial processing (Ten Brink, Van der Stigchel, et al., 2016). Furthermore, the absence of a clear relationship between the WAIS digit span performance and SWM thresholds indicates that the SWM thresholds do not reflect a general level of working memory, but very specific visuospatial working memory processes. We warrant some caution with this last statement because our sample size for the neuropsychological tasks was relatively small for the VSN+ group, which could mean that we did not have sufficient power to observe small relations.

After establishing SWM impairments in patients with VSN, we further explored the relationship between SWM performance and search behaviour. Even though our group classification (VSN- vs. VSN+) was based on the absolute difference in omissions on the left and right side of the cancellation task, the correlations cover different aspects of visual search performance. Moreover, the group classification was based on the cancellation test with visible markings, whereas the correlations between SWM and search performance were based on both the cancellation tests with visible and with invisible markings. We observed positive relations between SWM performance and the number of revisits, and with organization of the search pattern (best R; Mark et al., 2004). These correlations were only observed in the data of a cancellation test in which the cancellation markings were invisible, but not when the markings were visible. Previous studies also suggested that cancellation tests with invisible markings are more sensitive in detecting VSN and re-visits, possibly because the invisibility of the markings requires more SWM capacity to keep track of all previous markings (Husain et al., 2001; Wojciulik et al., 2001; Wojciulik, Rorden, Clarke, Husain, & Driver, 2004). Disorganized visual search in VSN is also observed with behavioural tasks other than cancellation tests (Kristjánsson & Vuilleumier, 2010; Mannan et al., 2005; Ptak et al., 2007). It could therefore be that disorganized search is a common exemplar of impaired SWM (Ten Brink, Biesbroek, et al., 2016).

6

Problems in visual search seem to be different from the presence of VSN (Ten Brink et al., 2018). Here, we observed a relation between SWM performance and the number of revisits in the VSN- group: the lower the SWM threshold the higher the number of revisits. Even more precise, this observation seems to be specific to patients with right hemisphere lesions, in line with previous findings (Ten Brink, Biesbroek, et al., 2016).

One consideration that we cannot fully exclude is the possibility that patients with SWM impairments have low level visual deficits, such as scotoma's or low visual acuity somewhere along the vertical axis. When either Target 1 or Target 2 of the SWM task was presented in the impaired visual field, the patient would have missed one of the two targets, and would consequently have to guess the direction of the displacement. The final score would thus not reflect the ability to represent spatial information in working memory, but rather whether the patient had seen the two stimuli in the first place. However, although visual field impairments might explain the SWM threshold, it is unclear how this would explain the relation between search behaviour and SWM thresholds. Visual search typically adapts fast after a visual field defect, within a few minutes after onset of simulated hemianopia, which likely parallels actual hemianopia (Simpson, Abegg, & Barton, 2011). The patients in this study were tested several weeks after stroke onset, making it likely that their visual search strategy has already adapted to any visual field defects.

Another limitation of the current dataset is that we did not monitor eye-movements. Although we designed the SWM task such that between the presentation of the two stimuli, attention would be attracted to the fixation point, it could be that different strategies were employed by different participants. For example, when a participant kept fixating the location of the first stimulus – despite the instruction to maintain fixation at the central fixation point – it would have been easier to make the spatial discrimination because the second stimulus would be presented closer to the fovea where visual acuity is higher.

To summarize, we showed that SWM performance can be assessed easily with a brief, staircased discrimination task in stroke patients in a clinical setting. Performance on this SWM task correlates with visual search behaviour as assessed with a cancellation test with invisible markings. Although we could recommend using the same or a similar SWM task in the clinical assessment of VSN or in VSN research, we would prioritize two other possibilities. Given the relationship between SWM performance and search behaviour, we think it would be most informative to combine a standard cancellation task with eye-tracking, because eye movements reflect search behaviour directly. However, this option is

only viable when eye-tracking does not increase test duration too extensively and is compatible with the patient's physical status. The next best option is the cancellation test with invisible markings. As demonstrated here and elsewhere, a cancellation task without visible markings provides a better insight into the search behaviour of a participant compared to a cancellation task with visible markings, which in turn is related to the SWM performance (Wojciulik et al., 2004). The SWM discrimination task that we developed here is a direct measure of SWM performance, which could be a useful addition to neuropsychological assessments when a specific question concerning SWM is at hand. Moreover, the task is brief, easy to administer and could be implemented on any standard computer or tablet, which makes it suitable for clinical settings where testing time is limited.

The current results corroborate a series of findings of earlier experiments that demonstrated a relationship between VSN and SWM performance, where more severe VSN being related to lower SWM performance (Ferber & Danckert, 2006; Malhotra et al., 2005, 2004; Pisella et al., 2004; Ravizza et al., 2005; Wansard et al., 2015, 2014). Together, the previous studies and our current dataset suggest that 1) VSN is best regarded as a syndrome comprising both a lateralized attention impairment and a non-lateralized SWM impairment (Husain & Rorden, 2003) and 2) SWM impairments are associated with disorganized search (Husain et al., 2001; Wojciulik et al., 2001).

6

Chapter 6 – Supplementary information

Explanatory effect of general cognitive decline on SWM performance

Analysis

To examine the relationship between SWM and general cognitive decline more in depth, we checked whether performance on five standard tasks from the neuropsychological assessment could account for the observed group effect on the SWM thresholds. We repeated the linear model analysis once per neuropsychological test, only including the patients from whom we had the data of that neuropsychological test (Table S1). Moreover, we tested for a difference in performance on the neuropsychological test between the VSN- and VSN+ group using a Bayesian t-test. We report the results of three analyses per test. 1) SWM ~ group assesses the difference in SWM thresholds between the subsamples of the VSN- and VSN+ groups. The outcome of this analysis can be used to check how representative the subsamples are of the original sample, concerning the SWM thresholds. 2) Test ~ group assesses the difference in performance on the neuropsychological test between the subsamples of the VSN- and VSN+ groups. 3) SWM ~ group + test assesses the SWM thresholds as a function of 'group' when accounting for the performance the neuropsychological 'test'.

Results

In the main text, we assessed SWM performance in stroke patients with and without VSN. We observed lower SWM performance in patients with VSN than patients without VSN. To examine whether patients with VSN display an overall decline in cognitive performance, we analysed various tests from the neuropsychological assessment. We did not have access to the data of all patients (see Table S1 for an overview of all tasks for which we had data of more than 5 patients per group). The results from these analyses are summarized in Figure S1 and Table S1. As displayed in the first column of the Statistics part in Table S1 (SWM ~ group, Group), in all tested subsamples there was still evidence for a group difference in SWM thresholds between the VSN- and VSN+ groups (all $BF_{10} > 10$). This means that the subgroups are representative for the original sample concerning SWM performance. To further quantify this, we also tested whether the group difference in SWM performance in the subsample was different from the group difference in the patients that
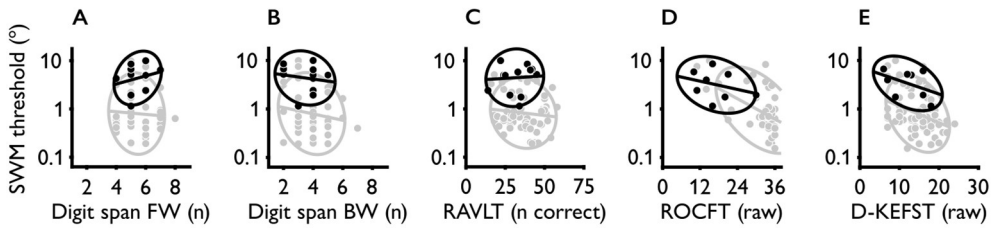
Figure S1. Relations between SWM threshold and performance on five neuropsychological tasks. Black represents the VSN+ group. Grey represents the VSN- group. Note that in these analyses we only included a subset of patients for which we had the data (see Table 4). **A.** WAIS digit span, forward, longest span. **B.** WAIS digit span, backwards, longest span. **C.** RAVLT, total number correct. **D.** ROCFT, raw score. **E.** D-KEFS Tower test, raw score.

were not included in the subsample (analysis not shown here). The group differences in the subsamples did not differ from the group difference in the original sample (all $BF_{10} < 0.13$). As displayed in the second column of the Statistics part in Table S1 (Test ~ group, Group), there was no clear evidence for group differences on the WAIS digit span forward, digit span backward, RAVLT and DKEFS Tower tests. However, there was strong evidence for a difference in performance on the ROCFT: on average, the VSN+ group had a lower performance on the ROCFT (mean = 17.25) than the VSN- group (mean = 30.63). Finally, we examined relationships between performances on the neuropsychological tasks and the SWM task (Table S1, final two columns, SWM ~ group + test, Group and Test). When accounting for performance on the WAIS digit span forward, WAIS digit span backward or 15 words task, we still observed a difference in the lower average SWM performance in the VSN+ group (all $BF_{10} > 50$).

Summary

These results suggest that, although the VSN+ group scored worse on the SWM task than the VSN- group, this is not due to a general worse performance on any cognitive task. However, when correcting for the performance on the ROCFT, there was no clear evidence for an effect of group on SWM performance ($BF_{10} = 0.251$). In contrast, there was a clear relationship between SWM performance and the performance on the ROCFT, where every point lost on the ROCFT related to an increase in SWM threshold of 0.03 base 10 log units (CrI: 0.01-0.05).

Table S1. Exploratory analyses. Number of cases per neuropsychological test and average score per subsample. In the Statistics columns, the second header shows the statistical model, the third header shows the effect name for which the Bayes Factor is shown in the column below (BF¬10). A $BF_{10} > 3$ indicate evidence in favour of an effect, whereas $BF_{10} < \frac{1}{3}$ indicate evidence in favour of the absence of an effect.

	VSN- (N = 158)			VSN+ (N = 24)			Statistics (BF_{10})			
	N	%	Mean	N	%	Mean	SWM~group	Test~group	SWM~group + test	
							Group	Group	Group	Test
WAIS fw[1]	47	29.7	5.38	11	45.8	5.46	7.62×10^4	0.329	1.82×10^5	0.135
WAIS bw[2]	47	29.7	3.89	11	45.8	3.46	7.62×10^4	0.544	6.34×10^4	0.280
RAVLT[3]	64	41.1	36.5	13	54.2	31.1	1.54×10^6	0.954	1.34×10^6	0.160
ROCFT[4]	41	25.9	30.6	8	33.3	17.3	11.0	1.94×10^4	0.251	365
D-KEFS[5]	76	48.1	14.6	8	33.3	12.2	298	0.940	53.0	15.5

[1]WAIS fw = Wechsler adult intelligence scale, digit span forward (score = max. span length),

[2]WAIS bw = Wechsler adult intelligence scale, digit span backward (score = max. span length),

[3]RAVLT = Rey auditory verbal learning test (score = number correct),

[4]ROCFT = Rey-Osterrieth complex figure test (score = raw total score)

[5]D-KEFS = Delis-Kaplan executive function system (score = raw total score

6

Chapter 7

Spatial inhibition of return as a function of fixation history, task, and spatial references

Author contributions

JHF, MJS and SvdS conceptualized and designed experiments. JHF programmed experiments, collected data and performed analyses. JHF, MJS and SvdS wrote and revised manuscript.

Abstract

In oculomotor selection, each saccade is thought to be automatically biased toward uninspected locations, inhibiting the inefficient behaviour of repeatedly refixating the same objects. This automatic bias is related to inhibition of return (IOR). Although IOR seems an appealing property that increases efficiency in visual search, such a mechanism would not be efficient in other tasks. Indeed, evidence for additional, more flexible control over refixations has been provided. Here, we investigated whether task demands implicitly affect the rate of refixations. We measured the probability of refixations after series of six binary saccadic decisions under two conditions: visual search and free viewing. The rate of refixations seems influenced by two effects. One effect is related to the rate of intervening fixations, specifically, more refixations were observed with more intervening fixations. In addition, we observed an effect of task set, with fewer refixations in visual search than in free viewing. Importantly, the history-related effect was more pronounced when sufficient spatial references were provided, suggesting that this effect is dependent on spatiotopic encoding of previously fixated locations. This known history-related bias in gaze direction is not the primary influence on the refixation rate. Instead, multiple factors, such as task set and spatial references, assert strong influences as well.

Introduction

Humans and other animals sample their environment with high spatial resolution by fixating different objects for short amounts of time. However, only a single location can be fixated at a time. Since the seminal work of Yarbus, it is known that not all parts of the visual world are fixated equally often (Yarbus, 1967). Hence, to efficiently sample the environment for visual information, humans continuously make decisions about where to move their eyes next. These saccadic decisions are influenced by a wide range of factors, such as the stimulus properties, task set, and expectations (Hayhoe & Ballard, 2011). In this context, refixations (fixating an already fixated location or object) have gained considerable attention. The interest in refixations has particularly grown since the first reports of inhibition of return (IOR) (Posner & Cohen, 1984; Posner, Rafal, Choate, & Vaughan, 1985). IOR is a delay in responses to recently attended locations at late cue – target onset asynchronies. It has been hypothesized that this temporal delay is enabled by the automatic placement of "inhibitory tags" at previously fixated locations (Abrams & Dobkin, 1994; Klein, 1988; Klein & MacInnes, 1999), thereby lowering the probability of making a refixation, and increasing sampling efficiency (Klein, 2000).

Despite the established temporal effect of IOR, a lowered probability of refixating any given location is often merely inferred from latency data. The increased latencies (temporal IOR) have been hypothesized to reflect a facilitation of saccades toward uninspected locations (spatial IOR), thus increasing sampling efficiency (Klein, 2000). Only a few studies have directly addressed refixation probabilities (Boot et al., 2004; Gilchrist & Harvey, 2000; Hooge, Over, van Wezel, & Frens, 2005; Luke, Smith, Schmidt, & Henderson, 2014; McCarley et al., 2003; T. J. Smith & Henderson, 2011). Unfortunately, what to use as a baseline when addressing refixation probabilities has been the subject of some debate. As was illustrated by Yarbus' work, some locations in a scene have a higher probability of being fixated, and therefore subsequently refixated. Hence, when addressing refixation probabilities, multiple parameters (e.g., saliency) have to be controlled for in the baseline probability (Bays & Husain, 2012; Gilchrist & Harvey, 2000; Hooge et al., 2005; Klein & Hilchey, 2011; T. J. Smith & Henderson, 2011). McCarley and colleagues (2003) circumvented a complex model with multiple parameters by using an artificial search task consisting of a series of binary saccadic decisions. Their subjects were presented a "hidden search display' where only two items of the entire search array were visible. Subjects made

a saccade to either of the two, in order to identify it as a target or a distractor. At some point in the trial, one of the two items was an item that had already been fixated. Hence, the a priori chances of a refixation and of a saccade to a new location were both 0.5. The results showed that the probability of making a refixation was indeed reduced, but this probability increased to baseline chance with more intermittent fixations, suggesting a limited lifetime of the inhibitory tags. This observation resulted in the hypothesis that IOR tags are stored in visual working memory (VWM) (Bays & Husain, 2012; Henderson & Hollingworth, 1999; Hollingworth & Luck, 2009; Peterson, Kramer, Wang, Irwin, & McCarley, 2001). The logic is that because the capacity of VWM is limited (Luck, 2008), information obtained at previous fixations is only available for a limited time. When the information is no longer available in VWM, a saccade might be executed to the location containing the interesting information again.

However, as was noted by Posner et al. (1985), IOR is "not the main determiner", but rather just one of the many factors contributing to oculomotor behaviour. Smith and Henderson (2011) also provided an integrative explanation of refixations, in which IOR is implemented as an initial delay in return saccades, that in more complex tasks might be obscured by other processes. This implies that in certain conditions the suppressing effect of IOR on refixations is stronger than in others. Interestingly, examples in the literature have suggested that the expression of temporal IOR is also modulated by different factors. For example, temporal IOR is observed most strongly when a subject performs a search task, but also to a lesser extent when the subject performs a memory task or is asked to rate a scene for its pleasantness (Dodd, Van der Stigchel, & Hollingworth, 2009). Another example is that temporal IOR diminishes when targets reliably appear at a particular, previously fixated location (Farrell, Ludwig, Ellis, & Gilchrist, 2010). Some flexibility in the rate of refixations has also been observed in the aforementioned binary saccadic decision paradigm (Boot et al., 2004). When subjects were explicitly instructed to intentionally make saccades to new targets instead of refixations, subjects made fewer refixations. This led to the conclusion that the rate of refixations can intentionally be altered. However, whether any flexibility in the rate of refixations is also implicitly influenced by task set has not yet been addressed. On a more global scale, previous studies have suggested that gaze direction is influenced by the current behavioural goals of the observer (Tatler, Wade, Kwan, Findlay, & Velichkovsky, 2010).

Here, we tested the hypothesis that refixations are flexibly inhibited when this is beneficial for task performance, but to a lesser extent when there is no explicit gain from

inhibiting refixations. In other words, do fewer refixations occur when task performance profits from inhibiting them, than under neutral, free viewing conditions? To address this question, we used a paradigm similar to that of McCarley et al. (2003). We manipulated the relevance of applying inhibition of refixations by having subjects perform two tasks within the same paradigm. In one task, subjects searched for a specific target (similar to McCarley et al., 2003), where inhibiting refixations would result in increased task performance. In the second task, subjects made saccades without any secondary objective. In this task, inhibiting refixations would not increase task performance.

Experiment 1

In Experiment 1, we assessed whether differences in the task set result in different saccadic decisions. Subjects completed two versions of a task in which they made six successive saccadic decisions. The decisions were binary ("fixate location A or location B"). The first five decisions were always between two locations that had not been fixated before. Crucially, the final decision was between a location that had been fixated and a novel location. To test the hypothesis that inhibiting refixations is task-dependent, subjects performed the task twice, once when they were instructed to locate a target ("search"), and once when they were instructed to make a series of saccades until a trial ended ("free viewing"). Additionally, we tested whether the probability of refixations increased with more intermittent fixations, since this had previously been observed in a similar search task (McCarley et al., 2003). For our paradigm, this meant that at the final saccadic decision, subjects had to choose between a novel location and a location that had been fixated either one, two, three, or four fixations back.

Method

Subjects

Ten naïve subjects (ages 20 – 27; nine female, one male) with normal or corrected-to-normal vision participated in Experiment 1. All subjects gave informed written consent and were paid for their participation. The study was approved by the faculty ethics committee of Utrecht University and was conducted in accordance with the Declaration of Helsinki.

Apparatus

Figure 1. Probes, distractor, and target. In both the search task (top labels) and the free viewing task (bottom labels), the probes were used as potential saccade targets. The actual diameter was 0.5°. The probe changed into either a distractor or a target in the search task. In the free viewing task, the probes did not change upon fixation. Only the final probe in each trial changed into the "endpoint" which was similar to a distractor in the search task.

All stimuli were presented on an LG 24MB65PM LCD-IPS monitor (50.7×33.9 cm) with a spatial resolution of 1280×800 pixels and a refresh rate of 60 Hz. The stimuli were generated using MATLAB (The MathWorks Inc., Natick, MA) and the Psychophysics Toolbox 3.0 (Brainard, 1997; Pelli, 1997). Eye movements were recorded with an EyeLink 1000 eye tracker (SR Research Ltd., Ottawa ON) with a sampling rate of 1000 Hz. The left eye was monitored. Subjects were seated in a darkened room and viewed the screen from a distance of 70 cm; their heads rested on a chinrest with a forehead rest, to minimize movements.

Stimuli

Locations were probed by small, thick grey rings (radius = 0.25°, radius inner circle = 0.14°; see Fig. 1), presented on a black background. In the search task, upon fixation the probes changed into thin grey rings, indicating a distractor (radius = 0.25°, radius inner circle = 0.2°), or a filled grey circle, indicating the target (radius = 0.25°). In the free-viewing probes, only the final probe changed from the thick grey ring to a thin grey ring, indicating the trial end. The corners of the area where the probes could appear were marked by differently coloured (red, green, yellow, and blue), orthogonal lines (2°), similar to those used in McCarley et al. (2003).

Procedure

Subjects completed two tasks: "search" and "free viewing". The order of the tasks was counterbalanced across subjects. Both consisted of 240 experimental trials. The search task had an additional 240 filler trials randomly interleaved with the experimental trials (explained below). The search task was divided into eight blocks, the free viewing task into four. All blocks started with the standard 9-point calibration and validation routines of the EyeLink 1000 eye tracker. In the experimental trials (Fig. 2), subjects initially fixated a central fixation point. After 500 ms of stable fixation, two location probes appeared. Subjects were
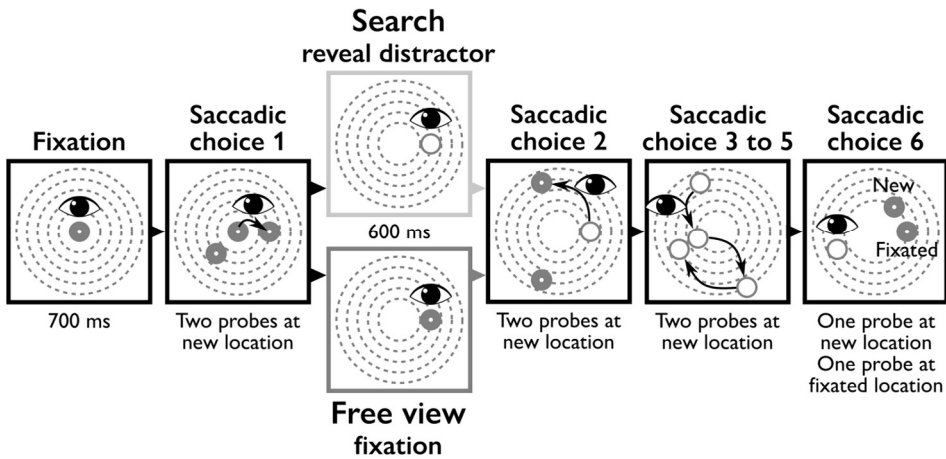
Figure 2. Sequence of events in a typical experimental trial with a lag of 4. In the actual display, the probe size was twice as small with respect to the dotted eccentricity rings depicted here. The actual background colour was black, and the dotted rings were not visible. **1.** A trial started with a central fixation for 700 ms, followed by the appearance of the first two location probes. **2.** Subjects were instructed to make a saccade to either probe. **3.** In the search task, the fixated probe turned into a distractor. In the free-viewing task, the probe did not change. There was always a delay of 600 ms between fixation and the onset of the two subsequent location probes. **4.** Another saccadic decision was made. **5.** For illustration purposes, the alternative probe locations for Saccades 3 to 5 are left out, so that only the fixated locations are shown. In the actual experiments, subjects were presented two location probes at each step. Note that the distractors displayed here would not remain on screen. Moreover, in the free viewing task, the probes never changed into a distractor until the final probe. **6.** At the final screen, one probe was located at a position that had been fixated before, and one at an uninspected location.

instructed to fixate one of the two probes. The alternative and the previously fixated probe (or fixation point) disappeared upon the new fixation. After 600 ms, two new probes were presented, and the subject made another saccadic decision and fixated one of the two probes. Subjects made six decisions per trial, in which each new probe pair was shown 600 ms after fixation onset. This interval was fixed. In the first five pairs, both probes were located at novel locations. In the final pair, one probe was located at a novel location, and the other probe was located at one of the previously fixated locations. The old location could be either one, two, three, or four fixations back. There were 60 trials for each of these lags. The choice in this final saccadic decision was used as a measure of saccadic choice preference.

The search task and free viewing task differed in their instructions. In the search task, subjects were instructed to locate a target stimulus. In the free viewing task, they were instructed to fixate one probe of each pair until the trial ended. In addition to the difference in instructions, the experimental trials differed slightly between the different tasks. In the

7

search task, a fixated probe "revealed its identity" upon fixation — that is, changed into a distractor (thin ring) or a target (filled circle). Importantly, this target was always located at the new location in the final probes. Thus, subjects would only find the target when they did not make a refixation. In the free viewing task, the location probes did not change, but remained thick grey rings. Only the last probe changed into a thin grey ring upon fixation, to indicate the trial end. However, in this task it did not matter whether a subject made a refixation; the trial would end, regardless. In both tasks, the alternative and previous probes disappeared from the screen upon a new fixation. Note that despite small differences in the foveal stimuli between the two tasks, peripheral visual stimulation during the crucial part of saccadic decision making was equal in both tasks.

In addition to the experimental trials, the search task contained 240 filler trials. In these filler trials, subjects would always find the target at either the first (20%), second (20%), third (20%), fourth (20%), or fifth (20%) fixation, irrespective of which location of a probe pair was fixated. All probes in the filler trials were shown at uninspected locations, similar to the first five probe pairs of the experimental trials. The filler trials were included to keep the subjects actively involved in their saccadic decisions, by giving the impression that the location of the target was really predetermined, whereas it was actually determined gaze-contingently. In other words, the location of the target was not set at the beginning of a trial, but rather the time at which it would be shown was set (i.e., always after the sixth decision in experimental trials, and always before the sixth decision in filler trials).

Probe locations

Locations were probed gaze-contingently, to ensure that two probes were placed equidistant from the currently fixated location. Locations were set in polar coordinates, using a set of five fixed eccentricities (ρ) with respect to the center of the screen (depicted as the dotted rings in Fig. 2). The ρ's were 3°, 4.5°, 6°, 7.5°, and 9° of visual angle. The sequence of ρ's was shuffled, with the constraint that for two consecutive probe pairs, the ρ's differed by at least 3° of visual angle. The angular separation (θ) between the first two probes was 120 deg. For the next probe pairs, the angular separation was 90 deg when ρ increased. When ρ decreased, the two probes were placed on opposing sides of the imaginary circle around screen center with a radius ρ (so, the distance between the two probes was 2ρ). These constraints yielded a median separation of 9.0° between the two probes in a pair (min 4.1°, max 18.0°) and a median distance of 8.7° between the currently fixated probe and the next probes (min 2.3°, max 16.3°). To anticipate and prevent

situations in which it would have been impossible to pick two locations meeting these constraints, all possible sequences for every trial (i.e., 26 sequences) were computed prior to the experiment.

Data analysis

Online gaze analysis was based on eye position. Targets were revealed when gaze was detected within a region of 2° around either probe. The saccades and fixations were reanalysed offline with a velocity-based algorithm (Nyström & Holmqvist, 2010). Trials were excluded when saccades after the presentation of the final probes were either too fast (<80 ms) or too slow (>1000 ms). Second, trials were excluded when no fixations were detected after the onset of the final probes or when the final fixation was not decisively close to one of the two probes (0.8% – 7.9%). A third exclusion criterion was when the online gaze-contingent algorithm failed to detect gaze samples at either probe within 2600 ms after probe onset (1.0% – 6.9% of trials per subject). These exclusion criteria resulted in a minimum of 45 trials per lag per subject in each task.

We performed a logit mixed-effects analysis using the lme4 package in R (Baayen et al., 2008; Bates et al., 2015; Jaeger, 2008). In this model we included task and lag as fixed effects, and for each subject a random intercept. "Lag 1" in the search task was set as the reference level. With these settings, all reported β's (in log probability) are relative to the rate of refixations at lag 1 in the search conditions.

Results

Refixation rate

Figure 3 (left panel) shows the proportions of refixations at different lags in both tasks: search and free viewing. As can be seen in the figure, the probability of refixations seems to increase until a lag of 4. After visual inspection of the data, we analysed a linear effect of lag (in log space) from lag 1 to lag 3. Including the data from four-back would reduce the fit of the model, or would require an overparameterized, nonlinear model. We believe it is fair to assume that from lag 3 onward, a constant "plateau" in the rate of refixations is reached, and that any fluctuations there are related to noise rather than a fixed effect.

We found a preference for saccades toward new targets in the search task at lag 1 (β = -0.52, z = 3.64, p < .001). However, there were more refixations with increasing lag in the
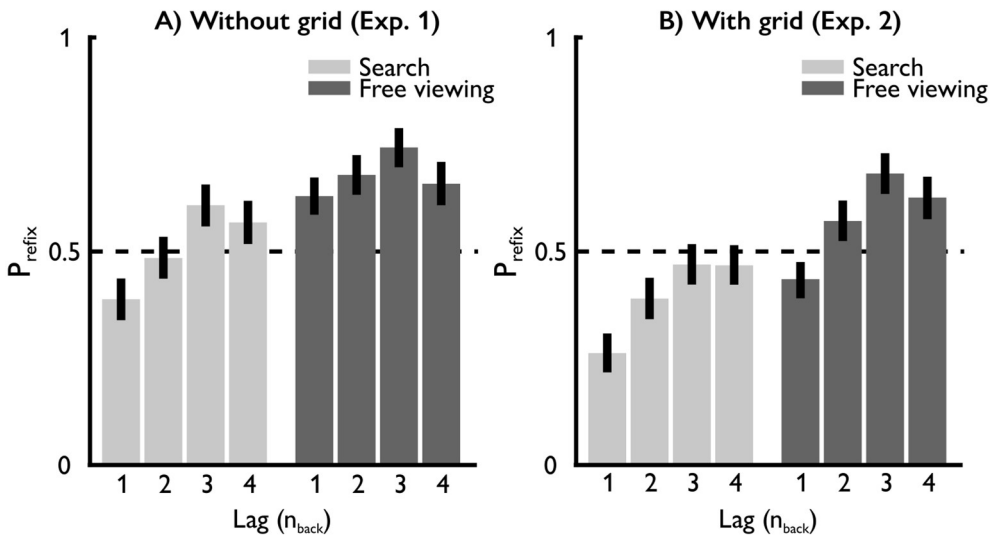
Figure 3. Proportions of refixations. **A.** Experiment 1: Subjects performed the tasks on a blank background. **B.** Experiment 2: Subjects performed the task with a continuously present background grid. In both panels, the left bars represent the group average proportions of refixations in the search task (light grey), and the right bars represent the group average proportions of refixations in the free viewing task (dark grey). Error bars represent the bootstrapped 95% confidence intervals of the sample mean (2,000 bootstrap samples). Values smaller than .5 indicate a preference for new locations, and values above .5 indicate a preference for refixations.

search task ($\beta = 0.48$, $z = 7.66$, $p < .001$). In the free viewing task, the rate of refixations at lag 1 was considerably higher than in the search task ($\beta = 1.06$, $z = 9.212$, $p < .001$). To inspect the free-viewing condition further, we reran the model with this task as a reference level. At lag 1, subjects showed a preference for refixations in the free viewing task ($\beta = 0.55$, $z = 3.79$, $p < .001$), in contrast to the preference for saccades to new targets in the search task. Moreover, although an effect of lag did emerge in the free viewing task ($\beta = 0.27$, $z = 4.02$, $p < .001$), it was substantially smaller than in the search task ($\beta = 0.21$, $z = 2.29$, $p = .022$).

On the basis of bootstrapped 95% confidence intervals (see Supplementary Table S1), we observed significant "absolute" inhibition of return only in the search task at lag 1. In contrast, we observed a preference for refixations at lags 3 and 4 in the search task and for all lags in the free viewing task. In summary, Experiment 1 shows a preference for refixations in the free viewing task that grows stronger with increasing lag. Furthermore, in the search task, in which refixations decreased task performance, there was a preference for saccades toward new locations at the shortest lag, but this increased with increasing lag. The

refixation rate increased even to the extent that a preference for refixations was observed for lags 3 and 4.

Saccade latency

Although subjects were not instructed to make saccades as quickly as possible, but rather to find as many targets as possible (in the search task), we analysed the saccadic latencies (see Supplementary Table S2 with all of the mean latencies). This analysis was performed because IOR is often defined as an increased latency between onset and response. Since we had no clear baseline latency, we included Choice (refixation vs. new) as a factor, so that the linear mixed-effects analysis on the saccadic latencies included Choice, Lag, and Task as fixed factors and subjects as an effect on the intercept. The reported β's are in milliseconds, with respect to the average latency for saccades toward new locations in the search task. Statistics are reported with t values only. As a rough approximation, t values higher than 2 are usually considered as a significant difference (Baayen et al., 2008).

The estimated latency for saccades toward new locations in the search task at lag 1 was 228.8 ms. This was not significantly different for saccades toward already fixated locations (β = -0.14, t = 0.019). Latencies in the free-viewing task were not significantly higher than in the search task (β = 0.4, t = 0.05), nor was the latency difference between saccades toward already fixated and new locations more pronounced (β = 6.0, t = 0.56). We found no effect of lag in either the search task (β = 4.5, t = 1.14) or the free-viewing task (β = -6.7, t = 1.054). In the search task, the effect of choice (refixation vs. new location) was not significantly different for shorter than for longer lags (β = -8.3, t = 1.47), which was also not different in the free viewing task (β = 2.8, t = 0.34). To summarize, neither choice, lag, nor task was a significant predictor of saccadic latencies (for a full overview of the estimated parameters and t statistics, see Supplementary Table S3). This presumably implies that factors other than the classic IOR effect more strongly affected latencies (for a similar notion, see Smith & Henderson, 2011). It should be noted that since subjects were not instructed to make speeded saccades, any subtle effect might have been obscured.

Discussion

In Experiment 1, we used a binary saccadic decision paradigm to quantify saccadic choice preferences for new locations and refixations under two different task sets. A similar paradigm has been used to show that in visual search, saccades toward new locations are

favoured over refixations (McCarley et al., 2003). This observation has been linked to the phenomenon of IOR (Macinnes & Klein, 2003), in which saccades to probes have been found to be slower when directed to probes presented at recently fixated locations. However, subsequent studies have shown that this temporal slowing of refixations is specific to visual search, and is not observed (or only to a lesser extent) in other visual tasks (Dodd et al., 2009; T. J. Smith & Henderson, 2009).

In Experiment 1, we showed that saccadic decisions are mediated by both a history-related effect and a task-related effect. With increasing lag between the initial fixation and the final decision, there was a higher rate of refixations. In addition to an effect of lag, we also observed an effect of task on the rate of refixations, with more refixations in the free viewing task as compared to the search task. Interestingly, we observed absolute spatial IOR only for the most recently fixated location and only in the search task. In contrast, in the free viewing task, refixations were favour

red over saccades to new locations. This suggests that refixations may occur frequently by default under task settings other than search. Moreover, they are actively inhibited during search, but the effect of lag on the rate of refixations is present in both search and free viewing. Hence, this effect might reflect an automatic process, such as IOR (Klein & MacInnes, 1999) or saccadic momentum (T. J. Smith & Henderson, 2009), that is intrinsic to the oculomotor system (Hooge & Frens, 2000; Posner et al., 1985).

Despite the similarities in paradigm, there is an important difference between the results of McCarley et al. (2003) and the present experiment: whereas in both experiments a similar lag-related effect was observed, we did not observe the absolute spatial IOR that was found in the original paradigm. We believe that small differences between the paradigms may have resulted in this difference. In McCarley et al.' s paradigm, stimuli that had been fixated could remain on screen over the course of several saccades. In contrast, in the present experiment, all stimuli except the fixated stimulus were removed from the screen at the onset of fixation. Therefore, in the present experiment, subjects only had a single opportunity to make a refixation in every trial, whereas in the original paradigm a previously fixated item could reappear several times on screen, or even remain on screen over several saccades. Importantly, this might have facilitated spatiotopic encoding of IOR in the original paradigm (Klein & MacInnes, 1999; Müller & von Mühlenen, 2000; Takeda & Yagi, 2000). Indeed, McCarley and colleagues noted that the rate of refixations was lower when items
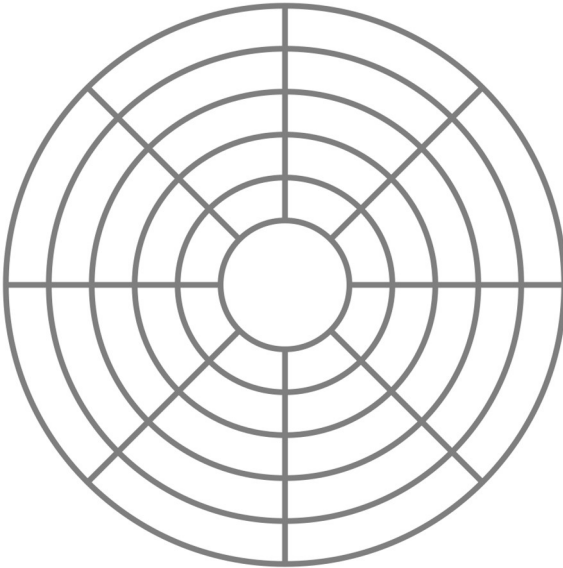
Figure 4. A radial grid was added to the display in Experiment 2. Targets could only appear between the concentric lines.

remained on screen (McCarley et al., 2003) or when more spatial references were provided (Kramer, McCarley, Boot, & Peterson, 2004).

To investigate whether sufficient spatial reference is a prerequisite for successfully inhibiting refixations of previously fixated locations, we performed a second experiment with a different group of subjects (n = 10). Experiment 2 was essentially a replication of Experiment 1, with the addition of a radial grid in the background display to provide more spatial reference.

Experiment 2

In Experiment 2, we investigated the hypothesis that with continuous spatial references, the rate of refixations can be reduced. Both tasks from Experiment 1 were repeated with a different set of subjects and the addition of a radial grid (Fig. 4) in the display, to facilitate the spatiotopic encoding of previously fixated locations.

Method

Ten different naïve subjects (ages 19-26; nine female, one male) participated in Experiment 2. All apparatus, stimuli, and procedures were identical to those of Experiment1, with the addition of a radial grid (Fig. 4) to the background of the display. This

grid was present during an entire trial, and the location probes appeared between the radial lines of the grid. The same exclusion criteria as in Experiment 1 were used, resulting in at least 46 trials per lag per condition.

Results

Refixation rate

Figure 3 (right panel) shows the logits of refixations at different lags for the two conditions obtained in Experiment 2. To investigate whether the addition of a radial grid to the display decreased the rate of refixations, we performed another linear mixed logit effects analysis. We included the factors Task, Lag, and Grid Presence as fixed effects, and subject as a random effect. The reference level for all subsequently reported β s is the search task in Experiment1 (without grid) at lag 1. As we found before, there was a significant preference for saccades toward new locations in the search task at lag 1 (β = -0.52, z = 3.95, p < .001). In Experiment2, this preference was even more pronounced (β = -0.49, z = 2.59, p =.009). The effect of lag in Experiment 1 had been expressed as an increasing preference for refixations with increasing lag (β = 0.48, z = 7.65, p < .001). In Experiment 2, a similar effect was observed, not significantly different from the effect of lag in Experiment 1 (β = 0.003, z = 0.031, p = .975). Furthermore, in Experiment 1 the refixation rate was higher in the free viewing task than in the search task (β = 1.06, z = 9.21, p < .001); in Experiment 2, this difference was slightly smaller (β = -0.33, z = 2.00, p = .045), although there was still a higher rate of refixations in the free viewing task than in the search task (β = 0.73, z = 6.25, p < .001). The effect of lag was smaller in the free viewing task than in the search task in Experiment 1 (β = -0.21, z = 2.29, p = .022). However, in Experiment2, the effect of lag was not different across the different tasks (β = 0.06, z = 0.64, p = .525). In summary, we observed a reduction in refixations in both the search and free viewing tasks when a background grid was present. Moreover, there was an effect of lag irrespective of grid presence, yet this effect was stronger in the free viewing task when a background grid was provided. This difference was not observed in the search task.

As in the analysis of Experiment1, we further inspected the observed refixation rates with bootstrapped 95% confidence intervals (see Supplementary Table S1). When a background grid was present, a preference for saccades toward new locations was apparent in both the search and the free viewing task at lag 1. In the search task, this was also the case at lag 2, but in the free viewing task, there was a preference for refixations at lag 2.

This preference for refixations was also found for lags 3 and 4 in the free viewing task. In the search task, however, no clear preference for either probe emerged at lags 3 and 4.

Saccade latency

As in Experiment 1, although we did not instruct subjects to finish a trial as quickly as possible, we analysed saccadic latencies, since they are such an important measure in the IOR literature (Table S2). We used a linear mixed-effects analysis with Choice, Task, Lag, and Grid Presence as fixed factors and subject as a random effect. The output of this analysis is provided in Supplementary Table S4. In short, this analysis showed that saccadic latencies in the search task increased with the introduction of a background grid (β = 10.8, t = 4.36), and that this increase was smaller in the free viewing task (β = − 5.4, t = 4.05). We observed no lag- or refixation-related effects (all t's< 1.2). The increased latency in the search task suggests that subjects might have employed more cognitive strategies to prevent refixations in the search task.

Discussion

To facilitate spatiotopic encoding of previously fixated locations, a radial grid was added to the background. This background grid was not relevant to the task in any way, but simply provided more spatial references to the display than in Experiment1. We observed that the rates of refixations were reduced when sufficient spatial references were provided. In regular search displays, these references can comprise the items in the search display itself. The data show that the reduction in refixations as a result of the background grid was not task specific. Importantly, with a background grid, we observed a quantitative preference for saccades toward new locations (i.e., spatial IOR) in the search task up to lag 2, and in the free viewing task at lag 1. However, there was still a preference for refixations in the free viewing task from lag 2 onward. We believe that the presence of continuous visual stimuli (as in Exp. 2) may account for the differences in absolute refixation rates between Experiment 1 and previous experiments (Boot et al., 2004; McCarley et al., 2003). In the previous experiments, stimuli could be present on the screen for several fixations, in contrast to the present study, in which stimuli always disappeared upon the next fixations. Instead of adding persistent probes to the display, we decided to use a background grid instead, to keep most parameters constant from Experiments 1 to 2, enabling a fairer comparison between the two.

7

General discussion

Biases in saccadic decisions have been found to favour saccades toward uninspected locations, at least during visual search (Gilchrist & Harvey, 2000; McCarley et al., 2003; Peterson et al., 2001). This bias has been hypothesized to result from an automatic process (Boot et al., 2004) such as IOR (Klein & MacInnes, 1999; Macinnes & Klein, 2003). IOR is commonly defined in the temporal domain as an increase in the latencies of responses to recently attended stimuli (Posner & Cohen, 1984). This increase in latencies has been suggested to facilitate visual search by decreasing the probability of making a refixation (Klein, 1988, 2000). Studies have indicated flexibility in the expression of temporal IOR under task sets other than visual search (Dodd et al., 2009; Farrell et al., 2010; Luke et al., 2014). Moreover, it has been stressed that the process of making a refixation is subject to multiple factors (Posner et al., 1985; T. J. Smith & Henderson, 2011), of which at least one can be flexibly adjusted. This has been interpreted to reflect an efficient flexibility to adapt oculomotor behaviour to meet the current task demands. Here we tested this functional interpretation of IOR by having subjects perform a nearly identical paradigm under two different sets of instructions.

The present data show both a task-dependent and a history-dependent effect on the rates of refixations. Moreover, refixation rates were lower when more spatial references were provided. It has been noted before that the refixation rate is inflexibly influenced by an automatic, history-dependent process (Boot et al., 2004; Gilchrist & Harvey, 2000; McCarley et al., 2003; Peterson et al., 2001). This process biases saccades in favour of new locations, suggestively corresponding with the conceptualization of IOR (Klein & MacInnes, 1999; Posner et al., 1985) or saccadic momentum (T. J. Smith & Henderson, 2009). Although the history-dependent effect in the present experiments was also present under both task sets, the strength of the effect interacted with task set. Even more, we observed a three-way interaction of task, lag, and spatial references, suggesting that a history-dependent effect can be modulated by task set, but that this modulation is weaker when sufficient spatial references are provided. Thus, speculatively, the influence of the history-dependent effect was stronger with sufficient spatial references, fitting with converging evidence that IOR is coded in spatiotopic coordinates (Z. Wang & Klein, 2010).

As a crucial addition to this history-dependent process, a more flexible process has been suggested to influence saccadic decision as well (Boot et al., 2004; Luke et al., 2014;

T. J. Smith & Henderson, 2011). Here, we confirmed such a second process, which is implicitly influenced by task demands. When subjects were searching for a target, they made fewer refixations than when they made saccadic decisions without specific search instructions. Moreover, the present data suggest that under specific conditions, refixating might actually be a default mode, even though immediate refixations tend to be inhibited through the aforementioned automatic process (i.e., the high probability of refixations at late lags in free viewing). Under natural viewing conditions, these locations may comprise the most salient regions within a scene (Bays & Husain, 2012; Wilming, Harst, Schmidt, & König, 2013). Moreover, the implicit benefit of inhibiting refixations in a search task only goes for static displays. When targets are mobile, re-inspecting a location might be fruitful.

For the oculomotor system to take previously fixated locations into account, those locations should have references in a spatiotopic map (Gabay, Pertzov, Cohen, Avidan, & Henik, 2013; Hilchey et al., 2012; Mathôt & Theeuwes, 2010; Posner & Cohen, 1984). It has been suggested that these locations are stored in working memory (Bays & Husain, 2012; Peterson et al., 2001; Shen, McIntosh, & Ryan, 2014). In the artificial search paradigm used here, the maintenance of these locations in working memory was particularly difficult, as all stimuli were removed from the screen when they were no longer fixated. This might be a substantial difference from the similar paradigms that have been used previously, in which stimuli could remain on screen, providing continuous spatial reference (Boot et al., 2004; Kramer et al., 2004; McCarley et al., 2003). Indeed, when we provided subjects with more spatial references, they were better at inhibiting refixations, perhaps as a result of improved working memory representations (Deubel, 2004; Golomb, Pulido, et al., 2010; Lisi et al., 2015).

The present results show that the probability of a refixation is influenced by at least two processes: one history-related process inhibiting immediate refixations, and one flexible process that can be implicitly influenced by task set. importantly, the expression of at least the history-related effect seems to be related to the degree to which fixated locations can be maintained spatiotopically. Together, these findings confirm the notion of Posner et al. (1985) that, although the oculomotor system may be intrinsically biased to making saccades toward new locations, other factors play a crucial role as well, even to such an extent that the probability of a refixation is higher than chance. Moreover, the observation of absolute spatial IOR is related to the presence of sufficient spatial references.

Chapter 7 – Supplementary information

Table S1. Bootstrapped 95% confidence intervals of the proportions of re-fixations (2000 bootstrap samples). Stars indicate confidence intervals that do not include 0.5

Task	Lag	No grid	Grid
Search	1	0.35 – 0.43 *	0.23 – 0.30 *
	2	0.45 – 0.52	0.35 – 0.43 *
	3	0.57 – 0.65 *	0.43 – 0.51
	4	0.53 – 0.61 *	0.43 – 0.51
Free saccades	1	0.59 – 0.67 *	0.40 – 0.47 *
	2	0.64 – 0.72 *	0.53 – 0.61 *
	3	0.71 – 0.78 *	0.64 – 0.72 *
	4	0.62 – 0.70 *	0.59 – 0.66 *

Table S2. Average saccadic reaction times in milliseconds

Task	Lag	Choice	No grid (s.e.m.)	Grid (s.e.m.)
Search	1	new	230.9 (13.5)	350.2 (36.3)
		re-fixation	238.2 (16.8)	344.6 (37.5)
	2	new	221.2 (12.2)	356.2 (35.3)
		re-fixation	218.2 (10.9)	352.3 (37.4)
	3	new	243.5 (15.6)	366.6 (43.0)
		re-fixation	230.0 (12.0)	344.1 (37.1)
	4	new	234.0 (15.8)	345.3 (33.8)
		re-fixation	219.0 (10.8)	334.8 (37.2)
Free saccades	1	new	251.6 (13.5)	322.5 (42.7)
		re-fixation	252.2 (22.9)	292.6 (31.5)
	2	new	239.3 (15.5)	292.5 (24.3)
		re-fixation	229.6 (8.5)	282.4 (21.5)
	3	new	226.8 (8.2)	295.4 (26.1)
		re-fixation	226.1 (11.3)	288.1 (27.2)
	4	new	239.6 (10.4)	278.8 (17.8)
		re-fixation	221.1 (7.8)	276.5 (23.1)

Table S3. Results of the linear mixed effects analysis of saccadic latencies in Experiment 1 (without grid)

Parameter	Estimate	Std. error	t-value
Intercept	228.8	9.1	24.98
Re-fixation	-0.1	7.3	-0.02
Free viewing	0.4	7.6	0.05
Lag	4.5	3.9	1.14
Re-fixation * Free viewing	6.0	10.6	0.56
Re-fixation * Lag	-8.3	5.6	-1.47
Free viewing * Lag	-6.7	6.4	-1.05
Re-fixation * Free viewing * Lag	2.8	8.3	0.34

Table S4. Results of the linear mixed effects analysis of saccadic latencies in Experiment 1 (without grid) and Experiment 2 (with grid) combined

Parameter	Estimate	Std. error	t-value
Intercept	229.3	17.6	13.03
Grid presence	10.8	24.7	4.36
Re-fixation	-0.1	9.6	0.01
Free viewing	0.3	10.1	0.03
Lag	4.5	5.2	0.86
Grid * Re-fixation	-15.7	14.1	1.12
Grid * Free viewing	-53.6	13.2	4.05
Re-fixation * Lag	6.1	14.0	0.43
Grid * Lag	0.7	7.0	0.10
Re-fixation * Lag	-8.3	7.4	1.12
Free viewing * Lag	-6.7	8.4	0.80
Grid * Re-fixation * Free viewing	-10.4	20.0	0.52
Grid * Re-fixation * Lag	-5.2	10.6	0.49
Grid * Free viewing * Lag	-1.4	11.2	0.13
Re-fixation * Free viewing * Lag	2.8	10.9	0.26
Grid * Re-fixation * Free viewing * Lag	-0.8	15.3	0.06

7
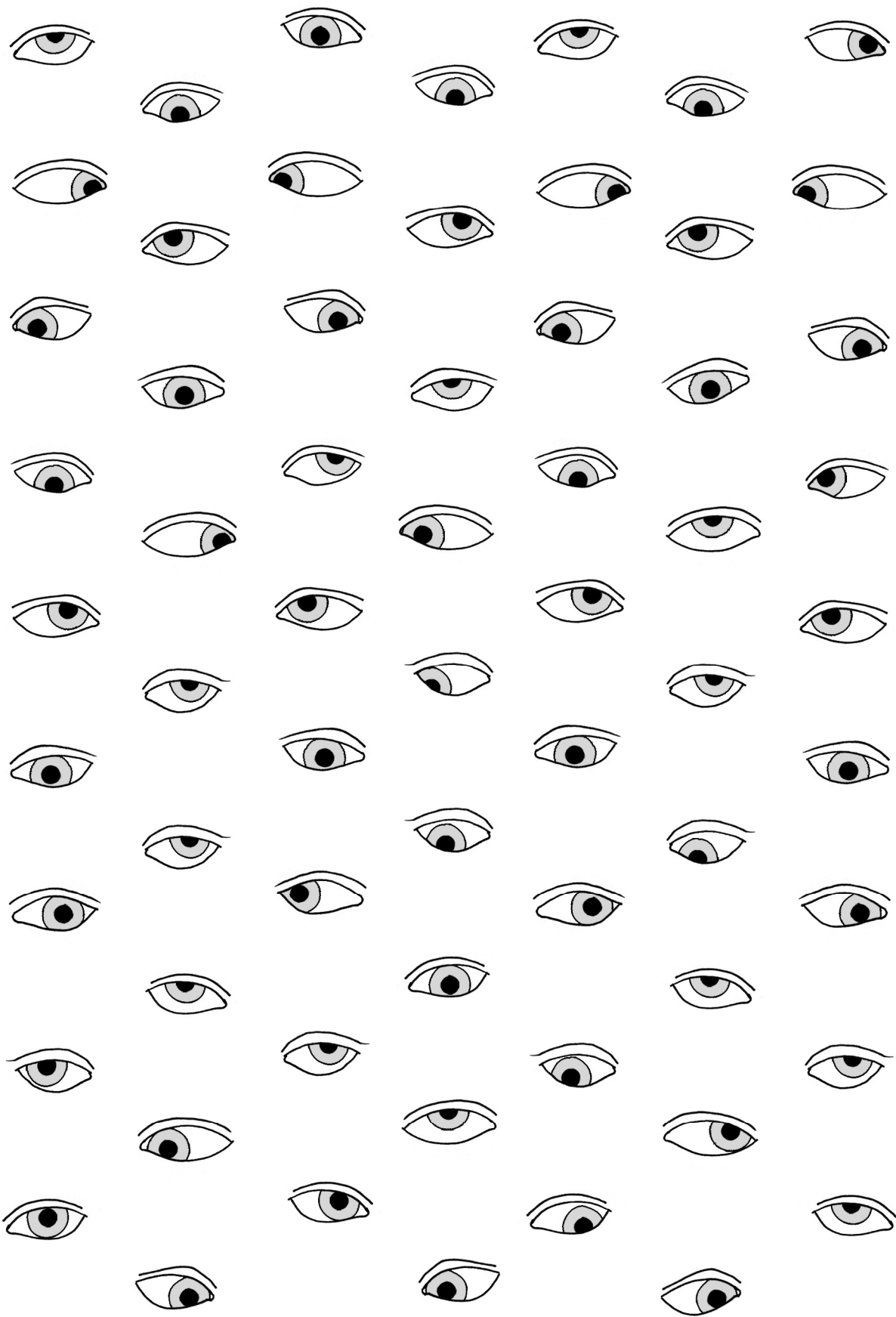
Chapter 8

Focus of spatial attention during spatial working memory maintenance: Evidence from pupillary light response

Author contributions
JHF, SM, and SvdS conceptualized and designed experiments. JHF programmed experiments, collected data and performed analyses. JHF, SM, MJS, TCNW and SvdS wrote and revised manuscript.

Abstract

In this experiment, we demonstrate modulation of the pupillary light response by spatial working memory (SWM). The pupillary light response has previously been shown to reflect the focus of covert attention, as demonstrated by smaller pupil sizes when a subject covertly attends a location on a bright background compared to a dark background. We took advantage of this modulation of the pupillary light response to measure the focus of attention during a SWM delay. Subjects performed two tasks in which a stimulus was presented in the periphery on either the bright or the dark half of a black and white display. Importantly, subjects had to remember the exact location of the stimulus in only one of the two tasks. We observed a modulation of pupil size by background luminance in the delay period, but only when subjects had to remember the exact location. We interpret this as evidence for a tight coupling between spatial attention and maintaining information in SWM. Interestingly, we observed particularly strong modulation of background luminance at the beginning and end of the delay, but not in between. This is suggestive of strategic guidance of spatial attention by the content of spatial working memory when it is task relevant.

Introduction

Successfully performing daily life spatial tasks, such as making coffee, partly depends on the capacity to select and remember the locations where crucial information has been or will be presented. Traditionally, the selection and temporary maintenance of locations is attributed to spatial attention and spatial working memory, respectively (SWM) (Baddeley & Hitch, 1974). A location is selected for further processing by attending to it and keeping that location available for a brief period is dependent on SWM. Despite the theoretical dichotomy between spatial attention and SWM, it has been argued that they both emerge from the same mechanism (Awh & Jonides, 2001; Postle, 2006). Thus, maintaining a location in SWM is equal to repeatedly attending a location during a retention delay (Awh et al., 1999).

Behavioural evidence for the involvement of spatial attention in SWM is obtained by experiments in which new spatial information interferes with information stored in SWM (Awh, Jonides, & Reuter-Lorenz, 1998; Herwig, Beisert, & Schneider, 2010; Lepsien, Griffin, Devlin, & Nobre, 2005; Van der Stigchel, Merten, Meeter, & Theeuwes, 2007). For example, Van der Stigchel et al. (2007) made subjects remember the location of a target. After a small delay, subjects clicked on the remembered location using a computer mouse. On some trials, a task-irrelevant distractor was presented at a different location. On these trials, the report of the remembered location shifted in the direction of the distractor. The authors concluded that the onset of the distractor attracted spatial attention away from the location of the remembered location, shifting the remembered location in SWM in the same direction. Although these studies provide support for a link between spatial attention and SWM, it is currently unclear whether the focus of attention is continuously located at the to be remembered location. To investigate this, we take advantage of a continuous signal that has recently been shown to be affected by the focus of covert attention: the pupillary light response.

Different groups have shown that the pupillary light response can be used as a measure of the deployment of covert attention (Binda & Murray, 2015; Binda et al., 2013; Mathôt et al., 2014; Mathôt, Melmi, van der Linden, & Van der Stigchel, 2016; Mathôt et al., 2013; Naber, Alvarez, & Nakayama, 2013). For example, while subjects maintained fixation at the centre of a black and white display, the sudden onset of a cue was used to attract attention

8

to a single side of the display, while not affecting the overall luminance of the display. When the onset was on the bright, white half of the display, pupils were more constricted than when the onset was presented on the dark, black half (Mathôt et al., 2014). This result shows that the pupillary light response reflects the focus of covert spatial attention.

Because working memory is conceptualized as the mental rehearsal of attentional allocation to specific features (D'Esposito & Postle, 2015), a recent study from our group examined whether the pupillary light response also reflects the content of visual working memory (Blom, Mathôt, Olivers, & Van der Stigchel, 2016). More specifically, subjects were presented a display with an equal number of bright and dark stimuli. Simultaneously, they were cued to remember either only the dark or only the bright stimuli, on which they performed a change detection task after a delay. The authors found differences in pupil size for dark or bright stimuli primarily when they were present on screen, but this difference diminished hen the stimuli were removed. There was no significant difference in pupil size in the working memory delay. Referring to the working memory model of Baddeley (Baddeley, 1992), they concluded that the pupillary light response reflects the encoding of stimuli into visual working memory, but not the maintenance.

The study by Blom et al. (2016) shows that visual working memory of bright or dark features does not affect the pupillary light response; we hypothesized that spatial working memory of a bright or dark location would affect the pupillary light response because we assume that this requires sustained (or repeated shifts of) visual attention. With the pupillary light response as a measure for attention, we can examine the focus of attention at each moment over the entire course over a working memory delay. In the current experiment, subjects performed two tasks: in the location discrimination (LD) task, they maintained a location for a period of 8.4 seconds in SWM to perform a spatial discrimination task; in the orientation change detection (OD) task, the same visual input was presented but the task instruction was different and there was no requirement to keep a location in memory. Crucially, locations (in the LD task) that had to be remembered were presented on either a bright or a dark background. During the working memory delay, we measured pupil size to estimate the focus of attention. The rationale here is, when spatial attention is continuously focused on the to be remembered location during a delay, we should observe differences in pupillary light responses when the location is presented on either a dark or bright background. Moreover, these differences should persist over the entire course of the working memory delay. Since the to be remembered location was relevant after the delay

in the LD task, but not in the OD task, we expected to find the hypothesized effect only in the LD task.

To preview the results, we observed an effect of background luminance on pupil size approximately 500 ms after the presentation of a stimulus, similar to previous studies (Binda & Murray, 2015; Mathôt et al., 2013). In the working memory delay, we observed an effect of background luminance in the LD task, where the location of the stimulus would become relevant after the delay. However, this effect did not persist over the entire working memory delay. Instead, we observed an effect at the beginning and at the end of the delay.

Methods

Subjects

Twelve subjects (age 18 – 26, nine female) with normal or corrected-to-normal acuity participated after giving written informed consent. All experimental procedures were approved by the local ethical committee of the Faculty of Social Sciences of Utrecht University.

Setup

Subjects were seated in a dark room with their heads resting on a chinrest. They were seated 70 cm in front of a 23″ LCD-IPS monitor with a spatial resolution of 1280×800 and a refresh rate of 60 Hz. All stimuli were created and presented using MATLAB (2016b) and the Psychophysics Toolbox 3.0 (Brainard, 1997; Kleiner et al., 2007; Pelli, 1997). Eye movements were recorded with an Eyelink 1000 (SR Research Ltd. Ottawa ON; sampling rate 1 kHz), using the Eyelink Toolbox for MATLAB (Cornelissen et al., 2002). The Eyelink was calibrated using the native 5-point calibration routine.

Stimuli

Subject were required to fixate a blue fixation point (r = 0.35°) in the centre of the screen. Stimuli were sinusoidal gratings (radius: 2°, contrast: 100%, spatial frequency: 2 cycles/deg.). Contrast decreased to 0 over the outer 0.5° of the grating. In a trial, multiple gratings were shown (see Procedure) all with a random phase. Stimuli were shown on a

8

black and white background annulus (inner radius: 5°; outer radius: 15°). Black and white layout (i.e., black-white or white-black) was randomly assigned for each participant.

Procedure

Each participant completed two tasks in a blocked design: Location Discrimination (LD) and Orientation Change Detection (OD). The order of tasks was counterbalanced across participants. All trials started with a single fixation point combined with the Eyelink 1000 drift check. In this drift check, gaze had to be closer than 2° to the fixation point and the subject had to press the spacebar. The sequence of visual events was equal in both tasks, until the response window. More importantly, the tasks varied in the task instructions given to the subjects.

Location discrimination

We measured the focus of attention with an LD task, where the location of a briefly presented stimulus would be relevant again after a delay. The LD task (Figure 1A) was a two alternative forced choice LD task. After the aforementioned drift check, a trial started with an adaptation period with a duration of 2500 ms. During this period, the first oriented grating was shown at fixation. This first grating was shown in order to have the same trial procedure as in the OD task, but was task-irrelevant in the LD task. Next, the grating was positioned on the black or white background annulus for 200 ms. This location – in polar coordinates – had a fixed radius (10° visual angle) and a variable polar angle. The polar angle was restricted to never take any values close to the border between black and white, where close was defined as 30°. Subjects were instructed to remember location of this stimulus. Then, a mask with a random texture (low pass filtered white noise) was presented for 400 ms in order to minimize the reliance on afterimages for task performance. Subjects had to keep the location of the first stimulus in working memory for another 8000 ms after the mask. We will refer to this period as the working memory delay. Finally, a third grating was presented (200 ms), slightly displaced clockwise or counter clockwise with respect to the location of the second grating. Subjects indicated whether this direction was upward or downward. We called this upward or downward since stimuli were never presented close to the vertical meridian. The spatial offset in polar angle between the second and third grating was determined by two interleaved QUEST staircases (Watson & Pelli, 1983), to keep the difficulty at a level where subjects should be at 0.75 accuracy, with a minimum displacement of 0.5°. Desired response (upward/leftward), background luminance
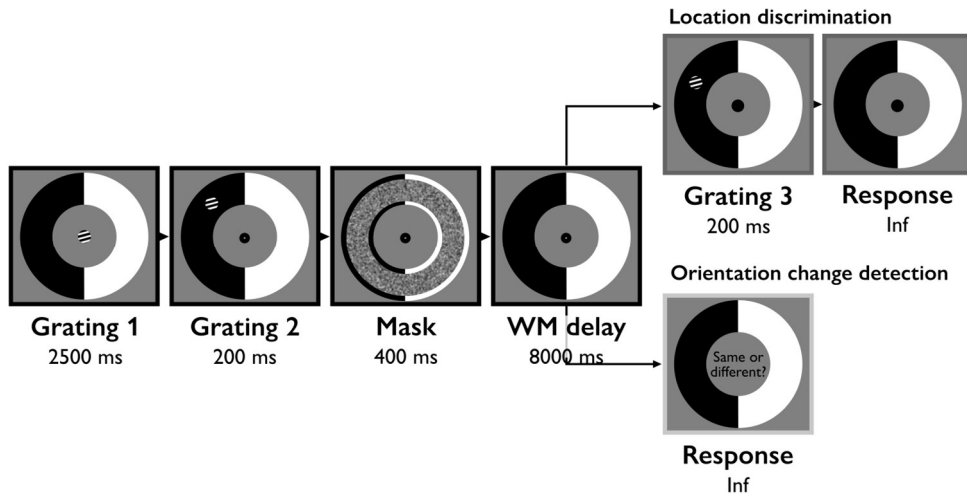
Figure 1. Trial timeline. **Location discrimination**: subjects had to remember the location of the Grating 2 (second panel), over the course of the working memory delay (fourth panel) and indicate whether the Grating 3 was displaced upward or downward. **Orientation change detection**: subjects had to compare the orientation of the Grating 2 (second panel) to the orientation of the Grating 1 (first panel) and indicate whether both had the same or a different orientation. They had to give their response after the working memory delay. In both tasks, we analysed pupil dilation from the onset of Grating 2 (second panel) to the offset of the working memory delay (fourth panel). Note that the visual stimulation is identical in both tasks up until the end of the working memory delay. **Abbreviations:** WM delay = working memory delay.

(black/white) and staircase index (1/2) were counterbalanced within blocks of 16 trials. Subjects completed six blocks in total (i.e., 48 trials per staircase and 48 trials per background luminance).

Orientation change detection

As a control task, we measured pupil size in an OD task, visually similar to the LD task, but the OD task instructions did not require the subjects to remember the location after the delay. The OD task was a 2AFC change detection task. In the OD task (Figure 1B), the sequence of events was similar to the LD task up until the end of the working memory delay. However, subjects were instructed to compare the orientation of the first grating (presented at fixation) to the orientation of the second grating. Hence, when the mask was presented, subjects were already presented with all the relevant information to complete their task. In the working memory delay, they only had to remember their response. At the end of the working memory delay, the fixation point disappeared and a text ("Same or Different") indicated that the subjects could respond. The left arrow key was used to

indicate a change in orientation, the right arrow to indicate no change. The orientation difference between the first and second stimulus was fixed at 35°. The number of trials in the OD task was identical to the number of trials in the LD task.

Data analysis

For the analysis of the pupil time series we used only trials where gaze was within 3° visual angle from the fixation point over the entire trial, and where all gaze samples were dispersed with a maximum of 2° visual angle (1707 trials in total, 74% of all trials). Missing samples due to blinks were reconstructed using cubic spline interpolation (Mathôt, 2013). We analysed pupil time series from the onset of the second grating to the offset of the working memory delay (total duration 8600 ms). Pupil time series were normalized by subtracting the average pupil size in the 100 ms prior to the onset of the second grating. This normalization was on a trial by trial basis. During this baseline period, differences in pupil size between tasks might arise, because Grating 1 (Figure 1, first panel) is task relevant in the OD task, but not in the LD task. Importantly, differences in pupil size that occur during the baseline period should not differentiate between the different background luminance.

For each 1 ms sample, we conducted a Bayesian linear mixed effects analysis. We analysed main effects of task (LD and OD), background luminance (dark or bright), and the interaction between the two. The interaction is the most important factor in the analysis as we expect an effect of background luminance in the LD task, but not in the OD task. Individual subjects were taken as random effects on the intercept. Moreover, we included the horizontal gaze position to account for effects in pupil dilation as a result of gaze shifts towards the white or black background. Horizontal gaze position was coded with positive values for shifts towards the white part of the background annulus.

For this analysis, we used the "generalTestBF" function from the R-package BayesFactor (Morey et al., 2015). This function computes Bayes Factors (BF_{10}) on the full model, with the restriction that the random intercept of subject was always included. Next, to estimate the BF of each factor (e.g., task), we used Bayesian model averaging (Hoeting et al., 1999; Rouder et al., 2017). Briefly, this entails summing the BF_{10} of the models that included that factor and divided that by the summed BF_{10} of the models without that factor. This method is possible as the BF_{10} for each submodel is calculated against a common denominator (i.e., the intercept only model). In the Supplemental data, we provide a more detailed description

of this method. Prior scales on the standardized effects were set to the default values (Rouder, Morey, Speckman, & Province, 2012). The interpretation of BF_{10} is straightforward: a BF_{10} of 3 indicates that the observed data are three times more likely under alternative hypothesis than the null hypothesis, and therefore provide evidence in favour of the alternative hypothesis. Conversely – and with an advantage over frequentist hypothesis testing – a BF_{10} of smaller than 1 can be interpreted as evidence in favour of the null hypothesis. alternatively, one could consider the BF_{01} (the inverse of BF_{10}): the amount by which the data are in favour of the null hypothesis, with respect to the alternative. We will use both BF_{10} and BF_{01} in describing our results. To facilitate the understanding of Bayes Factors (BF) in hypothesis testing, we adopt a common rule of thumb by interpreting BF_{10} > 3 as substantial evidence in favour of H_1, and BF_{01} of < ⅓ in favour of the H_0 (Jeffreys, 1961; Lee & Wagenmakers, 2013). Additionally, one can directly interpret larger BFs as larger amounts of evidence.

Thus, for each sample, we obtained the BF_{10} for each factor in the full model (i.e., task, background luminance, and their interaction). With these BFs, together with the slow dilation and constriction of the pupil, we can plot the development of the BF_{10} of each factor over time (a BF_{10} time series; Figure 2C). In discussing the results, we will report the maximum BF in favour of the alternative hypothesis (max BF_{10}) or in favour of the null hypothesis (max BF_{01}) for epochs where the BF exceeded our cut-off of BF > 3. Since BFs are obtained by MCMC sampling, this might result in occasional spikes in the BF time series. A brief introduction to MCMC sampling can be found elsewhere (Spiegelhalter & Rice, 2009). These spikes were smoothed using a third order one dimensional median filter.

We provide three important notes on interpreting the BF_{10} time series. First, the cut off value of 3 is rather arbitrary, meaning that short periods where the BF_{10} either exceeds or does not exceed that specific threshold value should not be interpreted to strictly. Such a period should rather be interpreted to not contain an overwhelming amount of evidence in favour of the presence of an effect in our dataset. Second, the onset and offset of an "interesting epoch" should not be interpreted too strictly either, because this is strongly influenced by the sensitivity of our measurement, e.g., increasing the number of trials in the analysis will always give more precise estimates of the average pupil size, therefore it will be easier to detect smaller differences between conditions. As a result, the BF_{10} will be above (or below) our threshold for a longer period. However, the mere presence of a period where the BF_{10} is above (or below) our threshold is indicative for the presence (or absence) of an effect of a condition, irrespective of the length of that period. Third, a large

8

BF_{10} indicates a large amount of evidence in favour of the presence of an effect, but it is not informative about the size of that effect. Hence, we encourage the reader to examine the figures in the result section to evaluate the results visually.
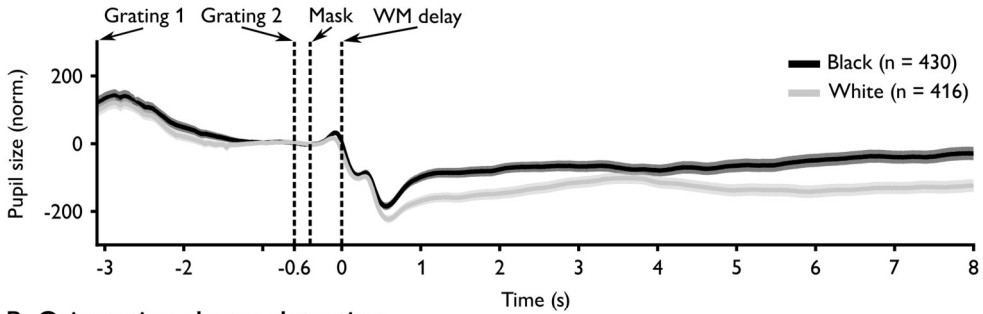
Results

Behavioural performance

We provide a small summary of the behavioural data to give the reader some insights into the performance of the subjects. However, we did not design the experiment to investigate differences in performance between for example task or background luminance. In the LD task, the average estimated displacement thresholds (75% correct) was 2.38° visual angle (±0.43 s.d.). In the OD, task we calculated sensitivity indices (D′) to estimate how well subjects could detect changes in orientation. Sensitivity to the change in orientation was very high (average D′ = 3.15, s.d. = 0.34), indicating that the task was easy to perform. In the OD task, there was no difference in performance for targets presented on the bright or on the dark background (Bayesian t-test, BF_{01} = 5.08, compared to a Cauchy prior with width 0.707; JASP Team, 2016). We were not able to make this comparison for the LD task because the size of the displacement was varied per trial by our staircase procedure.

Pupil time series analysis

Average pupil size in the LD task separated by background luminance is shown in Figure 2A. The average pupil size in the OD task is shown in Figure 2B. We will describe these pupil time series using the BF time series as depicted in Figure 2C. In all three subplots in Figure 2, the first data point is the onset of the second grating, the two vertical lines depict the onset of the mask and working memory delay, respectively. We report the maximum BF in favour of the alternative hypothesis (max BF_{10}) or in favour of the null hypothesis (max BF_{01}).

First, we will discuss the general differences in normalized pupil size between the LD and OD task. This is the difference in average pupil trace in Figure 2A (LD task) and Figure 2B (OD task). The BF of this general task effect is the depicted by the blue line in Figure 2C. At the start – i.e., the onset of the second grating – there is no clear effect of either condition, background luminance, or the interaction between the two (at t = -0.6, in Figure
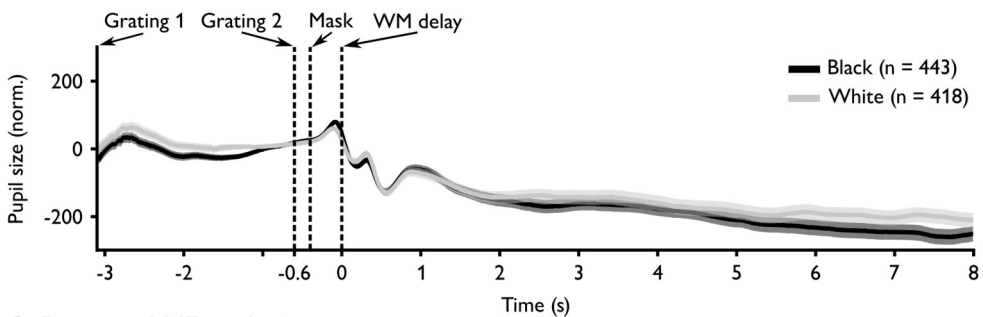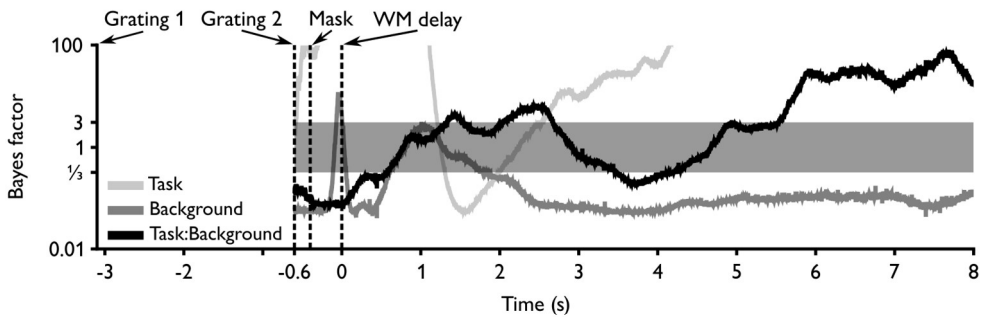
Figure 2. Pupil time series and results of Bayesian LME. In all panels, the x-axis represents time, aligned to the onset of the working memory delay and starting with the onset of the first grating. Vertical deshed lines represent the transition in trial phase, using the same phrasing as in Figure 1. **A.** Average normalized pupil size in the LD task for trials where the second grating was presented on a white background (grey) or black background (black). Shaded are represents 1 s.e.m. over all trials. **B.** Average normalized pupil size in the OD task for trials where the second grating was presented on a white background (grey) or black background (black). Shaded areas represent 1 s.e.m. over all trials. **C.** Bayes Factor (BF) time series. BF is the ratio of evidence in favour and against the presence an effect. The shaded grey region depicts BFs of 3 to ⅓. BFs within these commonly used bounds provide no clear evidence either in favour or against an effect of a factor. Roughly, points with a BF > 3 can be interpreted as evidence in favour of the presence of the factor they represent (but see our explanation in Methods for a more elaborate description on how to interpret the BF time series). Light grey is the main effect of condition. Dark grey is the main effect of background. Black is the interaction effect between background and condition. Note, the y-axis is scaled logarithmically to base 10. For visibility of the main effect of background (dark grey) and the interaction effect (black), the y-axis is limited to a maximum BF of 100. For the samples where the BF of the main effect of task (light grey) is outside this limit, the evidence for a main effect of task can be considered "very strong".

mask, a task difference begins to emerge (Figure 2C, blue line, from -585 ms), with larger average pupil sizes in the OD task (Figure 2B) than in the LD task (Figure 2A), irrespective of the background luminance on which the second grating was presented. Normalized pupil sizes are consistently larger in the OD task (Figure 2B) than in the LD task (Figure 2A) until 1209 ms in the working memory delay (Figure 2C). From this time point, the main effect of condition decreases and eventually reverses from 2533 ms until the end of the working memory delay, with larger normalized pupil sizes in the LD task (max $BF_{10} = 14.4 \times 10^9$). This general task effect likely reflects a general level of "mental effort" or higher states of arousal, reflecting that the OD task was initially more difficult than the LD task, but became easier later during the trial, when the OD task was effectively over (Hess & Polt, 1964; Kahneman & Beatty, 1966).

More interestingly, there was a short period with strong evidence in favour of a main effect of background luminance (Figure 2C, red line) before the onset of the working memory delay (max $BF_{10} = 11.26$). This main effect of background luminance indicates larger normalized pupil sizes when grating 2 was presented on a black background, as compared to when it was presented on a white background (Figure 2A and 2B, difference between black and yellow lines). The timing at which this background luminance effect is observed corresponds to the delay at which an effect of covert attentional orienting has previously been detected in pupil size (Binda & Murray, 2015; Binda et al., 2013; Mathôt et al., 2014, 2013). The period with evidence in favour of this task independent effect of background luminance lasted only briefly ($BF_{10} > 3$ for 76 ms), presumably as a result of the large effect of the onset and offset of the mask (although note that it is difficult to interpret the duration of these periods, as mentioned in the Methods section). We presented the mask to minimize subjects' reliance on after effects of the stimulus. The mask had a great impact on pupil size. After mask offset, there was no main effect of background luminance in the entire working memory delay. Rather, the effect of background luminance depended on the task (see below) and, for the majority of the samples, there was strong evidence against a main effect of background luminance (max $BF_{01} = 23.02$ in the working memory delay).

The interaction effect most directly represents the test of our hypothesis (the difference in separation of the black and yellow lines between Figure 2A and 2B), since we predicted that the storage of a location in spatial working memory is equivalent to allocating attention to that location. As indicated by the BF_{10} of the interaction (Figure 2C, green line), there is some evidence for an interaction effect from 1330 until 1541 and from 2248 until 2612 ms into the working memory delay (max $BF_{10} = 4.62$ and 6.92 in these intervals).
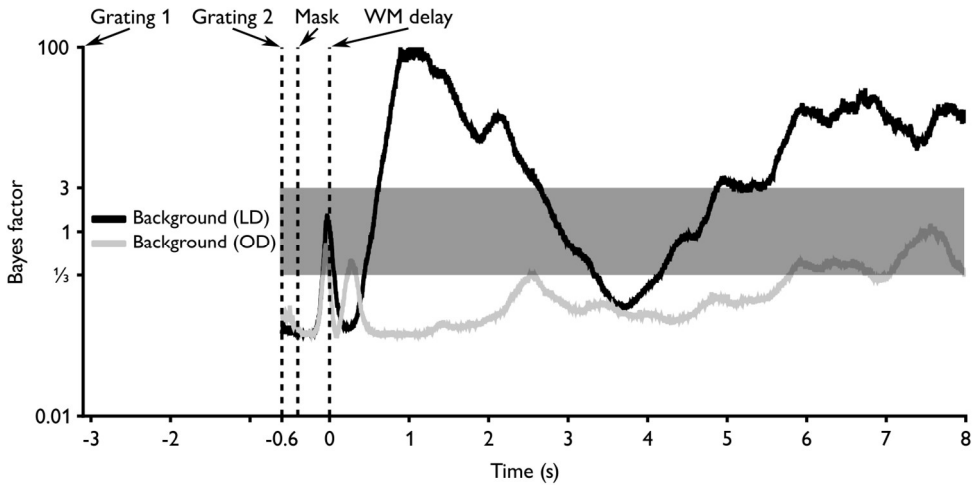
Figure 3. Bayes Factor (BF) time series for the effect of background luminance separately for the Location Discrimination task (black) and the OD task (grey). The shaded grey region depicts BFs of 3 to ⅓. BFs within these commonly used bounds provide no clear evidence either in favour or against an effect of a factor. Vertical dashed lines represent the transition in trial phase, using the same phrasing as in Figure 1.

However, from 5530 ms into the working memory delay until the end of the delay, there is strong evidence in favour of an interaction between task and background luminance, reaching its peak at 7678 ms (Figure 2C, green line, max $BF_{10} = 78.43$).

Next, we inspected the interaction effect more closely, by constructing two more Bayesian LME models (see Methods), one for the LD task and one for the OD task. With the results from these analyses we can evaluate the effect of background luminance on the modulation of the normalized pupil size in each task separately. In Figure 3, we show the time series of the BFs for the main effect of background luminance from the two additional LMEs. The dark blue line represents the background luminance effect in the LD task. The light blue line represents the background luminance effect in the OD task. As visible in Figure 2C (green line), there are roughly two periods with evidence in favour of an interaction effect between task and background luminance, one at the beginning of the WM delay and one at the end. In both these periods, pupil size was modulated by background luminance in the LD task (Figure 3, dark blue line). The first period is at the beginning of the working memory delay (in our data from 612 to 2646, max $BF_{10} = 106.48$), the second starts at 5437 ms in the working memory delay and continues until the end (max. $BF_{10} = 34.24$). In both periods, the normalized pupil size is larger when the to be remembered location was on a dark background (Figure 2A). Interestingly, these periods were separated

by a short period where there was more evidence against an interaction effect (Figure 2C, 3464 until 4187 ms, max BF_{01} = 5.48). In the same period, there was also more evidence against an effect of background luminance in both the LD task and OD task (Figure 3, black and grey lines, max BF_{01} = 6.94 and 10.19, respectively).

Gaze position control

To ensure that the observed luminance effects were not an artefact of gaze position, we ran a control analysis, testing the effect of task on the horizontal gaze position (Figure S1). The hypothesis here was that a stronger effect of background luminance in the LD task could have been the result of a drift of the eyes in the direction of the target. We performed another Bayesian LME analysis, where we modelled horizontal gaze position (coded such that positive values indicate drifts toward the target side) as a function of task, with a random intercept for each subject. This analysis showed that in the last second before the onset of the response window, there was evidence in favour of an effect of task on horizontal gaze position (max BF_{10} = 17.97; Figure S1). However, this was in the opposite direction from what we hypothesized: more drift in the OD task. Moreover, on average fixation position was still inside the area covered by the fixation point (radius = 0.35°). In other words, it is highly unlikely that the observed interaction between task and background luminance can be explained by gaze position.

Discussion

In the present experiment we tested the hypothesis that spatial attention is persistently allocated at a location that is stored in spatial working memory (Awh & Jonides, 2001). To determine where participants attended to, we took advantage of a recent finding that the pupillary light response reflects the focus of covert spatial attention (Binda & Murray, 2015; Binda et al., 2013; Mathôt et al., 2014, 2013). Subjects had to keep a location of a briefly flashed stimulus in memory. This stimulus was flashed either on a dark or on a bright background. Similar to previous studies, approximately 500 ms after stimulus presentation, the pupil dilated more when the stimulus was flashed on a dark background than on a white background (Binda & Murray, 2015; Mathôt et al., 2014, 2013). We interpret this as an effect of attending to the stimulus.

After flashing the stimulus, we presented a mask to minimize reliance on after images. The mask effectively abolished the main effect of background luminance that was present

after the onset of a stimulus on either a bright or dark background. However, our hypothesis specifically predicted an effect of background luminance only when a location has to be maintained in SWM. Indeed, examining the effect of background luminance over the course of the working memory delay, we observed effects of background luminance specifically in the SWM task, but not in the control task. Specifically, when subjects had to remember the location of the stimulus, pupils were more dilated when the stimulus was presented on a dark background than when they were presented on a bright background. These effects of SWM maintenance on pupillary light response clearly demonstrate a relation between the focus of attention and the content of spatial working memory (Awh & Jonides, 2001). Our results are in line with a recent study by Unsworth and Robison (Unsworth & Robison, 2017). The experiments by Unsworth and Robison (2017) and our own are similar in many ways, but also complement each other. Crucially, in one experiment, Unsworth and Robison (2017) used a retro-cue: participants first saw two stimuli, one on a dark background and one on a bright background. Next, after both stimuli had been removed from the display, a retro-cue indicated which of the two stimuli was to be remembered. The crucial finding was that the pupil was smaller when the bright, compared to the dark stimulus was retro-cued. This finding shows unambiguously that maintaining a location in working memory involves a shift of attention to that location. Our results support those of Unsworth and Robison (2017) and extend them by measuring pupil size during a much longer working memory interval (8 seconds here vs. 2.5/4.5 seconds in Unsworth & Robison, 2017). Interestingly, and contrary to our hypothesis, we did not find evidence for the continuous allocation of attention over the entire delay. We provide three possible explanations for this.

First, the influence of cognitive factors such as attention on the pupillary light response has been described only recently (Binda et al., 2013; Mathôt et al., 2013; Naber & Nakayama, 2013). As research into this is still developing (Mathôt & Van der Stigchel, 2015), it might be that these cognitive effects can only be detected in the pupillary light response when their effect size is large, i.e., that the pupillary light response is not very sensitive to small cognitive effects. The danger of this argument is that this can always be used to explain away the absence of an effect.

Second, another pupil-related issue is that the pupillary light response is a slow signal. One could therefore argue that the effects of background luminance in our experiment is an artefact of the slow development of the pupillary light response. Yet, the time to peak dilation in response to the onset of a stimulus has been estimated to be 930 ms, on average

8

(Hoeks & Levelt, 1993), and the late effect of background luminance on the pupillary light response in the current experiment was observed after approximately 5 seconds. This is considerably later in time than the expected time to peak dilation, making the slow development of the pupillary light response an unlikely explanation for the current results.

A third, more fundamental, explanation for the absence of a continuous effect of background luminance in the working memory delay is that the to-be-remembered location is not attended continuously. If we interpret the background-luminance effect as directly reflecting of the focus of covert attention, then we found evidence for attention rehearsal at the beginning and end of the working memory delay, but not in between. Interestingly, as in the current study, neurophysiological evidence for the rehearsal hypothesis of SWM has traditionally focused on persistent neural representation of working memory content (D'Esposito & Postle, 2015). For example, in one of the first studies that inspired many others, neurons in the prefrontal cortex were recorded, while a monkey had to remember the location of small food reward. During the memory delay, neurons in the PFC had higher spike rates than in rest (Fuster & Alexander, 1971). However, after decades of research, current views are drifting away from the idea of the necessity of continuously elevated neural representations during a working memory delay (Stokes, 2015). For example, in one study the authors tried to decode two stimuli with multi-voxel pattern analysis from visual cortex, while a retro cue indicated which of the two stimuli would be used later in the trial (Lewis-Peacock, Drysdale, Oberauer, & Postle, 2012). They also presented a second retro cue that could either indicate the same or the other stimulus. After the first retro cue, only the cued stimulus could reliably be decoded, the other not. However, when the second retro cue cued the other stimulus, the latter could be decoded again. This has been interpreted as evidence for working memory representations in the absence of input rehearsal. The current results could be interpreted similarly. Only when the location in working memory became task relevant (in anticipation of the response, at the end of the working memory delay), there was an effect of background luminance on pupil dilation, similar to the effects observed as a result of attentional orienting (Binda et al., 2013; Mathôt et al., 2013).

An interesting consequence of this is that not only spatial information, but also temporal information is used in the allocation of attention during a delay (Nobre, Correa, & Coull, 2007). Attention might be strategically focused at the beginning and end of the delay to optimize performance. Yet – at least when the duration of the working memory delay is predictable – in between there is no "need" to continuously activate the mental

representation of the to be remembered location. This is in line with a recent study where subjects performed a memory task and a concurrent search task (van Moorselaar, Theeuwes, & Olivers, 2016). Subjects had to remember the colour of a first stimulus. Then they performed a search task that contained a coloured distractor that either matched the colour of the memory stimulus or was unrelated. Importantly, the colour of the memory item was repeated nine times. With more repetitions, memory performance increased, yet simultaneously capture (i.e., slowed reaction times) by the matched distractor in the search task decreased. However, close to the end of a series of repetitions, interference increased again. The authors concluded that the active content of working memory guides attention, but that an item is only active in working memory when it is encoded (at the beginning of their repetition series) or when it is expected to be updated (at the end of their repetition series).

To conclude, we showed that a location stored in spatial working memory shifts the focus of attention to that location, which is reflected by the pupillary light response. When the to-be-remembered location was presented on a bright background, the pupil was more constricted than when it was presented on a dark background. The modulation of pupil dilation was most pronounced close the end of the working memory delay, when the location became task relevant. This suggests that the content of SWM guides attention when it is most relevant for the task at hand.

8

Chapter 8 – Supplementary information

Bayesian linear mixed effects analysis

Here, we provide an overview of the steps for the analysis of the pupil traces. We do this using the R-code we used. We use the function generalTestBF from the BayesFactor package for each 1 ms sample. For more information on this package by Richard Morey, see his website.

We model the pupil size per millisecond as a function of task and background luminance. In addition, we add the horizontal gaze position, to control for effects of gaze position. Lastly, we allow for between subject variation on the intercept.

```
p ~ task * luminance + x + subject
```

First, we load the BayesFactor pckage (Morey, Rouder & Jamil, 2015) and our data.

```
# load the BayesFactor package
library("BayesFactor")

# load data
data <- read.table( "datafile.dat", as.is=TRUE )

# set column names for readability
names(data) <- c( 'subject', 'task', 'luminance', 't', 'x',
'p' )

# make sure all variables have the correct class
data$subject   <- as.factor(data$subject)
data$task      <- as.factor(data$task)
data$luminance <- as.factor(data$luminance)
data$t         <- as.double(data$t)
data$x         <- as.double(data$x)
data$p         <- as.double(data$p)
```

As said, we analyse each sample separately. So, as an example, here we select the data from only the first sample.

```
tmpdata_t <- data[ data$t == 1, ]
```

And we make the models using generalTestBF and defining the full model. The function generalTestBF "successively removes terms from that model and tests the resulting sub-models" (Morey).

```
m <- generalTestBF( p ~ task * luminance + x + subject,
                    data = tmpdata,
                 whichRandom = 'subject',
                 whichModels = 'all',
                 iterations = 10000,
                 neverExclude = 'subject')
```

In total, 16 sub-models have been constructed. The variable 'm' contains (among others) the Bayes factors of each model. Here, is a list of all the models that were constructed. To stick with the R notation, the colon ':' represents an interaction effect, without the two main effects

```
1.    task + subject
2.    luminance + subject
3.    x + subject
4.    task:luminance + subject
5.    task + luminance + subject
6.    task + x + subject
7.    task + task:luminance + subject
8.    luminance + x + subject
9.    luminance + task:luminance + subject
10.   x + task:luminance + subject
11.   task + luminance + x + subject
12.   task + luminance + task:luminance + subject
13.   task + x + task:luminance + subject
14.   luminance + x + task:luminance + subject
15.   task + luminance + x + task:luminance + subject
16.   subject
```

Now, we have the Bayes factors for all models. To get the Bayes factor of each variable we use Bayesian model averaging, i.e. summing the BF of all the models that contain a specific variable and dividing that by the sum of all the BFs that do not contain that variable. So, in

case of the interaction between task and luminance, we select the models 4, 7, 9, 10, 12, 13 and 15.

```
# indices of models with the interaction effect
iWith <- c(4,7,9,10,12,13,15)

# indices of models without the interaction effect
iWithout <- !is.element(1:16, iWith)
```

We sum the Bayes factor of all the models with the interaction effect and divide by all the models that do not contain the interaction effect.

```
# put all Bayes factors in data frame
tmpbf <- as.data.frame(m)$bf

# summed Bayes factor of all the models with the interaction,
# divided by the fraction of models that include the
# interaction
bfWith <- sum( tmpbf[ iWith ] ) / (8/16)

# summed Bayes factor of all the models without the
# interaction, divided by the fraction of models that did not
# include the interaction
bfWithout <- sum( tmpbf[ iWithout] ) / (8/16)

# the Bayes factor of the interaction effect
bfInteraction <- bfWith / bfWithout
```

We can do this for each factor (main effect of task, main effect of background luminance and the interaction effect), and in each sample. The obtained Bayes factors are plotted in Figure 2 in the article.

A. Horizontal gaze position

B. Bayesian LME analysis
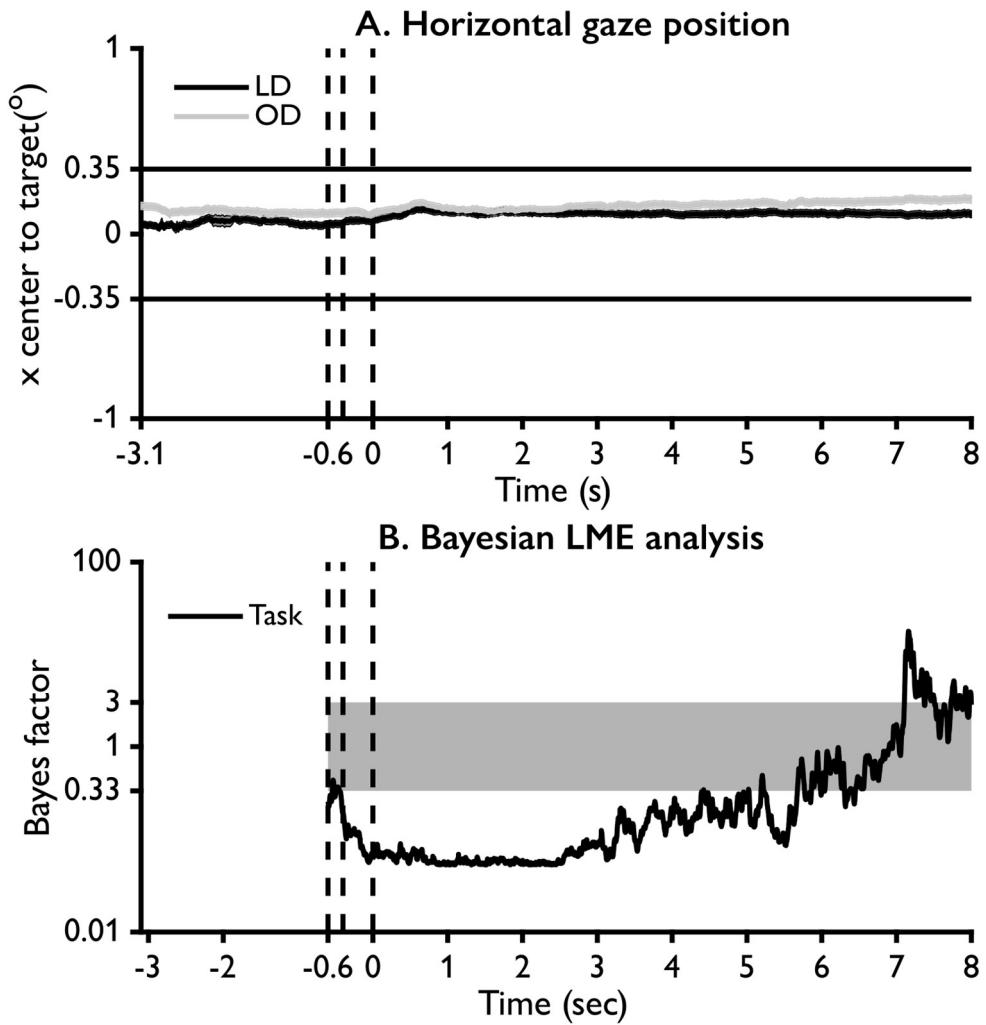
Figure S1. A. Horizontal gaze position over time, mean and s.e.m. (shaded area) separately for each task. Values > 0 indicate gaze positions in the direction of the target side. Values < 0 indicate values away from the target side. Horizontal lines mark the eccentricity of the fixation point. Hence, on average, gaze was positioned nicely on the fixation point. **B.** we constructed a Bayesian LME with the model x ~ task + subj. The evidence in favour of an effect of task on horizontal gaze position is depicted over time. At the end of the working memory delay, there seems to be a shortly lasting period where gaze is drifted more in the direction of the target in the OD task than in the LD task. Note that there was more drift in the OD task

8

Chapter 9

General discussion

Humans make frequent saccades – about three to four times per second. These eye movements create changes in sensory input that should be dissociated from changes in the outside world to accurately explore the environment. Visual perception is introspectively undisrupted and appears continuous. The question how perceptual continuity arises from the visual system has been investigated for decades. The results presented in this thesis address multiple aspects of perceptual continuity that are currently debated. The most prominent hypothesis today is that the visual system anticipates the sensory changes based on a predictive signal from the oculomotor system, using the principle of re-afference (Sperry, 1950; Von Holst & Mittelstaedt, 1950). However, this hypothesis is still quite vaguely formulated. What is the nature of the anticipation? Is any retinotopically encoded visual information updated in spatiotopic coordinates across saccades? And how is the anticipation implemented in visual processing?

Spatiotopic updating reflected in behaviour

In Chapter 2, 3 and 4 I provided evidence for spatiotopic updating of visual features across saccades. The data presented in Chapter 2 and 3 demonstrate that a visual stimulus before saccade onset influences the percept of the same stimulus immediately after saccade offset. Specifically, we showed that the rotation direction of a rotating ring is spatiotopically updated. To probe updating of visual information across saccades, we used a visual illusion consisting of two stages. First, a ring with a texture of random noise rotates slowly. Second, the random noise texture is rapidly replaced four times. The rapid replacement of noise textures creates the percept of a rotational step in the opposite direction of the preceding slow rotation. In Chapters 2 and 3, we presented the inducer in the periphery and asked subjects to make a saccade towards it. Immediately after the saccade we changed the textures, and subjects indicated the direction of the perceived step. Importantly, we compared two conditions: one where the ring was rotating slowly before the saccade and one where the ring remained static until the end of the saccade. After the saccade, the ring rotated only very briefly (for 20 or 50 milliseconds) in both conditions. The hypothesis was: if the rotational motion before the saccade is spatiotopically updated, the illusion should be stronger if the ring rotates before the saccade as compared to when it is static before the saccade. Both in Chapter 2 and Chapter 3, we provide data supporting this hypothesis.

In Chapter 2, we examined various alternative explanations of the effect we interpreted as spatiotopic updating. The most important alternative account was a spatially invariant

effect of the inducer. This account states that the rotation direction of an inducer anywhere in the visual field will induce the percept of a backward step when the textures of a different are changed. I.e. we presented subjects two rings, one around their point of fixation and one in the periphery. The peripheral ring rotated slowly, but the textures of the ring around fixation were changed. In terms of retinotopic stimulation, this condition is very similar to the spatiotopic condition, where subjects made a saccade towards the rotating ring, except that now they did not make a saccade. The results showed that this condition also induced slightly more frequent percepts of backwards steps as compared to a condition where the peripheral stimulus remained static. However, the frequency was lower than in the condition with a saccade. We concluded that although there is a small long range effect of the rotating annulus, this is not sufficient to explain the observed spatiotopic effect across saccades. Therefore, visual information about the rotation direction of the inducer must have been spatiotopically updated to explain the spatiotopic effect in the study. Together, these data show that visual feature information (here rotation direction) is spatiotopically updated and interacts with the visual feature information that is present immediately after saccade offset.

The data presented in Chapter 3 follow up on the results of Chapter 2. We tested the temporal characteristics of spatiotopic updating. It had previously been suggested that spatiotopic updating is slow, taking about 500 ms to develop (Zimmermann, Born, Fink, & Cavanagh, 2014; Zimmermann, Morrone, & Burr, 2016; Zimmermann, Morrone, Fink, et al., 2013). This is surprisingly slow because humans are known to make roughly three saccades per second. So, the visual system typically has less time than required for spatiotopic updating between two saccades, implying that spatiotopic updating would play a minor role in perceptual continuity across saccades. However, we noticed that the results of these studies do actually show that although spatiotopic updating increases in strength with longer saccade latencies, it develops faster than discussed by the authors. However, it is not immediately apparent from their results because the development of the spatiotopic effect, although beginning immediately, continuous to grow stronger when saccade execution is delayed.

To measure how spatiotopic updating develops over time, we modified the paradigm with the motion illusion, presented in Chapter 2, to give us a direct estimate the time course of spatiotopic updating. We asked participants to keep fixating a small point until the ring with random noise texture appeared. When the ring appeared subjects could immediately make a saccade towards it. The latencies of the saccades were low with a

9

median of 155 ms. Again, we had two conditions, one where the ring was rotating before the saccade and one where it remained static until saccade onset. Despite the low latencies, subjects reported more backward steps (indicating a stronger induction of the illusion) when the ring rotated before the saccade. This illusion was also stronger than in a control condition, where subjects remained fixation and the ring was brought to the central part of their visual field because we displaced it on the computer screen. We further tested the time course of updating with an additional experiment, where the ring would initially remain static upon appearance but then started rotating before saccade onset. With this manipulation we demonstrated that a longer preview increased the strength of the spatiotopically updated rotation information. Moreover, the data from this experiment show that the strength of the presaccadic stimulus is lower than the strength of the post-saccadic stimulus, similar to previous studies (Ganmor et al., 2015; Paeye, Collins, & Cavanagh, 2017; Schut, Van der Stoep, Fabius, & Van der Stigchel, 2018; Wolf & Schütz, 2015).

The findings of Chapter 2 and 3 highlight two important aspects of spatiotopic updating. First, motion information *can* be spatiotopically updated. Second, spatiotopic updating can develop quickly. Specifically, the results show that post-saccadic perception immediately after saccade offset is influenced by the pre-saccadic stimulus (Deubel et al., 1998; Fornaciai et al., 2018; Jüttner, 1997). Moreover, in the integration of pre- and post-saccadic visual information, the weight of the pre-saccadic stimulus – this stimulus is presented in the peripheral visual field, and earliest in time – is lower than that of the post-saccadic stimulus – presented in the central visual field, and most recently (Ganmor et al., 2015; Paeye et al., 2017; Schut et al., 2018; Wolf & Schütz, 2015).

Neural processes resulting in perceptual continuity

The data from Chapter 2 and 3 provide evidence that spatiotopic updating is reflected in human behaviour. As argued in the discussion of those chapters, these results could be explained by a predictive spatiotopic updating, i.e. that the information about the rotation direction of the ring is predictively transferred before saccade onset. However, the data in Chapter 2 and 3 are agnostic to the exact moment of information and transfer or the underlying mechanism per se. Behavioural studies on perception across saccades require a

response from the subject, typically a button press such as in the experiments presented in this thesis. These button presses are used to make inferences about the perception of the subject. Because of response latencies, the button presses are almost always recorded after saccade offset. Even when stimuli are presented close to saccade offset (such as in the experiments in Chapter 2 and 3), button presses typically lag by 400 ms. Therefore, behavioural studies cannot address whether spatiotopic updating is the result from pre- or post-saccadic neural processing.

The major hypothesis about the neural mechanism underlying spatiotopic updating is thought of as a forward model (Miall & Wolpert, 1996; Webb, 2004) using the principle of re-afference (Sperry, 1950; Von Holst & Mittelstaedt, 1950). In this model, the consequence of a saccade for visual processing is anticipated before saccade onset. Evidence for the neural implementation of a forward model in the visual system comes from monkey studies (Cavanaugh et al., 2016; Crapse & Sommer, 2012; Sommer & Wurtz, 2002, 2006). Moreover, neurons in several areas demonstrate predictive remapping of receptive fields (Duhamel, Colby, et al., 1992; Kusunoki & Goldberg, 2003; Umeno & Goldberg, 1997; Walker et al., 1995). In this model, the rotation direction of the pre-saccadic stimulus would have been transferred from neurons in the visual system whose receptive field cover the stimulus before saccade onset to the neurons that represent the stimulus after saccade offset.

Although the data presented in Chapter 2 and 3 are agnostic to this process, the data presented in Chapter 4 provided an alternative interpretation to a presaccadic process that enable spatiotopic updating. The results of the multivariate pattern analysis of the MEG data in Chapter 4 suggest that the pre-saccadic representation of a stimulus might linger in retinotopic coordinates, and that the new retinotopic representation of the stimulus develops rapidly after saccade offset (within 40 ms). Together, these two representations could be compared to evaluate visual continuity if the visual system has simultaneous access to the pre-saccadic and post-saccadic eye position. A recent neurophysiological study showed that it is possible to decode past, present and future eye positions from the same population of neurons in the parietal cortex, only by reading out the population response differently, i.e. re-weighting the output of each neuron in the population (Morris et al., 2016). This suggests that rather than predicting the post-saccadic visual image, if the pre-saccadic image can be briefly maintained it can be compared to the post-saccadic stimulus in implicit spatiotopic coordinates by reading out past and current eye positions. Interestingly, visual information might be retained with surprisingly rich details albeit in a

9

fragile, transient state that could easily be masked by other retinal input postsaccadically (Zerr et al., 2017). The visual information that is most likely to be available is in visual working memory (Irwin et al., 1990; Van der Stigchel & Hollingworth, 2018). Together, this proposed mechanism would be postdictive updating instead of predictive.

Degeneracy in neural circuits underlying spatiotopic updating

Neurons in the parietal cortex exhibit responses modulations around the time of saccades that are thought to be important for enabling spatiotopic updating (Duhamel, Colby, et al., 1992; Kusunoki & Goldberg, 2003; Medendorp et al., 2003; Merriam et al., 2003; Subramanian & Colby, 2014). It has been assumed that this modulation is the result from the integration of retinal and extra-retinal information (Wurtz, 2008). Thus, it seems that these neurons play an important role in enabling perceptual continuity across saccades. Although lesion studies with human subjects seemed to imply a crucial role of the parietal cortex in spatiotopic updating (Duhamel, Colby, et al., 1992; Heide et al., 1995), the data presented in Chapter 5, together with data from another recent study (Rath-Wilson & Guitton, 2015), argue differently. In our study, 9 patients with lesions to the right posterior parietal cortex performed the intra-saccadic displacement task. To measure the availability of extra-retinal information for perceptual judgement, the patients performed two conditions, one where the saccade target stepped during the saccade and one where it was briefly removed (250 ms blank screen) during the saccade before reappearing displaced. In subjects without brain damage the introduction of the blank leads to increased sensitivity (Deubel et al., 1996). This blank effect has been interpreted to demonstrate the use of extra-retinal signals in perceptual judgement over visual signals, when no visual signals are available immediately after saccade offset. Hence, we used the increase in sensitivity as an indication of the use of extra-retinal signals in perceptual judgments. Conversely, a decrease in sensitivity by the introduction of the blank is a sign of a lack of correct monitoring extra-retinal signals (Ostendorf et al., 2010). 7 of the 9 patients in our study showed an increase in sensitivity that was comparable to controls, only 2 out of 9 exhibited a decrease in sensitivity. Because some of the patients who displayed an increased sensitivity had substantial lesions to the posterior parietal cortex, we conclude that an intact posterior parietal cortex is not crucial for monitoring extra-retinal signals.

It is possible that the impairments in perceptual continuity are subtle and were not detected by the behavioural paradigms that have been used. But it could also be possible that perceptual continuity is either simply not dependent on neurons in parietal cortex or alternatively that the neural mechanisms underlying perceptual continuity are degenerate (Edelman & Gally, 2001; Price & Friston, 2002). The latter means that there are multiple neural circuits from which perceptual continuity could emerge, allowing the mechanism to be resilient from damage. Although this claim requires further experimentation, it is clear that both updating of visual information (Chapter 5) and motor plans (Rath-Wilson & Guitton, 2015) are still possible after a lesion to the posterior parietal cortex.

In Chapter 5 we specifically studied the effect of lesions to the posterior parietal cortex on perceptual continuity. Although clearly hypothesis driven and based on previous studies (Duhamel, Goldberg, et al., 1992; Heide et al., 1995), neurophysiological evidence identified a pathway that does not involve the posterior parietal cortex, but the superior colliculus, medial dorsal nucleus of the thalamus and the frontal eye fields (Sommer & Wurtz, 2008a). Moreover, focal thalamic lesions in humans (Ostendorf et al., 2010, 2013) or temporary inactivation of the medial dorsal nucleus (Cavanaugh et al., 2016) have resulted in seriously impaired performance on double step saccades and the intra-saccadic displacement task. It would therefore be interesting to investigate the effect of lesions to the frontal eye fields on performance on the intra-saccadic displacement task, because this is the cortical area that is part of the re-afference circuit.

The task designed for the study in Chapter 6 was originally conceived to be a screening task for the inclusion of a study like the study presented in Chapter 5. Because of limited time, we were not able to combine the two, unfortunately. The data presented in Chapter 6 show that stroke patients who have low performance on a brief spatial working memory task also perform lower than average on a visual search task. In the spatial working memory task, subjects had to precisely remember the location of a briefly presented stimulus for a delay of 2 seconds. After this delay another stimulus was shown slightly displaced from the initial location. The relationship with visual search and the ability to accurately remember visuospatial information has been identified before (Husain et al., 2001; Husain & Rorden, 2003; Mannan et al., 2005; Striemer et al., 2013). Because we ensured that the task was suited for a clinical environment, we did not use eye tracking in this study. Instead, we added a central fixation point that would remain visible on screen. Subjects were instructed to maintain fixation. The fixation point briefly expanded and contracted to capture attention of the subject after the first stimulus had been shown. However, it is possible that subjects

9

made saccade towards the stimuli. I am curious what the relationship is between performance on the spatial working memory task and performance on the intra-saccadic displacement task. Additional anatomical neuroimaging of the patients in that hypothetical study would allow for lesion symptom mapping. The approach taken in that new study would be opposite from the one in Chapter 5. In Chapter 5 we tested the hypothesis that the right posterior parietal cortex is crucially involved in enabling perceptual continuity. In the proposed new study, problems in perceptual continuity would be linked to a common lesion site. However, this would require a larger group of patients, which might be challenging given the extensiveness and duration of the intra-saccadic displacement task (i.e. a visit to an eye tracking lab of about 2 hours).

Maintenance of visuospatial information

In the first chapters of this thesis I used various techniques to pinpoint different aspects of spatiotopic updating (behavioural psychophysics, human neurophysiology and a lesion study). Chapters 7 and 8 were more exploratory in nature and focussed on the maintenance of visuospatial information either across saccades (Chapter 7) or while subjects maintained fixation (Chapter 8). In Chapter 7, I investigated inhibition of return (IOR). This is an effect primarily observed as an increased latency to previously attended or fixated locations (Klein, 2000). Because of longer response times to previously attended location, IOR has been suggested to promote exploration as it inhibits returning to previously inspected locations (Bays & Husain, 2012; Klein, 1988), but this has also been disputed (Hooge et al., 2005). For IOR to be effective in guiding saccade direction, the locations of previously fixated locations should be maintained in a spatiotopic reference frame, because with each new saccade, the retinotopic coordinates of each location changes with every saccade. In Chapter 7, we measured the probability of refixations after series of six binary saccadic decisions. Refixations were more frequent when a target had been fixated several fixations ago. Considering the preceding chapters, the most interesting result is that the history-related effect was more pronounced when sufficient spatial references were provided, suggesting that this effect is dependent on spatiotopic encoding of previously fixated locations. Other studies have also demonstrated that continuously present visual information is important for fast spatiotopic updating of attention (Golomb, Pulido, et al., 2010; Lisi et al., 2015). These findings are in line with the hypothesis that visual information immediately after saccade offset is the strongest factor in establishing perceptual continuity (Deubel et al., 1998).

In Chapter 8, I examined the deployment of covert attention during an interval in which a subject is asked to remember a location (conceptually similar to task in Chapter 6). To measure the location of covert attention we used the pupillary light response (PLR). Even though subjects maintain fixation at the center of the display, the average pupil size was larger when a to-be-remembered location was on the dark side of the screen than when it was on the bright side of the screen. We observed this modulation of pupil size for a long period at the beginning and at the end of the eight seconds working memory delay. We interpret this as evidence for a tight coupling between spatial attention and maintaining information in SWM. The study in Chapter 8 was exploratory from our side, in which we also checked whether we thought it would be useful to further use the PLR to study perceptual continuity. Although the result of this experiment was interesting on its own, we did not pursue the use of the PLR in experiments on perceptual continuity, because the PLR is relatively slow – almost 1 second to peak response (Hoeks & Levelt, 1993) – while the processing underlying perceptual continuity are fast.

Limitations and considerations for future studies

Although the data presented in Chapter 2 and 3 are consistent with other studies and each other. There are a few technical limitations. First, we included control conditions in which we tested whether the observed spatiotopic effects are unique to saccade execution. It could be argued that this control experiment is not optimal or even unsuitable. In our control experiment, a stimulus appeared in the periphery, disappeared and then reappeared around fixation, while the observer kept fixating a central fixation point. As remarked by emeritus professor Wertheim, motion on a monitor is not the same as motion of a moving object. The monitor can create apparent motion. A better way to simulate the saccade would be a setup with fast rotating mirrors, that in their rotation follow roughly the same velocity profile as typical saccades. This is possible with mirror galvanometer systems (Knöll, Morrone, & Bremmer, 2013). Unfortunately, this is not standard in the field, and I came across this solution too late to include it in this thesis. To be clear, I do think the control conditions we had are adequate, just not optimal.

The second limitation only applies to the data in Chapter 2. The accuracy and precision of the synchronization between the timing of the monitor (visual stimuli) and eye movement

9

recordings were not measured. Studies on perception across saccades have struggled with monitor issues. Most notably, one early study that demonstrated trans-saccadic fusion (Jonides, Irwin, & Yantis, 1982) was later corrected because the results were explained by slow phosphor decay times of the monitor that was used to present stimuli across saccades (Irwin et al., 1983). Because the decay time was slow, the stimulus was still visible after the saccade had ended. So, subjects did not need to integrate the pre- and post-saccadic stimuli spatiotopically but could simply use the post-saccadic stimulus and decaying pre-saccadic stimulus that was still visible after the saccade. Although the issue of phosphor decay times does not apply to LCD monitors, there are other issues that can affect the timing of the visual stimulus on these monitors, most notably, response time and input lag. Response time refers to the time it takes for a pixel to reach the requested luminance level. This issue is similar to the issue of decay time for CRT monitors. The response time of an LCD monitor can be measured with oscilloscope. However, in addition to the response time, LCD monitors typically have input lag, referring to the time between a change in luminance of a pixel and the time it was requested in the experimentation software using the graphics card of the computer.
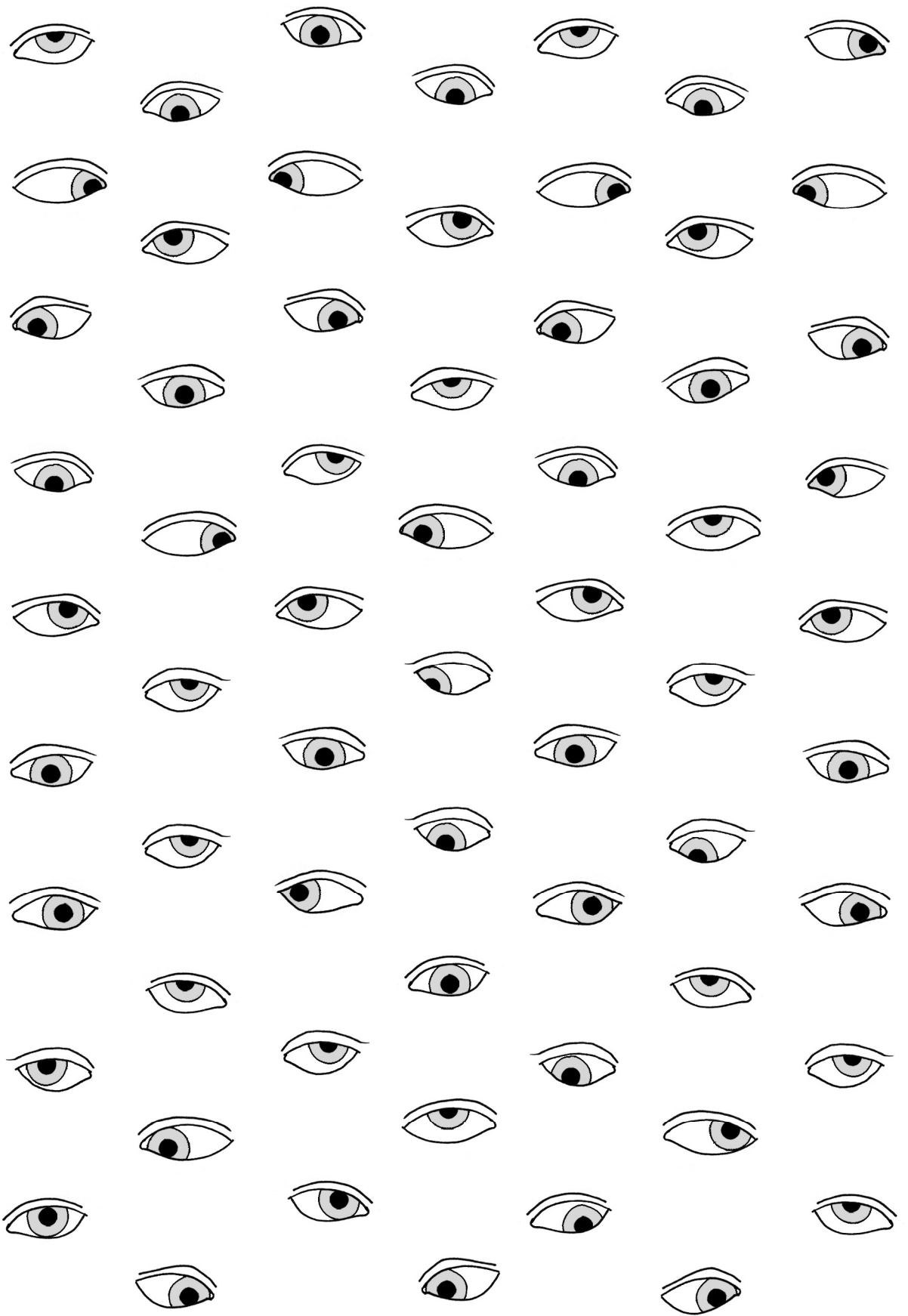
I used four different setups for the experiments presented in this thesis. The data presented in Chapter 2, 7 and 8 were performed using an LG 24 MB65PM LCD-IPS monitor with a refresh rate of 60 Hz. For the experiments presented in Chapter 7 and 8 this is sufficient, but for the experiments in Chapter 2, I am not convinced that this setup was optimal. For the experiments in Chapter 3, we had a new monitor, Asus RoG Swift PG278Q that we used with either a 100 Hz or 120 Hz refresh rate. On this monitor I did perform all measurements and complementary corrections that are required to accurately perform an experiment that requires high temporal precision and accuracy. Moreover, a study was published recently that argued that this monitor is suitable for experiments on visual perception that require high temporal precision when adequately accounting for the input lag (Zhang et al., 2018). The most ideal setup was used in Chapter 4, where stimulus presentation was done using a PROPixx projector, and the timing was recorded online using a photodiode. The PROPixx projector is designed for research and has a high temporal accuracy and precision. However, the projector is quite expensive. A photodiode that records all visual onsets allows for the complete synchronization of visual onsets and eye movements and is in my view the optimal solution. I think it should be standard for all studies on the interaction between eye movements and visual perception to report the procedure that was used to synchronize eye movement data with the timing of visual onset.

Strangely, this is not customary yet. Given that the results in Chapter 3 – where we did measure the timing of our monitor and corrected that visual onsets accordingly – conceptually replicate the findings presented in Chapter 2, I am confident that our interpretation of the results of Chapter 2 is valid.

One of the strengths of the paradigm used in Chapter 2 and 3 is that it allows to present a single stimulus at a single location, i.e. there is continuity in the presence of the stimulus. Several studies have already demonstrated that both behavioural and neural responses to transient stimuli are different from responses to stable and continuous stimuli (Churan, Guitton, & Pack, 2011; Deubel, 2004; H. M. Rao et al., 2016; Zimmermann et al., 2015). I would therefore advise to refrain from the use highly transient stimuli (e.g. flashes of light), but instead use continuously present stimuli to study visual perception across saccades.

Conclusion

How perceptual continuity across saccades emerges from the visual system is a long-standing question in visual neuroscience. As the experiments in this thesis support, this most likely arises from the interaction of retinal and extra-retinal signals, resulting in spatiotopic updating of visual information. The presented studies demonstrate that perceptual judgements reflect spatiotopic updating, and that this is robust to selective cortical lesions. In addition to existing suggestions for neural mechanisms underlying spatiotopic updating, I suggest an alternative explanation involving postdictive updating. Together these results provide clear directions for further investigations into perceptual continuity across saccades. The results of these future studies will be of interest to a broad scientific audience, because perceptual continuity across saccades is a case example that organisms dissociate the sensory input that result of changes outside themselves from the sensory input that result of their own motor output. As such, the processes underlying this dissociation might affect humans, ants and squirrels alike.

9

Appendix

References

Appendix

Abrams, R. A., & Dobkin, R. S. (1994). Inhibition of return: Effects of attentional cuing on eye movement latencies. *Journal of Experimental Psychology: Human Perception and Performance*, *20*(3), 467–477.

Aguilonius, F. (1613). *Opticorum Libri Sex: Philosophis iuxta ac Mathematicis utiles*. Antwerp: Antverpiæ: Ex officina Plantiniana, apud Viduam et filios J. Moreti.

Appelros, P., Karlsson, G. M., Seiger, A., & Nydevik, I. (2002). Neglect and anosognosia after first-ever stroke: Incidence and relationship to disability. *Journal of Rehabilitation Medicine*, *34*(5), 215–220. https://doi.org/10.1080/165019702760279206

Atsma, J., Maij, F., Koppen, M., Irwin, D. E., & Medendorp, W. P. (2016). Causal inference for spatial constancy across saccades. *PLoS Computational Biology*, *12*(3), e1004766. https://doi.org/10.1371/journal.pcbi.1004766

Awh, E., & Jonides, J. (2001). Overlapping mechanisms of attention and spatial working memory. *Trends in Cognitive Sciences*, *5*(3), 119–126. https://doi.org/10.1016/S1364-6613(00)01593-X

Awh, E., Jonides, J., & Reuter-Lorenz, P. A. (1998). Rehearsal in spatial working memory. *Journal of Experimental Psychology: Human Perception and Performance*, *24*(3), 780–790.

Awh, E., Jonides, J., Smith, E. E., Buxton, R. B., Frank, L. R., Love, T., … Gmeindl, L. (1999). Rehearsal in spatial working memory: Evidence from neuroimaging. *Psychological Science*, *10*(5), 433–437. https://doi.org/10.1111/1467-9280.00182

Azouvi, P., Samuel, C., Louis-Dreyfus, A., Bernati, T., Bartolomeo, P., Beis, J.-M., … Rousseaux, M. (2002). Sensitivity of clinical and behavioural tests of spatial neglect after right hemisphere stroke. *Journal of Neurology, Neurosurgery & Psychiatry*, *73*(2), 160–166. https://doi.org/10.1136/jnnp.73.2.160

Baayen, R. H., Davidson, D. J., & Bates, D. M. (2008). Mixed-effects modeling with crossed random effects for subjects and items. *Journal of Memory and Language*, *59*(4), 390–412. https://doi.org/10.1016/j.jml.2007.12.005

Baddeley, A. (1992). Working memory. *Science*, *255*, 556–559.

Baddeley, A., & Hitch, G. (1974). Working memory. In *The psychology of learning and motivation: Advances in research and theory* (Vol. 8, pp. 47–89). New York: Academic Press.

Bansal, S., Jayet Bray, L. C., Peterson, M. S., & Joiner, W. M. (2015). The effect of saccade metrics on the corollary discharge contribution to perceived eye location. *Journal of Neurophysiology*, *113*(9), 3312–3322. https://doi.org/10.1152/jn.00771.2014

Bates, D., Mächler, M., Bolker, B., & Walker, S. (2015). Fitting linear mixed-effects models using lme4. *Journal of Statistical Software*, *67*(1). https://doi.org/10.18637/jss.v067.i01

Bays, P. M., & Husain, M. (2007). Spatial remapping of the visual world across saccades: *NeuroReport*, *18*(12), 1207–1213. https://doi.org/10.1097/WNR.0b013e328244e6c3

Bays, P. M., & Husain, M. (2012). Active inhibition and memory promote exploration and search of natural scenes. *Journal of Vision*, *12*(8), 1–18. https://doi.org/10.1167/12.8.8

Behrmann, M., Watt, S., Black, S. E., & Barton, J. J. S. (1997). Impaired visual search in patients with unilateral neglect: an oculographic analysis. *Neuropsychologia*, *35*(11), 1445–1458. https://doi.org/10.1016/S0028-3932(97)00058-4

Bellebaum, C., & Daum, I. (2006). Time course of cross-hemispheric spatial updating in the human parietal cortex. *Behavioural Brain Research*, *169*(1), 150–161. https://doi.org/10.1016/j.bbr.2006.01.001

Bellebaum, C., Daum, I., Koch, B., Schwarz, M., & Hoffmann, K.-P. (2005). The role of the human thalamus in processing corollary discharge. *Brain*, *128*(5), 1139–1154. https://doi.org/10.1093/brain/awh474

Benjamins, J. S., Dalmaijer, E. S., Ten Brink, A. F., Nijboer, T. C. W., & Van der Stigchel, S. (2018). Multi-target visual search organisation across the lifespan: Cancellation task performance in a large and demographically stratified sample of healthy adults. *Aging, Neuropsychology, and Cognition*. https://doi.org/10.1101/307520

Biber, U., & Ilg, U. J. (2011). Visual stability and the motion aftereffect: A psychophysical study revealing spatial updating. *PLoS ONE*, *6*(1), e16265. https://doi.org/10.1371/journal.pone.0016265

Binda, P., & Murray, S. O. (2015). Spatial attention increases the pupillary response to light changes. *Journal of Vision*, *15*(2), 1–1. https://doi.org/10.1167/15.2.1

Binda, P., Pereverzeva, M., & Murray, S. O. (2013). Attention to bright surfaces enhances the pupillary light reflex. *Journal of Neuroscience*, *33*(5), 2199–2204. https://doi.org/10.1523/JNEUROSCI.3440-12.2013

Bisiach, E., & Vallar, G. (1988). Hemineglect in humans. In *Handbook of neuropsychology* (Vol. 1, pp. 195–222). New York, NY, US: Elsevier Science.

Blom, T., Mathôt, S., Olivers, C. N. L., & Van der Stigchel, S. (2016). The pupillary light response reflects encoding, but not maintenance, in visual working memory. *Journal of Experimental Psychology: Human Perception and Performance*, *42*(11), 1716–1723. https://doi.org/10.1037/xhp0000252

Boot, W. R., McCarley, J. S., Kramer, A. F., & Peterson, M. S. (2004). Automatic and intentional memory processes in visual search. *Psychonomic Bulletin & Review*, *11*(5), 854–861. https://doi.org/10.3758/BF03196712

Brainard, D. H. (1997). The Psychophysics Toolbox. *Spatial Vision*, *10*(4), 433–436. https://doi.org/10.1163/156856897X00357

Bray, L. C. J., Bansal, S., & Joiner, W. M. (2016). Quantifying the spatial extent of the corollary discharge benefit to transsaccadic visual perception. *Journal of Neurophysiology*, *115*, 1132–1145. https://doi.org/10.1152/jn.00657.2015

Bridgeman, B., Hendry, D., & Stark, L. (1975). Failure to detect displacement of the visual world during saccadic eye movements. *Vision Research*, *15*(6), 719–722. https://doi.org/10.1016/0042-6989(75)90290-4

Bridgeman, B., & Mayer, M. (1983). Failure to integrate visual information from successive fixations. *Bulletin of the Psychonomic Society*, *21*(4), 285–286. https://doi.org/10.3758/BF03334711

Bridgeman, B., Van der Heijden, A. H. C., & Velichkovsky, B. M. (1994). A theory of visual stability across saccadic eye movements. *Behavioral and Brain Sciences*, *17*(02), 247. https://doi.org/10.1017/S0140525X00034361

A

Appendix

Buxbaum, L. J., Ferraro, M. K., Veramonti, T., Farne, A., Whyte, J., Ladavas, E., … Coslett, H. B. (2004). Hemispatial neglect: Subtypes, neuroanatomy, and disability. *Neurology*, *62*(5), 749–756. https://doi.org/10.1212/01.WNL.0000113730.73031.F4

Carlson, T., Tovar, D. A., Alink, A., & Kriegeskorte, N. (2013). Representational dynamics of object vision: The first 1000 ms. *Journal of Vision*, *13*(10), 1–19. https://doi.org/10.1167/13.10.1

Castet, E., Jeanjean, S., & Masson, G. S. (2002). Motion perception of saccade-induced retinal translation. *Proceedings of the National Academy of Sciences*, *99*(23), 15159–15163. https://doi.org/10.1073/pnas.232377199

Castet, E., & Masson, G. S. (2000). Motion perception during saccadic eye movements. *Nature Neuroscience*, *3*(2), 177–183. https://doi.org/10.1038/72124

Cavanagh, P., Hunt, A. R., Afraz, A., & Rolfs, M. (2010). Visual stability based on remapping of attention pointers. *Trends in Cognitive Sciences*, *14*(4), 147–153. https://doi.org/10.1016/j.tics.2010.01.007

Cavanaugh, J., Berman, R. A., Joiner, W. M., & Wurtz, R. H. (2016). Saccadic corollary discharge underlies stable visual perception. *Journal of Neuroscience*, *36*(1), 31–42. https://doi.org/10.1523/JNEUROSCI.2054-15.2016

Chen, C.-Y., Sonnenberg, L., Weller, S., Witschel, T., & Hafed, Z. M. (2018). Spatial frequency sensitivity in macaque midbrain. *Nature Communications*, *9*(1). https://doi.org/10.1038/s41467-018-05302-5

Churan, J., Guitton, D., & Pack, C. C. (2011). Context dependence of receptive field remapping in superior colliculus. *Journal of Neurophysiology*, *106*(4), 1862–1874. https://doi.org/10.1152/jn.00288.2011

Cicchini, G. M., Binda, P., Burr, D. C., & Morrone, M. C. (2013). Transient spatiotopic integration across saccadic eye movements mediates visual stability. *Journal of Neurophysiology*, *109*(4), 1117–1125. https://doi.org/10.1152/jn.00478.2012

Cornelissen, F. W., Peters, E. M., & Palmer, J. (2002). The Eyelink Toolbox: Eye tracking with MATLAB and the Psychophysics Toolbox. *Behavior Research Methods, Instruments, & Computers*, *34*(4), 613–617. https://doi.org/10.3758/BF03195489

Crapse, T. B., & Sommer, M. A. (2008a). Corollary discharge across the animal kingdom. *Nature Reviews Neuroscience*, *9*(8), 587–600. https://doi.org/10.1038/nrn2457

Crapse, T. B., & Sommer, M. A. (2008b). The frontal eye field as a prediction map. In *Progress in Brain Research* (Vol. 171, pp. 383–390). https://doi.org/10.1016/S0079-6123(08)00656-0

Crapse, T. B., & Sommer, M. A. (2012). Frontal eye field neurons assess visual stability across saccades. *Journal of Neuroscience*, *32*(8), 2835–2845. https://doi.org/10.1523/JNEUROSCI.1320-11.2012

Crespi, S., Biagi, L., d'Avossa, G., Burr, D. C., Tosetti, M., & Morrone, M. C. (2011). Spatiotopic coding of BOLD signal in human visual cortex depends on spatial attention. *PLoS ONE*, *6*(7), e21661. https://doi.org/10.1371/journal.pone.0021661

Crouzet, S. M. (2010). Fast saccades toward faces: Face detection in just 100 ms. *Journal of Vision*, *10*(4), 1–17. https://doi.org/10.1167/10.4.16

Curcio, C. A., Sloan, K. R., Kalina, R. E., & Hendrickson, A. E. (1990). Human photoreceptor topography. *The Journal of Comparative Neurology*, *292*(4), 497–523. https://doi.org/10.1002/cne.902920402

Currie, C. B., McConkie, G. W., Carlson-Radvansky, L. A., & Irwin, D. E. (2000). The role of the saccade target object in the perception of a visually stable world. *Perception & Psychophysics*, *62*(4), 673–683. https://doi.org/10.3758/BF03206914

d'Avossa, G., Tosetti, M., Crespi, S., Biagi, L., Burr, D. C., & Morrone, M. C. (2007). Spatiotopic selectivity of BOLD responses to visual motion in human area MT. *Nature Neuroscience*, *10*(2), 249–255. https://doi.org/10.1038/nn1824

Dalmaijer, E. S., Van der Stigchel, S., Nijboer, T. C. W., Cornelissen, T. H. W., & Husain, M. (2015). CancellationTools: All-in-one software for administration and analysis of cancellation tasks. *Behavior Research Methods*, *47*(4), 1065–1075. https://doi.org/10.3758/s13428-014-0522-7

Demeyer, M., De Graef, P., Wagemans, J., & Verfaillie, K. (2009). Transsaccadic identification of highly similar artificial shapes. *Journal of Vision*, *9*(4), 1–14. https://doi.org/10.1167/9.4.28

Demeyer, M., De Graef, P., Wagemans, J., & Verfaillie, K. (2010). Object form discontinuity facilitates displacement discrimination across saccades. *Journal of Vision*, *10*(6), 1–14. https://doi.org/10.1167/10.6.17

D'Esposito, M., & Postle, B. R. (2015). The Cognitive Neuroscience of Working Memory. *Annual Review of Psychology*, *66*(1), 115–142. https://doi.org/10.1146/annurev-psych-010814-015031

Deubel, H. (2004). Localization of targets across saccades: Role of landmark objects. *Visual Cognition*, *11*(2–3), 173–202. https://doi.org/10.1080/13506280344000284

Deubel, H., Bridgeman, B., & Schneider, W. X. (1998). Immediate post-saccadic information mediates space constancy. *Vision Research*, *38*(20), 3147–3159. https://doi.org/10.1016/S0042-6989(98)00048-0

Deubel, H., Schneider, W. X., & Bridgeman, B. (1996). Postsaccadic target blanking prevents saccadic suppression of image displacement. *Vision Research*, *36*(7), 985–996. https://doi.org/10.1016/0042-6989(95)00203-0

Dodd, M. D., Van der Stigchel, S., & Hollingworth, A. (2009). Novelty is not always the best policy: Inhibition of return and facilitation of return as a function of visual task. *Psychological Science*, *20*(3), 333–339. https://doi.org/10.1111/j.1467-9280.2009.02294.x

Drew, T., Mance, I., Horowitz, T. S., Wolfe, J. M., & Vogel, E. K. (2014). A soft handoff of attention between cerebral hemispheres. *Current Biology*, *24*(10), 1133–1137. https://doi.org/10.1016/j.cub.2014.03.054

Duhamel, J.-R., Colby, C. L., & Goldberg, M. E. (1992). The updating of the representation of visual space in parietal cortex by intended eye movements. *Science*, *255*(5040), 90–92. https://doi.org/10.1126/science.1553535

Duhamel, J.-R., Goldberg, M. E., Fitzgibbon, E. J., Sirigu, A., & Grafman, J. (1992). Saccadic dysmetria in a patient with a right frontoparietal lesion: The importance of corollary discharge for accurate spatial behavior. *Brain*, *115*(5), 1387–1402. https://doi.org/10.1093/brain/115.5.1387

Dunkley, B. T., Baltaretu, B., & Crawford, J. D. (2016). Trans-saccadic interactions in human parietal and occipital cortex during the retention and comparison of object orientation. *Cortex*, *82*, 263–276. https://doi.org/10.1016/j.cortex.2016.06.012

Edelman, G. M., & Gally, J. A. (2001). Degeneracy and complexity in biological systems. *Proceedings of the National Academy of Sciences*, *98*(24), 13763–13768. https://doi.org/10.1073/pnas.231499798

A

Appendix

Edwards, G., VanRullen, R., & Cavanagh, P. (2018). Decoding trans-saccadic memory. *Journal of Neuroscience*, *38*(5), 1114–1123. https://doi.org/10.1523/JNEUROSCI.0854-17.2017

Eglin, M., Robertson, L. C., & Knight, R. T. (1989). Visual search performance in the neglect syndrome. *Journal of Cognitive Neuroscience*, *1*(4), 372–385. https://doi.org/10.1162/jocn.1989.1.4.372

Fabius, J. H., Fracasso, A., Nijboer, T. C. W., & Van der Stigchel, S. (2019). Time course of spatiotopic updating across saccades. *Proceedings of the National Academy of Sciences*, 6.

Fabius, J. H., Fracasso, A., & Van der Stigchel, S. (2016). Spatiotopic updating facilitates perception immediately after saccades. *Scientific Reports*, *6*(1). https://doi.org/10.1038/srep34488

Fairhall, S. L., Schwarzbach, J., Lingnau, A., Van Koningsbruggen, M. G., & Melcher, D. (2017). Spatiotopic updating across saccades revealed by spatially-specific fMRI adaptation. *NeuroImage*, *147*, 339–345. https://doi.org/10.1016/j.neuroimage.2016.11.071

Farrell, S., Ludwig, C. J. H., Ellis, L. A., & Gilchrist, I. D. (2010). Influence of environmental statistics on inhibition of saccadic return. *Proceedings of the National Academy of Sciences*, *107*(2), 929–934. https://doi.org/10.1073/pnas.0906845107

Ferber, S., & Danckert, J. (2006). Lost in space—The fate of memory representations for non-neglected stimuli. *Neuropsychologia*, *44*(2), 320–325. https://doi.org/10.1016/j.neuropsychologia.2005.04.018

Ferber, S., & Karnath, H.-O. (2001). How to assess spatial neglect - Line bisection or cancellation tasks? *Journal of Clinical and Experimental Neuropsychology*, *23*(5), 599–607. https://doi.org/10.1076/jcen.23.5.599.1243

Findlay, J. M., & Gilchrist, I. D. (2003). *Active vision: The psychology of looking and seeing*. Oxford University Press.

Fornaciai, M., Binda, P., & Cicchini, G. M. (2018). Trans-saccadic integration of orientation information. *Journal of Vision*, *18*(4), 1–11. https://doi.org/10.1167/18.4.9

Fracasso, A., Caramazza, A., & Melcher, D. (2010). Continuous perception of motion and shape across saccadic eye movements. *Journal of Vision*, *10*(13), 1–17. https://doi.org/10.1167/10.13.14

Friston, K., Adams, R. A., Perrinet, L., & Breakspear, M. (2012). Perceptions as hypotheses: Saccades as experiments. *Frontiers in Psychology*, *3*. https://doi.org/10.3389/fpsyg.2012.00151

Fuster, J. M., & Alexander, G. E. (1971). Neuron activity related to short-term memory. *Science*, *173*(3997), 652–654. https://doi.org/10.1126/science.173.3997.652

Gabay, S., Pertzov, Y., Cohen, N., Avidan, G., & Henik, A. (2013). Remapping of the environment without corollary discharges: Evidence from scene-based IOR. *Journal of Vision*, *13*(8), 1–10. https://doi.org/10.1167/13.8.22

Ganmor, E., Landy, M. S., & Simoncelli, E. P. (2015). Near-optimal integration of orientation information across saccades. *Journal of Vision*, *15*(16), 1–12. https://doi.org/10.1167/15.16.8

Gardner, J. L., Merriam, E. P., Movshon, J. A., & Heeger, D. J. (2008). Maps of visual space in human occipital cortex are retinotopic, not spatiotopic. *Journal of Neuroscience*, *28*(15), 3988–3999. https://doi.org/10.1523/JNEUROSCI.5476-07.2008

Gibson, J. J., & Radner, M. (1937). Adaptation, after-effect and contrast in the perception of tilted lines. I. Quantitative studies. *Journal of Experimental Psychology*, *20*(5), 453–467. https://doi.org/10.1037/h0059826

Gilchrist, I. D., & Harvey, M. (2000). Refixation frequency and memory mechanisms in visual search. *Current Biology*, *10*(19), 1209–1212. https://doi.org/10.1016/S0960-9822(00)00729-6

Golomb, J. D., Nguyen-Phuc, A. Y., Mazer, J. A., McCarthy, G., & Chun, M. M. (2010). Attentional facilitation throughout human visual cortex lingers in retinotopic coordinates after eye movements. *Journal of Neuroscience*, *30*(31), 10493–10506. https://doi.org/10.1523/JNEUROSCI.1546-10.2010

Golomb, J. D., Pulido, V. Z., Albrecht, A. R., Chun, M. M., & Mazer, J. A. (2010). Robustness of the retinotopic attentional trace after eye movements. *Journal of Vision*, *10*(3), 1–12. https://doi.org/10.1167/10.3.19

Greenlee, M. W., & Magnussen, S. (1987). Saturation of the tilt aftereffect. *Vision Research*, *27*(6), 1041–1043. https://doi.org/10.1016/0042-6989(87)90017-4

Grill-Spector, K., Henson, R., & Martin, A. (2006). Repetition and the brain: neural models of stimulus-specific effects. *Trends in Cognitive Sciences*, *10*(1), 14–23. https://doi.org/10.1016/j.tics.2005.11.006

Grüsser, O.-J. (1995). On the history of the ideas of efference copy and reafference. *Clio Medica*, (33), 35–55.

Guthrie, B., Porter, J., & Sparks, D. (1983). Corollary discharge provides accurate eye position information to the oculomotor system. *Science*, *221*(4616), 1193–1195. https://doi.org/10.1126/science.6612334

Hallett, P. E., & Lightstone, A. D. (1976). Saccadic eye movements to flashed targets. *Vision Research*, *16*(1), 107–114. https://doi.org/10.1016/0042-6989(76)90084-5

Harrison, W. J., & Bex, P. J. (2014). Integrating retinotopic features in spatiotopic coordinates. *Journal of Neuroscience*, *34*(21), 7351–7360. https://doi.org/10.1523/JNEUROSCI.5252-13.2014

Hartline, H. K. (1938). The response of single optic nerve fibers of the vertebrate eye to illumination of the retina. *American Journal of Physiology-Legacy Content*, *121*(2), 400–415. https://doi.org/10.1152/ajplegacy.1938.121.2.400

Hartmann, T. S., Zirnsak, M., Marquis, M., Hamker, F. H., & Moore, T. (2017). Two Types of Receptive Field Dynamics in Area V4 at the Time of Eye Movements? *Frontiers in Systems Neuroscience*, *11*. https://doi.org/10.3389/fnsys.2017.00013

Hayhoe, M. M., & Ballard, D. H. (2011). Mechanisms of gaze control in natural vision. In *The Oxford handbook of eye movements* (pp. 607–617). Oxford, UK: Oxford University Press.

Heide, W., Blankenburg, M., Zimmermann, E., & Kompf, M. D. (1995). Cortical control of double-step saccades: Implications for spatial orientation. *Annals of Neurology*, *38*, 739–748.

Henderson, J. M., & Hollingworth, A. (1998). Eye movements during scene viewing: An overview. In G. Underwood (Ed.), *Eye Guidance in Reading and Scene Perception* (pp. 269–293). https://doi.org/10.1016/B978-008043361-5/50013-4

Henderson, J. M., & Hollingworth, A. (1999). High-level scene perception. *Annual Review of Psychology*, *50*(1), 243–271. https://doi.org/10.1146/annurev.psych.50.1.243

A

Herwig, A. (2015). Transsaccadic integration and perceptual continuity. *Journal of Vision*, *15*(16), 1–6. https://doi.org/10.1167/15.16.7

Herwig, A., Beisert, M., & Schneider, W. X. (2010). On the spatial interaction of visual working memory and attention: Evidence for a global effect from memory-guided saccades. *Journal of Vision*, *10*(5), 1–10. https://doi.org/10.1167/10.5.8

Hess, E. H., & Polt, J. M. (1964). Pupil size in relation to mental activity during simple problem-solving. *Science*, *143*(3611), 1190–1192.

Higgins, E., & Rayner, K. (2015). Transsaccadic processing: stability, integration, and the potential role of remapping. *Attention, Perception, & Psychophysics*, *77*(1), 3–27. https://doi.org/10.3758/s13414-014-0751-y

Hilchey, M. D., Klein, R. M., Satel, J., & Wang, Z. (2012). Oculomotor inhibition of return: How soon is it "recoded" into spatiotopic coordinates? *Attention, Perception, & Psychophysics*, *74*(6), 1145–1153. https://doi.org/10.3758/s13414-012-0312-1

Hoeks, B., & Levelt, W. J. M. (1993). Pupillary dilation as a measure of attention: a quantitative system analysis. *Behavior Research Methods, Instruments, & Computers*, *25*(1), 16–26. https://doi.org/10.3758/BF03204445

Hoeting, J. A., Madigan, D., Raftery, A. E., & Volinsky, C. T. (1999). Bayesian Model Averaging: A Tutorial. *Statistical Science*, *14*(4), 382–417.

Hollingworth, A., & Luck, S. J. (2009). The role of visual working memory (VWM) in the control of gaze during visual search. *Attention, Perception, & Psychophysics*, *71*(4), 936–949. https://doi.org/10.3758/APP.71.4.936

Holm, S. (1979). A simple sequentially rejective multiple test procedure. *Scandinavian Journal of Statistics*, *6*(2), 65–70.

Hooge, I. Th. C., & Frens, M. A. (2000). Inhibition of saccade return (ISR): spatio-temporal properties of saccade programming. *Vision Research*, *40*(24), 3415–3426. https://doi.org/10.1016/S0042-6989(00)00184-X

Hooge, I. Th. C., Over, E. A. B., van Wezel, R. J. A., & Frens, M. A. (2005). Inhibition of return is not a foraging facilitator in saccadic search and free viewing. *Vision Research*, *45*(14), 1901–1908. https://doi.org/10.1016/j.visres.2005.01.030

Hubel, D. H., & Wiesel, T. N. (1959). Receptive fields of single neurones in the cat's striate cortex. *The Journal of Physiology*, *148*(3), 574–591. https://doi.org/10.1113/jphysiol.1959.sp006308

Huber-Huber, C., Buonocore, A., Hickey, C., & Melcher, D. (2018). Previewing a face in the periphery reduces the fN170: Combined EEG and eye-tracking suggests two stages of trans-saccadic predictive processes. *BioRxiv*. https://doi.org/10.1101/468900

Husain, M., Mannan, S. K., Hodgson, T. L., Wojciulik, E., Driver, J., & Kennard, C. (2001). Impaired spatial working memory across saccades contributes to abnormal search in parietal neglect. *Brain*, *124*(5), 941–952. https://doi.org/10.1093/brain/124.5.941

Husain, M., & Rorden, C. (2003). Non-spatially lateralized mechanisms in hemispatial neglect. *Nature Reviews Neuroscience*, *4*(1), 26–36. https://doi.org/10.1038/nrn1005

Inaba, N., & Kawano, K. (2016). Eye position effects on the remapped memory trace of visual motion in cortical area MST. *Scientific Reports*, *6*(1). https://doi.org/10.1038/srep22013

Irwin, D. E., Yantis, S., & Jonides, J. (1983). Evidence against visual integration across saccadic eye movements. *Perception & Psychophysics*, *34*(1), 49–57. https://doi.org/10.3758/BF03205895

Irwin, D. E., Zacks, J. L., & Brown, J. S. (1990). Visual memory and the perception of a stable visual environment. *Perception & Psychophysics*, *47*(1), 35–46. https://doi.org/10.3758/BF03208162

Jaeger, T. F. (2008). Categorical data analysis: Away from ANOVAs (transformation or not) and towards logit mixed models. *Journal of Memory and Language*, *59*(4), 434–446. https://doi.org/10.1016/j.jml.2007.11.007

Jeffreys, H. (1961). *Theory of probability* (3. ed., reprinted). Oxford: Clarendon Press.

Joiner, W. M., Cavanaugh, J., FitzGibbon, E. J., & Wurtz, R. H. (2013). Corollary discharge contributes to perceived eye location in monkeys. *Journal of Neurophysiology*, *110*(10), 2402–2413. https://doi.org/10.1152/jn.00362.2013

Jonides, J., Irwin, D. E., & Yantis, S. (1982). Integrating visual information from successive fixations. *Science*, *215*(4529), 192–194. https://doi.org/10.1126/science.7053571

Jonikaitis, D., & Theeuwes, J. (2013). Dissociating oculomotor contributions to spatial and feature-based selection. *Journal of Neurophysiology*, *110*(7), 1525–1534. https://doi.org/10.1152/jn.00275.2013

Jüttner, M. (1997). Effects of perceptual context on transsaccadic visual matching. *Perception & Psychophysics*, *59*(5), 762–773. https://doi.org/10.3758/BF03206022

Jüttner, M., & Röhler, R. (1993). Lateral information transfer across saccadic eye movements. *Perception & Psychophysics*, *53*(2), 210–220. https://doi.org/10.3758/BF03211731

Kahneman, D., & Beatty, J. (1966). Pupil Diameter and Load on Memory. *Science*, *154*(3756), 1583–1585.

Kanai, R., & Verstraten, F. A. J. (2005). Perceptual manifestations of fast neural plasticity: Motion priming, rapid motion aftereffect and perceptual sensitization. *Vision Research*, *45*(25–26), 3109–3116. https://doi.org/10.1016/j.visres.2005.05.014

Kass, R. E., & Raftery, A. E. (1995). Bayes Factors. *Journal of American Statistical Association*, *90*(430), 773–795.

Kesten, H. (1958). Accelerated Stochastic Approximation. *The Annals of Mathematical Statistics*, *29*(1), 41–59. https://doi.org/10.1214/aoms/1177706705

Khayat, P. S., Spekreijse, H., & Roelfsema, P. R. (2006). Attention lights up new object representations before the old ones fade away. *Journal of Neuroscience*, *26*(1), 138–142. https://doi.org/10.1523/JNEUROSCI.2784-05.2006

Kinsbourne, M. (1987). Mechanisms of Unilateral Neglect. In M. Jeannerod (Ed.), *Advances in Psychology* (Vol. 45, pp. 69–86). https://doi.org/10.1016/S0166-4115(08)61709-4

Kirchner, H., & Thorpe, S. J. (2006). Ultra-rapid object detection with saccadic eye movements: Visual processing speed revisited. *Vision Research*, *46*(11), 1762–1776. https://doi.org/10.1016/j.visres.2005.10.002

Klein, R. M. (1988). Inhibitory tagging system facilitates visual search. *Nature*, *334*(6181), 430–431. https://doi.org/10.1038/334430a0

Klein, R. M. (2000). Inhibition of return. *Trends in Cognitive Sciences*, *4*(4), 138–147.

A

Appendix

Klein, R. M., & Hilchey, M. D. (2011). Oculomotor inhibition of return. In *The Oxford handbook of eye movements* (pp. 471–492). Oxford, UK: Oxford University Press.

Klein, R. M., & MacInnes, W. J. (1999). Inhibition of return is a foraging facilitator in visual search. *Psychological Science*, *10*(4), 346–352. https://doi.org/10.1111/1467-9280.00166

Kleiner, M., Brainard, D. H., & Pelli, D. G. (2007). What's new in Psychtoolbox-3? *Perception*, *36*(14).

Knapen, T., Rolfs, M., & Cavanagh, P. (2009). The reference frame of the motion aftereffect is retinotopic. *Journal of Vision*, *9*(5), 1–6. https://doi.org/10.1167/9.5.16

Knapen, T., Rolfs, M., Wexler, M., & Cavanagh, P. (2010). The reference frame of the tilt aftereffect. *Journal of Vision*, *10*(1), 1–13. https://doi.org/10.1038/srep40525

Knöll, J., Morrone, M. C., & Bremmer, F. (2013). Spatio-temporal topography of saccadic overestimation of time. *Vision Research*, *83*, 56–65. https://doi.org/10.1016/j.visres.2013.02.013

Kramer, A. F., McCarley, J. S., Boot, W. R., & Peterson, M. S. (2004). Landmarks help guide attention during visual search. *Spatial Vision*, *17*(4), 497–510. https://doi.org/10.1163/1568568041920230

Kristjánsson, Á., & Vuilleumier, P. (2010). Disruption of spatial memory in visual search in the left visual field in patients with hemispatial neglect. *Vision Research*, *50*(14), 1426–1435. https://doi.org/10.1016/j.visres.2010.03.001

Kusunoki, M., & Goldberg, M. E. (2003). The time course of perisaccadic receptive field shifts in the lateral intraparietal area of the monkey. *Journal of Neurophysiology*, *89*(3), 1519–1527. https://doi.org/10.1152/jn.00519.2002

Lee, M. D., & Wagenmakers, E.-J. (2013). *Bayesian cognitive modeling: A practical course* (1st ed.). Retrieved from http://doi.org/10.1017/CBO9781139087759

Lepsien, J., Griffin, I. C., Devlin, J. T., & Nobre, A. C. (2005). Directing spatial attention in mental representations: Interactions between attentional orienting and working-memory load. *NeuroImage*, *26*(3), 733–743. https://doi.org/10.1016/j.neuroimage.2005.02.026

Lescroart, M. D., Kanwisher, N., & Golomb, J. D. (2016). No evidence for automatic remapping of stimulus features or location found with fMRI. *Frontiers in Systems Neuroscience*, *10*. https://doi.org/10.3389/fnsys.2016.00053

Lewis-Peacock, J. A., Drysdale, A. T., Oberauer, K., & Postle, B. R. (2012). Neural evidence for a distinction between short-term memory and the focus of attention. *Journal of Cognitive Neuroscience*, *24*(1), 61–79. https://doi.org/10.1162/jocn_a_00140

Lisi, M., Cavanagh, P., & Zorzi, M. (2015). Spatial constancy of attention across eye movements is mediated by the presence of visual objects. *Attention, Perception, & Psychophysics*, *77*(4), 1159–1169. https://doi.org/10.3758/s13414-015-0861-1

Liversedge, S. P., Gilchrist, I. D., & Everling, S. (Eds.). (2011). *The Oxford handbook of eye movements* (1. ed). Oxford: Oxford Univ. Press.

Luck, S. J. (2008). Visual short-term memory. In *Visual memory* (pp. 43–85). Oxford University Press.

Luke, S. G., Smith, T. J., Schmidt, J., & Henderson, J. M. (2014). Dissociating temporal inhibition of return and saccadic momentum across multiple eye-movement tasks. *Journal of Vision*, *14*(14), 1–12. https://doi.org/10.1167/14.14.9

Macinnes, W. J., & Klein, R. M. (2003). Inhibition of return biases orienting during the search of complex scenes. *The Scientific World JOURNAL*, *3*, 75–86. https://doi.org/10.1100/tsw.2003.03

Mackay, D. M. (1972). Visual stability. *Investigative Ophtalmology*, *11*(6), 518–524.

Malhotra, P., Jäger, H. R., Parton, A., Greenwood, R., Playford, E. D., Brown, M. M., … Husain, M. (2005). Spatial working memory capacity in unilateral neglect. *Brain*, *128*(2), 424–435. https://doi.org/10.1093/brain/awh372

Malhotra, P., Mannan, S., Driver, J., & Husain, M. (2004). Impaired spatial working memory: One component of the visual neglect syndrome? *Cortex*, *40*(4–5), 667–676. https://doi.org/10.1016/S0010-9452(08)70163-1

Mannan, S. K., Mort, D. J., Hodgson, T. L., Driver, J., Kennard, C., & Husain, M. (2005). Revisiting previously searched locations in visual neglect: Role of right parietal and frontal lesions in misjudging old locations as new. *Journal of Cognitive Neuroscience*, *17*(2), 340–354. https://doi.org/10.1162/0898929053124983

Marino, A. C., & Mazer, J. A. (2016). Perisaccadic updating of visual representations and attentional states: Linking behavior and neurophysiology. *Frontiers in Systems Neuroscience*, *10*. https://doi.org/10.3389/fnsys.2016.00003

Maris, E., & Oostenveld, R. (2007). Nonparametric statistical testing of EEG- and MEG-data. *Journal of Neuroscience Methods*, *164*(1), 177–190. https://doi.org/10.1016/j.jneumeth.2007.03.024

Mark, V. W., Woods, A. J., Ball, K. K., Roth, D. L., & Mennemeier, M. (2004). Disorganized search on cancellation is not a consequence of neglect. *Neurology*, *63*(1), 78–84. https://doi.org/10.1212/01.WNL.0000131947.08670.D4

Mathôt, S. (2013). *Pupil size reconstruction examples*. Retrieved from https://dx.doi.org/10.6084/m9.figshare.688002.v1

Mathôt, S., Dalmaijer, E., & Grainger, J. (2014). The pupillary light response reflects exogenous attention and inhibition of return. *Journal of Vision*, 9.

Mathôt, S., Melmi, J.-B., van der Linden, L., & Van der Stigchel, S. (2016). The mind-writing pupil: A human-computer interface based on decoding of covert attention through pupillometry. *PLOS ONE*, *11*(2), e0148805. https://doi.org/10.1371/journal.pone.0148805

Mathôt, S., & Theeuwes, J. (2010). Gradual remapping results in early retinotopic and late spatiotopic inhibition of return. *Psychological Science*, *21*(12), 1793–1798. https://doi.org/10.1177/0956797610388813

Mathôt, S., & Theeuwes, J. (2011). Visual attention and stability. *Philosophical Transactions of the Royal Society B: Biological Sciences*, *366*(1564), 516–527. https://doi.org/10.1098/rstb.2010.0187

Mathôt, S., & Theeuwes, J. (2013). A reinvestigation of the reference frame of the tilt-adaptation aftereffect. *Scientific Reports*, *3*(1). https://doi.org/10.1038/srep01152

Mathôt, S., van der Linden, L., Grainger, J., & Vitu, F. (2013). The pupillary light response reveals the focus of covert visual attention. *PLoS ONE*, *8*(10), e78168. https://doi.org/10.1371/journal.pone.0078168

A

Appendix

Mathôt, S., & Van der Stigchel, S. (2015). New light on the mind's eye: The pupillary light response as active vision. *Current Directions in Psychological Science*, *24*(5), 374–378. https://doi.org/10.1177/0963721415593725

Maunsell, J. H. R., & Gibson, J. R. (1992). Visual response latencies in striate cortex of the macaque monkey. *Journal of Neurophysiology*, *68*(4), 1332–1344. https://doi.org/10.1152/jn.1992.68.4.1332

Mazer, J. A., Vinje, W. E., McDermott, J., Schiller, P. H., & Gallant, J. L. (2002). Spatial frequency and orientation tuning dynamics in area V1. *Proceedings of the National Academy of Sciences*, *99*(3), 1645–1650. https://doi.org/10.1073/pnas.022638499

McCarley, J. S., Wang, R. F., Kramer, A. F., Irwin, D. E., & Peterson, M. S. (2003). How much memory does oculomotor search have? *Psychological Science*, *14*(5), 422–426.

McConkie, G. W., & Currie, C. B. (1996). Visual stability across saccades while viewing complex pictures. *Journal of Experimental Psychology: Human Perception and Performance*, *27*(3), 563–581.

Medendorp, W. P., Goltz, H. C., & Vilis, T. (2006). Directional selectivity of BOLD activity in human posterior parietal cortex for memory-guided double-step saccades. *Journal of Neurophysiology*, *95*(3), 1645–1655. https://doi.org/10.1152/jn.00905.2005

Medendorp, W. P., Goltz, H. C., Vilis, T., & Crawford, J. D. (2003). Gaze-centered updating of visual space in human parietal cortex. *Journal of Neuroscience*, *23*(15), 6209–6214. https://doi.org/10.1523/JNEUROSCI.23-15-06209.2003

Melcher, D. (2005). Spatiotopic Transfer of Visual-Form Adaptation across Saccadic Eye Movements. *Current Biology*, *15*(19), 1745–1748. https://doi.org/10.1016/j.cub.2005.08.044

Melcher, D. (2009). Selective attention and the active remapping of object features in trans-saccadic perception. *Vision Research*, *49*(10), 1249–1255. https://doi.org/10.1016/j.visres.2008.03.014

Melcher, D. (2011). Visual stability. *Philosophical Transactions of the Royal Society B: Biological Sciences*, *366*(1564), 468–475. https://doi.org/10.1098/rstb.2010.0277

Melcher, D., & Colby, C. L. (2008). Trans-saccadic perception. *Trends in Cognitive Sciences*, *12*(12), 466–473. https://doi.org/10.1016/j.tics.2008.09.003

Melcher, D., & Fracasso, A. (2012). Remapping of the line motion illusion across eye movements. *Experimental Brain Research*, *218*(4), 503–514. https://doi.org/10.1007/s00221-012-3043-6

Melcher, D., & Morrone, M. C. (2003). Spatiotopic temporal integration of visual motion across saccadic eye movements. *Nature Neuroscience*, *6*(8), 877–881. https://doi.org/10.1038/nn1098

Merriam, E. P., Genovese, C. R., & Colby, C. L. (2003). Spatial updating in human parietal cortex. *Neuron*, *39*(2), 361–373. https://doi.org/10.1016/S0896-6273(03)00393-3

Merriam, E. P., Genovese, C. R., & Colby, C. L. (2007). Remapping in human visual cortex. *Journal of Neurophysiology*, *97*(2), 1738–1755. https://doi.org/10.1152/jn.00189.2006

Miall, R. C., & Wolpert, D. M. (1996). Forward models for physiological motor control. *Neural Networks*, *9*(8), 1265–1279. https://doi.org/10.1016/S0893-6080(96)00035-4

Mirpour, K., & Bisley, J. W. (2012). Anticipatory remapping of attentional priority across the entire visual field. *Journal of Neuroscience*, *32*(46), 16449–16457. https://doi.org/10.1523/JNEUROSCI.2008-12.2012

Mirpour, K., & Bisley, J. W. (2016). Remapping, spatial stability, and temporal continuity: From the pre-saccadic to postsaccadic representation of visual space in LIP. *Cerebral Cortex*, *26*(7), 3183–3195. https://doi.org/10.1093/cercor/bhv153

Morey, R. D., Rouder, J. N., & Jamil, T. (2015). *Computation of Bayes Factors for common designs*. Retrieved from https://CRAN.R- project.org/package=BayesFactor

Morris, A. P., Bremmer, F., & Krekelberg, B. (2016). The dorsal visual system predicts future and remembers past eye position. *Frontiers in Systems Neuroscience*, *10*. https://doi.org/10.3389/fnsys.2016.00009

Morris, A. P., Liu, C. C., Cropper, S. J., Forte, J. D., Krekelberg, B., & Mattingley, J. B. (2010). Summation of visual motion across eye movements reflects a nonspatial decision mechanism. *Journal of Neuroscience*, *30*(29), 9821–9830. https://doi.org/10.1523/JNEUROSCI.1705-10.2010

Müller, H. J., & von Mühlenen, A. (2000). Probing distractor inhibition in visual search: Inhibition of return. *Journal of Experimental Psychology: Human Perception and Performance*, *26*(5), 1591–1605. https://doi.org/10.10371/0096-1523.26.5.1591

Naber, M., Alvarez, G. A., & Nakayama, K. (2013). Tracking the allocation of attention using human pupillary oscillations. *Frontiers in Psychology*, *4*. https://doi.org/10.3389/fpsyg.2013.00919

Naber, M., & Nakayama, K. (2013). Pupil responses to high-level image content. *Journal of Vision*, *13*(6), 7–7. https://doi.org/10.1167/13.6.7

Nakamura, K., & Colby, C. L. (2002). Updating of the visual representation in monkey striate and extrastriate cortex during saccades. *Proceedings of the National Academy of Sciences*, *99*(6), 4026–4031. https://doi.org/10.1073/pnas.052379899

Nakashima, Y., & Sugita, Y. (2017). The reference frame of the tilt aftereffect measured by differential Pavlovian conditioning. *Scientific Reports*, *7*(1). https://doi.org/10.1038/srep40525

Neupane, S., Guitton, D., & Pack, C. C. (2016). Two distinct types of remapping in primate cortical area V4. *Nature Communications*, *7*, 10402. https://doi.org/10.1038/ncomms10402

Niemeier, M., Crawford, J. D., & Tweed, D. B. (2003). Optimal transsaccadic integration explains distorted spatial perception. *Nature*, *422*(6927), 76–80. https://doi.org/10.1038/nature01439

Nijboer, T. C. W., Kollen, B. J., & Kwakkel, G. (2013). Time course of visuospatial neglect early after stroke: A longitudinal cohort study. *Cortex*, *49*(8), 2021–2027. https://doi.org/10.1016/j.cortex.2012.11.006

Nijboer, T. C. W., van de Port, I., Schepers, V., Post, M., & Visser-Meily, J. M. A. (2013). Predicting functional outcome after stroke: The influence of neglect on basic activities in daily living. *Frontiers in Human Neuroscience*, *7*. https://doi.org/10.3389/fnhum.2013.00182

Nobre, A., Correa, A., & Coull, J. (2007). The hazards of time. *Current Opinion in Neurobiology*, *17*(4), 465–470. https://doi.org/10.1016/j.conb.2007.07.006

Nyström, M., & Holmqvist, K. (2010). An adaptive algorithm for fixation, saccade, and glissade detection in eyetracking data. *Behavior Research Methods*, *42*(1), 188–204. https://doi.org/10.3758/BRM.42.1.188

A

Appendix

Ong, W. S., Hooshvar, N., Zhang, M., & Bisley, J. W. (2009). Psychophysical evidence for spatiotopic processing in area MT in a short-term memory for motion task. *Journal of Neurophysiology*, *102*(4), 2435–2440. https://doi.org/10.1152/jn.00684.2009

Oosterhof, N. N., Connolly, A. C., & Haxby, J. V. (2016). CoSMoMVPA: Multi-modal multivariate pattern analysis of neuroimaging data in Matlab/GNU Octave. *Frontiers in Neuroinformatics*, *10*. https://doi.org/10.3389/fninf.2016.00027

Oostwoud Wijdenes, L., Marshall, L., & Bays, P. M. (2015). Evidence for optimal integration of visual feature representations across saccades. *Journal of Neuroscience*, *35*(28), 10146–10153. https://doi.org/10.1523/JNEUROSCI.1040-15.2015

O'Regan, J. K., & Lévy-Schoen, A. (1983). Integrating visual information from successive fixations: does trans-saccadic fusion exist? *Vision Research*, *23*(8), 765–768.

Ostendorf, F., Liebermann, D., & Ploner, C. J. (2010). Human thalamus contributes to perceptual stability across eye movements. *Proceedings of the National Academy of Sciences*, *107*(3), 1229–1234. https://doi.org/10.1073/pnas.0910742107

Ostendorf, F., Liebermann, D., & Ploner, C. J. (2013). A role of the human thalamus in predicting the perceptual consequences of eye movements. *Frontiers in Systems Neuroscience*, *7*. https://doi.org/10.3389/fnsys.2013.00010

Paeye, C., Collins, T., & Cavanagh, P. (2017). Transsaccadic perceptual fusion. *Journal of Vision*, *17*(1), 1–11. https://doi.org/10.1167/17.1.14

Parks, N. A., & Corballis, P. M. (2008). Electrophysiological correlates of presaccadic remapping in humans. *Psychophysiology*, *45*(5), 776–783. https://doi.org/10.1111/j.1469-8986.2008.00669.x

Parks, N. A., & Corballis, P. M. (2010). Human transsaccadic visual processing: Presaccadic remapping and postsaccadic updating. *Neuropsychologia*, *48*(12), 3451–3458. https://doi.org/10.1016/j.neuropsychologia.2010.07.028

Parton, A., Malhotra, P., Nachev, P., Ames, D., Ball, J., Chataway, J., & Husain, M. (2006). Space re-exploration in hemispatial neglect: *NeuroReport*, *17*(8), 833–836. https://doi.org/10.1097/01.wnr.0000220130.86349.a7

Pelli, D. G. (1997). The VideoToolbox software for visual psychophysics: Transforming numbers into movies. *Spatial Vision*, *10*(4), 437–442.

Pertzov, Y., Zohary, E., & Avidan, G. (2010). Rapid formation of spatiotopic representations as revealed by inhibition of return. *Journal of Neuroscience*, *30*(26), 8882–8887. https://doi.org/10.1523/JNEUROSCI.3986-09.2010

Peterburs, J., Gajda, K., Hoffmann, K.-P., Daum, I., & Bellebaum, C. (2011). Electrophysiological correlates of inter- and intrahemispheric saccade-related updating of visual space. *Behavioural Brain Research*, *216*(2), 496–504. https://doi.org/10.1016/j.bbr.2010.08.025

Peterson, M. S., Kramer, A. F., Wang, R. F., Irwin, D. E., & McCarley, J. S. (2001). Visual search has memory. *Psychological Science*, *12*(4), 287–292.

Pisella, L., Berberovic, N., & Mattingley, J. B. (2004). Impaired working memory for location but not for colour or shape in visual neglect: A comparison of parietal and non-parietal lesions. *Cortex*, *40*(2), 379–390. https://doi.org/10.1016/S0010-9452(08)70132-1

Poletti, M., Burr, D. C., & Rucci, M. (2013). Optimal multimodal integration in spatial localization. *Journal of Neuroscience*, *33*(35), 14259–14268. https://doi.org/10.1523/JNEUROSCI.0523-13.2013

Pollatsek, A., Rayner, K., & Collins, W. E. (1984). Integrating pictorial information across eye movements. *Journal of Experimental Psychology: General*, *113*(3), 426–442.

Posner, M. I., & Cohen, Y. (1984). Components of visual orienting. In *Attention and Performance* (Vol. 10, pp. 531–556). Hilldale, NJ: Erlbaum.

Posner, M. I., Rafal, R. D., Choate, L. S., & Vaughan, J. (1985). Inhibition of return: Neural basis and function. *Cognitive Neuropsychology*, *2*, 211–228. https://doi.org/10.1080/02643298508252866

Postle, B. R. (2006). Working memory as an emergent property of the mind and brain. *Neuroscience*, *139*(1), 23–38. https://doi.org/10.1016/j.neuroscience.2005.06.005

Price, C. J., & Friston, K. J. (2002). Degeneracy and cognitive anatomy. *Trends in Cognitive Sciences*, *6*(10), 416–421. https://doi.org/10.1016/S1364-6613(02)01976-9

Prime, S. L., Niemeier, M., & Crawford, J. D. (2006). Transsaccadic integration of visual features in a line intersection task. *Experimental Brain Research*, *169*(4), 532–548. https://doi.org/10.1007/s00221-005-0164-1

Ptak, R., Schnider, A., Golay, L., & Muri, R. (2007). A non-spatial bias favouring fixated stimuli revealed in patients with spatial neglect. *Brain*, *130*(12), 3211–3222. https://doi.org/10.1093/brain/awm234

Purves, D., Augustine, G. J., Fitzpatrick, D., Hall, W., LaMantia, A.-S., McNamara, J. O., & White, L. E. (2008). *Neuroscience* (4th ed.). Sunderland, MA: Sinauer Associates, Inc.

Ramkumar, P., Jas, M., Pannasch, S., Hari, R., & Parkkonen, L. (2013). Feature-specific information processing precedes concerted activation in human visual cortex. *Journal of Neuroscience*, *33*(18), 7691–7699. https://doi.org/10.1523/JNEUROSCI.3905-12.2013

Rao, H. M., Abzug, Z. M., & Sommer, M. A. (2016). Visual continuity across saccades is influenced by expectations. *Journal of Vision*, *16*(5), 1–18. https://doi.org/10.1167/16.5.7

Rao, R. P. N., & Ballard, D. H. (1999). Predictive coding in the visual cortex: a functional interpretation of some extra-classical receptive-field effects. *Nature Neuroscience*, *2*(1), 79–87. https://doi.org/10.1038/4580

Rapcsak, S. Z., Cimino, C. R., & Heilman, K. M. (1988). Altitudinal neglect. *Neurology*, *38*(2), 277. https://doi.org/10.1212/WNL.38.2.277

Rath-Wilson, K., & Guitton, D. (2015). Refuting the hypothesis that a unilateral human parietal lesion abolishes saccade corollary discharge. *Brain*, *138*(12), 3760–3775. https://doi.org/10.1093/brain/awv275

Ravizza, S. M., Behrmann, M., & Fiez, J. A. (2005). Right parietal contributions to verbal working memory: Spatial or executive? *Neuropsychologia*, *43*(14), 2057–2067. https://doi.org/10.1016/j.neuropsychologia.2005.03.014

A

Appendix

Ronchi, R., Posteraro, L., Fortis, P., Bricolo, E., & Vallar, G. (2009). Perseveration in left spatial neglect: Drawing and cancellation tasks. *Cortex*, *45*(3), 300–312. https://doi.org/10.1016/j.cortex.2008.03.012

Rorden, Chris, & Brett, M. (2000). Stereotaxic display of brain lesions. *Behavioural Neurology*, *12*(4), 191–200. https://doi.org/10.1155/2000/421719

Rorden, Christopher, & Karnath, H.-O. (2010). A simple measure of neglect severity. *Neuropsychologia*, *48*(9), 2758–2763. https://doi.org/10.1016/j.neuropsychologia.2010.04.018

Rouder, J. N., Morey, R. D., Speckman, P. L., & Province, J. M. (2012). Default Bayes factors for ANOVA designs. *Journal of Mathematical Psychology*, *56*(5), 356–374. https://doi.org/10.1016/j.jmp.2012.08.001

Rouder, J. N., Morey, R. D., Verhagen, J., Swagman, A. R., & Wagenmakers, E.-J. (2017). Bayesian analysis of factorial designs. *Psychological Methods*, *22*(2), 304–321. https://doi.org/10.1037/met0000057

Russell, C., Deidda, C., Malhotra, P., Crinion, J. T., Merola, S., & Husain, M. (2010). A deficit of spatial remapping in constructional apraxia after right-hemisphere stroke. *Brain*, *133*(4), 1239–1251. https://doi.org/10.1093/brain/awq052

Saslow, M. G. (1967). Effects of components of displacement-step stimuli upon latency for saccadic eye movement. *Journal of the Optical Society of America*, *57*(8), 1030. https://doi.org/10.1364/JOSA.57.001030

Schall, J. D. (1995). Neural basis of saccade target selection. *Reviews in the Neurosciences*, *6*(1). https://doi.org/10.1515/REVNEURO.1995.6.1.63

Schut, M. J., Van der Stoep, N., Fabius, J. H., & Van der Stigchel, S. (2018). Feature integration is unaffected by saccade landing point, even when saccades land outside of the range of regular oculomotor variance. *Journal of Vision*, *18*(7), 6. https://doi.org/10.1167/18.7.6

Schut, M. J., Van der Stoep, N., Postma, A., & Van der Stigchel, S. (2017). The cost of making an eye movement: A direct link between visual working memory and saccade execution. *Journal of Vision*, *17*(6), 1–20. https://doi.org/10.1167/17.6.15

Schütt, H. H., Harmeling, S., Macke, J. H., & Wichmann, F. A. (2016). Painfree and accurate Bayesian estimation of psychometric functions for (potentially) overdispersed data. *Vision Research*, *122*, 105–123. https://doi.org/10.1016/j.visres.2016.02.002

Shen, K., McIntosh, A. R., & Ryan, J. D. (2014). A working memory account of refixations in visual search. *Journal of Vision*, *14*(14), 1–11. https://doi.org/10.1167/14.14.11

Shimozaki, S. S., Hayhoe, M. M., Zelinsky, G. J., Weinstein, A., Merigan, W. H., & Ballard, D. H. (2003). Effect of parietal lobe lesions on saccade targeting and spatial memory in a naturalistic visual search task. *Neuropsychologia*, *41*(10), 1365–1386. https://doi.org/10.1016/S0028-3932(03)00042-3

Shioiri, S., & Cavanagh, P. (1989). Saccadic suppression of low-level motion. *Vision Research*, *29*(8), 915–928. https://doi.org/10.1016/0042-6989(89)90106-5

Simons, D. J., & Rensink, R. A. (2005). Change blindness: past, present, and future. *Trends in Cognitive Sciences*, *9*(1), 16–20. https://doi.org/10.1016/j.tics.2004.11.006

Simpson, S. A., Abegg, M., & Barton, J. J. S. (2011). Rapid adaptation of visual search in simulated hemianopia. *Cerebral Cortex*, *21*(7), 1593–1601. https://doi.org/10.1093/cercor/bhq221

Smith, S., & Nichols, T. (2009). Threshold-free cluster enhancement: Addressing problems of smoothing, threshold dependence and localisation in cluster inference. *NeuroImage*, *44*(1), 83–98. https://doi.org/10.1016/j.neuroimage.2008.03.061

Smith, T. J., & Henderson, J. M. (2009). Facilitation of return during scene viewing. *Visual Cognition*, *17*(6–7), 1083–1108. https://doi.org/10.1080/13506280802678557

Smith, T. J., & Henderson, J. M. (2011). Does oculomotor inhibition of return influence fixation probability during scene search? *Attention, Perception, & Psychophysics*, *73*(8), 2384–2398. https://doi.org/10.3758/s13414-011-0191-x

Solomon, T. M., DeBros, G. B., Budson, A. E., Mirkovic, N., Murphy, C. A., & Solomon, P. R. (2014). Correlational analysis of 5 commonly used measures of cognitive functioning and mental status: An update. *American Journal of Alzheimer's Disease and Other Dementias*, *29*(8), 718–722. https://doi.org/10.1177/1533317514534761

Sommer, M. A., & Wurtz, R. H. (2002). A pathway in primate brain for internal monitoring of movements. *Science*, *296*(5572), 1480–1482. https://doi.org/10.1126/science.1069590

Sommer, M. A., & Wurtz, R. H. (2006). Influence of the thalamus on spatial visual processing in frontal cortex. *Nature*, *444*(7117), 374–377. https://doi.org/10.1038/nature05279

Sommer, M. A., & Wurtz, R. H. (2008a). Brain circuits for the internal monitoring of movements. *Annual Review of Neuroscience*, *31*(1), 317–338. https://doi.org/10.1146/annurev.neuro.31.060407.125627

Sommer, M. A., & Wurtz, R. H. (2008b). Visual perception and corollary discharge. *Perception*, *37*(3), 408–418. https://doi.org/10.1068/p5873

Sparks, D. L., & Mays, L. E. (1983). Spatial localization of saccade targets. I. Compensation for stimulation-induced perturbations in eye position. *Journal of Neurophysiology*, *49*(1), 45–63. https://doi.org/10.1152/jn.1983.49.1.45

Sparks, D. L., Mays, L. E., & Porter, J. D. (1987). Eye movements induced by pontine stimulation: interaction with visually triggered saccades. *Journal of Neurophysiology*, *58*(2), 300–318. https://doi.org/10.1152/jn.1987.58.2.300

Sperry, R. W. (1950). Neural basis of the spontaneous optokinetic response produced by visual inversion. *Journal of Comparative and Physiological Psychology*, *43*(6), 482–489. https://doi.org/10.1037/h0055479

Spiegelhalter, D., & Rice, K. (2009). Bayesian statistics. Retrieved from Scholarpedia website: http://doi.org/10.4249/scholarpedia.5230

Spratling, M. W. (2017). A predictive coding model of gaze shifts and the underlying neurophysiology. *Visual Cognition*, *25*(7–8), 770–801. https://doi.org/10.1080/13506285.2017.1336141

Steinbach, M. J. (1987). Proprioceptive knowledge of eye position. *Vision Research*, *27*(10), 1737–1744. https://doi.org/10.1016/0042-6989(87)90103-9

Stokes, M. G. (2015). 'Activity-silent' working memory in prefrontal cortex: a dynamic coding framework. *Trends in Cognitive Sciences*, *19*(7), 394–405. https://doi.org/10.1016/j.tics.2015.05.004

A

Appendix

Straka, H., Simmers, J., & Chagnaud, B. P. (2018). A New Perspective on Predictive Motor Signaling. *Current Biology*, *28*(5), R232–R243. https://doi.org/10.1016/j.cub.2018.01.033

Strasburger, H., Rentschler, I., & Jüttner, M. (2011). Peripheral vision and pattern recognition: A review. *Journal of Vision*, *11*(5), 13–13. https://doi.org/10.1167/11.5.13

Striemer, C. L., Ferber, S., & Danckert, J. (2013). Spatial working memory deficits represent a core challenge for rehabilitating neglect. *Frontiers in Human Neuroscience*, *7*. https://doi.org/10.3389/fnhum.2013.00334

Subramanian, J., & Colby, C. L. (2014). Shape selectivity and remapping in dorsal stream visual area LIP. *Journal of Neurophysiology*, *111*(3), 613–627. https://doi.org/10.1152/jn.00841.2011

Sun, L. D., & Goldberg, M. E. (2016). Corollary discharge and oculomotor proprioception: Cortical mechanisms for spatially accurate vision. *Annual Review of Vision Science*, *2*(1), 61–84. https://doi.org/10.1146/annurev-vision-082114-035407

Szinte, M., & Cavanagh, P. (2011). Spatiotopic apparent motion reveals local variations in space constancy. *Journal of Vision*, *11*(2), 1–20. https://doi.org/10.1167/11.2.4

Szinte, M., Wexler, M., & Cavanagh, P. (2012). Temporal dynamics of remapping captured by peri-saccadic continuous motion. *Journal of Vision*, *12*(7), 1–18. https://doi.org/10.1167/12.7.12

Takeda, Y., & Yagi, A. (2000). Inhibitory tagging in visual search can be found if search stimuli remain visible. *Perception & Psychophysics*, *62*(5), 927–934. https://doi.org/10.3758/BF03212078

Tatler, B. W., Wade, N. J., Kwan, H., Findlay, J. M., & Velichkovsky, B. M. (2010). Yarbus, eye movements, and vision. *I-Perception*, *1*(1), 7–27. https://doi.org/10.1068/i0382

Taulu, S., & Kajola, M. (2005). Presentation of electromagnetic multichannel data: The signal space separation method. *Journal of Applied Physics*, *97*(12), 124905. https://doi.org/10.1063/1.1935742

Taulu, S., Kajola, M., & Simola, J. (2003). Suppression of interference and artifacts by the signal space separation method. *Brain Topography*, *16*(4), 269–275. https://doi.org/10.1023/B:BRAT.0000032864.93890.f9

Taulu, S., Simola, J., & Kajola, M. (2005). Applications of the signal space separation method. *IEEE Transactions on Signal Processing*, *53*(9), 3359–3372. https://doi.org/10.1109/TSP.2005.853302

Ten Brink, A. F., Biesbroek, J. M., Kuijf, H. J., Van der Stigchel, S., Oort, Q., Visser-Meily, J. M. A., & Nijboer, T. C. W. (2016). The right hemisphere is dominant in organization of visual search—A study in stroke patients. *Behavioural Brain Research*, *304*, 71–79. https://doi.org/10.1016/j.bbr.2016.02.004

Ten Brink, A. F., Van der Stigchel, S., Visser-Meily, J. M. A., & Nijboer, T. C. W. (2016). You never know where you are going until you know where you have been: Disorganized search after stroke. *Journal of Neuropsychology*, *10*(2), 256–275. https://doi.org/10.1111/jnp.12068

Ten Brink, A. F., Visser-Meily, J. M. A., & Nijboer, T. C. W. (2018). What Does It Take to Search Organized? The Cognitive Correlates of Search Organization During Cancellation After Stroke. *Journal of the International Neuropsychological Society*, *24*(05), 424–436. https://doi.org/10.1017/S1355617717001254

Thaler, L., Schütz, A. C., Goodale, M. A., & Gegenfurtner, K. R. (2013). What is the best fixation target? The effect of target shape on stability of fixational eye movements. *Vision Research*, *76*, 31–42. https://doi.org/10.1016/j.visres.2012.10.012

Thorpe, S., Fize, D., & Marlot, C. (1996). Speed of processing in the human visual system. *Nature*, *381*(6582), 520–522. https://doi.org/10.1038/381520a0

Tolias, A. S., Moore, T., Smirnakis, S. M., Tehovnik, E. J., Siapas, A. G., & Schiller, P. H. (2001). Eye Movements Modulate Visual Receptive Fields of V4 Neurons. *Neuron*, *29*(3), 757–767. https://doi.org/10.1016/S0896-6273(01)00250-1

Treutwein, B. (1995). Minireview: Adaptive Psychophysical Procedures. *Vision Research*, *35*(12), 25032522.

Tzourio-Mazoyer, N., Landeau, B., Papathanassiou, D., Crivello, F., Etard, O., Delcroix, N., … Joliot, M. (2002). Automated anatomical labeling of activations in SPM using a macroscopic anatomical parcellation of the MNI MRI single-subject brain. *NeuroImage*, *15*(1), 273–289. https://doi.org/10.1006/nimg.2001.0978

Umeno, M. M., & Goldberg, M. E. (1997). Spatial processing in the monkey frontal eye field. I. Predictive visual responses. *Journal of Neurophysiology*, *78*(3), 1373–1383. https://doi.org/10.1152/jn.1997.78.3.1373

Unsworth, N., & Robison, M. K. (2017). Pupillary correlates of covert shifts of attention during working memory maintenance. *Attention, Perception, & Psychophysics*, *79*(3), 782–795. https://doi.org/10.3758/s13414-016-1272-7

Van der Stigchel, S., & Hollingworth, A. (2018). Visuospatial working memory as a fundamental component of the eye movement system. *Current Directions in Psychological Science*, *27*(2), 136–143. https://doi.org/10.1177/0963721417741710

Van der Stigchel, S., Meeter, M., & Theeuwes, J. (2006). Eye movement trajectories and what they tell us. *Neuroscience & Biobehavioral Reviews*, *30*(5), 666–679. https://doi.org/10.1016/j.neubiorev.2005.12.001

Van der Stigchel, S., Merten, H., Meeter, M., & Theeuwes, J. (2007). The effects of a task-irrelevant visual event on spatial working memory. *Psychonomic Bulletin & Review*, *14*(6), 1066–1071. https://doi.org/10.3758/BF03193092

Van der Stoep, N., Visser-Meily, J. M. A., Kappelle, L. J., de Kort, P. L. M., Huisman, K. D., Eijsackers, A. L. H., … Nijboer, T. C. W. (2013). Exploring near and far regions of space: Distance-specific visuospatial neglect after stroke. *Journal of Clinical and Experimental Neuropsychology*, *35*(8), 799–811. https://doi.org/10.1080/13803395.2013.824555

Van Der Werf, J., Buchholz, V. N., Jensen, O., & Medendorp, W. P. (2013). Reorganization of oscillatory activity in human parietal cortex during spatial updating. *Cerebral Cortex*, *23*(3), 508–519. https://doi.org/10.1093/cercor/bhr387

van Doorn, J., Ly, A., Marsman, M., & Wagenmakers, E.-J. (2016). Bayesian inference for Kendall's rank correlation coefficient. *The American Statistician*, 1–6. https://doi.org/10.1080/00031305.2016.1264998

van Moorselaar, D., Theeuwes, J., & Olivers, C. N. L. (2016). Learning changes the attentional status of prospective memories. *Psychonomic Bulletin & Review*, *23*(5), 1483–1490. https://doi.org/10.3758/s13423-016-1008-7

van Opstal, A. J., & van Gisbergen, J. A. M. (1989). Scatter in the metrics of saccades and properties of the collicular motor map. *Vision Research*, *29*(9), 1183–1196. https://doi.org/10.1016/0042-6989(89)90064-3

A

Appendix

Vetter, P., Edwards, G., & Muckli, L. (2012). Transfer of predictive signals across saccades. *Frontiers in Psychology*, *3*. https://doi.org/10.3389/fpsyg.2012.00176

Volkmann, F. (1962). Vision during voluntary saccadic eye movements. *Journal of the Optical Society of America*, *52*, 8.

Von Holst, E., & Mittelstaedt, H. (1950). Das reafferenz princip: (Wechselwirkungen zwischen Zentralnervensystem und Peripherie.). *Die Naturwissenschaften*, *37*, 464–476.

Vuilleumier, P., Sergent, C., Schwartz, S., Valenza, N., Girardi, M., Husain, M., & Driver, J. (2007). Impaired perceptual memory of locations across gaze-shifts in patients with unilateral spatial neglect. *Journal of Cognitive Neuroscience*, *19*(8), 1388–1406. https://doi.org/10.1162/jocn.2007.19.8.1388

Walker, M. F., Fitzgibbon, E. J., & Goldberg, M. E. (1995). Neurons in the monkey superior colliculus predict the visual result of impending saccadic eye movements. *Journal of Neurophysiology*, *73*(5), 1988–2003. https://doi.org/10.1152/jn.1995.73.5.1988

Wandell, B. A. (1995). A brief organized list. Retrieved from https://web.stanford.edu/group/vista/cgi-bin/wandell/a-brief-organized-list/

Wandell, B. A., Dumoulin, S. O., & Brewer, A. A. (2007). Visual field maps in human cortex. *Neuron*, *56*(2), 366–383. https://doi.org/10.1016/j.neuron.2007.10.012

Wang, X., Fung, C. C. A., Guan, S., Wu, S., Goldberg, M. E., & Zhang, M. (2016). Perisaccadic receptive field expansion in the lateral intraparietal area. *Neuron*, *90*(2), 400–409. https://doi.org/10.1016/j.neuron.2016.02.035

Wang, Z., & Klein, R. M. (2010). Searching for inhibition of return in visual search: A review. *Vision Research*, *50*(2), 220–228. https://doi.org/10.1016/j.visres.2009.11.013

Wansard, M., Bartolomeo, P., Bastin, C., Segovia, F., Gillet, S., Duret, C., & Meulemans, T. (2015). Support for distinct subcomponents of spatial working memory: A double dissociation between spatial–simultaneous and spatial–sequential performance in unilateral neglect. *Cognitive Neuropsychology*, *32*(1), 14–28. https://doi.org/10.1080/02643294.2014.995075

Wansard, M., Meulemans, T., Gillet, S., Segovia, F., Bastin, C., Toba, M. N., & Bartolomeo, P. (2014). Visual neglect: Is there a relationship between impaired spatial working memory and re-cancellation? *Experimental Brain Research*, *232*(10), 3333–3343. https://doi.org/10.1007/s00221-014-4028-4

Watson, A. B., & Pelli, D. G. (1983). Quest: A Bayesian adaptive psychometric method. *Perception & Psychophysics*, *33*(2), 113–120. https://doi.org/10.3758/BF03202828

Webb, B. (2004). Neural mechanisms for prediction: do insects have forward models? *Trends in Neurosciences*, *27*(5), 278–282. https://doi.org/10.1016/j.tins.2004.03.004

Wenderoth, P., & Wiese, M. (2008). Retinotopic encoding of the direction aftereffect. *Vision Research*, *48*(19), 1949–1954. https://doi.org/10.1016/j.visres.2008.06.013

Wexler, M., & Collins, T. (2014). Orthogonal steps relieve saccadic suppression. *Journal of Vision*, *14*(2), 1–9. https://doi.org/10.1167/14.2.13

Wexler, M., Glennerster, A., Cavanagh, P., Ito, H., & Seno, T. (2013). Default perception of high-speed motion. *Proceedings of the National Academy of Sciences*, *110*(17), 7080–7085. https://doi.org/10.1073/pnas.1213997110

Wichmann, F. A., & Hill, N. J. (2001). The psychometric function: I. Fitting, sampling, and goodness of fit. *Perception & Psychophysics*, *63*(8), 1293–1313. https://doi.org/10.3758/BF03194544

Wilming, N., Harst, S., Schmidt, N., & König, P. (2013). Saccadic momentum and facilitation of return saccades contribute to an optimal foraging strategy. *PLoS Computational Biology*, *9*(1), e1002871. https://doi.org/10.1371/journal.pcbi.1002871

Wittenberg, M., Bremmer, F., & Wachtler, T. (2008). Perceptual evidence for saccadic updating of color stimuli. *Journal of Vision*, *8*(14), 1–9. https://doi.org/10.1167/8.14.9

Wojciulik, E., Husain, M., Clarke, K., & Driver, J. (2001). Spatial working memory deficit in unilateral neglect. *Neuropsychologia*, *39*(4), 390–396. https://doi.org/10.1016/S0028-3932(00)00131-7

Wojciulik, E., Rorden, C., Clarke, K., Husain, M., & Driver, J. (2004). Group study of an "undercover" test for visuospatial neglect: invisible cancellation can reveal more neglect than standard cancellation. *Journal of Neurology, Neurosurgery & Psychiatry*, *75*(9), 1356–1358. https://doi.org/10.1136/jnnp.2003.021931

Wolf, C., & Schütz, A. C. (2015). Trans-saccadic integration of peripheral and foveal feature information is close to optimal. *Journal of Vision*, *15*(16), 1–18. https://doi.org/10.1167/15.16.1

Wolfe, B. A., & Whitney, D. (2015). Saccadic remapping of object-selective information. *Attention, Perception, & Psychophysics*, *77*(7), 2260–2269. https://doi.org/10.3758/s13414-015-0944-z

Wurtz, R. H. (2008). Neuronal mechanisms of visual stability. *Vision Research*, *48*(20), 2070–2089. https://doi.org/10.1016/j.visres.2008.03.021

Wurtz, R. H., Joiner, W. M., & Berman, R. A. (2011). Neuronal mechanisms for visual stability: progress and problems. *Philosophical Transactions of the Royal Society B: Biological Sciences*, *366*(1564), 492–503. https://doi.org/10.1098/rstb.2010.0186

Xu, Y., Wang, X., Peck, C., & Goldberg, M. E. (2011). The time course of the tonic oculomotor proprioceptive signal in area 3a of somatosensory cortex. *Journal of Neurophysiology*, *106*(1), 71–77. https://doi.org/10.1152/jn.00668.2010

Yao, T., Treue, S., & Krishna, B. S. (2016). An attention-sensitive memory trace in macaque MT following saccadic eye movements. *PLoS Biology*, *14*(2), e1002390. https://doi.org/10.1371/journal.pbio.1002390

Yarbus, A. L. (1967). *Eye movements and vision*. Retrieved from //www.springer.com/us/book/9781489953810

Zerr, P., Gayet, S., Mulder, K., Pinto, Y., Sligte, I., & Van der Stigchel, S. (2017). Remapping high-capacity, pre-attentive, fragile sensory memory. *Scientific Reports*, *7*(1). https://doi.org/10.1038/s41598-017-16156-0

Zhang, G.-L., Li, A.-S., Miao, C.-G., He, X., Zhang, M., & Zhang, Y. (2018). A consumer-grade LCD monitor for precise visual stimulation. *Behavior Research Methods*, *50*(4), 1496–1502. https://doi.org/10.3758/s13428-018-1018-7

A

Appendix

Zimmermann, E., Born, S., Fink, G. R., & Cavanagh, P. (2014). Masking produces compression of space and time in the absence of eye movements. *Journal of Neurophysiology*, *112*(12), 3066–3076. https://doi.org/10.1152/jn.00156.2014

Zimmermann, E., Morrone, M. C., & Burr, D. (2015). Visual mislocalization during saccade sequences. *Experimental Brain Research*, *233*(2), 577–585. https://doi.org/10.1007/s00221-014-4138-z

Zimmermann, E., Morrone, M. C., & Burr, D. (2016). Adaptation to size affects saccades with long but not short latencies. *Journal of Vision*, *16*(7), 1–8. https://doi.org/10.1167/16.7.2

Zimmermann, E., Morrone, M. C., & Burr, D. C. (2013). Spatial position information accumulates steadily over time. *Journal of Neuroscience*, *33*(47), 18396–18401. https://doi.org/10.1523/JNEUROSCI.1864-13.2013

Zimmermann, E., Morrone, M. C., & Burr, D. C. (2014). Buildup of spatial information over time and across eye-movements. *Behavioural Brain Research*, *275*, 281–287. https://doi.org/10.1016/j.bbr.2014.09.013

Zimmermann, E., Morrone, M. C., Fink, G. R., & Burr, D. C. (2013). Spatiotopic neural representations develop slowly across saccades. *Current Biology*, *23*(5), R193–R194. https://doi.org/10.1016/j.cub.2013.01.065

Zimmermann, E., Weidner, R., Abdollahi, R. O., & Fink, G. R. (2016). Spatiotopic adaptation in visual areas. *Journal of Neuroscience*, *36*(37), 9526–9534. https://doi.org/10.1523/JNEUROSCI.0052-16.2016

Zimmermann, E., Weidner, R., & Fink, G. R. (2017). Spatiotopic updating of visual feature information. *Journal of Vision*, *17*(12), 1–9. https://doi.org/10.1167/17.12.6

Zirnsak, M., & Moore, T. (2014). Saccades and shifting receptive fields: anticipating consequences or selecting targets? *Trends in Cognitive Sciences*, *18*(12), 621–628. https://doi.org/10.1016/j.tics.2014.10.002

Zirnsak, M., Steinmetz, N. A., Noudoost, B., Xu, K. Z., & Moore, T. (2014). Visual space is compressed in prefrontal cortex before eye movements. *Nature*, *507*(7493), 504–507. https://doi.org/10.1038/nature13149

A

Appendix

Dutch summary

Nederlandse samenvatting

Perceptuele continuïteit over saccades heen

Wanneer mensen de wereld om zich heen bekijken, wordt licht omgezet in een neurale reactie door de fotoreceptoren in het netvlies. De neurale reactie wordt doorgegeven in het visuele systeem van het brein waardoor een bewuste waarneming ontstaat. Maar het zicht is niet overal even scherp; het is het scherpst in het midden van het visuele veld. Om een zo gedetailleerd mogelijk beeld van de omgeving te krijgen, maken mensen drie à vier saccades (= snelle oogbewegingen) per seconde. Elke saccade zorgt ervoor dat de hele wereld over het netvlies schiet. Daardoor ontstaat er ambiguïteit over de bron van de beweging: bewoog er iets in de buitenwereld, of bewogen de ogen waardoor alles op het netvlies zich verplaatste? De subjectieve ervaring van deze verschillende oorzaken (externe beweging of oogbeweging) is verschillend. Ondanks de hoge frequentie van oogbewegingen is de subjectieve ervaring ononderbroken en stabiel. Hoe is het mogelijk dat de perceptie continu is, terwijl de instroom van visuele informatie elke 300 ms wordt onderbroken door saccades?

Het onderzoek naar perceptuele continuïteit over saccades heen kent een lange geschiedenis. De meest prominente hypothese is dat er een signaal van het oogbewegingssysteem (een extra-retinaal signaal) naar het visuele systeem wordt gestuurd waarmee de verandering in visuele input (een retinaal signaal) door een volgende oogbeweging kan worden geanticipeerd in het visuele systeem. Met het anticiperen zou het mogelijk kunnen worden om perceptuele representaties spatiotopisch bij te werken. De definitie van spatiotopisch updaten (*spatiotopic updating*) staat in Box 1 aan het einde van Hoofdstuk 1. Voor en na een oogbeweging stimuleert een stimulus twee verschillende plaatsen op het netvlies. "Updaten" refereert aan de verandering in de perceptie van een stimulus als die meerdere keren wordt getoond. "Spatiotopisch" betekent in coördinaten in de externe wereld. "Spatiotopisch updaten" is dus het veranderen of verscherpen van de perceptie van een stimulus, die, ondanks twee verschillende locaties op het netvlies te stimuleren, wel wordt gezien als een en dezelfde stimulus.

Ondanks de lange geschiedenis van onderzoek zijn meerdere aspecten van perceptuele continuïteit nog onduidelijk. Komt de subjectieve ervaring overeen met meetbaar gedrag? Wat wordt er precies geanticipeerd? En hoe werkt dat op neuraal niveau? In Hoofdstuk 2, 3 en 4 van mijn proefschrift ben ik ingegaan op deze fundamentele aspecten van perceptuele continuïteit over saccades heen, gebruikmakend van psychofysica en magneto-encefalografie. In Hoofdstuk 5 heb ik onderzocht of perceptuele continuïteit veranderd is

bij proefpersonen waarbij de posterieure pariëtaal kwab– een corticaal gebied waarin neuronen eigenschappen bezitten die een belangrijke rol kunnen spelen voor het bewerkstelligen van perceptuele continuïteit - beschadigd is. Voor Hoofdstuk 6 ontwikkelde ik een taak waarmee problemen in het ruimtelijke werkgeheugen in kaart kunnen worden gebracht, wat – naar ik vermoed – gerelateerd is aan verminderde perceptuele continuïteit. Hoofdstuk 7 en 8 zijn meer exploratief. In Hoofdstuk 7 heb ik onderzocht in hoeverre proefpersonen gebruik maken van (de informatie van de plek) waar ze al hebben gekeken om te bepalen waar ze vervolgens gaan kijken. In hoofdstuk 8 heb ik onderzocht wat er gebeurt met de ruimtelijke aandacht wanneer mensen een locatie voor een korte periode onthouden.

Spatiotopisch updaten

De data uit Hoofdstuk 2 en 3 laten zien dat een stimulus gepresenteerd voorafgaand aan een saccade, de perceptie van een stimulus na de saccade beïnvloedt wanneer beide stimuli in dezelfde spatiotopische coördinaten worden getoond. In de experimenten maakten we gebruik van een bewegingsillusie. In deze illusie krijgen proefpersonen een langzaam draaiende ring te zien. De ring heeft een gerandomiseerd zwart-wit patroon. Als de ring even gedraaid heeft, wordt het patroon van de ring snel achter elkaar veranderd met vier verschillende gerandomiseerde patronen. Deze nieuwe patronen draaien niet, maar creëren toch het percept van een snelle, rotationele sprong in de tegenovergestelde richting van de aanvankelijke draairichting. De draaiende ring met het eerste patroon wordt de inductor genoemd. In Hoofdstuk 2 en 3 lieten we proefpersonen de inductor in de periferie zien, gevolgd door de instructie om een oogbeweging naar de ring te maken. Nadat de oogbeweging gemaakt was, veranderden we het patroon en vroegen we proefpersonen te rapporteren naar welke kant ze de ring zagen springen (met de klok mee of tegen de klok in). Als de eerste langzame rotatie spatiotopisch bijgewerkt wordt, zullen proefpersonen een sprong tegen de eerste draairichting in rapporteren na de oogbeweging. Als dat niet het geval is, zullen proefpersonen in de helft van de gevallen een sprong de ene kant op rapporteren en in de andere helft een sprong de andere kant op. De data van zowel Hoofdstuk 2 als 3 komen meer overeen met het eerstgenoemde geval, en laten daarmee zien dat de rotatie richting spatiotopisch wordt bijgewerkt.

In Hoofdstuk 2 voerden we verschillende controle experimenten uit. Die laten onder andere zien dat het spatiotopisch updaten van de rotatie richting zwakker is wanneer de stimulus kunstmatig wordt verplaatst terwijl de proefpersonen hun ogen houden. Die

A

bevinding suggereert dat het zelf maken van een oogbeweging belangrijk is voor het volledig tot uiting komen van het spatiotopisch updaten van visuele informatie. De vereiste van het zelf uitvoeren klopt met de hypothese dat perceptuele continuïteit samenhangt met een signaal uit het oogbewegingssysteem dat ervoor zorgt dat het visuele systeem de veranderde input als gevolg van een saccade kan anticiperen.

In hoofdstuk 3 hebben we de temporele aspecten van spatiotopisch updaten onderzocht omdat gesuggereerd werd dat spatiotopisch updaten een langzaam proces is, dat meer dan 500 ms nodig heeft om een meetbaar effect te hebben. Dat zou bijzonder langzaam zijn, aangezien saccades ongeveer elke 300 ms worden uitgevoerd. Daarmee lijkt het onwaarschijnlijk dat spatiotopisch updaten een rol speelt in het tot stand komen van perceptuele continuïteit. Het viel ons op dat deze conclusie was gebaseerd op data waaruit spatiotopisch updaten steeds duidelijker meetbaar wordt met langere intervallen tussen saccades, maar dat het ook al meetbaar is bij korte intervallen. In Hoofdstuk 3 hebben we een aangepaste versie gebruikt van het experiment met de bewegingsillusie uit Hoofdstuk 2 om direct te kunnen meten hoe spatiotopisch updaten verloopt. De illusie wordt inderdaad sterker wanneer de inductor lang draait voordat de saccade wordt uitgevoerd, maar het effect is al meetbaar in de responsen van de proefpersonen als de inductor slechts kort voordat de saccade wordt uitgevoerd verschijnt. In deze experimenten lieten we de inductor (de draaiende ring) ook nog kort zien na de saccade. Het effect van de inductor vóór de oogbeweging was minder sterk dan het effect van de inductor na de saccade. Samengevat wijzen de data uit Hoofdstuk 2 en 3 uit dat er een directe relatie is tussen de stimulus voor en na de saccade, waarbij beweging van de stimulus spatiotopisch wordt bijgewerkt. Het effect van de stimulus van voor de oogbeweging is meetbaar wanneer deze slechts kort van tevoren wordt getoond, maar wordt substantieel sterker wanneer hij langer zichtbaar is.

Neurale processen en perceptuele continuïteit

In Hoofdstuk 4 hebben we met magneto-encefalografie (MEG) gemeten wat er op neuraal niveau gebeurt wanneer visuele informatie spatiotopisch wordt bijgewerkt. In dit experiment kregen proefpersonen een gestreepte cirkel te zien met ofwel enkele dikke strepen ofwel een groot aantal dunne strepen. Deze twee streeppatronen worden verschillend verwerkt door het visuele systeem. Daardoor konden we uit de MEG-data aflezen of de proefpersoon in een specifieke trial de dikke of de dunne strepen te zien kreeg. Dat deden we door het algoritme te trainen op 90% van de MEG-data. Daarmee leert het

algoritme om onderscheid te maken in neurale respons op het dunne streeppatroon en het dikke streeppatroon. Vervolgens testen we hoe goed dit onderscheid is door de overige 10% van de data te classificeren. Vanaf ongeveer 40 ms nadat de stimulus verscheen kon dit onderscheid gemaakt worden.

In dit experiment maakten proefpersonen een saccade waardoor het streeppatroon eerst in de linkerhelft en toen in de rechterhelft van het visuele veld verscheen. Met behulp van het algoritme konden we het streeppatroon van de stimulus bepalen uit de MEG-data vanaf ~40 ms na het verschijnen van de stimulus tot meer dan 200 ms na het uitvoeren van de saccade aflezen. Bovendien was er ~40 ms na het uitvoeren van de saccade een tweede neurale response waaruit we konden aflezen wat het streeppatroon was. Met de lange nasleep van de eerste respons en de snelle tweede respons na de oogbeweging is het theoretisch mogelijk om voor, tijdens en na de oogbeweging het streeppatroon van de stimulus uit de neurale data uit te lezen. Het spatiotopisch updaten van perceptuele representaties zou daarmee vanaf ~40 ms na de oogbeweging kunnen beginnen.

Perceptuele continuïteit na hersenbeschadiging

Meerdere neurofysiologische experimenten hebben laten zien dat de respons op visuele stimuli van neuronen in de posterieure pariëtale cortex (PPC) gemoduleerd wordt door opvolgende saccades. Er wordt aangenomen dat deze modulatie een reflectie is van het integreren van retinale en extra-retinale signalen. Daarmee is het waarschijnlijk dat deze neuronen een cruciale rol spelen in het tot stand komen van perceptuele continuïteit. In Hoofdstuk 5 testen we deze hypothese. Negen patiënten met schade aan de PPC na een beroerte voeren de intra-saccadische verplaatsingstaak uit, waarin retinale en extra-retinale signalen gecombineerd moeten worden. In deze taak moeten proefpersonen een saccade maken naar een stip. Tijdens de oogbeweging wordt de stip verplaatst, waardoor de stip na de saccade niet alleen in andere retinotopische, maar ook in andere spatiotopische coördinaten staat. De proefpersoon moet aangeven naar welke kant de stip is verplaatst. Rekening houdend met de retinotopische coördinaten van de stip, moet de proefpersoon dus de verplaatsing door de saccade onderscheiden van de verplaatsing van de stip zelf. Uit eerdere onderzoeken is gebleken dat deze taak door gezonde proefpersonen accurater wordt uitgevoerd wanneer de stip kort verdwijnt tijdens de saccade en dan weer verschijnt. De interpretatie van deze verbetering is dat proefpersonen gemiddeld meer gebruik maken van de extra-retinale signalen als de stip even verdwenen is. In onze studie gebruikten we deze verbetering als maat voor het gebruik van extra-retinale signalen. De hypothese was

A

dat de invloed van extra-retinale signalen op de perceptie bij patiënten met PPC schade afwezig of verminderd is. Dat was echter niet duidelijk het geval. Bij zeven van de negen patiënten was de invloed vergelijkbaar met die bij dertien controle proefpersonen zonder PPC schade. Een mogelijke verklaring hiervoor is dat er voor perceptuele continuïteit *degeneracy* is in neurale circuits, dat wil zeggen dat er meerdere neurale systemen zijn die tot perceptuele continuïteit kunnen leiden. Deze hypothese moet echter nog verder onderzocht worden.

In Hoofdstuk 6 wordt het begin gemaakt van een andere aanpak om veranderingen in perceptuele continuïteit te onderzoeken. Waar we in Hoofdstuk 5 patiënten includeerden op basis van laesielocatie (de PPC), werden voor Hoofdstuk 6 juist zoveel mogelijk patiënten geïncludeerd ongeacht laesielocatie of cognitieve problematiek. Patiënten uit revalidatiekliniek de Hoogstraat hebben een taak gedaan waarin niet expliciet gekeken werd naar perceptuele continuïteit, maar naar het vermogen om ruimtelijke informatie voor korte tijd op te slaan, dat wil zeggen gebruik te maken van het spatieel werkgeheugen. Patiënten kregen 500 ms een stip te zien, die vervolgens verdween voor 2 seconden en daarna weer terugkeerde, maar net iets verplaatst was ten opzichte van de eerste locatie. De taak voor de patiënt was om aan te geven naar welke kant de stip was verplaatst. Naast de prestatie op deze taak hadden we beschikking over een aantal andere gegevens van deze patiënten waar we uit afleidden dat het vermogen van het spatieel werkgeheugen correleert met de prestatie op een zoektaak. Eerder onderzoek suggereert dat een lage prestatie op een vergelijkbare zoektaak kan samenhangen met problemen in perceptuele continuïteit. Een mogelijke verklaring hiervoor kan dus zijn dat problemen met het vasthouden van ruimtelijke informatie leiden tot verminderde perceptuele continuïteit. De taak uit Hoofdstuk 6 kan gemakkelijk gebruikt worden in vervolgonderzoek om deze relatie verder uit te diepen.

Vasthouden van visueel-ruimtelijke informatie

In de laatste hoofdstukken van mijn proefschrift heb ik niet direct perceptuele continuïteit onderzocht, maar wel het vasthouden van visueel-ruimtelijke informatie. In Hoofdstuk 7 heb ik terugkeer inhibitie (*inhibition of return; IOR*) onderzocht. IOR beschrijft een vertraging in reactietijden wanneer proefpersonen snel moeten reageren op een stimulus, maar wanneer ~300 ms voor het verschijnen van de stimulus een cue de aandacht al naar de locatie van de stimulus had getrokken. Wanneer de tijd tussen cue en stimulus kort is kan dit juist voor versnelling van reactietijden zorgen, maar vanaf een verschil van

~300 ms wordt juist een vertraging gezien. Eerdere onderzoeken hebben deze vertraging geïnterpreteerd als een neiging om niet herhaaldelijk dezelfde plek te inspecteren (dus om niet meer "terug te keren", vandaar de naam terugkeer inhibitie). In hoofdstuk 7 hebben we gemeten hoe vaak proefpersonen terugkijken naar een plek waar ze al eens gekeken hadden, terwijl ze een soort zoektaak uitvoerden. De mate van terugkijken hing in dit experiment samen met de taak die de proefpersonen uitvoerden (ze keken minder vaak terug tijdens een zoektaak), de tijd (ze keken minder vaak terug naar plekken die ze net bekeken hadden, maar wat vaker als dat al langer geleden was) en de hoeveelheid referenties (ze keken minder vaak terug als er meer referenties geven werden). Het laatste effect is in de context van dit proefschrift met name interessant, want het kan suggereren dat het accurate opslaan en spatiotopisch updaten van bekeken locaties alleen goed mogelijk is wanneer er voldoende visuele informatie continu aanwezig is in het visuele veld.

In Hoofdstuk 8 hebben we een experiment gedaan om te kijken waar proefpersonen hun aandacht houden wanneer ze een locatie moeten onthouden zonder hun ogen te bewegen. In deze taak moeten proefpersonen naar het midden van een computerscherm kijken. Dan verschijnt er in de periferie van het visuele veld kort een stimulus, terwijl de proefpersoon naar het midden van het scherm blijft kijken. Na 8 seconden verschijnt de stimulus weer, maar is deze iets verplaatst ten opzichte van de eerste locatie. De proefpersoon moet aangeven welke kant de stip op is verplaatst. In dit experiment hebben we gekeken naar de aandacht tijdens de 8 seconden dat de locatie onthouden moet worden. We hebben aandacht gemeten met de lichtreflex van de pupil. Dat konden we doen door de helft van het scherm zwart en de andere helft wit te maken. Eerder onderzoek heeft laten zien dat wanneer de aandacht naar de lichte kant verschuift, dus zonder dat de lichtintensiteit verandert, de pupil kleiner wordt dan wanneer de aandacht naar de donkere kant verschuift. Voor het grootste deel van de 8 seconden waarin de locatie onthouden moest worden zagen we lange tijd ook deze pupil lichtreflex. Daaruit concluderen we dat het vasthouden van ruimtelijke informatie en het richten van aandacht nauw aan elkaar verbonden zijn.

Conclusie

Hoe perceptuele continuïteit over saccades heen ontstaat in het visuele systeem is een oude vraag in de visuele neurowetenschappen. Zoals de experimenten in dit proefschrift ondersteunen, komt dit hoogstwaarschijnlijk voort uit de interactie van retinale en extra-retinale signalen, resulterend in een update van percepties. De gepresenteerde onderzoeken

A

tonen aan dat menselijk gedrag spatiotopische updaten weerspiegelt en dat dit robuust is tegen selectieve corticale laesies. Naast de bestaande suggesties voor neurale mechanismen die ten grondslag liggen aan spatiotopische updaten, stel ik een alternatieve verklaring voor met betrekking tot het updaten van visuele perceptie in spatiotopische coördinaten. Gezamenlijk bieden deze resultaten duidelijke aanwijzingen voor verder onderzoek naar perceptuele continuïteit over saccades. De resultaten van deze toekomstige studies zullen van belang zijn voor een breed wetenschappelijk publiek, omdat perceptuele continuïteit over saccades heen een voorbeeld is van een "probleem" waar elke bewegend organisme mee te maken heeft: het succesvol onderscheiden van verandering in sensorische prikkels die veroorzaakt worden door de eigen beweging en prikkels die veroorzaakt worden door veranderingen in de buitenwereld.

A

Appendix

Acknowledgements

Stefan, I am very grateful that you offered me a place in your lab immediately after you had received your VIDI grant to study visual perception across eye movements. Your style of supervising and lab management has created a productive working environment for me. Your mental speed is unparalleled. I have experienced this with essentially any request for feedback, as it was answered virtually instantaneously – whether the nature was input for new experiments, problems with teaching, corrections on manuscripts or the need for newly discovered music. I have always felt supported by you in all the endeavours that were included in my PhD studies. I have enjoyed them all and I am glad we already have new projects ahead of us in which we will continue our collaboration.

Tanja, thank you for being a very enthusiastic and energetic co-promotor. Although our main research interests may have diverged a little during the last years, I highly appreciate your drive in improving the clinical applications of cognitive neuroscience. I am thankful for the opportunities you gave me to study trans-saccadic perception in a population of stroke patients.

Alessio, I feel lucky that we both decided to have lunch with John Reynolds when he was in Utrecht for a Helmholtz lecture, and that the topic of conversation was shifted to a – then – new study on remapping of receptive fields. Thank you for joining my team of co-promotoren since then. I have enjoyed working with you very much, and am delighted to continue to collaborate in the upcoming 3 years as your post-doc.

Martijn, I am very happy you were the second member to join the lab. Coping with the frustrations from everyday activities like dealing with publication-nuisances, delving into new statistics, balancing work-life and supervising students became so much easier thanks to your absurd sense of humour. I am glad you introduced me to various brilliant sources of entertainment (Rick & Morty, DHMIS, Alan tutorial etc.). And beside the entertainment, you have also greatly improved my programming skills. Thank you for making my Ph.D. worthwhile on multiple levels.

Yun, thank you for all the interesting chats about experiments, science, Mongolian throat singing and life in general on our many bike rides home and the nice train ride to Venice. Thank you for the beautiful handmade wallet and notebook. Your craftsmanship is reflected in your scientific experiments as well. Also, it was a very interesting experience to eat fish eyeballs, thanks for that too.

A

iedereen open staat voor nieuwe ideeën en nieuwe avonturen. En dat iedereen geduldig luistert naar de hakkelende uitlegjes die ik heb gegeven over mijn onderzoek op menig verjaardagsfeest. In het bijzonder wil ook mijn anderhalve maand jongere nichtjes bedanken. **Bernardien** en **Marieke**, dank dat we al sinds baby leeftijd wel en wee kunnen delen over school, studie en nu werk. **Tilly & Bob, Bonne-Jan, Maarten, Annemarie & Florian**, dank dat ik ook jullie onder familie mag scharen – wellicht een jaartje voorbarig, maar ik heb er vertrouwen in. Ik vind het fijn om te zien dat jullie Suzanne en mij steunen in onze gezamenlijk avonturen, ook als dat betekent dat we een tijdje verder weg van elkaar wonen, erg veel dank daarvoor.

Papa & mama, Timon & Mariska, Lidwien & Erik, jullie wil ik graag bedanken voor jullie enthousiasme voor uitgebreide discussies over geneeskundige, juridische, psychologische en culturele onderwerpen. Het kan niet anders dan dat die discussies van invloed zijn geweest op dit proefschrift. Maar net zo goed ook bedankt voor alle ontspanning en afleiding die onze gezamenlijk weekenden weg naar bijvoorbeeld een Waddeneiland hebben geboden. Ik voel me onvoorwaardelijk gesteund door jullie in alle keuzes die ik heb gemaakt. Zelfs toen ik in mijn slaapkamer op de Amers een drumstel had.

En als laatste, lieve **Suzanne**, er zijn erg veel eigenschappen van jou waar ik gek op ben. Maar een verdient in de context van dit proefschrift speciaal de aandacht: jouw engelengeduld. Zelfs nu wacht je op me terwijl ik bezig ben met het schrijven van de laatste woorden. Je hebt me daarmee erg veel rust kunnen geven, waarmee ik zelfs de stressvollere periodes kon doorkomen. Dankjewel dat je tegenwicht kon bieden als ik me verloor in de onderzoeksvragen en analyses door duidelijk te maken dat er meerdere belangrijke zaken bestaan in het leven, niet alleen onderzoek. En toen zei je ook nog 'ja' op de meest bijzondere onderzoeksvraag die ik de afgelopen jaren heb gesteld. Niet een vraag over visuele perceptie of oogbewegingen, maar of je met mij wil trouwen. Ik hoop dat je gedoogt dat ik eerst met de universiteit zal trouwen, en daarna met jou. Ik beloof dat die volgorde niet symbool staat voor mijn prioriteiten, want ik wil vooral samen met jou nieuwe ontdekkingen doen.

A
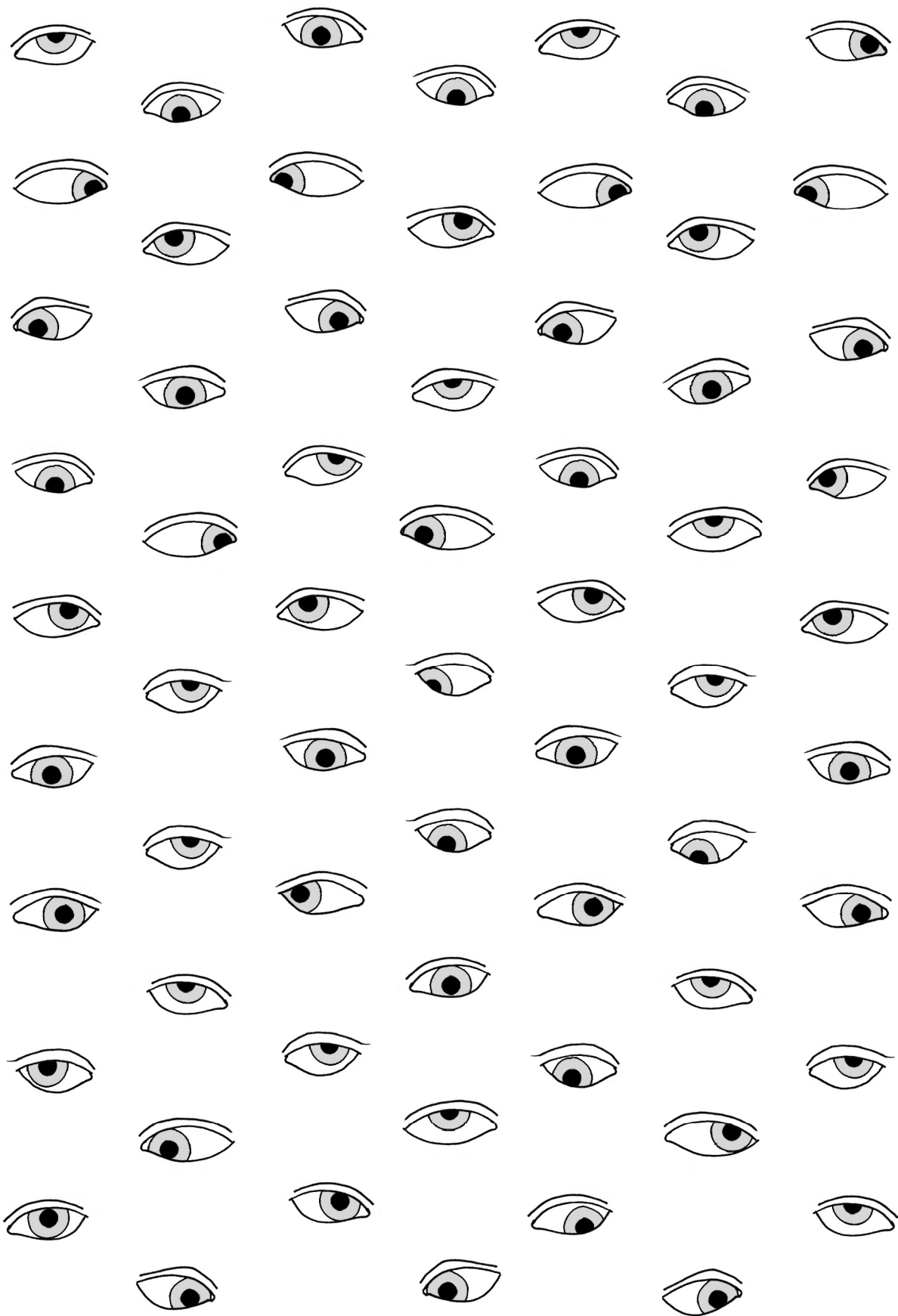
Appendix

Curriculum vitae

Curriculum vitae

Jasper Fabius was born on March 28th, 1989 in Amsterdam. Before turning 1 year old, he moved to Leiden where he learned to talk. And before his 6th birthday he moved to Beetsterzwaag. He graduated from gymnasium CSG Liudger in 2007 after which he moved to Utrecht to obtain his bachelor's in psychology. He completed the bachelor track Cognitive Neuroscience with a minor in Neuroscience (Life Sciences) in 2010. In doubt of pursuing a clinical or research career, Jasper then completed both the research master Neuroscience & Cognition (2013) and the Clinical Neuropsychology master's programme (2014). After research internships at the UMC Utrecht and Donders Institute in Nijmegen and an internship in clinical neuropsychology at the Zuwe Hofpoort Ziekenhuis in Woerden, he decided to go for research. In 2015, he started his Ph.D. research with Stefan Van der Stigchel (promotor) and Tanja Nijboer (co-promotor). Alessio Fracasso became a second co-promotor after Jasper learned that Alessio completed his Ph.D. on a similar topic, and Alessio was willing to collaborate on the new projects. During his Ph.D. Jasper spent 3 months in Rovereto (IT) in the lab of David Melcher to perform an experiment with magnetoencephalography. After his Ph.D. candidacy, Jasper worked as a post-doctoral researcher in Stefan Van der Stigchel's lab. Starting May 1st, he will work as a research associate with Alessio Fracasso at the University of Glasgow (UK).

Beside working on visual perception and eye movements, Jasper also spends a fair amount of time drumming. He was the former drummer in the Medics, but decided he was unable to combine the rock 'n roll life style with his scientific career. In a dramatic series of events his membership of the Medics came to an end. Still, the rhythmic gap in his life had to be filled. With his new band Red Panel the combination of science and music culminated in a performance in Reykjavik (IS) combining basic science and live music. While writing the last chapters of his Ph.D. thesis, Red Panel simultaneously recorded their first EP, to be released in 2019.

A
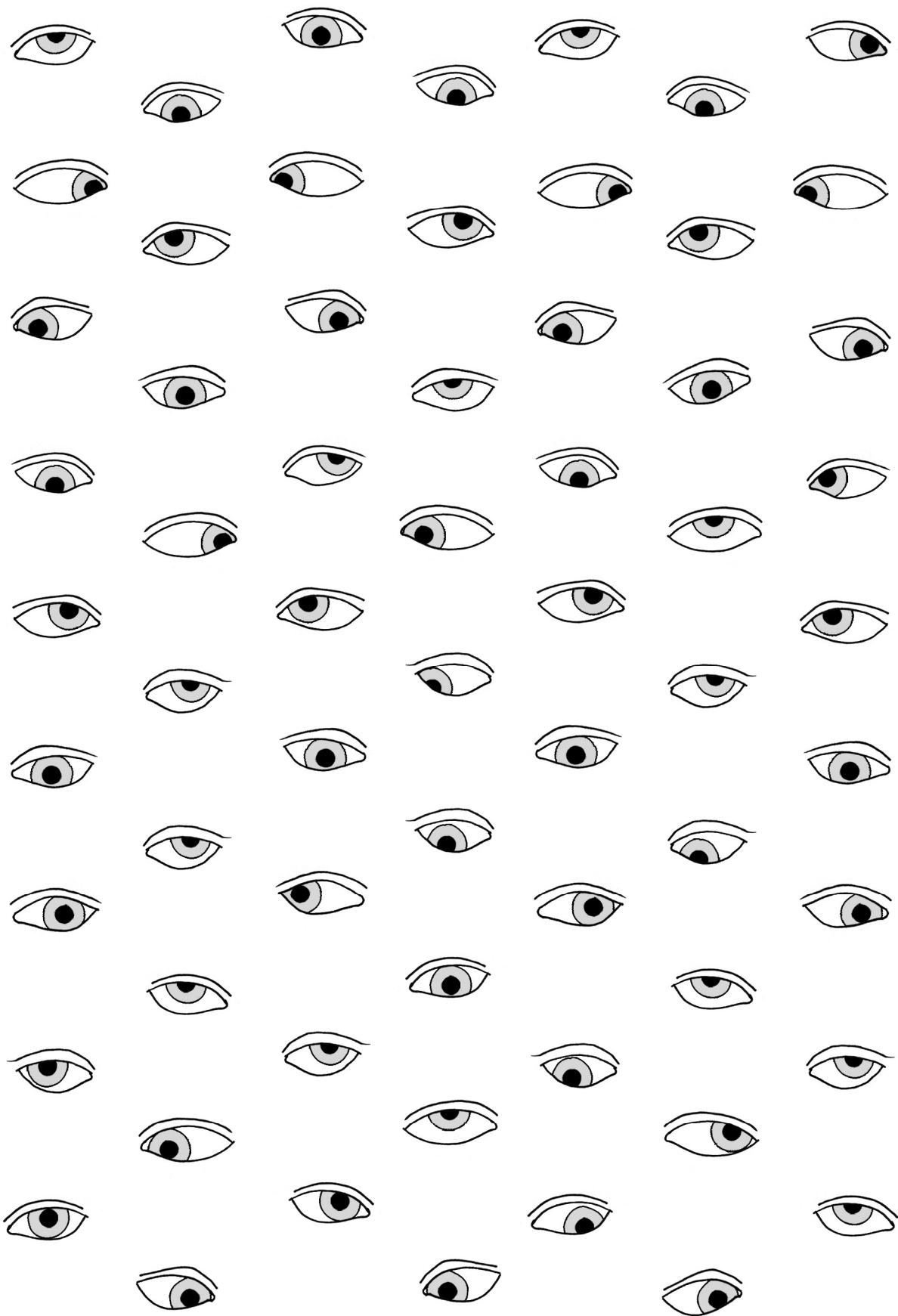
Appendix

Publications

Published peer-reviewed articles

First author

Fabius, J. H., Fracasso, A., Nijboer, T. C. W., & Van der Stigchel, S. (2019). Time course of spatiotopic updating across saccades. *Proceedings of the National Academy of Sciences*, 6.

Fabius, J. H., Mathôt, S., Schut, M. J., Nijboer, T. C. W., & Van der Stigchel, S. (2017). Focus of spatial attention during spatial working memory maintenance: Evidence from pupillary light response. *Visual Cognition*, 25(1–3), 10–20. https://doi.org/10.1080/13506285.2017.1311975

Fabius, J. H., Fracasso, A., & Van der Stigchel, S. (2016). Spatiotopic updating facilitates perception immediately after saccades. *Scientific Reports*, 6(1). https://doi.org/10.1038/srep34488

Fabius, J. H., Schut, M. J., & Van der Stigchel, S. (2016). Spatial inhibition of return as a function of fixation history, task, and spatial references. *Attention, Perception, & Psychophysics*, 78(6), 1633–1641. https://doi.org/10.3758/s13414-016-1123-6

Other

Ten Brink, A. F., Nijboer, T. C. W., Fabius, J. H., & Van der Stigchel, S. (2019). No direction specific costs in trans-saccadic memory. *Neuropsychologia*, 125, 23–29. https://doi.org/10.1016/j.neuropsychologia.2019.01.014

Mathôt, S., Fabius, J. H., Van Heusden, E., & Van der Stigchel, S. (2018). Safe and sensible preprocessing and baseline correction of pupil-size data. *Behavior Research Methods*, 50(1), 94–106. https://doi.org/10.3758/s13428-017-1007-2

Schut, M. J., Van der Stoep, N., Fabius, J. H., & Van der Stigchel, S. (2018). Feature integration is unaffected by saccade landing point, even when saccades land outside of the range of regular oculomotor variance. *Journal of Vision*, 18(7), 6. https://doi.org/10.1167/18.7.6

Schut, M. J., Fabius, J. H., Van der Stoep, N., & Van der Stigchel, S. (2017). Object files across eye movements: Previous fixations affect the latencies of corrective saccades. *Attention, Perception, & Psychophysics*, 79(1), 138–153. https://doi.org/10.3758/s13414-016-1220-6

Schut, M. J., Fabius, J. H., & Van der Stigchel, S. (2016). Investigating the parameters of transsaccadic memory: inhibition of return impedes information acquisition near a saccade target. *Visual Cognition*, 24(2), 141–154. https://doi.org/10.1080/13506285.2016.1206050

Articles in preparation (data presented in this thesis)

Fabius, J.H., Ten Brink, A.F., Van der Stigchel, S. & Nijboer, T.C.W. (under review). Spatial working memory impairment and search behavior in visuospatial neglect.

Fabius, J.H., Nijboer, T.C.W., Fracasso, A., & Van der Stigchel, S. (submitted). Perceptual continuity across eye movements after a lesion to the posterior parietal cortex

Fabius, J.H., Fracasso A., Acunzo, D.A., Van der Stigchel, S. & Melcher, D. (in preparation) Perceptual continuity across eye movements after a lesion to the posterior parietal cortex.

Presentations

Talks

Fabius, J,H,, Fracasso, A., Nijboer, T.C.W., & Van der Stigchel, S. (2018). Rapid spatiotopic updating across saccades. Presented at *Tagung Experimentall Arbeitender Psychologen 2018*, Marburg, Germany.

Fabius, J,H,, Fracasso, A., Nijboer, T.C.W., & Van der Stigchel, S. (2017). Perceptual continuity across saccades: evidence for rapid spatiotopic updating. Presented at *European Conference on Eye Movements 2017*, Wuppertal, Germany

Fabius, J,H,, Fracasso, A., & Van der Stigchel, S. (2017). Spatiotopic updating facilitates post-saccadic perception. Presented at *Perception Day 2016*, Nijmegen, The Netherlands.

Fabius, J,H,, Fracasso, A., & Van der Stigchel, S. (2016). Visual continuity across saccades. Presented at *Annual Meeting of the Vision Sciences Society 2016,* St. Pete Beach, Florida.

Posters

Fabius, J.H., Fracasso, A., Acunzo, D.A., Deflorio, D., Van der Stigchel, S., & Melcher, D. Presaccadic spatiotopic updating across visually-guided saccades investigated with time-resolved MEG classification. Presented at *European Conference on Visual Perception 2018*, Trieste, Italy

Fabius, J.H., Fracasso, A., Acunzo, D.A., Deflorio, D., Van der Stigchel, S., & Melcher, D. Presaccadic spatiotopic updating across visually-guided saccades investigated with time-resolved MEG classification. Presented at *Perception day 2018*, Nijmegen, The Netherlands

Fabius, J,H,, Fracasso, A., Nijboer, T.C.W., & Van der Stigchel, S. (2017). Perceptual continuity across saccades: evidence for rapid spatiotopic updating. Presented at *Annual Meeting of the Vision Sciences Society 2017*, St. Pete Beach, Florida.

Fabius, J.H., Schut, M.J., & Van der Stigchel, S. (2015). Preventing re-fixations is not a general principle, despite inhibition of return. Presented at *Winter Conference of the Nederlandse Vereniging voor Psychonomie*, Egmond aan Zee, The Netherlands.

A